

# **For Reference**

---

**NOT TO BE TAKEN FROM THIS ROOM**

Ex LIBRIS  
UNIVERSITATIS  
ALBERTAENSIS











T H E   U N I V E R S I T Y   O F   A L B E R T A

CHROMATOGRAPHY AND TWO PHASE PHOTOMETRIC TITRATIONS  
FOR THE DETERMINATION OF DRUGS AND OTHER SUBSTANCES

BY



HUSSAIN Y. MOHAMMED

A THESIS

SUBMITTED TO THE FACULTY OF GRADUATE STUDIES AND  
RESEARCH IN PARTIAL FULFILMENT OF THE REQUIREMENTS  
FOR THE DEGREE OF DOCTOR OF PHILOSOPHY

IN

CHEMISTRY

EDMONTON, ALBERTA

FALL, 1979



THE UNIVERSITY OF ALBERTA

FACULTY OF GRADUATE STUDIES AND RESEARCH

The undersigned certify that they have read, and recommend to the Faculty of Graduate Studies and Research for acceptance, a thesis entitled, "Chromatography and Two-Phase Photometric Titrations for the Determination of Drugs and Other Substances," submitted by HUSSAIN Y. MOHAMMED in partial fulfilment of the requirements for the degree of Doctor of Philosophy in Chemistry.



This thesis is dedicated to my parents;  
without their help this work would never  
have been started.



## ABSTRACT

In Part I of this thesis, the chromatographic determination of drugs in pharmaceutical syrups on a column of Amberlite XAD-2 will be discussed in detail. Syrups were directly injected onto a short pre-column, without sample pretreatment. The apparatus in Figure 1A and B were used for the analysis of phenylephrine hydrochloride, acetaminophen, glyceryl guaiacolate, and dextromethorphan hydrobromide in commercial syrups.

The chromatographic retention behavior of drug samples was studied as a function of five different mobile phase variables including the type and percent of organic solvent in the aqueous-organic mobile phase, pH, and nature and concentration of inert electrolyte in the mobile phase.

Chromatographic retention volumes of a monobasic amine (promethazine) and a dibasic amine (pheniramine) were studied as a function of pH of the mobile phase. Theoretical expressions were derived for both cases and verified experimentally.

In Part II of this thesis a novel heterogeneous photometric titration technique is described. The heart of the titration apparatus is the filter-probe which allows only one of the two immiscible liquid phases (aqueous or organic) to be continuously pumped out of a vigorously stirred two-phase solvent mixture.



The filtered phase is pumped through a spectrophotometer flow cell, and returned to the titration vessel.

This system has been used for many applications including the acid-base and ion-pair titrations of drug compounds of the  $BH^+$  charge type and the ion-pair titrations of cationic and anionic surfactants. Several pharmaceutical amines were titrated with sodium hydroxide and picrate ion, and the absorbance of the aqueous phase was monitored. Cationic drugs and surfactants were titrated with picrate ion and the absorbance of the organic phase was monitored. Also anionic surfactants were titrated with methylene blue cation and the organic phase was again monitored.

Theoretical titration equations were derived, for these acid-base and ion-pair titrations which take into account the common side reactions, and in most cases the theoretical equations were verified experimentally by titrating drug or surfactant sample compounds. These equations were used to illustrate the influence of various parameters on the overall photometric titration curves. Among these parameters are the distribution coefficients of various sample and titrant species, the  $pK_a$  and  $pK_b$  values of sample and titrant, and the aqueous phase pH. The theoretical titration equations facilitate prediction of optimum titration conditions.



## ACKNOWLEDGEMENTS

The author wishes to express his sincere gratitude to Dr. Frederick F. Cantwell of this institution for his guidance and encouragement during the course of this work.

Sincere thanks are also extended to Mrs. L. Ziola for her excellent secretarial work and to Mrs. F. Nagle for her helpfulness and her excellent drafting work.

Finally, the author acknowledges Leslie Chatten of the College of Pharmacy, University of Alberta, and C. F. Hiskey of Endo Laboratories, Inc., for their supply of sample drugs.



## TABLE OF CONTENTS

### PART I

#### CHAPTER

1.	INTRODUCTION .....	2
2.	EXPERIMENTAL .....	9
2.1	Apparatus .....	9
2.2	Chemicals .....	15
2.3	Reagents .....	16
2.4	Resins .....	18
2.5	Syrups .....	19
2.6	Blank and Spiked Blank Syrup .....	19
2.7	Potentiometric Titration .....	22
2.8	Photometric Determination of $pK_{a,1}$ for Pheniramine Cation .....	22
3.	RESULTS AND DISCUSSION .....	24
3.1	Retention of Drugs from Methanol/Water ...	24
3.2	Retention of Drugs from Acetonitrile/ Water .....	35
3.3	Retention of Drugs from Dioxane/Water ....	40
3.4	Predicting Separation Conditions .....	40
3.5	Influence of pH on Retention .....	48
3.5.1	Phenols and Carboxylic Acids .....	48
3.5.2	Monobasic Amines .....	49
3.5.3	Dibasic Amines .....	53
3.6	Influence of Electrolyte on Retention ....	60
3.7	Retention of Inert Ingredients .....	64



3.8	Analysis of Syrups .....	66
3.8.1	Phenylephrine and Acetaminophen ...	67
3.8.2	Glyceryl Guaiacolate .....	72
3.8.3	Dextromethorphan Hydrobromide .....	74
4.	CONCLUSION .....	76
5.	FURTHER WORK .....	78

## PART II

### CHAPTER

1.	INTRODUCTION .....	80
2.	THEORETICAL .....	86
2.1	Acid-Base Titrations .....	86
2.1.1	Proposed Model .....	86
2.1.2	Predicted Acid-Base Titration Behavior .....	91
2.1.3	Dilution Correction for Acid- Base Titrations .....	100
2.2	Ion-Pair Titrations .....	103
2.2.1	Proposed Model .....	104
2.2.2	Predicted Ion-Pair Titration Behavior .....	111
2.2.2.1	Absorbance of Aqueous Phase Monitored; Titrant A <sup>-</sup> .....	111
2.2.2.2	Absorbance of Organic Phase Monitored; Titrant A <sup>-</sup> .....	126
2.2.3	Dilution Correction for Ion-Pair Titrations .....	131



3.	EXPERIMENTAL .....	136
3.1	Apparatus .....	136
3.2	Chemicals .....	144
3.3	Reagents .....	147
3.4	Distribution Isotherms and Molar Absorptivities .....	149
3.5	Titration Procedure .....	153
4.	RESULTS AND DISCUSSION.....	156
4.1	Acid-Base Titrations .....	156
4.1.1	Dextromethorphan Hydrobromide .....	156
4.1.2	Assay of Drugs .....	161
4.1.3	Advantages of the Method .....	163
4.2	Ion-Pair Titrations .....	165
4.2.1	Monitoring the Absorbance of the Aqueous Phase .....	165
4.2.1.1	Promethazine Hydro- chloride .....	165
4.2.1.2	Assay of Drugs .....	170
4.2.2	Monitoring the Absorbance of the Organic Phase .....	174
4.2.2.1	Titration of Cations .....	175
4.2.2.2	Titration of Anions .....	182
4.2.2.3	Emulsions and Adsorption .	185
5.	CONCLUSION .....	188
6.	FURTHER WORK .....	195
	REFERENCES .....	197
	APPENDIX I. Tables of all of the data in Figures 2, 3, and 4 .....	207



APPENDIX II.	Derivation of the distribution ratio expressions for acids $BH^+$ and $BH_2^{2+}$ in the presence of XAD-2 resin .....	215
APPENDIX III.	Derivation of photometric acid-base titration equations for a weak acid $BH^+$ titrated with NaOH .....	219
APPENDIX IV.	Derivation of photometric ion-pair titration equations for a weak acid cation with anionic titrant .....	226
APPENDIX V.	Derivation of photometric ion-pair titration equations for a weak base anion with cationic titrant. Absorbance of organic phase monitored .....	236



## LIST OF TABLES

NUMBER	TITLE	PAGE
I	Composition of Blank Syrups.	20
II	Names, Identifying Numbers, Structures and Ionization Constants of Drugs Studied	25
III	Results of Syrup Analyses	68
IV	Equilibrium Constant Expressions for the Acid-Base Titrations	88
V	Equilibrium Constant Expressions for the Ion-Pair Titrations	107
VI	Assay Values (%) for Several Drugs by Three Titration Methods	162
VII	Values of Constants for the Ion-Pair Titrations	171
VIII	Assay Values (%) and Average Deviations for Several Drugs by Three Titration Methods	173
IX	Assay Values (%) and Average Deviations for Cations Titrated with Picrate	181



NUMBER	TITLE	PAGE
X	Assay Values (%) and Average Deviations for Anions Titrated with Methylene Blue	183



## LIST OF FIGURES

NUMBER	TITLE	PAGE
1	Two arrangements of the liquid chromatograph.	10
2	Relationship between $\log V_N$ and percent water in methanol/water mobile phases, on a 30 cm x 0.20 cm column of Amberlite XAD-2.	29
3	Relationship between $\log V_N$ and percent water in acetonitrile/water mobile phases, on a 15 cm x 0.28 cm column of Amberlite XAD-2.	36
4	Relationship between $\log V_N$ and percent water in dioxane/water mobile phases, on a 15 cm x 0.28 cm column of Amberlite XAD-2.	41
5	Relationship between $p_{aH}^*$ and $\log (n_{NaOH}/n_X - n_{NaOH})$ for promethazine.HCl.	54
6	Relationship between the distribution ratio and $p_{aH}^*$ for promethazine.HCl in 10% water/methanol, on a 15 cm x 0.28 cm column of Amberlite XAD-2.	55



NUMBER	TITLE	PAGE
7	Relationship between the distribution ratio and $p_{a_H}^*$ for pheniramine maleate in 30% water/methanol, on a 15 cm x 0.28 cm column of Amberlite XAD-2.	57
8	Relationship between $A_2$ and $a_H^*$ ( $A_2^{II} - A_2$ ) for pheniramine maleate.	59
9	Dependence of $V_N$ for acetaminophen (---) and phenylephrine (—) on concentration of chloride (●) and perchlorate (O) on a 15 cm x 0.28 cm column of Amberlite XAD-2.	61
10	Typical syrup chromatograms of phenylephrine.HCl and acetaminophen (A); glyceryl guaia-colate (B); and dextromethorphan.HBr (C), on a 15 cm column under the conditions described in the text.	69
11	Theoretical titration curves for acid $BH^+$ in a two phase system (monitoring the aqueous phase). First effect of $K_I$ on the shape of the titration curve.	94



NUMBER	TITLE	PAGE
12	Theoretical titration curves for acid $BH^+$ in a two phase system (monitoring the aqueous phase). Second effect of $K_I$ on the shape of the titration curve.	96
13	Theoretical titration curves for acid $BH^+$ in a two phase system (monitoring the aqueous phase). First effect of $K_B$ on the shape of the titration curve.	97
14	Theoretical titration curves for acid $BH^+$ in a two phase system (monitoring the aqueous phase). Second effect of $K_B$ on the shape of the titration curve.	99
15	Theoretical titration curves for acid $BH^+$ in a two phase system (monitoring the aqueous phase). Effect of $K_S$ on the shape of the titration curve.	113
16	Theoretical titration curves for acid $BH^+$ in a two phase system (monitoring the aqueous phase). Effect of $K_{I,BHX}$ on the shape of the titration curve.	116



NUMBER	TITLE	PAGE
17	Theoretical titration curves for acid $BH^+$ in a two phase system (monitoring the aqueous phase). Effect of $K'_a$ on the shape of the titration curve.	118
18	Theoretical titration curves for acid $BH^+$ in a two phase system (monitoring the aqueous phase). Effect of $K_B$ on the shape of the titration curve.	119
19	Theoretical titration curves for acid $BH^+$ in a two phase system (monitoring the aqueous phase). Effect of $K_{I,MA}$ on the shape of the titration curve.	120
20	Theoretical titration curves for acid $BH^+$ in a two phase system (monitoring the aqueous phase). Effect of $K'_b$ on the shape of the titration curve.	122
21	Theoretical titration curves for acid $BH^+$ in a two phase system (monitoring the aqueous phase). Effect of $K_{HA}$ on the shape of the titration curve.	123



NUMBER	TITLE	PAGE
22	Theoretical titration curves for acid $BH^+$ in a two phase system (monitoring the aqueous phase). Effect of pH on the shape of the titration curve.	124
23	Theoretical titration curves for acid $BH^+$ in a two phase system (monitoring the organic phase). Effect of $K_s$ on the shape of the titration curve.	128
24	Theoretical titration curves for acid $BH^+$ in a two phase system (monitoring the organic phase). Effect of pH on the shape of the titration curve.	129
25	Diagram of the titration apparatus	137
26	Exploded view of the end of the filter-probe.	140
27	Spectrophotometric recorder tracing for the titration of dextromethorphan.HBr with sodium hydroxide at 275 nm.	155
28	Photometric titration curves for dextro-methorphan.HBr with sodium hydroxide titrant.	157



NUMBER	TITLE	PAGE
29	Distribution isotherm for dextromethorphanium ion ( $\text{BH}^+$ ) and dextromethorphan base (B) between $\text{CCl}_4/\text{CHCl}_3$ (1:1) and 0.1 M NaCl aqueous electrolyte. Curve A, pH = 2 ( $\text{BH}^+$ ); Curve B, pH = 13 (B).	160
30	Titration curve for promethazine.HCl with picrate titrant.	167
31	Distribution isotherm for promethazinium ion between chloroform and aqueous 0.052 M phosphate buffer pH = 2.90.	169
32	Titration of benzethonium chloride with picrate.	176
33	Distribution isotherm for benzethonium chloride between chloroform and aqueous buffer pH = 7.50.	178
34	Titration of promethazine.HCl with picrate.	180
35	Experimental titration curve of sodium laury sulfate with Methylene Blue.	184



NUMBER	TITLE	PAGE
36	Experimental titration curve of silver ion with dithizone.	192



PART I

CHROMATOGRAPHIC DETERMINATION OF  
DRUGS IN PHARMACEUTICAL SYRUPS



## CHAPTER 1

### INTRODUCTION

Pharmaceutical syrups are complex mixtures containing various active ingredients along with several inert components such as dyes, flavoring agents, sweeteners, preservatives and buffers. Because of their complexity, assay of these syrups presents a time-consuming and difficult problem. For this reason gas chromatography and high efficiency liquid chromatography have been popular for their analysis.

The applicability of gas chromatography to pharmaceutical analysis is well documented in the literature (1-15), and the resolution of many types of mixtures has been published. Gas chromatographic assay methods often require an initial liquid-liquid extraction of the drugs from the aqueous syrup to eliminate water (16), and sometimes to remove the organic soluble flavor and coloring additives which interfere with the chromatogram (17). Furthermore, serious difficulties are often encountered when relatively polar compounds such as phenylephrine are chromatographed. These materials often exhibit excessive tailing, and the selection of the liquid phase becomes critical if resolution is to be obtained.



Hishta and Laubach (18) analyzed a mixture of phenylpropanolamine, phenylephrine, phenyltoloxamine and chlorpheniramine by gas chromatography after forming the bistrimethylsilylacetamide (BSA) derivative. Watson and Lawrence (19) converted phenylephrine to a less polar derivative before gas chromatography. In recent review articles Nicholson (20,21) described the various means available for derivative formation.

Using the ion exchange mode of liquid chromatography Spreick (22) analyzed phenylpropanolamine, pseudoephedrine, and pheniramine in syrups on a pellar cation exchange column by direct injection. Pyrillamine maleate was separated from phenylephrine hydrochloride, and naphazoline hydrochloride by high pressure anion exchange chromatography (23).

The development and commercial availability of hydrolytically stable stationary phases chemically bonded onto microparticulate substrates has given the chromatographer an efficient and versatile partition medium for HPLC. One of the most widely used HPLC bonded phase functional groups is octadecylsilane, which is employed in a reversed-phase mode with eluents composed of water-methanol or water-acetonitrile. Honigberg and co-workers (24) recently described the LC separation and quantification of the active components of a typical cough-cold preparation con-



taining pseudoephedrine hydrochloride, codeine phosphate, triprolidine hydrochloride, and strychnine sulfate. Drugs were chromatographed on diphenyldichlorosilane(phenyl) column in less than 10 min. Syrup samples were not analyzed. The liquid chromatographic behavior of a number of drugs on non-polar bonded phases (25) was found to be highly predictable on the basis of  $pK_a$  and partition coefficient, and the authors claimed that these stationary phases should be especially valuable for the separation of acidic and neutral drugs. Chromatography of syrup samples on a non-polar bonded phase (octadecylsilyl) required preliminary liquid-liquid extraction (26) to eliminate interference. When chromatographing amines on non-polar bonded phases, the pH was adjusted to a value at which the non-ionized free-base was the adsorbed species (24-27).

Most drug substances are ionizable and some of them are present in aqueous solution only in ionized form, e.g., quaternary ammonium compounds and sulphate conjugates. Ionized compounds can be extracted into organic solvents as ion pairs with suitable counter ions. This technique has found wide application in drug analysis owing to the superior selectivity and the possibility of an increased sensitivity for quantitative determinations. Schill (28) has surveyed



the use of ion-pair extraction in drug analysis.

Ion-pair partition has also been applied successfully in liquid-liquid chromatography. For example, Doyle and Levine (29,30) have popularized gravity-flow liquid-liquid partition chromatography employing ion-pair distribution of the salts of amine drugs with simple anions such as  $\text{Cl}^-$ ,  $\text{Br}^-$ , and  $\text{NO}_3^-$ .

High efficiency liquid-liquid chromatography has also been achieved, particularly when silica microparticles are used as the support for the stationary liquid phase (31-36). Recently, octadecylsilyl bonded packings have been used as stationary phases for reverse-phase "ion-pair" chromatography of cationic sample components using a large organic anion as the counterion (37-40), and for anionic sample components using quaternary ammonium counterions (40-43). Knox and co-workers (44,45) demonstrated the use of ion-pair partition in liquid-liquid, adsorption and bonded phase chromatography. Recently Gloor and Johnson (46) have discussed the effects of counterion type, size, and concentration on separation of alkylbenzene sulfonates, catecholamines, and dyestuffs in "ion-pair" chromatography on reverse-phase bonded packings.

In the present investigation Amberlite XAD-2 resin has been used as a stationary phase for liquid chromatography of drugs. Amberlite XAD-2 is a styrene divinylbenzene copolymer produced commercially as white, insoluble 20-50 mesh beads. Each bead is an agglomeration



of a large number of microspheres. As a result, the beads have a "macroreticular" or "macroporous" structure, a uniform pore size, and a high specific surface area. Some of the physical characteristics of XAD-2 are:

- (a) surface area  $330 \text{ m}^2/\text{g}$ ,
- (b) porosity  $0.40 - 0.45 \text{ mL/mL}$ ,
- (c) average pore diameter  $90 \text{ \AA}$ , and
- (d) skeletal density  $1.07 \text{ g/mL}$ . (47)

In recent years XAD-2, due to its physical durability, low cost, and useful pH range (48), has been used as a packing material for liquid chromatography. Scoggins and Miller used it for separation and analysis of both alkyl- and arylsulfonic acids (49). Zaika used XAD-2 to separate a nucleoside from its corresponding nucleotide and free base, the order of elution being nucleotide-base-nucleoside (50). Pietrzyk and Chu used it to separate various organic bases, substituted benzenes, phenols, benzoic acids, sulfonic acids and phenoxyacetic acids (51-53). Recent work of Pietrzyk et al. involved studies on the effect of solute ionization on chromatographic retention on XAD-2 (54), and extended the theory to separation and retention of amino acids, peptides and derivatives (55). Cantwell (56) has demonstrated the utility of this stationary phase in the chromatographic analysis of preservatives in pharmaceutical syrups. In that



study a short pre-column was used to facilitate on-column clean-up, allowing direct injection of the syrup. Cantwell and co-workers also used the XAD-2 column to analyze various pharmaceutical compounds (57,58). More recently, Cantwell discussed its future role in reversed-phase HPLC (59).

XAD-2 is capable of adsorbing both neutral and ionic chemical species from solution. The neutral form of the weak acids and bases is generally much more strongly adsorbed than the anionic or cationic conjugate species (52,57,60,61). Gustafson et al. (60) reported that the distribution coefficients of aliphatic and aromatic sulfonates increase with increasing concentration of sodium chloride. In other studies sulfonate, benzoate and phthalate were chromatographically separated, and retention volumes were also found to increase with increasing concentration of sodium chloride in the mobile phase (49,62). More recent studies (54,55) have confirmed this electrolyte effect and have led to the suggestion that ion-pairing might account for the increased retention.

Cantwell and Puon (63) have studied the adsorption of ions on XAD-2 using two different experimental techniques to evaluate the adsorption mechanism:

(i) Adsorption isotherms, and (ii) Microelectrophoresis. The quantitative results from both types of experiments



suggest that adsorption of ions onto Amberlite XAD-2 can be explained in terms of the Stern-Guoy-Chapman model of the electrical double layer.

In Part I of this thesis the chromatographic retention, on XAD-2, of twenty-nine drugs which are common components of cough-cold preparations has been investigated as a function of mobile phase composition. Both neutral and ionic conjugate species are retained. Retention volumes depend on type and percentage of organic solvent in the aqueous-organic eluent, pH, and nature and concentration of electrolyte in the eluent. The observed retention diagrams are used to predict appropriate mobile phase composition for a given analysis. When combined with short pre-columns of XAD-2 and anion exchange resin, chromatographic columns of XAD-2 are used for the analysis of phenylephrine hydrochloride, acetaminophen, glyceryl guaia-colate and dextromethorphan hydrobromide in commercial syrups.



## CHAPTER 2

### EXPERIMENTAL

#### 2.1 Apparatus

Diagrams of two variations of the liquid chromatograph are presented in Figure 1. A Chromatronix model CMP-2VK pump ( $P_1$ ), chromatographic columns, injectors, fittings and Teflon tubing were of the "Cheminert" variety, obtained from Laboratory Data Control, Riviera Beach, Florida. In Figure 1A, with valve  $V_1$  (model R6031 SVP) in the position shown, pump  $P_1$  pumped solvent 1 through the sample injection valve  $V_2$  (model CSV), the pre-column  $C_1$  and the analytical column  $C_2$ . Simultaneously, pump  $P_2$ , a constant pressure pump based on the design of Fritz (64), pumped solvent 2 to waste. When valve  $V_1$  was switched (dashed lines) it allowed solvent 1 to flow directly into the analytical column and diverted solvent 2 through  $C_1$ .

In Figure 1B, pump  $P_1$  pumped solvent 1 through the analytical column  $C_2$ . Simultaneously, pump  $P_2$  pumped solvent 2 through the sample injection valve  $V_2$  and the pre-columns  $C_3$  and  $C_1$  to waste. When valve  $V_1$  was switched (dashed lines) it allowed solvent 1 to flow into  $C_1$  and the analytical column  $C_2$  and diverted solvent 2 to waste. The use of the chromatograph is described below.





FIGURE 1. Two arrangements of the liquid chromatograph.

P1, Main pump;

P2, Auxiliary pump;

C1, Pre-column (3 cm long);

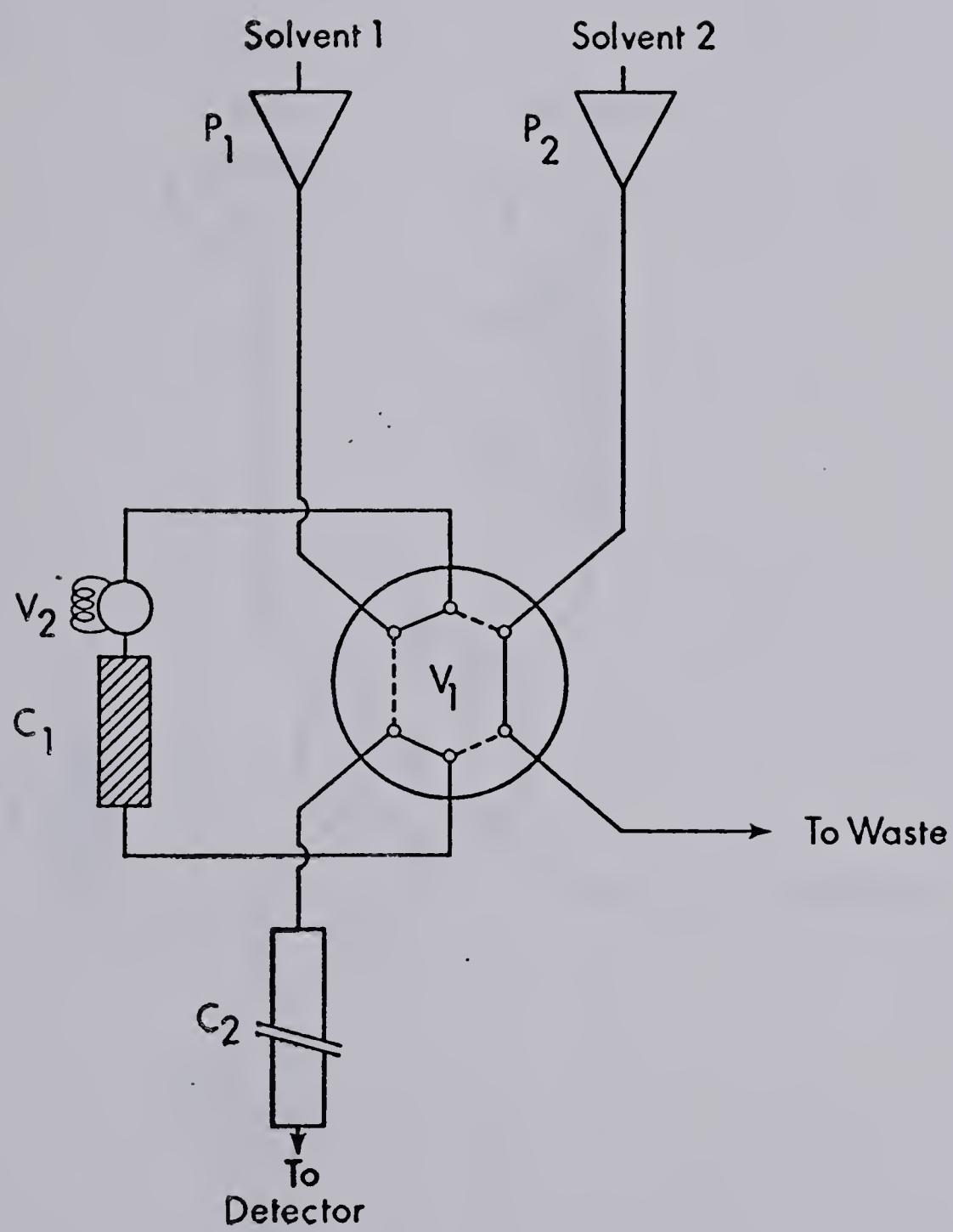
C2, Analytical column (30 cm or 15 cm long);

C3, Pre-column (2 cm long)

V1, Rotary valve;

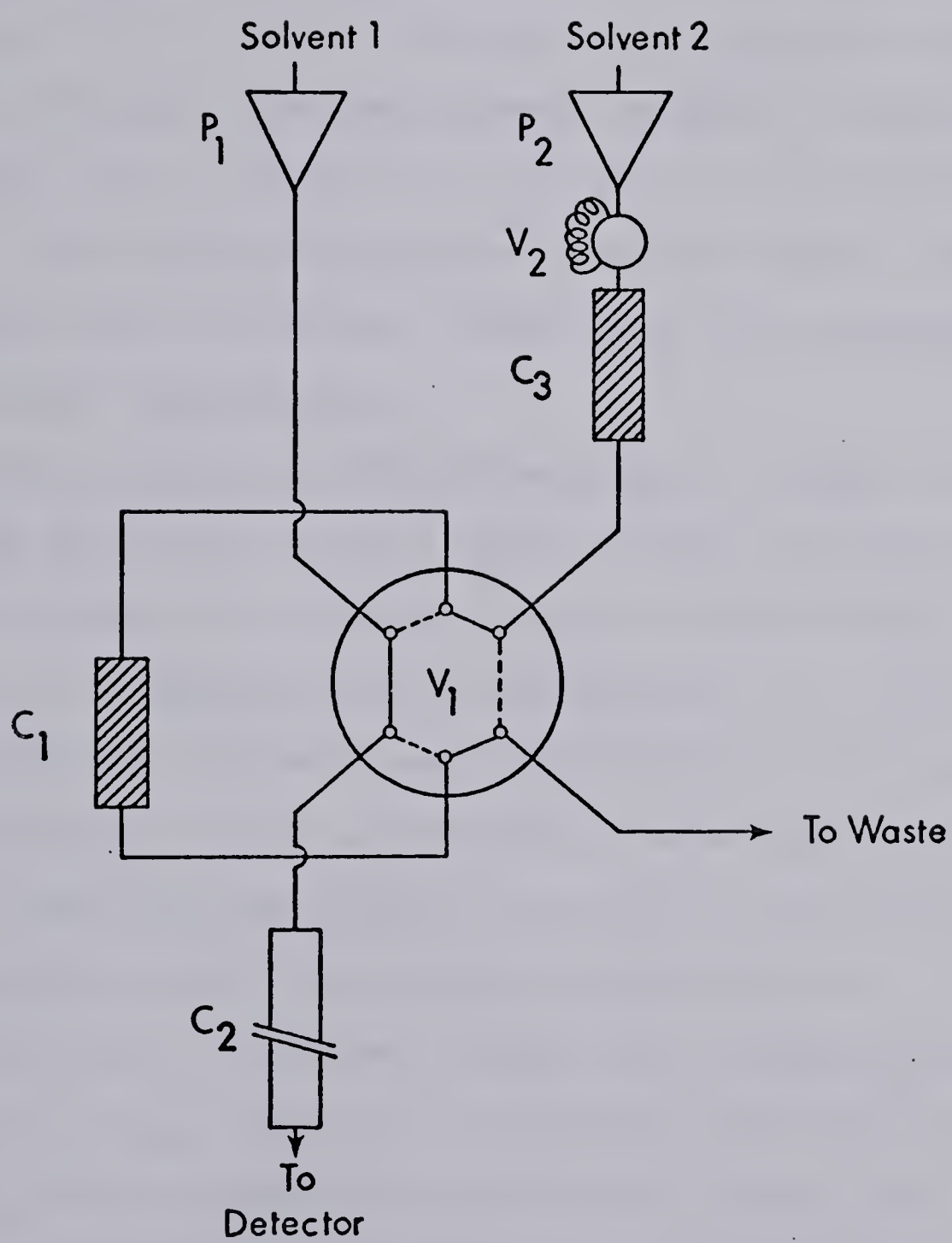
V2, Sample injection valve.

A





B





The UV detector was a model 770 Spectroflow Monitor (Schoeffel Instrument Corp., Westwood, N.J.), the recorder a Model SR (Sargent-Welch Co., Skokie, Ill.), and the electronic integrator a Model CSI-38 (Columbia Scientific Industries, Austin, Texas). The glass analytical column  $C_2$  was either 30 cm x 0.20 cm I.D. or 15 cm x 0.28 cm I.D. (Type MB) packed with 0.25 g of < 325 mesh Amberlite XAD-2. Pre-column  $C_1$  was 3 cm x 0.28 cm I.D. and  $C_3$  was 2 cm x 0.28 cm I.D. Pre-column packings are described below. All columns were dry packed. Experiments were performed at ambient temperature.

When measuring adjusted retention volumes, either  $P_2$  was connected directly to the 30 cm x 0.20 cm analytical column via a septum injector (Model 183A8) and 5  $\mu$ L of sample solution containing 2.5 - 5.0  $\mu$ g of a soluble drug salt was injected with a Pressure-Lok microsyringe (Precision Sampling, Baton Rouge, La.), or  $P_1$  was connected directly to the 15 cm x 0.28 cm analytical column via a sample injection valve. Adjusted (net) retention volumes were calculated as  $V_N = V_R - V_M$ . Here  $V_R$  is the sample retention volume and  $V_M$  is the retention volume of an unretained component (0.70 mL in this case).  $V_M$  is found by injection of a small amount of water onto a column while using a mobile phase containing a high percent



methanol. Water is unretained and produces a peak as it elutes, due to a large change in refractive index.

Potentiometric titration equipment used for the determination of  $pK_a$ 's consisted of a thermostatted titration vessel with a Teflon stopper, electrodes, pH meter, and micrometer buret. The titration vessel was a lipless glass beaker with a volume of about 150 mL. The stopper was machined to fit the vessel. It has three holes, two of which are for the electrodes, the third for the microburette tip. The pH meter was a Fisher Scientific Model 320. It was equipped with a glass electrode (Fisher Scientific Company) and a saturated calomel electrode (Fisher Scientific Company). The pH meter was standardized with buffer solutions of pH 4.00, 7.00, 10.00 (Fisher Scientific Company, Cat. No. SO-B-98, SO-B-108, SO-B-116 respectively). The titrant was delivered from a 2 mL micrometer burette (Roger Gilmont Instruments, Great Neck, N.Y.). The glass barrel of the burette was connected to a three way valve (Model CAV3031, Laboratory Data Control, Riviera Beach, Fla.). Another length of Teflon tubing connected the valve to the glass burette tip. The third valve port was connected to the titrant stored in a polyethylene reservoir bottle, and allowed rapid refilling of the buret barrel between titrations by simply switching the valve and retracting the buret



piston.

## 2.2 Chemicals

Dextromethorphan Hydrobromide was kindly supplied by Endo Laboratories (Garden City, N.Y.). It was analyzed by Fajan's argentimetric titration (65) and by nonaqueous titration using glacial acetic acid as a solvent and perchloric acid in glacial acetic acid as titrant (65) as 95.4%. (Structure in Table II).

Phenylephrine Hydrochloride was supplied by Endo Laboratories. It was analyzed by Fajan's titration as 100.0%. (Structure in Table II).

Acetaminophen was supplied by L. Chatten (College of Pharmacy, University of Alberta) and was analyzed spectrophotometrically using NF Reference Standard as 99.4%. (Structure in Table II).

Glyceryl guaiacolate, supplied by Endo Laboratories, was analyzed spectrophotometrically using USP Reference Standard as 99.6%. (Structure in Table II).

Other Drug Substances were supplied by Endo Laboratories and L. Chatten and were USP or equivalent grades. (Structures in Table II).

Other chemicals included dyes, which were Certified colors; flavors and caramel coloring, which were food grade; sodium chloride, sodium bromide, sodium carbonate, sodium perchlorate, sodium hydroxide,



potassium phosphate monobasic and dibasic, hydrochloric acid, perchloric acid, ammonium hydroxide, glacial acetic acid, citric acid, and silver nitrate which were all analytical reagent grade chemicals. Potassium acid phthalate was primary standard grade.

### 2.3 Reagents

Double distilled water was prepared by distilling the laboratory distilled water from alkaline permanganate. The first 10 - 20% of the distillate was discarded and the middle fraction was used. This water was used to prepare all aqueous solutions in this work.

1 Molar Hydrochloric Acid was prepared from the concentrated reagent by diluting with double distilled water and standardized against sodium carbonate.

0.1 Molar Ammonium Hydroxide was prepared from the concentrated reagent by diluting with double distilled water and standardized against hydrochloric acid.

0.1 Molar Perchloric Acid in glacial acetic acid was prepared by combining, in a one liter volumetric flask, several hundred mL of glacial acetic acid, 8.5 mL of 70% perchloric acid and 20 mL of acetic anhydride, diluting to volume with acetic acid and allowing to stand overnight before use. This solution was standardized against primary standard potassium



acid phthalate.

1 Molar Sodium Hydroxide was prepared by diluting 1:1 sodium hydroxide solution to the appropriate volume with freshly boiled and cooled double distilled water. The sodium hydroxide solution was stored in a polyethylene bottle and standardized with primary standard potassium acid phthalate.

Organic Solvents, methanol (J. T. Baker Chemical Co., Phillipsburg, N.J.), dioxane and acetonitrile (Caledon Laboratories, Georgetown, Ontario) were distilled before use.

Mobile Phases. All methanol-water, dioxane-water, and acetonitrile-water mobile phase solvents were prepared volumetrically by transferring measured volumes of water and aqueous reagent solutions into a volumetric flask and diluting to volume with the organic solvent. Solvent composition is therefore reported as V/V percent water.

Mobile phases used to measure the dependence of  $V_N$  on chloride and perchlorate concentration were prepared to contain  $1.0 \times 10^{-3}$  M HCl or  $\text{HClO}_4$  plus sufficient amount of added NaCl or  $\text{NaClO}_4$  to yield the desired anion concentration, in 100% water (i.e., no organic solvent).

Mobile phases used to measure the dependence of  $V_N$  or  $D$  on  $p_{\text{aH}}^*$  in Figures 6 and 7 (where  $p_{\text{aH}}^*$  is the negative log of the hydrogen ion activity referred to the standard state in the mixed solvent, calculated as discussed in Section 3.5.2 below) were prepared as



follows: Aqueous buffers were prepared in a beaker by combining sufficient volume of 1.0 M HCl (for final pH's 1 to 3), 0.50 M citric acid (for final pH's 3 to 6), 0.05 M  $\text{KH}_2\text{PO}_4$  (for final pH's 6 to 8), 0.05 M  $\text{NH}_3$  (for final pH's 8.5 to 10.5), or 0.1 M NaOH (for final pH's 11 to 13) with the volume of either dilute NaOH or dilute  $\text{NH}_4\text{Cl}$  water required to produce the desired pH, as indicated by a pH meter. Then a 100 mL or a 300 mL aliquot of this solution was transferred into a 1 liter volumetric flask. Enough NaCl was added to yield a final  $[\text{Cl}^-]$  of 0.1 M and the solution was diluted to volume with methanol. The pH's of these final 10% or 30% water solutions were measured with a glass-calomel electrode combination. The pH meter reading was corrected to  $\text{p}a_{\text{H}}^*$  as discussed in Section 3.5.2 below.

## 2.4 Resins

Amberlite XAD-2 macroreticular resin (Rohm and Haas Co., Philadelphia, Pa., Lot No. 2-0218), was ground in a triple porcelain roller mill (Erweka-Apparatebau-GmbH, Chemical and Pharmaceutical Industry Co., N.Y.), dried and classified on standard sieves (W. S. Tyler Company of Canada). The < 325 mesh portion was washed with 3 M hydrochloric acid, extracted with methanol in a Soxhlet extractor, "de-fined" by decantation



in methanol and dried in a 50°C vacuum oven. Amber-lyst A-26 macroreticular strongly basic anion exchange resin was ground in a mortar and classified on standard sieves. The 120 - 325 mesh portion was purified by alternately washing with 1 M potassium hydroxide, methanol and 4 M hydrochloric acid. After washing out excess acid and removing fines by decantation in water, the resin was air dried.

## 2.5 Syrups

Commercial cough-cold syrups were purchased at a local pharmacy. The undiluted syrups were drawn into the sample injection valve and injected directly onto the pre-column.

## 2.6 Blank and Spiked Blank Syrups

In order to demonstrate the lack of interference by other likely active and inert syrup components, blank syrups were prepared to contain the ingredients listed in Table 1. Quantitative recovery of the analyte component was demonstrated with a Spiked Blank syrup prepared by adding a known concentration of analyte compound to a portion of the appropriate blank syrup before injecting it.



TABLE I.  
Composition of Blank Syrups.<sup>a</sup>

<u>Drug</u>	<u>mg/mL</u>	Blank for Phenyl- ephrine· HCl and Aceta- minophen	Blank for Glyceryl Guaia- colate	Blank for Dextro- methor- phan.HBr
Acetaminophen	20.0	A	+	+
Phenylephrine.HCl	2.0	A	+	+
Glyceryl Guaiacolate	20.0	+	A	+
Dextromethorphan.HBr	3.0	+	+	A
Codeine Phosphate	2.4	-	+	+
Methoxyphenamine Maleate	3.4	-	+	+
Diphenhydramine.HCl	2.0	-	+	+
Diphenylpyraline.HCl	0.4	+	+	+
Ephedrine.HCl	6.0	+	+	+
Brompheniramine Maleate	0.8	+	+	+
Chlorpheniramine Maleate	0.4	+	+	+
Phenylpropanolamine.HCl	4.0	+	+	+
Pheniramine Maleate	1.5	+	+	+
Pyrilamine Maleate	2.5	+	+	+
Promethazine.HCl	1.0	+	+	+
Phenyltoloxamine Citrate	2.0	+	+	- <sup>b</sup>
Methdilazine.HCl	0.4	+	+	+
<u>Dyes and Excipients</u>				
F.D. & C Red No. 2	0.1	+	+	+
F.D. & C Yellow No. y	0.3	+	+	+



TABLE I (continued)

	<u>mg/mL</u>	Blank for Phenyl- ephrine. HCl and Aceta- minophen	Blank for Glyceryl Guaia- colate	Blank for Dextro- methor- phan.HBr
<u>Dyes and Excipients (con't)</u>				
Casiline orange	0.1	+	+	+
Minoline green	0.1	+	+	+
Sucrose	568	+	+	+
Sorbitol	64	+	+	+
Citric acid monohydrate	12	+	+	+
Caramel color	3	+	+	+
<u>Flavors</u>				
Imitation cherry	3	+	+	+
Imitation wild cherry	3	+	+	+
Imitation banana	3	+	+	+
Butterscotch	3	+	+	+
<u>Others</u>				
p-Hydroxybenzoic acid	1.0	+	+	+
Vanillic acid	1.0	+	+	+
Benzoic acid	1.0	+	+	+
Cinnamaldehyde	1.0	+	+	+
Ammonium chloride	12	+	+	+

<sup>a</sup>A (+) indicates presence in the Blank syrup. An (A) indicates the analyte component, which is absent from the blank. A (-) indicates drugs omitted from Blank.

<sup>b</sup>Not found in combination with dextromethorphan.HBr in commercial syrups.



## 2.7 Potentiometric Titration

Potentiometric titrations were carried out in 50.0 mL of water/methanol solvent for the determination of  $pK'_{a,1}$  for promethazine and  $pK'_{a,2}$  for pheniramine. The total amount of sample added to the beaker was about  $10^{-4}$  mole. Sodium hydroxide titrant concentration was 0.1070 M. Thus the amount of added titrant was never more than 2 mL.

Before a titration was begun, sufficient amount of sodium chloride was added to 25.0 mL of water/methanol solvent (10% and 30% water/methanol for promethazine and pheniramine respectively) to yield a final  $[Cl^-]$  of 0.1 M. A 25.0 mL aliquot of a solution of the sample compound dissolved in the same water/methanol solvent was then pipetted into the beaker and titration was begun.

After each increment of titrant was added to the stirred solution the pH meter reading was recorded when the reading had drifted to a steady value. Meter readings were converted to  $pa_H^*$  as discussed in Section 3.5.2.

## 2.8 Photometric Determination of $pK'_{a,1}$ for Pheniramine

Photometric determinations were carried out by dissolving about  $10^{-4}$  mole of pheniramine maleate in 50 mL volumes of a series of 30% water/methanol



solvents each at a different  $\text{p}a_{\text{H}}^*$  (1.5 to 6) and each containing a  $[\text{Cl}^-]$  of 0.1 M. Solvents were prepared in the same manner as described in Section 2.3.

Spectrophotometric measurements were made on a Cary 118 spectrophotometer (Varian Instruments, Palo Alto, Calif.) at 262 nm.



## CHAPTER 3

### RESULTS AND DISCUSSION

#### 3.1 Retention of Drugs from Methanol/Water

Twenty nine different drugs were chromatographed on a 30 cm x 0.20 cm column of XAD-2 using acidic, neutral and alkaline mobile phases, each containing various ratios of water and methanol. The chromatographic behavior is presented in Figure 2 as plots of  $\log V_N$  vs. percent water, and the data from Figure 2 are tabulated in Appendix I. Adjusted retention volumes above about 17 mL are too long and those below about 0.1 mL are too short to measure accurately. In the 0.010 M ammonia mobile phases (Figure 2A and B) compounds 1 - 24 are present as neutral species and are adsorbed on the resin as such (see Table II for compound name and identifying numbers). For many of the compounds there is a linear relationship between  $\log V_N$  and percent  $H_2O$  as has been observed before (56,66).

Compounds 25 - 29 possess a phenolic or carboxyl proton. They are ionized in ammonia solution and show greatly reduced retention volumes. Their retention behavior was studied in water-methanol mobile phase without added base (Figure 2E) as well as in 0.10 M HCl (Figure 2 , Compounds 25 - 27). Of this group of compounds, only phenylephrine (No. 27) possesses a



TABLE II.

Names, Identifying Numbers, Structures and Ionization Constants of Drugs Studied

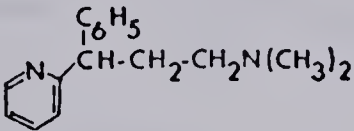
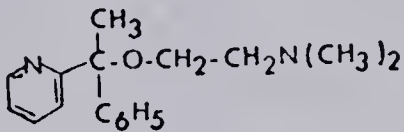
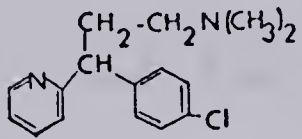
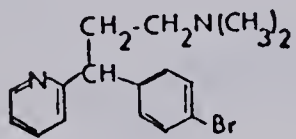
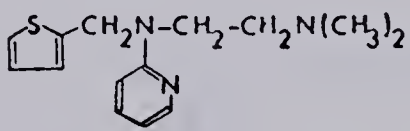
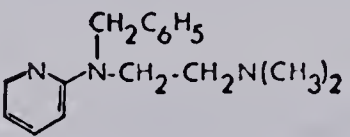
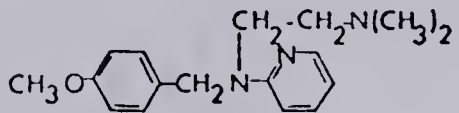
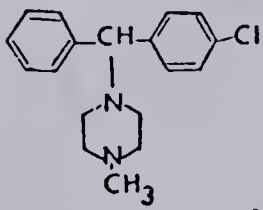
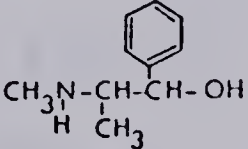
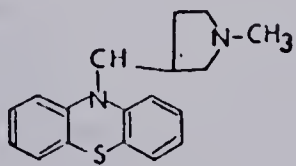
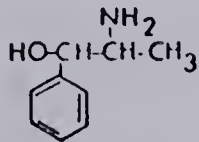
Identifying Number	Name	Structure (Neutral Drug Species)	pK <sub>a1</sub>	pK <sub>a2</sub>	Ref.
1	Pheniramine. (Maleate)		4.2	9.3	30,124
2	Doxylamine. (Succinate)		4.4	9.2	30,124
3	Chlorpheniramine. (Maleate)		4.0	9.2	30,124
4	Brompheniramine. (Maleate)				
5	Methapyrilene. (Maleate)		3.66	8.91	124
6	Tripelennamine. (HCl) <sub>2</sub>		3.92	8.96	124
7	Pyrilamine. (Maleate)		4.0	8.9	30,124
8	Chlorcycl zine. (HCl) <sub>2</sub>		2.43	7.81	124
9	Ephedrine. (HCl)		---	9.6	124
10	Methdilazine. (HCl)				
11	Phenylpropanolamine. (HCl)		9.4	---	30

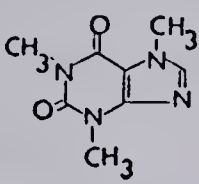
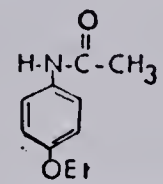
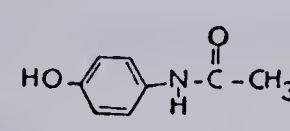
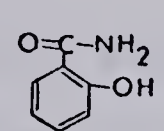
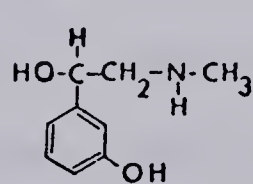
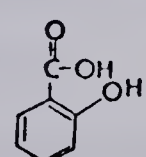
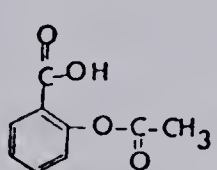


TABLE II (continued)

Identifying Number	Name	Structure (Neutral Drug Species)	pK <sub>a1</sub>	pK <sub>a2</sub>	Ref.
12	Caramiphen. (Ethanesulfonate)		---	---	
13	Codeine. (Phosphate)		8.2	---	124
14	Phenothiazine <sup>a</sup>				
15	Methoxyphenamine. (HCl)		10.1	---	30
16	Diphenhydramine. (HCl)		9.0	---	124
17	Diphenylpyraline. (HCl)				
18	Dimethoxanate. (HCl)			---	
19	Promethazine. (HCl)		9.0	---	124
20	Phenyltoloxamine. (Citrate)		9.1	---	30
21	Dextromethorphan. (HBr)		8.3	---	30
22	Glyceryl Guaiacolate		---	---	



TABLE II (con't)

Identifying Number	Name	Structure (Neutral Drug Species)	pK <sub>a1</sub>	pK <sub>a2</sub>	Ref.
23	Caffeine		< 1		124
24	Phenacetin		---	---	
25	Acetaminophen				
26	Salicylamide				
27	Phenylephrine. (HCl)		9.0	10.2	30
28	Salicylic Acid		3.0	13.82	70
29	Acetylsalicylic Acid		3.48	---	70

<sup>a</sup>See text for anomalous behavior of this compound.



basic functional group. Consequently, the neutral conjugate species for all but phenylephrine is the predominant species in both water and 0.10 M HCl and the plots of adjusted retention volume vs. percent water are similar for these compounds in both acidic and neutral solvents.

Compounds 22 - 24 are not significantly ionized in 0.10 M HCl, water or in 0.01 M  $\text{NH}_3$  and their retention behavior is independent of mobile phase acidity in this range.

In 0.10 M HCl mobile phases (Figure 2C and D) compounds 1 - 21 (except 14) and phenylephrine are cations. Of this group, compounds 1 - 8 are divalent cations and the remainder are univalent. These cationic species are adsorbed by Amberlite XAD-2, although to a much smaller extent than are their neutral conjugate species.

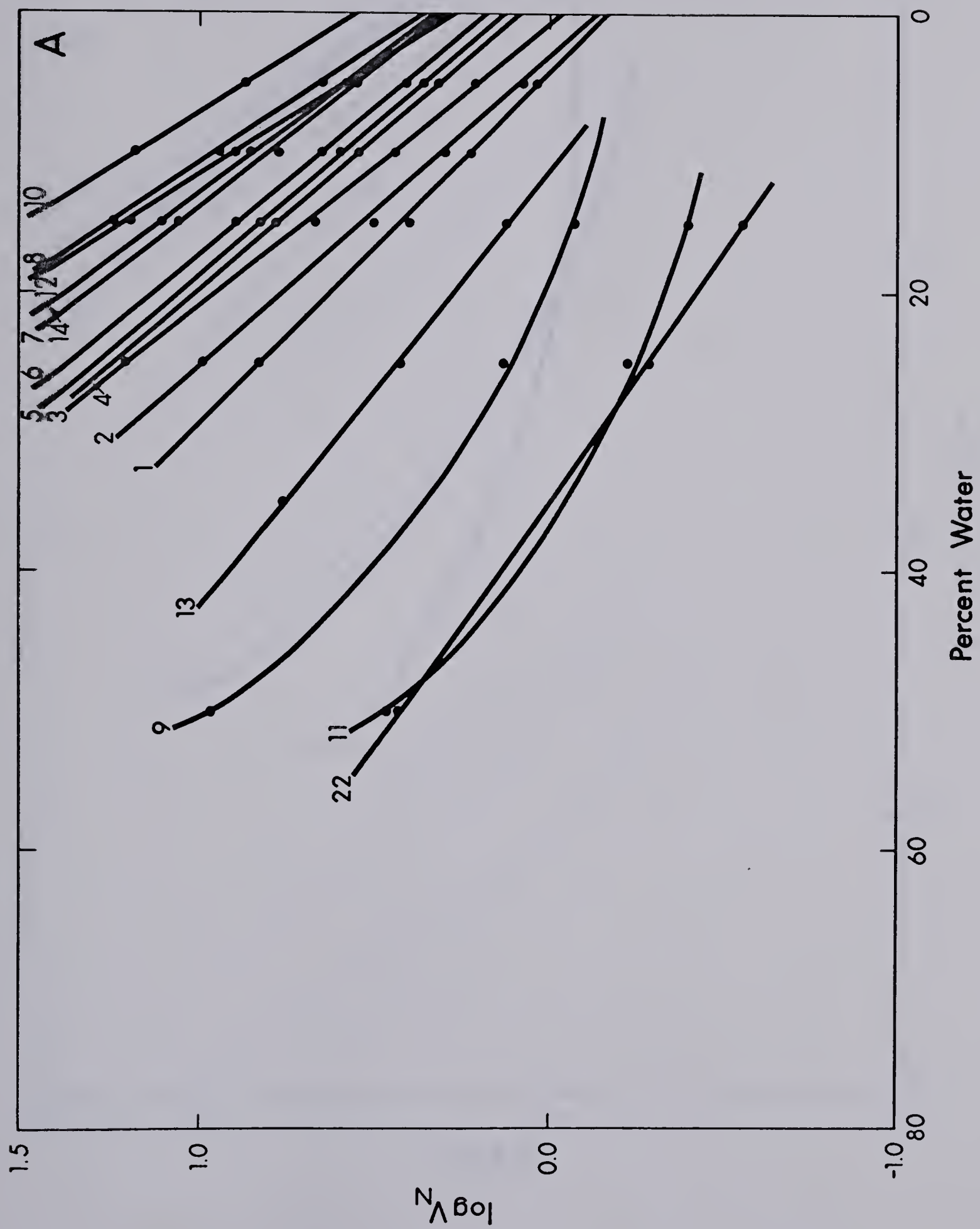
Compound 14, phenothiazine, is actually too weak a base to be protonated in 0.10 M HCl and its retention volume is the same in acidic mobile phases as it is in those containing 0.01 M  $\text{NH}_3$ . However, the compound is rapidly decomposed in an acidic solvent (77) and the decomposition product elutes with a much shorter retention volume than phenothiazine. The curve for compound 14 in Figure 2C is that of its decomposition product.



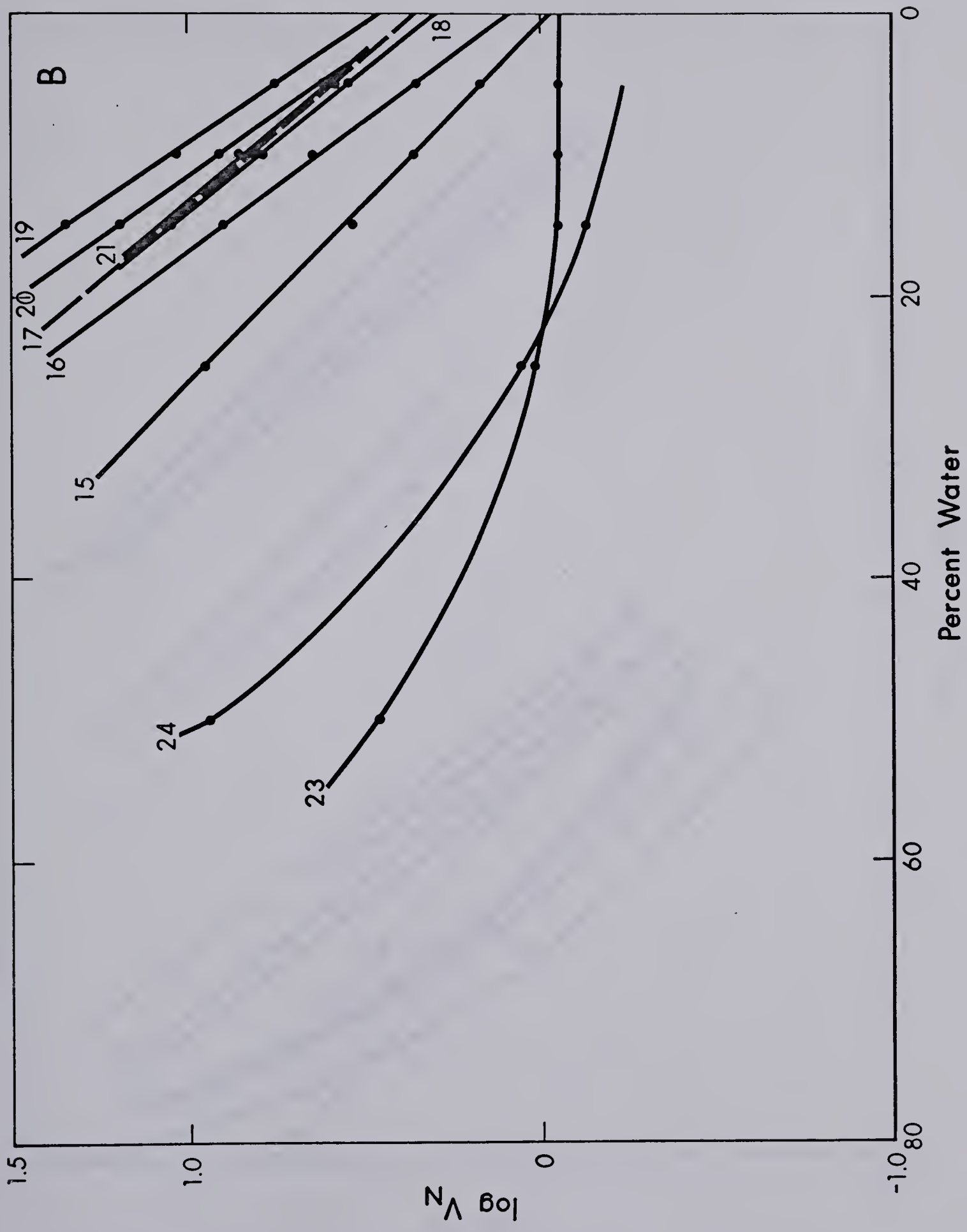


THE UNIVERSITY OF CHICAGO  
LIBRARY  
1100 EAST 58TH STREET  
CHICAGO, ILL. 60637  
TEL: 773-936-3000  
WWW.CHICAGO.LIBRARY.EDU

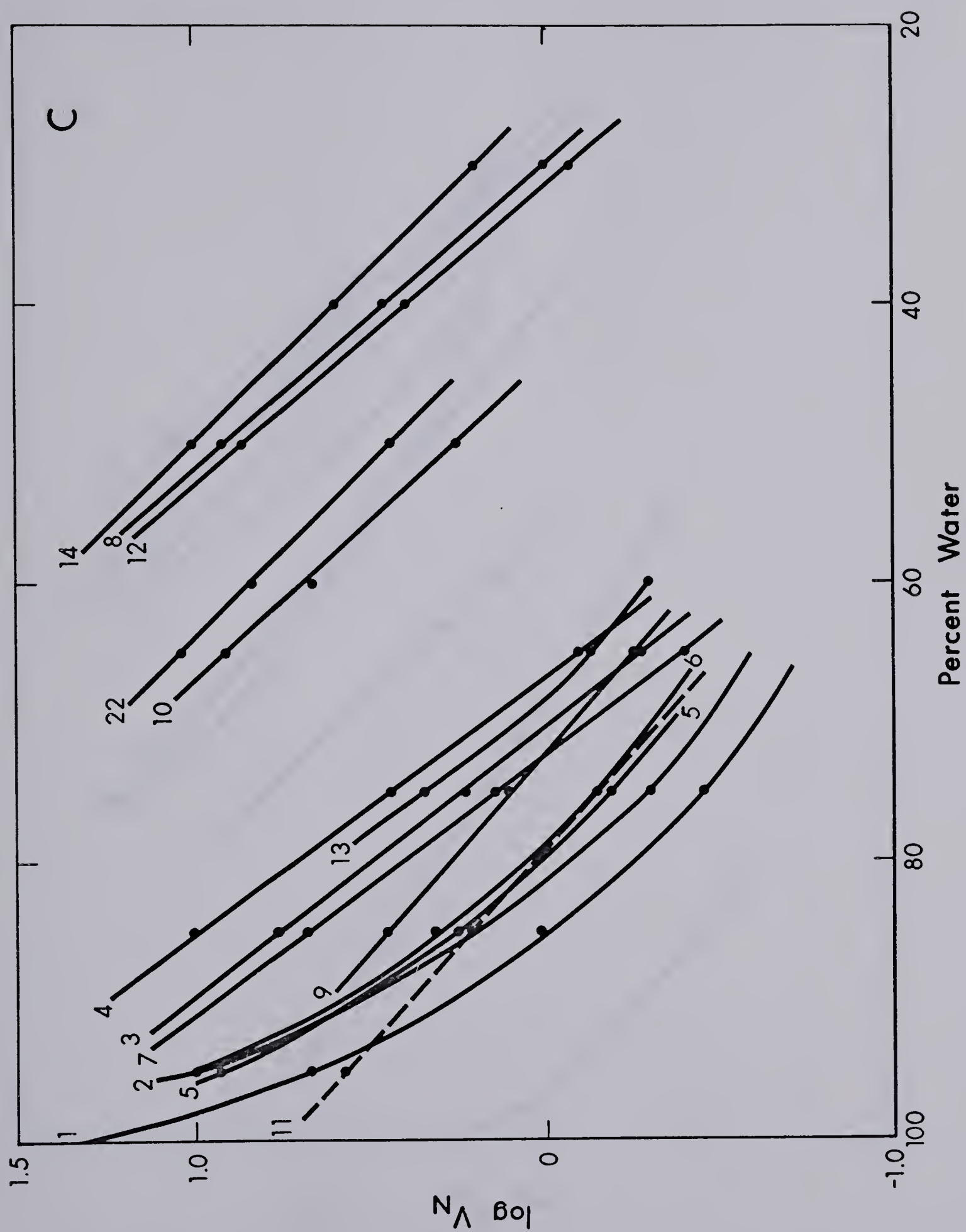
FIGURE 2. Relationship between  $\log V_N$  and percent water in methanol/water mobile phases for 0.010 M  $\text{NH}_3$  (A and B), 0.10 M HCl (C and D), and with no added acid or base (E), on a 30 cm x 0.20 cm column of Amberlite XAD-2. Compounds identified in Table II.



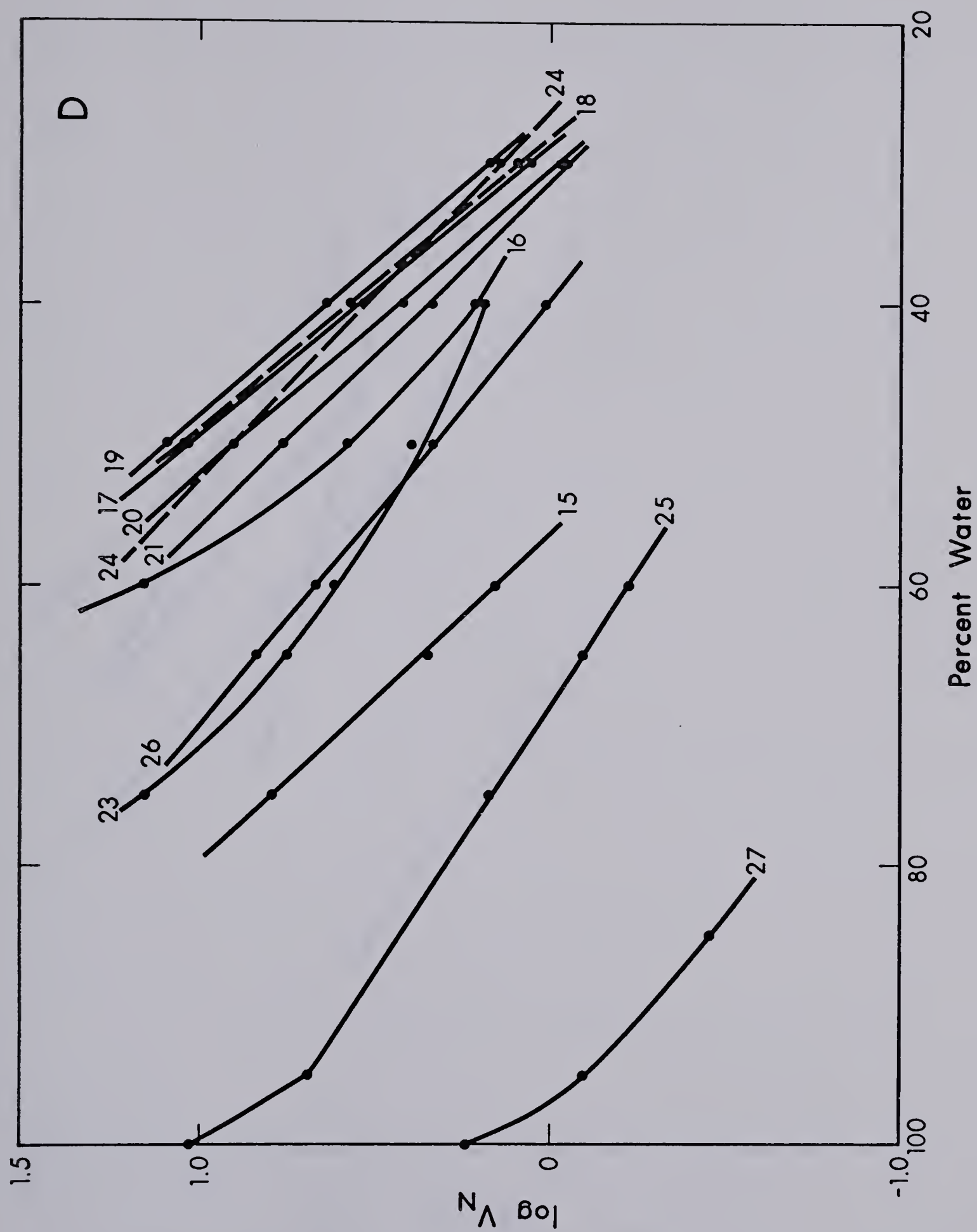




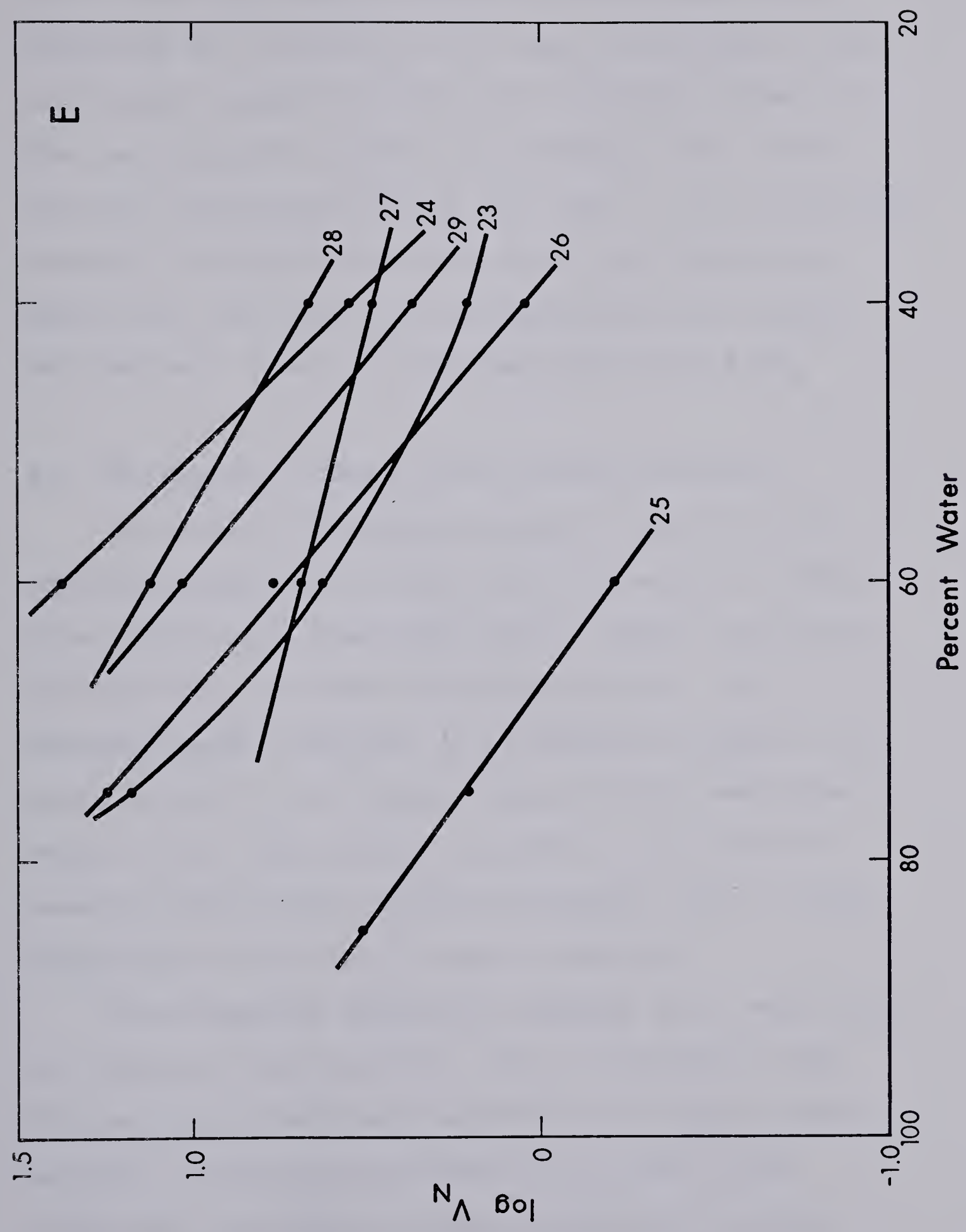














For a given methanol-water composition the retention volume of a monofunctional acid or base can be predicted as a function of pH from a knowledge of its ionization constant and the net retention volumes of its two conjugate species (see Section 3.5). Likewise for difunctional bases (e.g. No. 1 - 8), retention volumes intermediate between those for the divalent cation and free-base are obtained with mobile phase pH's between those of 0.10 M HCl and 0.010 M  $\text{NH}_3$ .

### 3.2 Retention of Drugs from Acetonitrile/Water

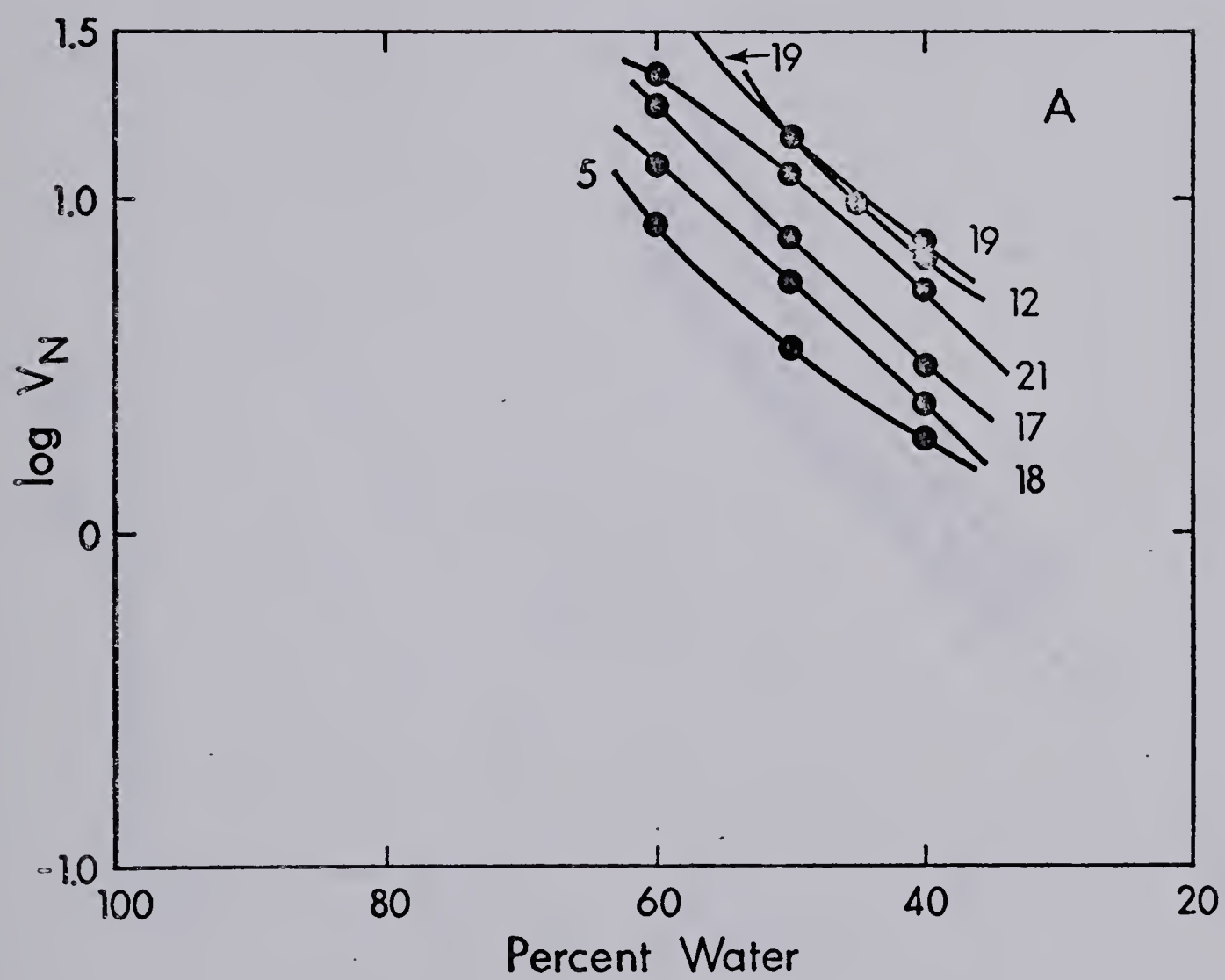
Thirteen of the drugs listed in Table II were chromatographed on a 15 cm x 0.28 cm column of Amberlite XAD-2 using ammoniacal mobile phases containing various ratios of water and acetonitrile. The chromatographic behavior is presented in Figure 3 as plots of  $\log V_N$  vs. percent water and the data from Figure 3 are tabulated in Appendix I. In 0.010 M ammonia mobile phase (Figure 3A and b), all of these compounds are present as neutral species.

The retention volume of compound 26 is very short in alkaline mobile phases. Also, compounds 22 and 23 should be relatively independent of mobile phase acidity. The retention behavior of these three compounds was studied in water-acetonitrile mobile phase without added ammonia (Figure 3C).

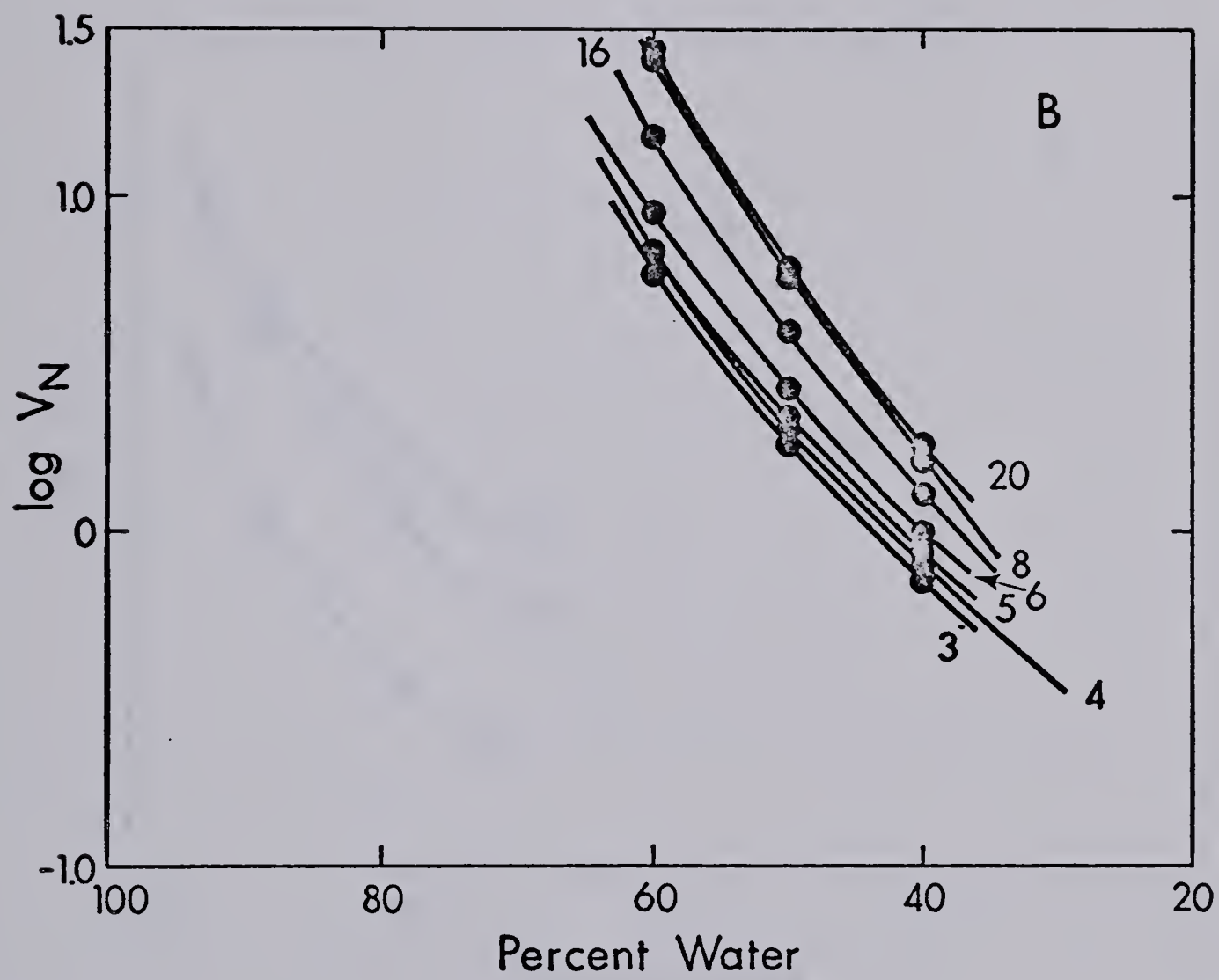




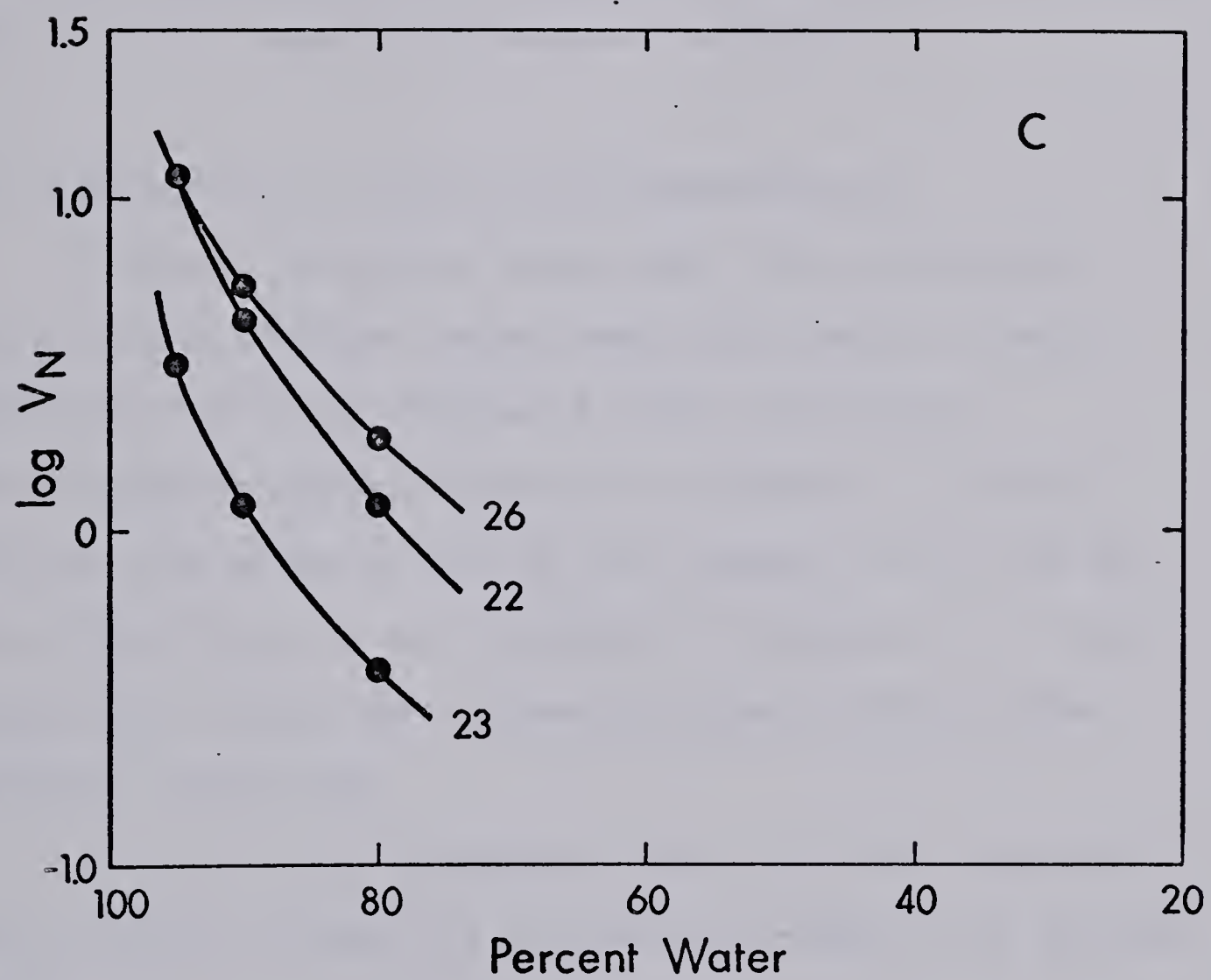
FIGURE 3. Relationship between  $\log V_N$  and percent water in acetonitrile/water mobile phases for 0.010 M  $\text{NH}_3$  (A and B), and with no added acid or base (C), on a 15 cm x 0.28 cm column of Amberlite XAD-2. Compounds identified in Table II.













The elution sequence of all sixteen compounds is approximately the same as in methanol-water with some exceptions. The most obvious difference between the two solvent systems is the greater "strength" of acetonitrile as an eluent and the improved separation of the compound pairs 12 and 18, 18 and 21, and 23 and 26, with the acetonitrile-water solvents.

### 3.3 Retention of Drugs from Dioxane/Water

Thirteen different drugs were chromatographed on a column of XAD-2 using ammoniacal mobile phases containing various ratios of water and dioxane. The chromatographic behavior is presented in Figure 4A and B as plots of  $\log V_N$  vs. percent water and the data from Figure 4 are tabulated in Appendix I. Three additional drugs were chromatographed without added ammonia, Figure 4C.

The retention characteristics of these compounds are similar to those in acetonitrile-water (see Section 3.2).

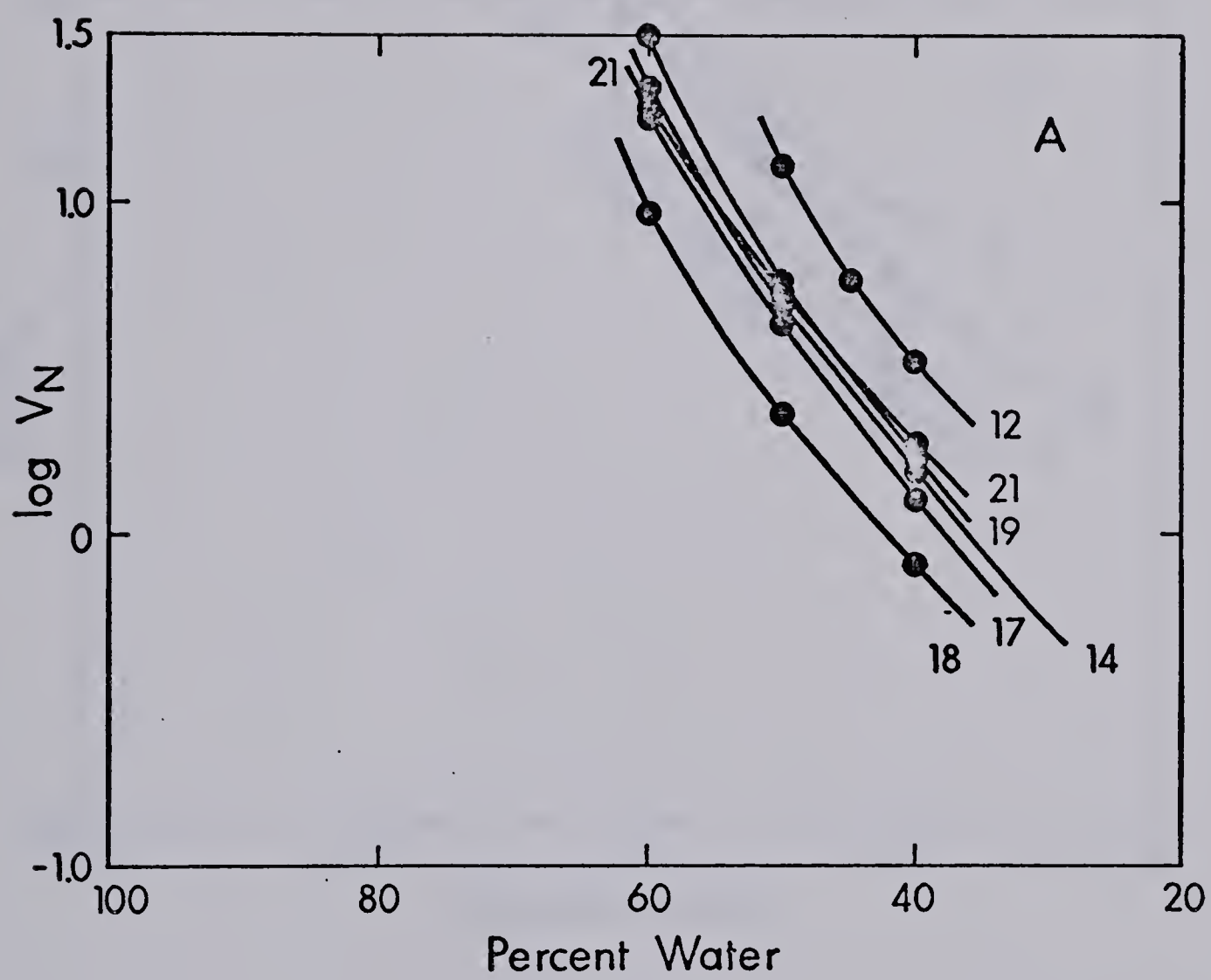
### 3.4 Predicting Separation Conditions

The plots in Figures 2, 3 and 4 may be used to select the column length and mobile phase composition required to separate any two syrup components  $i$  and  $j$ , where  $j$  has a larger retention volume than  $i$ .

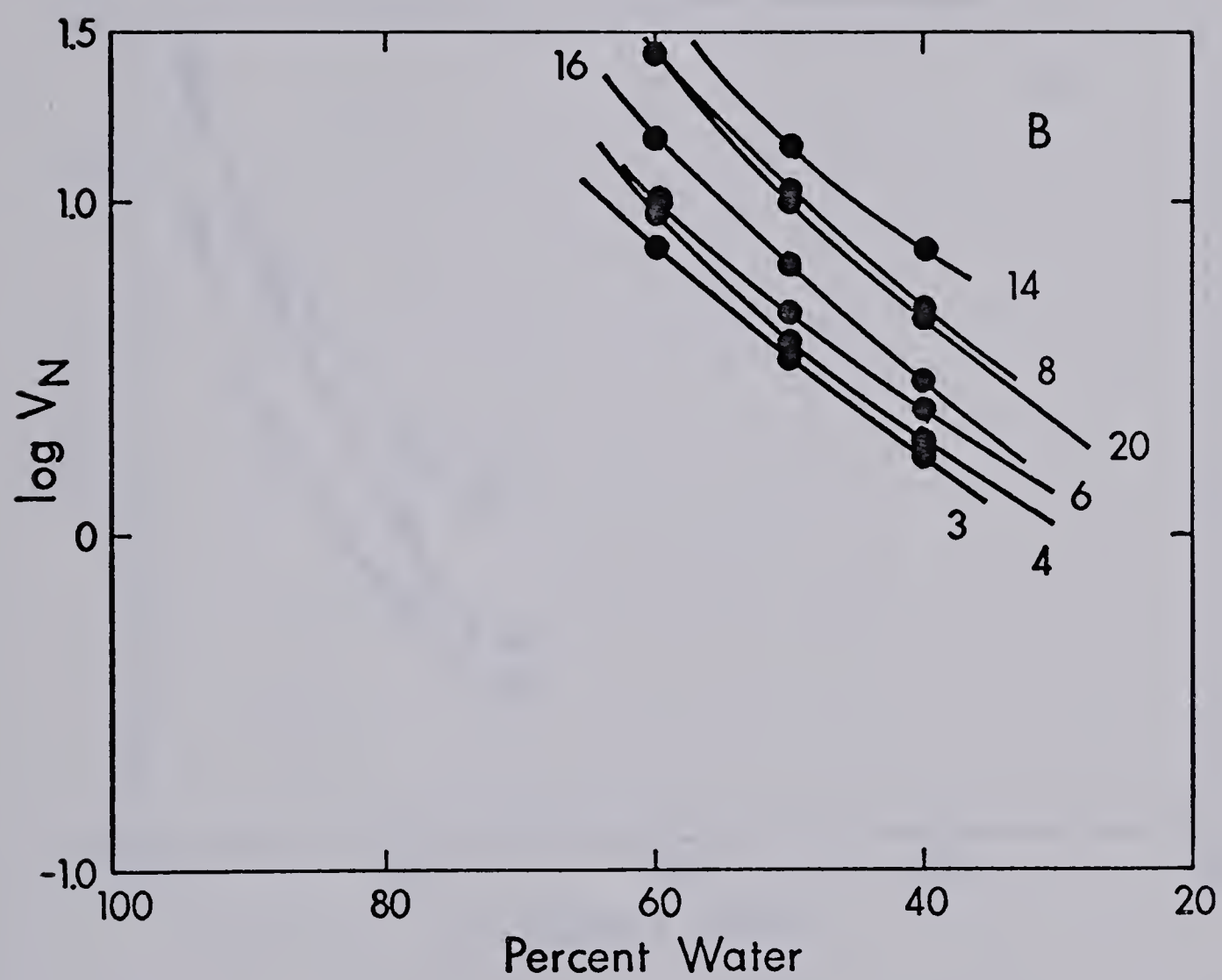




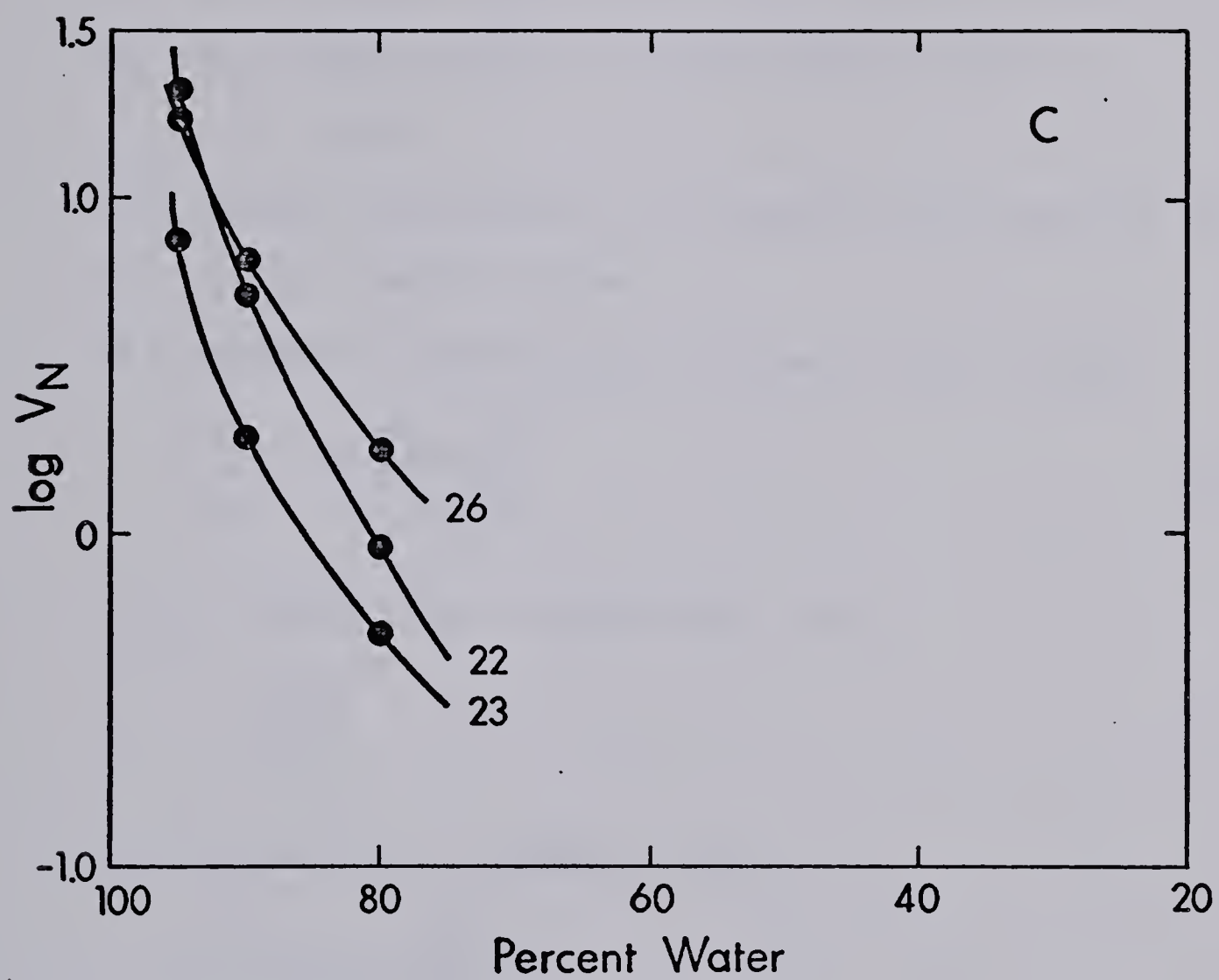
FIGURE 4. Relationship between  $\log V_N$  and percent water in dioxane/water mobile phases for 0.010 M  $\text{NH}_3$  (A and B), and with no added acid or base (C), on a 15 cm x 0.28 cm column of Amberlite XAD-2. Compounds identified in Table II.













The following symbols are defined:

$V_{N,i}, V_{N,j}$  = net retention volumes in mL for i

and  $j = V_{R,i} - V_M, V_{R,j} - V_M$

$k'_i, k'_j$  = capacity factors for i and j

$$= \frac{V_{N,i}}{V_M}, \frac{V_{N,j}}{V_M} \quad (1)$$

$W_i, W_j$  = band width of eluted peaks i and j  
in mL

$H$  = height equivalent to a theoretical plate in cm

$L$  = column length in cm

$N$  = number of theoretical plates in the column

$$= \frac{L}{H} = 16 \left( \frac{V_{R,j}}{W_j} \right)^2 \quad (2)$$

$\alpha_{j,i}$  = separation factor for j and i

$$= \frac{V_{N,j}}{V_{N,i}} \quad (3)$$

$R_S$  = resolution between i and j

$$\begin{aligned} &= \frac{2(V_{N,j} - V_{N,i})}{W_j + W_i} \\ &\approx \frac{\sqrt{N}}{4} \left( \frac{\alpha_{j/i} - 1}{\alpha_{j/i}} \right) \left( \frac{k'_j}{1 + k'_j} \right) \end{aligned} \quad (4)$$

Equation 2 implies that the plate height  $H$  is independent of the sample component whose peak is used to calculate  $N$ , which is only approximately true.



Also the right hand form of equation 4 assumes that the retention volumes for peaks  $i$  and  $j$  are not too different, so that their widths may be considered approximately equal (67).

Figures 2, 3 and 4 and Equations 1 - 4 are used as follows. If columns are packed with resin in a reproducible manner, then the column void volume  $V_M$  and the retention volume  $V_R$  are both directly proportional to the amount of packing in the column, and the values in Figures 2, 3 or 4 can be adjusted to apply to any column size. In order to select a mobile phase which gives baseline resolution ( $R_S = 1.5$ ) between the first retained component and any unretained components (including "solvent peaks"), first calculate the number of theoretical plates,  $N$  (68).

The 15 cm x 0.28 cm column used for syrup analyses exhibited plate heights ( $H$ ) between 0.1 and 0.2 cm for a variety of methanol-water compositions at linear velocities between 0.14 and 0.4 cm/sec (0.4 and 1.1 ml/min). Thus  $N \approx 100$  plates for this column. Peak width for an unretained component  $W_u$  is calculated as 0.28 mL by using equation 2 and the measured value of  $V_M = 0.70$  mL. Assuming that the first retained component has a similar width when it is just baseline resolved from the unretained peak, then the minimum allowable net retention volume for the first retained



component is calculated as 0.42 mL from the expression

$$R_S = 1.5 \approx \frac{V_R - V_M}{0.28} \quad (5)$$

From Figure 2, 3 or 4 it is possible to find the mobile phase compositions which give  $V_N=0.42$  mL for the first retained component. This requirement places an upper limit on solvent strength. The next step is to choose a solvent composition, whose strength is not greater than this maximum, that will yield adequate resolution between sample components  $i$  and  $j$ . Since  $N$  is known for the column, equation 4 can be used to predict the minimum  $\alpha_{j/i}$  required to achieve the desired resolution.

An example using the methanol/water data from Figure 2 will illustrate the approach: In order to separate the first retained component (exemplified by dextromethorphan No. 21) from the unretained component, a mobile phase composition which gives  $V_N \geq 0.42$  mL must contain not less than 25% water in an acidic mobile phase is used (Figure 2D) in order to achieve baseline resolution. This condition is fulfilled by all methanol/water mobile phase compositions containing ammonia (Figure 2B). In order to separate dextromethorphan (No. 21) from promethazine (No. 19) with a resolution  $R_S = 1.0$  (i.e., about 2% mutual overlap of similar size peaks) one would select a mobile phase



that will elute the more strongly retained promethazine with  $k'_j$  between 5 and 10. Using equation (1) and the measured value of  $V_M = 0.70$  mL, it is evident that  $V_{N,j}$  should be about 3.5 mL ( $\log V_{N,j} = 0.54$ ) in order to have  $k'_j = 5$ . Either 0.010 M  $\text{NH}_3$  in 2% water or 0.10 M HCl in 38% water would be satisfactory. (At intermediate mobile phase pH's intermediate methanol-water composition is appropriate, Section 3.5.) From equation 4 the value of  $\alpha_{j/i}$  necessary to produce  $R_S = 1.0$  is 1.9 ( $\log \alpha_{j/i} = 0.28$ ). This corresponds in Figure 2 to a vertical distance between the lines for compounds 19 and 21 of 0.28. The observed distance in the ammoniacal solvent is 0.12 and in the acidic solvent it is 0.28. Hence  $R_S = 1.0$  separation can be achieved in this case by chromatographing the cationic form of the drugs but not by chromatography of the free bases. Since  $R_S$  is proportional to  $N$  it would require a 34 cm column to achieve  $R_S = 1.0$  with the ammoniacal mobile phase.

### 3.5 Influence of pH on Retention

The effect of pH on the retention of the compounds listed in Table II will be examined in more detail.

3.5.1 Phenols and Carboxylic Acids (compounds 25 - 29) are weak acids. Their retention on XAD-2 is

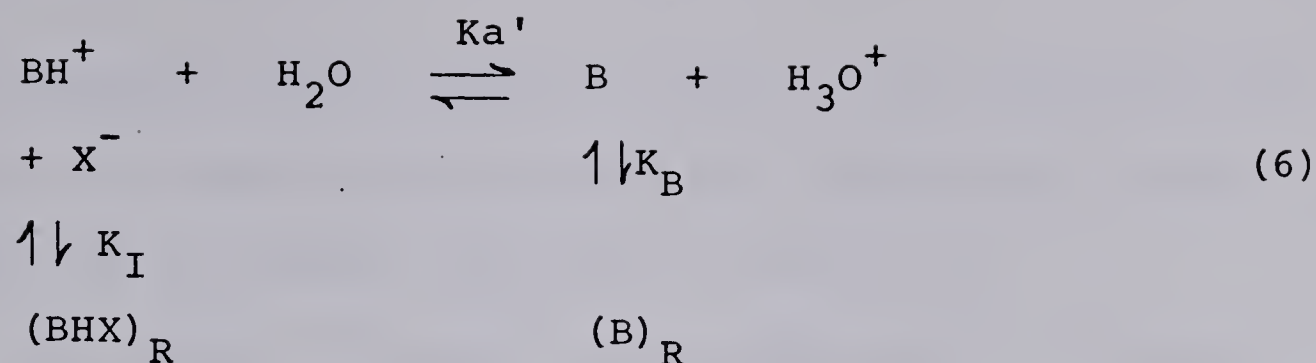


affected by the pH of the mobile phase. Adsorption of this type of compound is relatively high and constant at low pH's (where the neutral species predominates) and is low at a pH exceeding the  $pK_a$  of the drug (where it exists mainly as the anionic species). Because of the anticipated low retention of compounds 25 - 29 in an ammoniacal mobile phase, they were studied only in neutral and/or acidic mobile phases (Figures 2, 3 and 4).

Pietrzyk et al. (52-54,69) have studied the retention behavior of organic acids on Amberlite XAD-2 as a function of pH. They have reported the distribution coefficients for a series of nitro- and chloro-phenols (69) and chlorinated phenoxyacetic acids (52) as a function of pH. Also studied was the retention behavior of phenol, carboxylic acid derivatives and p-substituted benzenesulfonic acid derivatives (52,53). An expression for capacity factors was derived for both mono- and diprotic acids, in terms of pH and other equilibria in that system (54).

3.5.2 Monobasic Amines (compounds 9 - 21) are retained on XAD-2 as both the ionic acid and the neutral conjugate free base. The equilibria can be represented as:





where the subscript R refers to the resin phase and  $\text{X}^-$  is the conjugate base of a strong acid (e.g.  $\text{Cl}^-$ ) which is added in great excess. The constants are defined in Appendix IIA. When the pH of the mobile phase is low, essentially the only amine species is the protonated form  $\text{BH}^+$ . The  $\text{BH}^+$  species is adsorbed by XAD-2 in the presence of  $\text{X}^-$  in the mobile phase (Figure 2C and 2D).

As the pH of the mobile phase is increased, increasing amounts of the free amine, B, are adsorbed. The distribution ratio, D, can be expressed in terms of the total amine concentration, C, in each phase and solved for the independent variable  $a_{\text{H}}^*$ . Details of the derivation are given in Appendix II.

$$D = \frac{[\text{C}]_R}{[\text{C}]} = \frac{K'_a \cdot K_B + K_I \cdot a_{\text{H}}^*}{K'_a + a_{\text{H}}^*} \quad (7)$$

where  $K'_a = \frac{[\text{B}] \cdot a_{\text{H}}^*}{[\text{BH}^+]}$

$$K_B = \frac{[\text{B}]_R}{[\text{B}]}$$

$$K_I = \frac{[\text{BHX}]_R}{[\text{BH}]}$$

and  $a_{\text{H}}^*$  is defined in the next paragraph.



This equation can be used to calculate the distribution ratio as a function of pH from the experimental value of  $K_B$  and  $K_I$  and the ionization constant  $K'_a$ .

The values of  $K_B$  and  $K_I$  are obtained as follows: In the region where  $pH \gg pK'_a$ , the distribution ratio is approximately equal to  $K_B$ . In regions where  $pH \ll pK'_a$ ,  $(a_H^*/K_a)$  is much greater than unity and the distribution ratio is approximately equal to  $K_I$ .

The chromatographic retention of promethazine was studied as a function of mobile phase  $pa_H^*$  to illustrate the behavior of monobasic amines. Promethazine.HCl was chromatographed on a 15 cm x 0.28 cm column of XAD-2 using 10% water/methanol eluent solution at  $pa_H^*$ 's of 1.55, 4.5, 7.0, 7.95, 8.75, 10.55, 11.75 and 12.85. Here  $pa_H^*$  is the negative log of the hydrogen ion activity referred to the standard state in the mixed solvent (75), given by:

$$pa_H^* = pH - \delta \quad (8)$$

$pH$  is the experimental (meter) value and  $\delta = \bar{E}_j - \log_m \gamma_H$ , where  $\bar{E}_j$  is the liquid junction potential and  $\log_m \gamma_H$  is the transfer activity coefficient of the hydrogen ion.  $\delta$  is constant for a medium of given composition (75).

The value of  $pa_H^*$  is calculated by substituting into equation 8 the tabulated  $\delta$  correction values (75) and the pH meter reading furnished by a pH meter standardized



with aqueous buffer solution. Weight percent methanol in solution was calculated from volume percent methanol using published data (76).

The experimental values of  $K_I$  and  $K_B$  were measured in the manner discussed above, as  $K_I = 1.2$ ,  $K_B = 40$ . The  $pK'_a$  value for promethazine.HCl was determined potentiometrically in 10% water/methanol (70). The following relationship applies to the titration with sodium hydroxide:

$$pa_H^* = pK'_a + \log \left( \frac{n_{NaOH}}{n_X - n_{NaOH}} \right) \quad (9)$$

where  $n_{NaOH}$  is the number of moles of titrant added,  $n_X$  is the number of moles of promethazine. Plotting  $pa_H^*$  vs.  $\log (n_{NaOH}/n_X - n_{NaOH})$  (Figure 5) gives an intercept equal to  $pK'_a$ . It was  $7.8 \pm 0.07$  ( $pK_a = 9.0$  in aqueous solution (30)). The distribution ratio,  $D$ , is related to  $V_N$  by the expression:

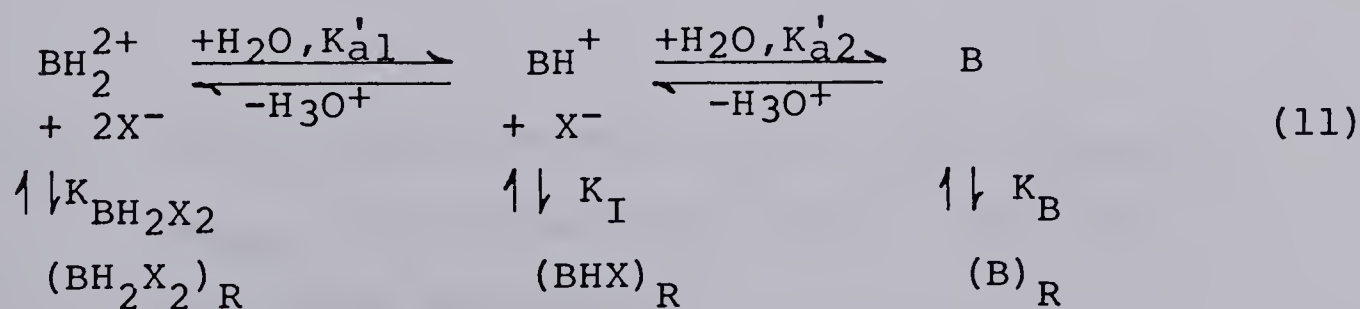
$$V_N = D \cdot W_S \quad (10)$$

where  $W_S$  is the weight of resin in the column (0.25 g).



The chromatographic behavior of promethazine.HCl is presented in Figure 6 as a plot of the distribution ratio (D) vs.  $\text{pa}_\text{H}^*$  in 10% water/methanol. There is good agreement between experimental (points) and calculated line, using equation 7. The major change in D with  $\text{pa}_\text{H}^*$  occurs in the region of  $\text{pK}_\text{a}$  for promethazine.HCl. At this point, a slight increase in the  $\text{pa}_\text{H}^*$  converts a large percentage of  $\text{BH}^+$  species, which is weakly adsorbed, to the neutral form B, which is highly adsorbed. Similar behavior was obtained for weak monobasic amine by Pietrzyk's group (51-54).

3.5.3 Dibasic Amines (compounds 1 - 8) may be adsorbed on XAD-2 in all three conjugate forms, viz.  $\text{BH}_2^{2+}$ ,  $\text{BH}^+$  and B, with the most highly charged species being least strongly adsorbed. The equilibria are:





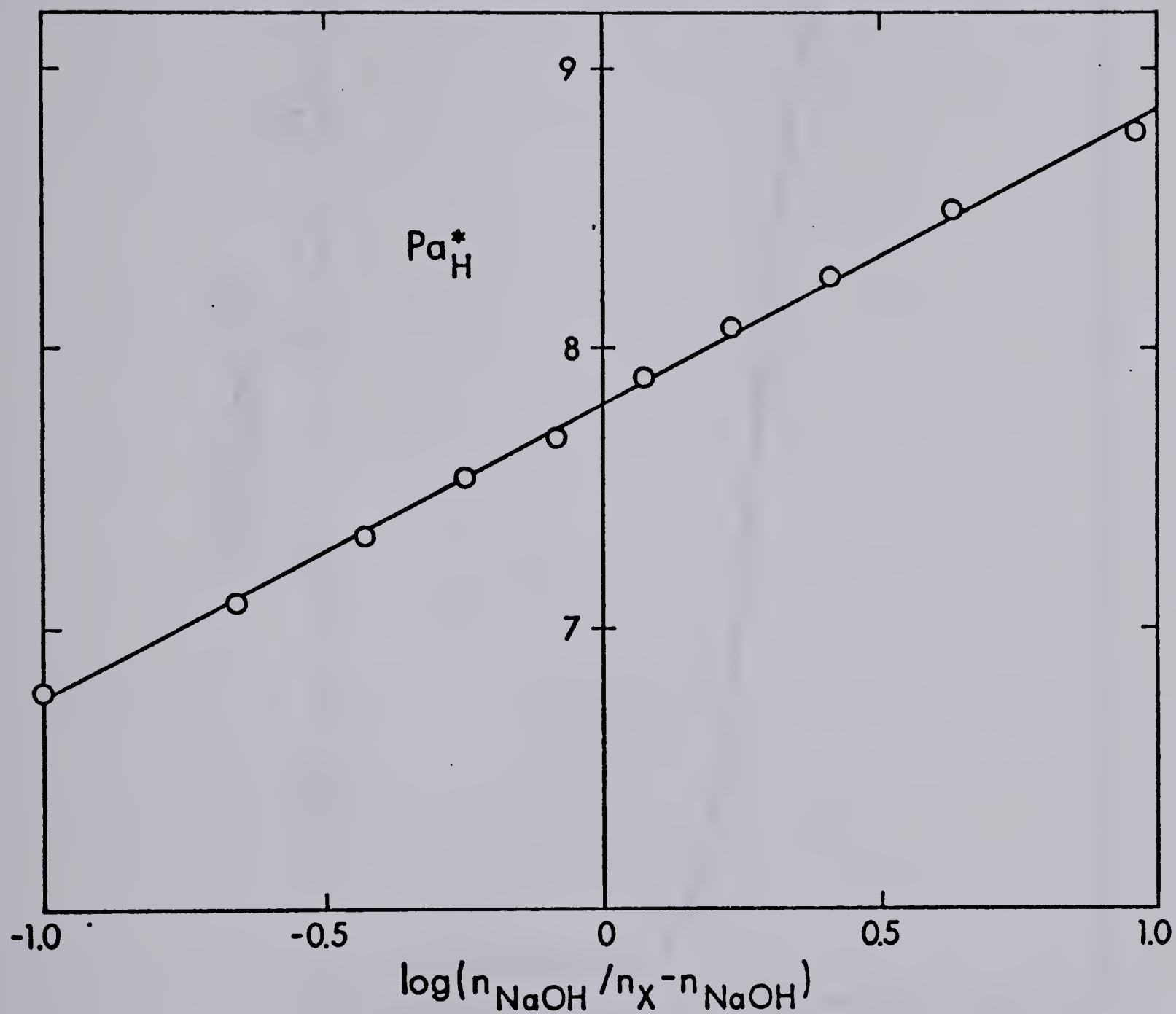


FIGURE 5. Relationship between  $p_{aH}^*$  and  $\log (n_{NaOH}/n_X - n_{NaOH})$  for promethazine.HCl. The line is the least squares fit.



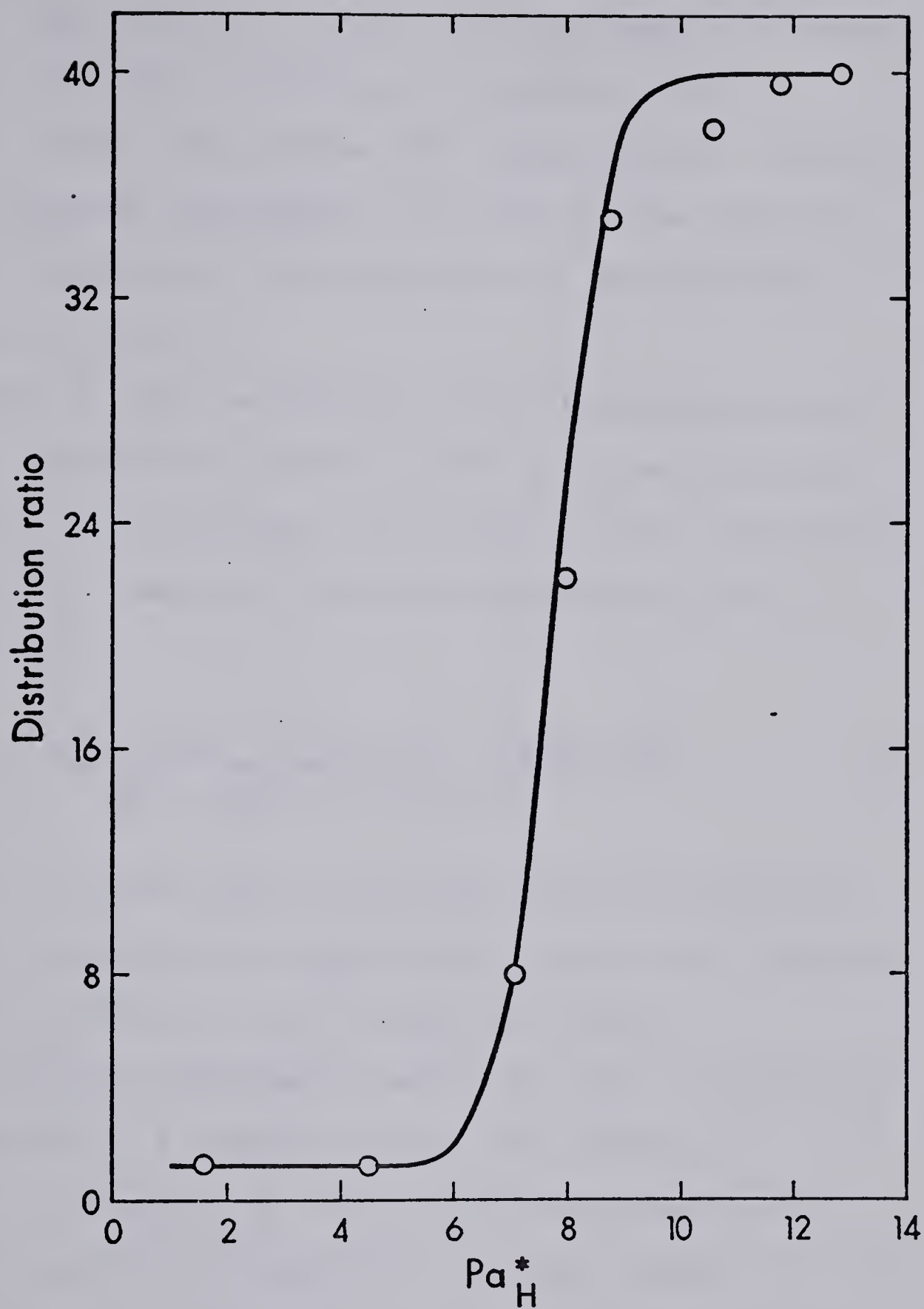


FIGURE 6. Relationship between the distribution ratio and  $p^*_{aH}$  for promethazine.HCl in 10% water/methanol, on a 15 cm x 0.28 cm column of Amberlite XAD-2. The line is calculated from equation 7 and points are experimental.  $K_B = 40$ ,  $K_I = 1.2$ ,  $pK'_a = 7.80$ .



where  $X^-$  and subscript R have the same meaning as above and the constants are defined in Appendix IIB.

At low pH, the species  $BH_2^{2+}$  predominates. As the pH is increased the species  $BH^+$  and B become more predominant in turn and the adsorption of the compound increases (Figure 6).

From the above equilibria, the distribution ratio D can be expressed in terms of the total amine concentration, C, in each phase and solved for the independent variable  $a_H^*$ . Details of the derivation are given in Appendix IIB.

$$D = \frac{K_B \cdot K'_{a1} \cdot K'_{a2} + K_I \cdot K'_{a1} a_H^* + K_{BH_2X_2} a_H^{*2}}{a_H^{*2} + K'_{a1} \cdot a_H^* + K'_{a1} \cdot K'_{a2}} \quad (12)$$

Equation 12 can be used to calculate the distribution ratio as a function of  $pa_H^*$  once the ionization constants and the distribution coefficients are known.

A study of pheniramine was performed to illustrate the behavior of a dibasic amine. The values of  $K_{BH_2X_2}$  ( $= 0$ ) and  $K_B$  ( $= 71.2$ ) were determined from the flat portions of the plot D vs.  $pa_H^*$  (Figure 7) at low and high  $pa_H^*$  in a manner analogous to that used to obtain  $K_I$  and  $K_B$  in section 3.5.2 above. The value of  $K_I$  ( $= 1.0$ ) was obtained by using Equation 12 as follows: The net retention volume measured at pH = 5.5 was converted to the corresponding value of D using



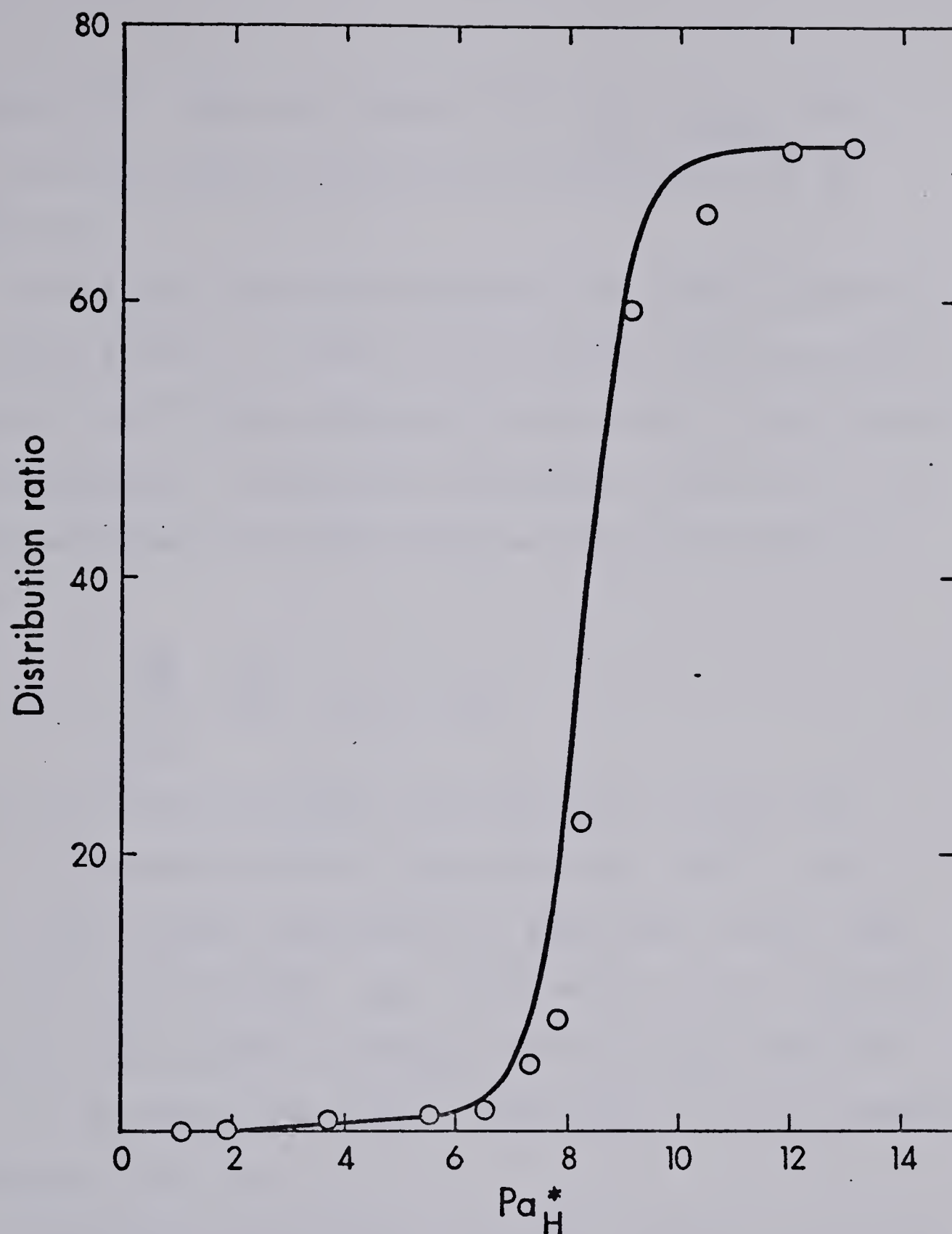


FIGURE 7. Relationship between the distribution ratio and  $p_{aH}^*$  for pheniramine maleate in 30% water, on a 15 cm x 0.28 cm column of Amberlite XAD-2. The line is calculated from Equation 12, points are experimental.

$$K_{BH_2X_2} = 0, K_I = 1.0, K_B = 71.2, pK'_{a1} = 3.03, \\ pK'_{a2} = 8.27.$$



Equation 10. Then the values of  $D$ ,  $K_B$ ,  $K_{BH_2X_2}$ ,  $a_H^*$ ,  $K'_{a,1}$  and  $K'_{a,2}$  were substituted into Equation 12 to obtain  $K_I$ .

The first ionization constant was measured photometrically (70). A set of seven buffer solutions were prepared in 30% water/methanol containing a known amount of pheniramine. Using the absorbance at 262 nm of all seven solutions, the following equation was applied (70):

$$A_2 = \frac{a_H^*}{K_{a,1}} (A_2^{II} - A_2) + A_2^I \quad (13)$$

where  $A_2$  is the observed absorbance at a given pH,  $A_2^{II}$  is the absorbance of pure dication ( $BH_2^{2+}$ ), and  $A_2^I$  is the unknown absorbance of pure mono-cation ( $BH^+$ ). Plotting  $A_2$  vs  $a_H^*(A_2^{II} - A_2)$  (Figure 8) gives a straight line of slope equal to  $1/K_{a,1}$  and intercept equal to  $A_2^I$ . It is found that  $pK'_{a1} = 3.03$  ( $pK_{a1} = 4.2$  in aqueous solution, ref. 30).

The second ionization constant, measured potentiometrically as discussed in Section 3.5.2, was  $pK'_{a2} = 8.27$  ( $pK_{a2} = 9.3$  in aqueous solution, ref. 30).

The dependence of  $D$  on  $pa_H^*$  for the compound pheniramine is shown in Figure 7 in 30% water/methanol. The line is calculated from equation 12 and the points are experimental. The steeply rising theoretical line in the vicinity of  $pK'_{a,2}$  occurs a few tenths of a  $pa_H^*$  unit below the experimental points. The reason



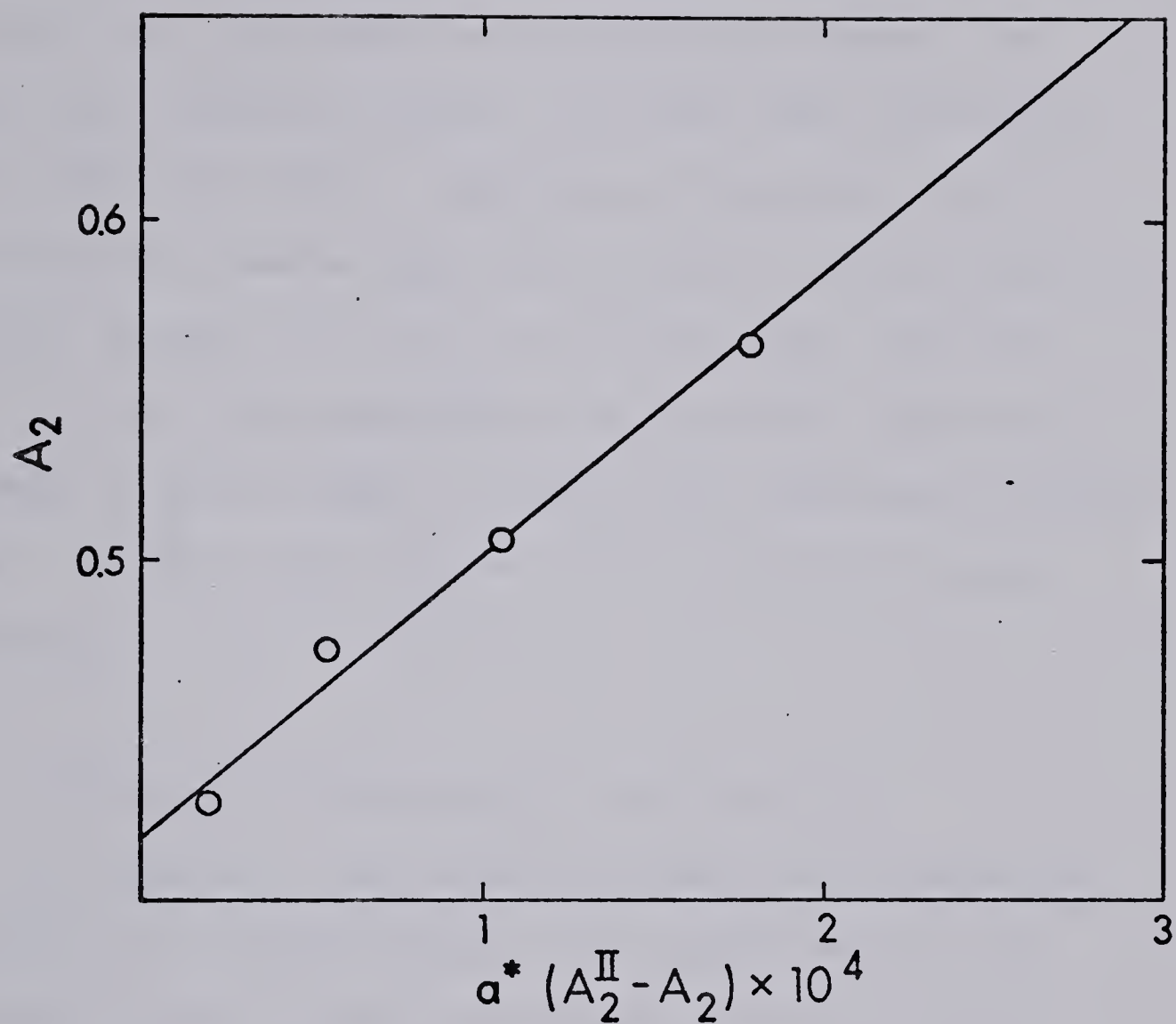


FIGURE 8. Relationship between  $A_2$  and  $a_H^* (A_2^{\text{II}} - A_2)$  for pheniramine maleate. The line is the least squares fit.



for this discrepancy is not known but it is relatively minor.

Mobile phase pH can be used as a variable to improve chromatographic resolution of compounds which are not well separated as the fully protonated and fully deprotonated species, provided that compounds have different pKa's. Equations 10 and 12, and for the monobasic amine equation 10 and 7, can be used to predict values of  $D$  or  $V_N$  at various pH. From the  $V_N$ 's for any two compounds at a given pH, equations 1 through 4 can be used to predict the resolution between them. In this way, optimum mobile phase pH can be selected.

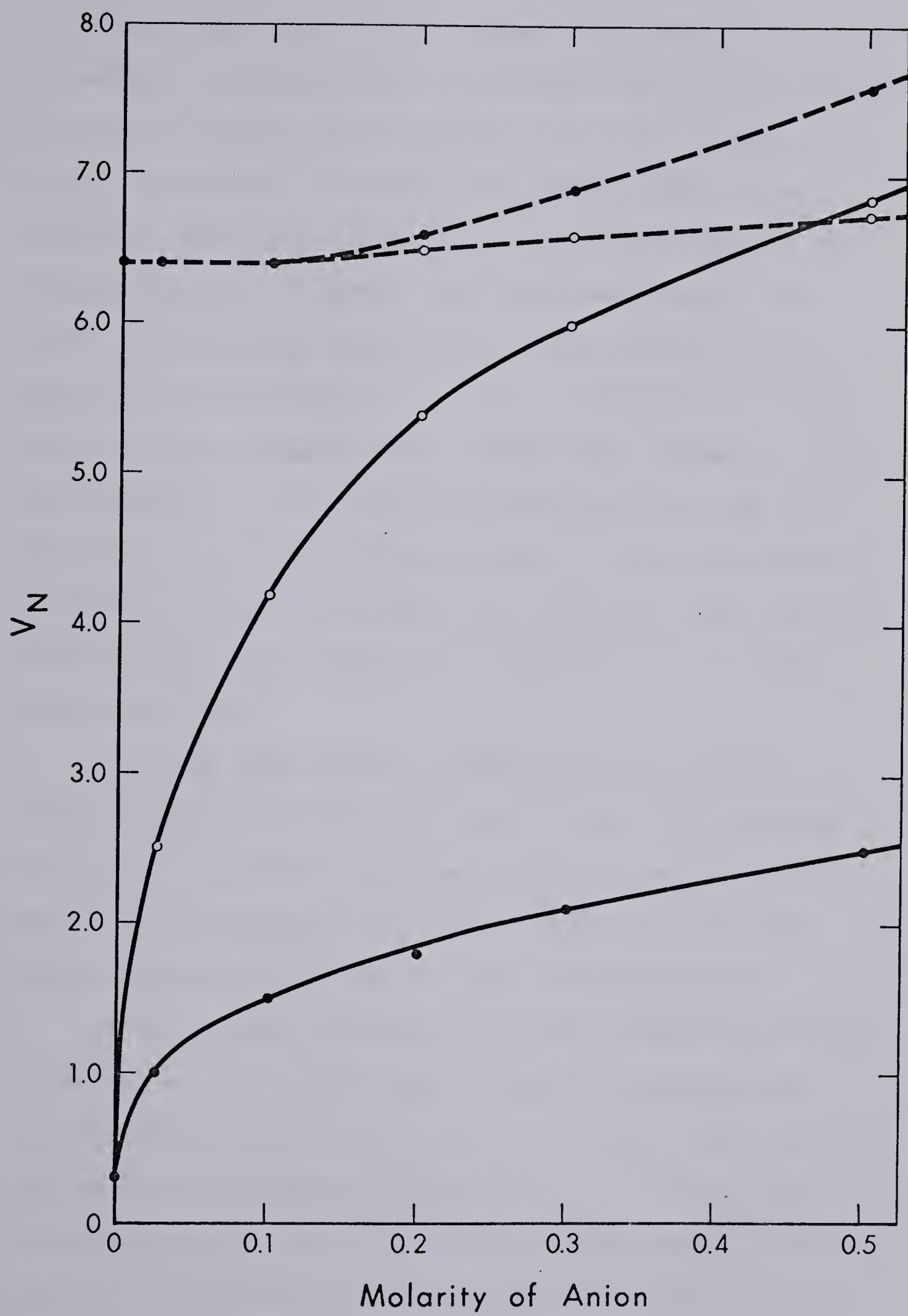
### 3.6 Influence of Electrolyte on Retention

In Figure 9, the adjusted retention volumes for phenylephrine hydrochloride and acetaminophen are plotted against anion concentration in the mobile phase for the anions chloride and perchlorate. The relatively small increase in  $V_N$  for acetaminophen above 0.1 M  $\text{Cl}^-$  is a "salting-out" effect (69,71). It is less pronounced for  $\text{ClO}_4^-$ . In contrast to the slight influence of salt concentration on the retention of the neutral species, acetaminophen, it has a profound effect on the retention of the cation phenylephrine. Furthermore,  $\text{ClO}_4^-$  has a significantly greater effect





FIGURE 9. Dependence of  $V_N$  for acetaminophen (---) and phenylephrine (—) on concentration of chloride (●) and perchlorate (o) on a 15 cm x 0.28 cm column of Amberlite XAD-2. Mobile phase contains no organic solvent.





than  $\text{Cl}^-$ .

There are similarities between the retention behavior of cations (exemplified by phenylephrine) in this system and in a liquid-liquid ion-pair partition system (33). First, the marked increase in  $V_N$  with anion concentration, though non-linear in the present system, is common to both. Second, the effectiveness of the anion in promoting adsorption of the organic cation improves in the order  $\text{Cl}^- < \text{ClO}_4^-$ . (Experiments with other organic cations and a wider range of anions show the order  $\text{Cl}^- < \text{Br}^- < \text{ClO}_4^- < \text{d-camphorsulfonate}$  (74)). However, a detailed investigation of the mechanism of sorption of cations on XAD-2 has revealed that ion-pair formation is not involved, at least when  $\text{Cl}^-$  is the counterion (63).

In other experiments, adsorption of organic anions (exemplified by the propyl ester of p-hydroxybenzoate) onto XAD-2 increases with concentration of NaCl, and adsorption is greater from KCl solutions than from NaCl solutions of equal concentration.

It is evident that not only the concentration but also the nature of the inert electrolyte dissolved in the mobile phase can be used to control retention volumes and separation factors ( $\alpha_{j/i}$ ). Use of the data in Figure 9 to optimize the chromatographic determination of a mixture of phenylephrine hydrochloride



and acetaminophen will be described in Section 3.8.1 below.

### 3.7 Retention of Inert Ingredients

When the soluble azosulfonate dyes used to color syrups are injected onto an XAD-2 column the elution peaks occur at the void volume of the system but "tailing" of the peaks is severe. The presence of this dye on the resin causes a very large increase in the retention volumes of the cationic drug species (56). Most likely the strong sorption of azosulfonate dye results from the presence in the resin of a very small number of cationic functional groups which serve as anion exchange sites. These may be amine groups in the resin which are protonated in acid mobile phases. In support of this view is the observation that a 1.5 M ammonia solution in 50% methanol readily eluted most of the sorbed dye from the column (56). This view may also explain the observation of Zaika (50) that after passage of sodium hydroxide solution through an XAD-2 column, some of the hydroxide was "difficult" to wash out.

If this explanation of the strong sorption of dye is correct, then the marked increase in the retention time of the cationic drug species may be understood to be due to cation exchange of the drug cation on the



anionic sorbed dye. Most of the azosulfonate dyes used have at least two sulfonate functional groups. If the dye sorbed onto widely spaced cationic resin sites via one sulfonate group, the other sulfonate groups on the dye ion are available to interact with the cationic drug species (56).

In any event, it is desirable to prevent these dyes from entering the XAD-2 column. This can be done by placing a short pre-column of Amberlyst A-26 macroreticular anion exchange resin immediately downstream from the sample injection valve. The anionic dyes in the injected syrup are strongly sorbed on the ion exchanger and are therefore "stripped out" of the injected sample before it reaches the XAD-2. After 30 syrup injections, a 1-cm length of the ion exchanger showed no sign of dye breakthrough.

Any U.V. absorbing components which may be present in the common syrup ingredients sucrose, sorbitol and caramel coloring, elute nearly unretained from the XAD-2 column and present no interference in the analyses. Net retention volumes of the preservatives methyl and propyl p- hydroxybenzoate, of the flavor components vanillin, benzaldehyde and cinnamaldehyde, and of their decomposition products p-hydroxybenzoic acid, vanillic acid, benzoic acid and cinnamic acid can be estimated for any XAD-2 column with an



acidic, aqueous/methanol mobile phase from Figure 2 in reference (56) by multiplying the net retention volume from that figure by the ratio of the weight of resin in the two columns. Maleic acid from maleate salts of the drugs has  $k' \approx 1$  in a 100% water acidic mobile phase and is nearly unretained at higher methanol percentages. In an alkaline mobile phase all of these compounds except benzaldehyde and cinnamaldehyde exist as anions and are trapped on the anion exchange resin along with the azosulfonate dyes.

### 3.8 Analysis of Syrups

Application of the data in Figure 2 to the analysis of real syrups will be illustrated by three examples: determination of phenylephrine hydrochloride and acetaminophen; determination of glyceryl guaiacolate; and determination of dextromethorphan hydrobromide. In these analyses the analytical column  $C_2$  was a 15 cm x 0.28 cm column of XAD-2. The composition of Blank syrups and of Spiked Blank syrups is presented in the Experimental section above. In each case Blank syrup chromatograms showed straight base-lines in the region of interest. Quantification was based on comparison with standard curves obtained by injecting aqueous solutions of the analyte drug. Both peak height and peak area measurements yielded linear calibration



curves and similar syrup assay values. Relative standard deviations for replicate injections were about 1.4% for area measurements and 1.6% for height measurements. Assay values reported in Table III are the average of both height and area values. The three Spiked Blank syrups and eight commercial syrups, each containing two or more of the four drug compounds of interest, were analyzed. In Table III assay values are compared with the known amounts added to Spiked Blanks and with label claims of commercial syrups. Typical chromatograms of syrups are shown in Figure 10.

3.8.1. Phenylephrine and Acetaminophen. Using 0.10 M HCl in 100% water these two compounds are well resolved from one another ( $\Delta \log V_N = 0.8$ , Figure 2D). Of the twenty seven other drugs investigated all are well resolved from phenylephrine and only ephedrine and phenylpropanolamine might interfere with acetaminophen. At 275 nm, however, both of these potential interferents have sufficiently low molar absorptivities that they do not interfere with the acetaminophen peak. In 0.10 M HCl the resolution between phenylephrine and acetaminophen is actually too large so that when acetaminophen elutes with  $k' \approx 12$  phenylephrine has  $k' \approx 2$  and overlaps components such as maleic acid which are nearly unretained. Since phenylephrine is



TABLE III.

## Results of Syrup Analyses

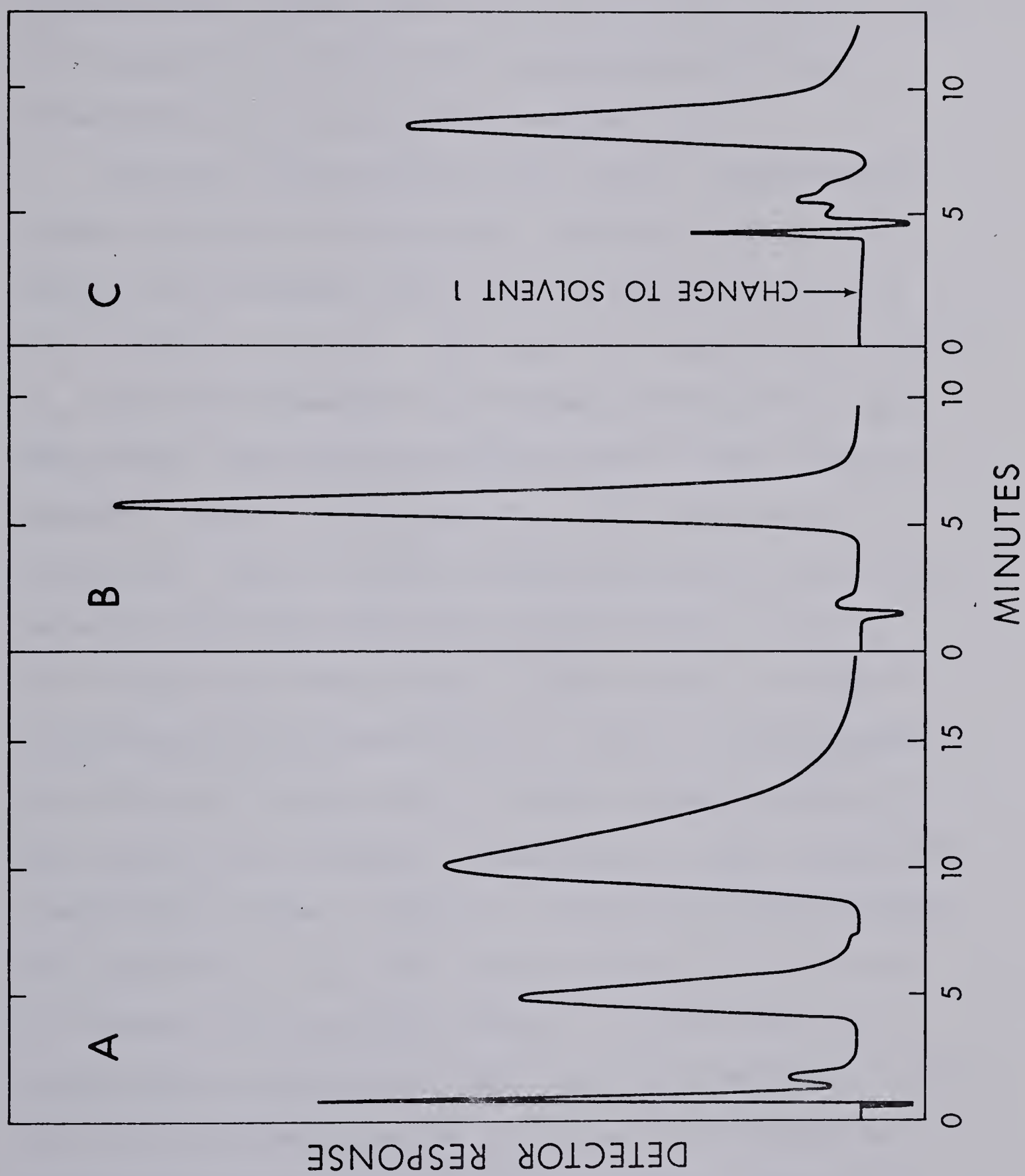
Product	Found mg/mL (Label Claim mg/mL)				Other Drugs Present
	Phenyl eph rine. HCl	Aceta- minophen	Glyceryl Guaia- colate	Dextro- methorphan. HBr	
Spiked Blank <sup>a</sup>	1.10(1.10)	20.4(20.3)	10.6(10.6)	2.49(2.50)	Table I
A	---	---	10.1(10.0)	1.91(2.00)	Phenylpropanolamine.HCl
B	0.46(0.50)	21.7(21.6)	10.1(10.0)	1.48(1.50)	---
C	2.04(2.00)	---	---	---	Diphenylpyraline.HCl
D	0.92(1.00)	---	19.8(20.0)	---	Phenylpropanolamine.HCl Brompheniramine Maleate
E	---	16.4(16.0)	---	---	Triprolidine.HCl Pseudoephedrine.HCl
F	---	---	20.1(20.0)	2.89(3.00)	Phenylpropanolamine.HCl Pheniramine Maleate Pyrilamine Maleate
G	---	---	---	2.80(3.00)	Diphenhydramine.HCl
H	0.4 <sub>3</sub> (1.00) <sup>b</sup>	---	---	0.94(1.00)	Carbinoxamine Maleate

<sup>a</sup>Amount in parentheses in this row is amount added to Spiked Blank.<sup>b</sup>Peak height data only.





FIGURE 10. Typical syrup chromatograms of phenyl-  
ephedrine.HCl (AUFS = 0.1,  $\lambda$  = 275 nm) and  
acetaminophen (AUFS = 1.0,  $\lambda$  = 275 nm)  
(A); glyceryl guaiacolate (AUFS = 1.0,  
 $\lambda$  = 275 nm) (B); and dextromethorphan.HBr  
(AUFS = 0.4,  $\lambda$  = 280 nm) (C), on a 15 cm  
column under the conditions described in  
the text. AUFS is the absorbance unit  
full scale.





retained via "salt-adsorption" while acetaminophen is adsorbed as a neutral species, it is possible to selectively increase the retention volume of the former by changing the nature and concentration of inert electrolyte as discussed in section 3.6.

For this determination the liquid chromatograph shown in Figure 1A was used. Solvent 1 was 0.030 M  $\text{HClO}_4$  in 100% water and Solvent 2 was 0.030 M  $\text{HClO}_4$  in 5% water/methanol. The upper one-third of pre-column  $C_1$  contained Amberlyst A-26 anion exchange resin and the lower two-thirds contained XAD-2. With Solvent 1 pumping through  $P_1$ ,  $C_1$  and  $C_2$  a 10  $\mu\text{L}$  sample was injected. After 6.0 min, when phenylephrine and acetaminophen had quantitatively eluted from  $C_1$  onto  $C_2$ , but before the other drugs, preservatives or flavor ingredients had eluted from  $C_1$ , valve  $V_1$  was switched and Solvent 2 washed all of these components from  $C_1$  to waste, while Solvent 1 continued to pass through the analytical column. After the elution of acetaminophen,  $V_1$  was switched back and another injection made after a 3-minute equilibration period. If the syrup contains drugs which elute right after acetaminophen (e.g. No. 1) then some fraction of them may be transferred onto column  $C_2$  along with acetaminophen. These are washed off by the "slug" of Solvent 2 from  $C_1$  which passes through  $C_2$  when valve  $V_1$  is switched back.



The recovery of both phenylephrine hydrochloride and acetaminophen in the Spiked Blank is quantitative (Table III). Label claim by manufacturer generally has a  $\pm 10\%$  tolerance. That is, the manufacturer is required to adjust the actual concentration of drug to within these limits of his label claim. Phenylephrine hydrochloride and acetaminophen are within label claim for all commercial syrups analyzed except syrup "H" (Table III).

The phenylephrine·HCl content of Syrup "H" is well below label claim and the phenylephrine chromatographic peak for this sample is overlapped by another peak with a longer retention time. A similar peak appears in chromatograms of aerated alkaline solutions of phenylephrine·HCl that have been stored at elevated temperature and is accompanied by a decrease in the phenylephrine peak. This presumed decomposition product can be resolved from phenylephrine on a 30 cm column of XAD-2 using as mobile phase 0.010 M  $\text{HClO}_4$  plus 0.10 M  $\text{NaClO}_4$ .

3.8.2 Glyceryl Guaiacolate. In an alkaline mobile phase glyceryl guaiacolate is well resolved from all twenty-eight other drugs studied except caffeine and phenylpropanolamine (Figure 2A and B). The former is not present in commercial syrups along with glyceryl



guaiacolate and the latter has such a low molar absorptivity at 275 nm that it shows negligible absorbance at the detector sensitivity employed. The chromatograph for this determination was identical to that used for phenylephrine and acetaminophen except that Solvent 1 was 0.010 M NaOH in 50% water/methanol, Solvent 2 was 0.010 M NaOH in 5% water/methanol and column  $C_1$  contained 2.0 cm of anion exchange resin followed by 1.0 cm of XAD-2.

With Solvent 1 flowing through  $P_1$ ,  $C_1$  and  $C_2$ , a 2- $\mu$ L syrup sample was injected. After 2.5 min the glyceryl guaiacolate had all been eluted from column  $C_1$  onto  $C_2$  and valve  $V_1$  was then switched to allow Solvent 2 to wash off the syrup components that were retained on  $C_1$ , while glyceryl guaiacolate continues to move down the analytical column,  $C_2$ . With Solvent 1 as mobile phase all of the preservatives, flavor ingredients and their decomposition products except benzaldehyde and cinnamaldehyde were trapped on the anion exchange resin, while the latter two compounds were retained on the XAD-2 resin in Column  $C_1$  along with the other drug components and subsequently washed off to waste by Solvent 2.

Recovery of glyceryl guaiacolate in the Spiked Blank is quantitative, and it is well within the label claim tolerance for the commercial syrups (Table III).



3.8.3 Dextromethorphan Hydrobromide. This compound is the major non-narcotic cough suppressant used in syrups. With 0.10 M HCl in 35% water/methanol as mobile phase the only unresolved drugs, of those which are found in combination with dextromethorphan, are diphenylhydramine hydrochloride and diphenylpyraline hydrochloride. At 280 nm both of these compounds absorb too weakly to interfere with dextromethorphan. The chromatograph used for this determination is shown in Figure 1B. Pre-column  $C_1$  contained 3 cm XAD-2 while pre-column  $C_3$  contained 2 cm of anion exchange resin. Solvent 1 was 0.10 M HCl in 35% water/methanol and Solvent 2 was 0.010 M NaOH in 35% water/methanol. Before injecting the sample, valve  $V_1$  was set to allow Solvent 2 to pump through  $V_2$ ,  $C_3$  and  $C_1$  to waste, while Solvent 1 passed through the analytical column only. When a 10  $\mu$ L sample was injected all of the components which are anions in an alkaline solution were trapped on the anion exchange resin while dextromethorphan was adsorbed on pre-column  $C_1$ . Weakly retained compounds like the drugs acetaminophen, glyceryl guaiacolate and codeine and the flavor components benzaldehyde and cinnamaldehyde elute from  $C_1$  to waste during this time. After 2.5 minutes  $V_1$  was switched to allow Solvent 1 to pass through pre-column  $C_1$  eluting dextromethorphan through both  $C_1$  and  $C_2$ . Compounds such as meth-



dilazine and promethazine which are adsorbed onto  $C_1$  from an alkaline solvent elute from  $C_2$  either before or after dextromethorphan. After a total of 12 min, valve  $V_1$  is switched back to its original position and the next injection is made after a short equilibration period.

Again, the recovery was quantitative for the Spiked Blank (Table III), and all of the commercial samples are within label claim tolerance.

It is important to remember that the determinations of phenylephrine.HCl and acetaminophen, of glyceryl guaiacolate, and of dextromethorphan.HBr reported for the Spiked Blank are obtained on a sample which contains all of the ingredients listed in Table I. Likewise, the syrups A through H are real commercial products which contain large numbers of the dyes, excipients, flavors and other components listed in Table I, along with the "Other Drugs Present" which are noted in Table III. Thus the chromatographic methods described here are quite specific.



## CHAPTER 4

### CONCLUSIONS

Using pre-columns of XAD-2 and anion exchange resin in conjunction with the analytical column allows drugs to be determined in cough-cold syrups by direct injection without sample pretreatment. In this study drugs were chromatographed as both their neutral and ionic conjugate species which permitted the control of retention volume and resolution by choice not only of nature and concentration of organic solvent in the aqueous mobile phase, but also of pH and nature and concentration of counterion in the mobile phase. The later two variables have been shown to have a profound effect on retention volumes of charged species. Another study in this laboratory (63) has shown that large organic coions (i.e., ions with the same charge sign as the sample ion) can also have a profound effect on sample retention. Thus, there are at least five mobile phase variables, excluding temperature, which can be used to control retention and resolution of drugs on columns of XAD-2.

High efficiency XAD-2 columns have been obtained by making small (5 - 10  $\mu\text{m}$ ) particles through grinding and elutriation (73). Such columns yield a plate height  $\approx 0.05$  mm, which is comparable to those of commercial bonded phases. High efficiency, compata-



bility with all pH, long column life and low cost of such columns make them an attractive alternative to both low efficiency liquid-liquid partition systems (29,30) and high efficiency bonded phases for many applications.

Finally, it is obvious from the principles outlined in the discussion and from the data in Figures 2 - 4 that separation factors for many drug pairs are large enough that quantitative separation can be achieved on very short columns with low pressures or gravity flow (56,68). This is a potentially attractive feature for small laboratories operating on a low budget.



## CHAPTER 5

### FURTHER WORK

(a) This work is being extended to the analysis of drugs in body fluids (blood and urine) on high efficiency columns of XAD-2, using pre-columns for clean-up. The use of pre-columns and solvent switching valves will eliminate the need for preliminary concentration and clean-up steps prior to injection.

(b) Higher column efficiencies can be obtained by using microparticulate resin with a narrow particle size range and preferably with spherical shape. Efforts should be made to obtain XAD-2-like materials which fulfill these requirements.



## PART II

### TWO-PHASE PHOTOMETRIC TITRATIONS FOR THE DETERMINATION OF DRUGS AND OTHER SUBSTANCES



## CHAPTER 1

### INTRODUCTION

Photometric titrations are performed by measuring the absorbance of a sample solution as a function of amount of titrant added. In general, either the reactant, the product, or the titrant may be light-absorbing, or any combination of these may be light-absorbing. Photometric titrations based on acid-base, redox, precipitation and complex formation reactions have been described. The theoretical as well as practical aspects of photometric titrations have been reviewed (78-80). In part II of this thesis two-phase photometric titrations based on both acid-base reactions and ion-pair reactions are reported.

Any method for the determination of weak acids in aqueous solution is limited in its scope by two fundamental requirements: The substance to be determined must be appreciably stronger than water as an acid, and the concentration must be appreciably larger than the concentration of hydrogen ions from the water. In order to overcome the above limitations, titrations in a solvent other than water have been investigated. Nonaqueous solvents with small autoprotolysis constants, or nonpolar solvents have been used widely (81,82). Titrations in mixed aqueous-organic solvents and aqueous solvents containing a high concentration of neutral



electrolyte have also been investigated (83).

Heterogeneous titrations, in which acids and bases are titrated in a well-stirred aqueous solution in the presence of a second phase, have been described for systems in which the second phase is either an ion exchange resin (84-86), a nonionic resin (72,74) or an immiscible organic solvent (87,88-92). In these titrations, one or more species from the acid-base equilibrium is removed from the aqueous to the second phase. This process can be expressed as a phase distribution equilibrium. If the phase distribution favors the product of an acid-base titration then, according to Le Chatelier's principle, the acid-base equilibrium will shift to the right (product side). The net effect in a titration is that the compound titrates as though it were a stronger acid or base. On the other hand, if the phase distribution involves a reactant from the acid-base equilibrium, the compound titrates as a weaker acid or base.

Cantwell and Pietrzyk (84-86) studied the potentiometric and photometric titration of weak bases with hydrochloric acid in an aqueous slurry of cation exchange resin and found that the resulting titration could be quantitatively described in terms of the aqueous phase acid-base equilibria and the phase distribution equilibria of the conjugate acid-base species of the sample.



Puon and Cantwell (72,74) described the potentiometric titration of weak acids with sodium hydroxide in the presence of Amberlite XAD-2 nonionic resin. In that study theoretical titration equations were derived and verified experimentally for several different charge type acids.

Dyrssen (88) employed potentiometric titrations in a two phase aqueous organic solvent mixture in order to evaluate high distribution coefficients of acids. Christiansen (89) and Davis and Kreutler (90) have used the same technique for evaluating distribution coefficients of acids and bases of charge type HA and B. Ratajewics and Ratajewics (91) studied potentiometric titrations of sparingly soluble diprotic bases in a two liquid phase system and the result was used to determine the dissociation constants of the bases. Komar (92) has derived an expression for the differentiating effect resulting from phase distribution when titrating a mixture of two acids of the charge type HA in an immiscible aqueous-organic solvent system.

Another class of chemical reaction, which has been used for two phase photometric titrations, is complex formation. Galik et al. (93-96) have titrated metal ions with ligands such as dithizone. The titration is performed in an aqueous-carbon tetrachloride medium



and the resulting neutral metal-ligand complex extracts into the organic phase. After the addition of each increment of ligand titrant and agitation, the bulk phases are allowed to separate and the absorbance of the organic phase is measured. Titration equations have been derived for these titrations (97) and the subject has been reviewed (80,98).

The formation of extractable ion-pairs is a type of complex forming reaction which has found extensive use in the analysis of ionic surfactants by two-phase titration. High molecular weight quaternary ammonium cations are used to titrate anionic surfactants in water in the presence of an immiscible organic solvent (99-101). The resulting ion-pair is extracted into the organic phase. In the reverse process a high molecular weight anionic surfactant is used as titrant for a cationic surfactant analyte (102-105). In these titrations a cationic or anionic dye which has been added to the solution transfers from one phase into the other in the presence of a slight excess of titrant, making possible visual detection of the end point.

Anionic surfactants have also been used to titrate the ammonium form of amine drugs in a two-phase system. Here again the resultant ion-pair extracts from the aqueous into the organic phase and a cationic dye undergoes a color change at the endpoint when it forms



an extractable ion-pair with the first excess of titrant (106). In a related approach anionic dyes such as bromthymol blue have been used as titrants for the ammonium form of drugs (107). The drug-dye ion-pair extracts into the organic phase and the endpoint is indicated by the appearance of the color of the first excess of titrant in the aqueous phase.

Behrends (108) has derived the photometric titration equation for a two-phase ion-pair titration of a non-absorbing ion such as tetraphenylarsonium with an absorbing titrant such as permanganate, in which the absorbance of one of the phases is monitored. In the derivation the titrant and analyte ions were assumed to undergo no side reactions which would change their charge. He has also derived the titration equation for the case in which neither titrant nor analyte absorbs, but an absorbing indicator ion is added which forms an extractable ion-pair with the titrant. Several examples of the latter type of titration are presented (108,109) such as the titration of hexafluorophosphate with tetraphenylarsonium ion in the presence of 1,2-dichloroethane as a second phase and permanganate as indicator.

In all of the above two-phase titrations whether the endpoint was observed visually or photometrically, it was necessary to allow the two bulk phases to separate



after adding each increment of titrant. Furthermore, titration equations for two-phase ion pair titrations have been derived only for the rather limited case in which neither titrant nor analyte participates in any side reactions (108).

In part II of this thesis, a simple titration apparatus is described which allows one liquid phase to be continually pumped out of a vigorously stirred two-phase solvent mixture, passed through a spectrophotometer flow cell, and returned to the mixture. In one category of titration where the absorbance of the aqueous phase was monitored, several pharmaceutical amines of  $BH^+$  charge type were titrated with sodium hydroxide. In another category, drugs of this charge type were titrated with picrate anion in a buffered two phase system and the aqueous phase absorbance was again monitored. In a third category, cationic drugs and surfactants were titrated with picrate and the absorbance of the organic phase was monitored. Finally, in a fourth category, anionic surfactants were titrated with the cationic dye methylene blue and the organic phase absorbance was monitored. In all of these categories theoretical titration equations were derived which take into account several common side reactions, and in most categories the theoretical equations were verified experimentally by titrating drug or surfactant sample compounds.



## CHAPTER 2

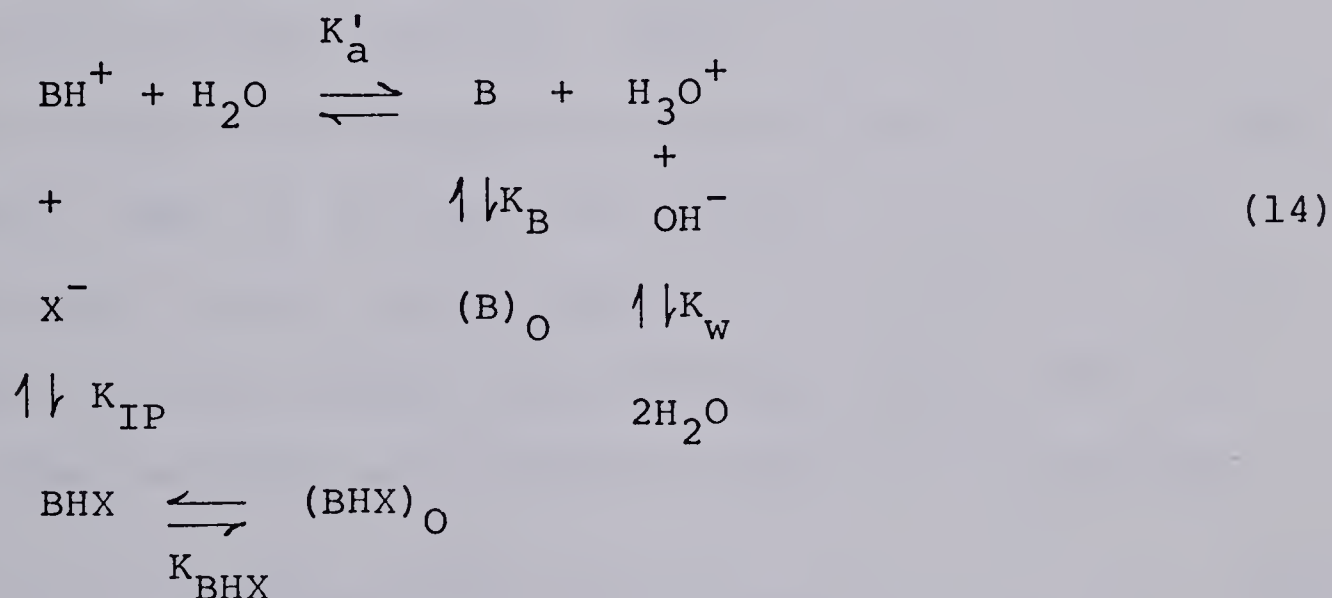
### THEORETICAL

#### 2.1 Acid-Base Titrations

The two-phase photometric titration of a weak acid ( $\text{BH}^+$ ) with sodium hydroxide will be described for the cases in which the absorbance of the aqueous or of the organic phase is monitored.

2.1.1 Proposed Model. In this section a physico-chemical model will be established which describes the titration of a monofunctional acid of the charge  $\text{BH}^+$ , in the presence of two immiscible liquids. The mathematical details of the derivation are given in Appendix III.

In the titration of a  $\text{BH}^+$  species, an overall equilibrium equation can be given:



where B is the conjugate base (titration product) of  $\text{BH}^+$ , and BHX is an ion-pair formed between  $\text{BH}^+$  and anion



$X^-$ . Here  $X^-$  is the conjugate base of a strong acid (e.g.,  $Cl^-$ ). Species without a subscript are in the aqueous phase and those with subscript 0 are in the organic phase. The thermodynamic constants appropriate to these equilibria are presented in the left-hand column of Table IV. The formation of an extractable ion-pair  $BHX$  has been well documented for a large number of protonated amines (28). In the titration equation it is useful to use concentrations,  $[i]$ , instead of activities,  $a_i$ , for all species,  $i$ , except  $H_3O^+$  and  $OH^-$ . In the right-hand column of Table IV the forms of the equilibrium constant expressions used in the titration equation are presented. It is evident that  $K'_a = K_a^T \cdot \gamma_{BH} / \gamma_B$ , where  $\gamma_{BH}$  and  $\gamma_B$  are the activity coefficients of conjugate species  $BH^+$  and  $B$  in the aqueous phase. Since the species  $B$  is neutral  $\gamma_B \approx 1$  at low electrolyte concentrations. Also,  $K_B = K_B^T$ , assuming that activity coefficients of  $B$  are equal to one in both phases. Now, if an inert electrolyte  $MX$  (e.g.  $NaCl$ ) is present in the aqueous phase at concentrations much higher than the sample, all activity coefficients in the aqueous phase are constants and  $K_I$  is a constant:

$$K_I = K_{IP}^T \cdot K_{BHX}^T \cdot [X^-] \cdot \gamma_{BH} \cdot \gamma_X / \gamma_{BHX,0} \quad (15)$$

Furthermore, it has been found (28) for ion pairs involving organic ammonium ions that  $K_{BHX}^T \gg K_{IP}^T \cdot [X^-]$ .



TABLE IV  
Equilibrium Constant Expressions  
For the Acid-Base Titrations

Thermodynamic Constants

$$K_a^T = \frac{a_B \cdot a_H}{a_{BH}}$$

$$K_w = a_H \cdot a_{OH}$$

$$K_B^T = \frac{a_{B,o}}{a_B}$$

$$K_{IP}^T = \frac{a_{BHX}}{a_{BH} \cdot a_X}$$

$$K_{BHX}^T = \frac{a_{BHX,o}}{a_{BHX}}$$

Constant Used

$$K'_a = \frac{[B] \cdot a_H}{[BH]}$$

$$K_w = a_H \cdot a_{OH}$$

$$K_B = \frac{[B]_o}{[B]}$$

$$K_I = \frac{[BHX]_o}{[BH]}$$



This means that the concentration of the species BH<sub>X</sub> is negligibly small in the aqueous phase.

Neglecting the concentration of BH<sub>X</sub> in the aqueous phase and assuming that all chemical species are in one or another of the bulk liquid phases, the following titration equation is derived for the case in which the aqueous phase absorbance is monitored by combining the equilibrium constant expressions with mass balance equations, with the electroneutrality condition, and with Beer's Law expressions for BH<sup>+</sup> and B in the aqueous phase (Appendix IIIA).

$$n_{OH} = X + Y \cdot \frac{K_w \cdot V}{K'_a \cdot \gamma_{OH}} - \frac{K'_a \cdot V}{\gamma_H} \quad (16)$$

where

$$X = \frac{[\epsilon'_{BH} \cdot n_{BH} - A_{obs} (V + K_I \cdot V_O)] \cdot [V + K_B \cdot V_O]}{[\epsilon'_{BH} (V + K_B \cdot V_O) - \epsilon'_B (V + K_I \cdot V_O)]} \quad (17)$$

$$Y = \frac{n_{BH} \cdot \epsilon'_{BH} - A_{obs} (V + K_I \cdot V_O)}{A_{obs} (V + K_B \cdot V_O) - n_{BH} \cdot \epsilon'_B} \quad (18)$$

$$Z = 1/Y \quad (19)$$

The photometric titration equation for the case where the organic phase absorbance is monitored can be derived by combining the equilibrium constant expressions with mass balance and electroneutrality equations and



with Beer's Law expressions for BHX and B in the organic phase. All chemical species are assumed to be in one or another of the bulk liquid phases. It is the same as equation 16, except that:

$$X = \frac{[\epsilon'_{\text{BHX},O} \cdot n_{\text{BH}} \cdot K_I - A_{\text{obs},O} (V + K_I \cdot V_O)] (V + K_B \cdot V_O)}{[\epsilon'_{\text{BHX},O} \cdot K_I \cdot (V + K_B \cdot V_O) - \epsilon'_{\text{B},O} \cdot K_B \cdot (V + K_I \cdot V_O)]} \quad (20)$$

$$Y = \frac{n_{\text{BH}} \cdot \epsilon'_{\text{BHX},O} \cdot K_I - A_{\text{obs},O} (V + K_I \cdot V_O)}{A_{\text{obs},O} (V + K_B \cdot V_O) - n_{\text{BH}} \cdot K_B \cdot \epsilon'_{\text{B},O}} \quad (21)$$

$$Z = 1/Y \quad (22)$$

In these equations  $\epsilon'_{\text{BH}}$  and  $\epsilon'_{\text{B}}$  as well as  $\epsilon'_{\text{BHX},O}$  and  $\epsilon'_{\text{B},O}$  are the products of molar absorptivities, at the wavelength used, and cell pathlength for species  $\text{BH}^+$  and B, in the aqueous and the organic phase, respectively.  $A_{\text{obs}}$  and  $A_{\text{obs},O}$  are the observed absorbances in the aqueous phase and the organic phase, corrected for dilution if necessary;  $V$  and  $V_O$  are volumes of aqueous and organic phases in liters;  $n_{\text{BH}}$  and  $n_{\text{OH}}$  are moles of sample and titrant added to the titration vessel;  $\gamma_{\text{H}}$  and  $\gamma_{\text{OH}}$  are ionic activity coefficients for  $\text{H}_3\text{O}^+$  and  $\text{OH}^-$ .



### 2.1.2 Predicted Acid-Base Titration Behavior.

(84,86,87). An examination of equations 16-19 for the case in which the aqueous phase absorbance is followed reveals that the right hand side of equation 16 contains three terms. The first term is a linear term in which  $A_{\text{obs}}$ , the observed absorbance, is a linear function of  $n_{\text{OH}}$ , the amount of added titrant. The straight line corresponding to this term connects a point at  $n_{\text{OH}} = 0$  and

$$A_{\text{obs}} = n_{\text{BH}} \cdot \epsilon'_{\text{BH}} / (V + K_{\text{I}} \cdot V_{\text{O}}) \quad (23)$$

and with a point at  $n_{\text{OH}} = n_{\text{BH}}$  and

$$A_{\text{obs}} = n_{\text{BH}} \cdot \epsilon'_{\text{B}} / (V + K_{\text{B}} \cdot V_{\text{O}}) \quad (24)$$

The second term on the right in equation 16 is responsible for the curvature which occurs near the endpoint of a titration curve. This curvature is away from the ordinate and is more severe the weaker the acid being titrated or the more dilute its solution. If the second term alone is equated to  $n_{\text{OH}}$  and the resulting equation is rearranged, it may be shown that an expression of the following form is obtained.

$$n_{\text{OH}} \cdot A_{\text{obs}} + n_{\text{OH}} C_1 + A_{\text{obs}} \cdot C_2 + C_3 = 0 \quad (25)$$

where  $C_1$ ,  $C_2$  and  $C_3$  are constants. This is the equation for a rectangular hyperbola with horizontal and vertical



asymptotes, or of a degenerate hyperbola consisting of a horizontal and vertical line (84). The coordinates of the center of the hyperbola are:

$$n_{OH} = -\left(\frac{K_w \cdot V}{K'_a \cdot \gamma_{OH}}\right) \cdot \frac{(V + K_I \cdot V_O)}{(V + K_B \cdot V_O)} \quad (26)$$

and

$$A_{obs} = \frac{n_{BH} \epsilon'_B}{(V + K_B \cdot V_O)} \quad (27)$$

and the asymptotes are vertical and horizontal lines (parallel with the axes) which pass through this point. These equations reveal that when  $\epsilon'_B$  is equal to zero then the horizontal asymptotes will be coincident with the abscissa. In contrast, however, it can be seen that the vertical asymptote will never be coincident with the ordinate, but will always be to the left of it.

The third term on the right in Equation 16 is responsible for the curvature which occurs in the early part of a titration curve. In this region the curvature is toward the ordinate and is more severe the stronger the acid or the more dilute its solution. This term, like the second term, may also be shown to represent a rectangular hyperbola or a degenerate hyperbola, with its center coordinates as follows:

$$n_{OH} = \frac{(V + K_B \cdot V_O)}{(V + K_I \cdot V_O)} \left( \frac{K'_a \cdot V}{\gamma_H} \right) \quad (28)$$



and

$$A_{\text{obs}} = \frac{n_{\text{BH}} \cdot \epsilon'_{\text{BH}}}{(V + K_{\text{I}} \cdot V_{\text{O}})} \quad (29)$$

The asymptotes are vertical and horizontal lines passing through this point. The horizontal asymptote may coincide with the abscissa, but the vertical asymptote in this case will always be to the right of the ordinate.

An overall photometric titration curve is, of course, a composite of all three component curves — a linear and two hyperbolic curves, with only the zero and positive values of  $A_{\text{obs}}$  and  $n_{\text{OH}}$  having physical significance.

The influence of the various parameters on the overall photometric titration curve can be summarized by plotting theoretical titration curves using equation 16 in which only one parameter is allowed to vary at a time. This is shown in Figures 11 to 14 for an acid of the charge type  $\text{BH}^+$ .

The parameter  $K_{\text{I}}$  will be seen to effect the titration curve in two distinct ways which are illustrated in Figures 11 and 12. First in Figure 11, as  $K_{\text{I}}$  increases the initial absorbance progressively decreases. Therefore, if  $K_{\text{I}}$  were large enough, all the acid  $\text{BH}^+$  species would be in the organic phase and the titration curve would nearly coincide with the abscissa along its entire length and would, therefore, be analytically



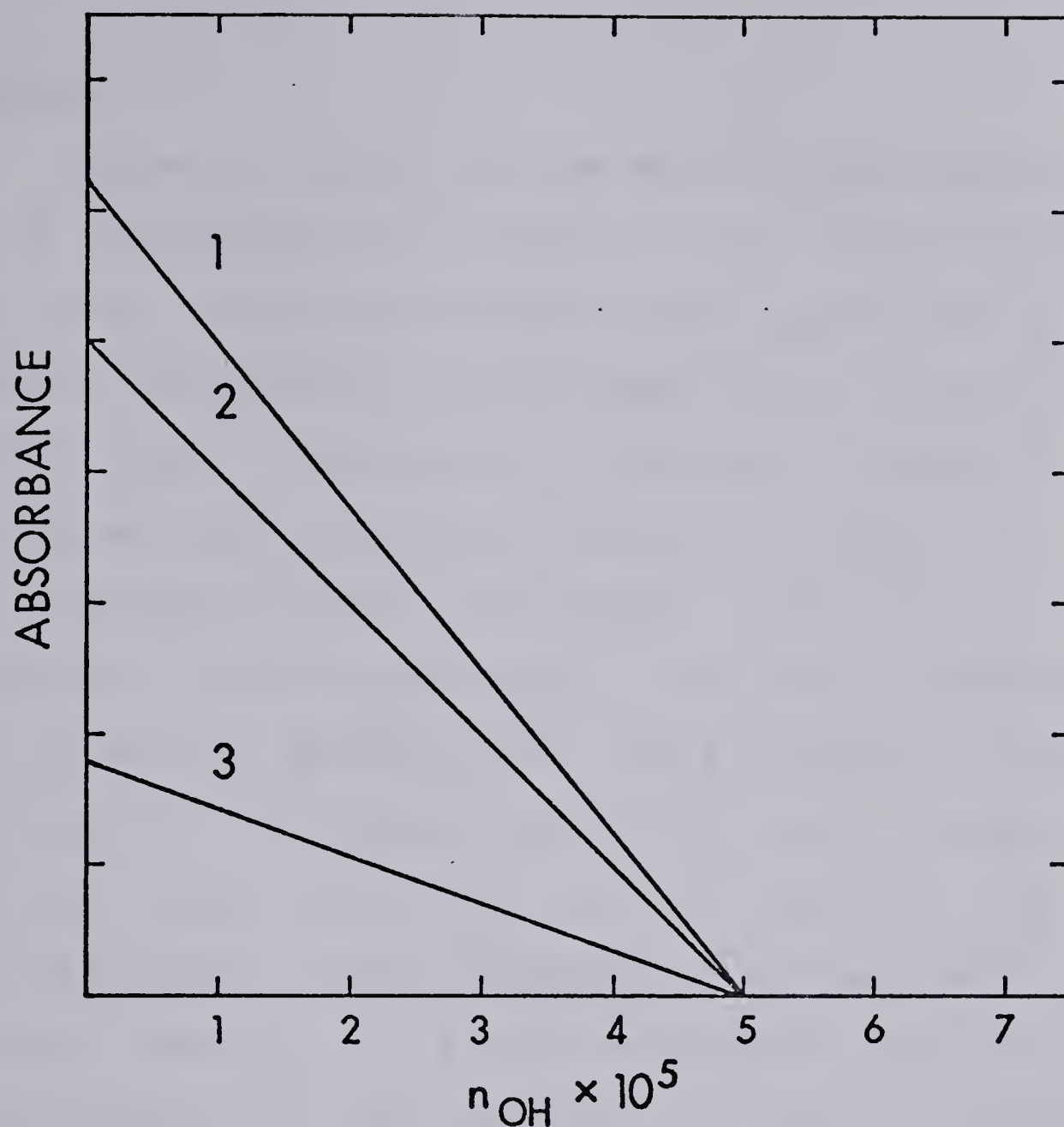


FIGURE 11. Theoretical titration curves for acid  $\text{BH}^+$  in a two phase system. First effect of  $K_I$  on the shape of the titration curve.

(Curves calculated from Equation 16  
for absorbance of aqueous phase.)

---

$\gamma_H = \gamma_{OH} = 1.0$ ;  $K_B = 0.0$ ;  $\epsilon'_{BH} = 200$ ;  $\epsilon'_B = 0.0$ ;  
 $K'_a = 1.0 \times 10^{-7}$ ;  $K_w = 1.0 \times 10^{-14}$ ;  $n_{BH} = 5.0 \times 10^{-5}$ ;  
 $V_O = 0.02 \text{ L}$ ;  $V = 0.08 \text{ L}$ .

---

Curve No.	1	2	3
$K_I$	0.01	1.0	10.0

---



useless.

Figure 12 illustrates the second effect that  $K_I$  has on the photometric titration curve. In this example, the initial absorbance is zero since  $\epsilon'_{BH} = 0$ , and is therefore unaffected by an increase in  $K_I$ . Figure 12 reveals that an increase in  $K_I$  produces an effect similar to that produced by a decrease in  $K'_a$  (i.e., when titrating a weak acid (78,80)). That is, it generates a greater curvature in the part of the titration curve near the end point. This increase in the curvature in the latter part of the curve is associated with the second term in the titration equation. If the acid chosen for the illustration had been much stronger than  $pK'_a = 7$  it would be evident (since  $Z = 1/Y$  in equation 18) that an increase in  $K_I$  would also have the effect of decreasing the curvature in the early part of the titration curve which is associated with the third term in the titration equation.

The  $K_B$  parameter, like  $K_I$ , also exerts two distinct effects on the photometric titration curve of an acid  $BH^+$ . In Figure 13 is presented a family of titration curves for a hypothetical acid of  $pK'_a = 10$ , for which both conjugate species have identical molar absorptivities. As  $K_B$  increases, a downward shift of the final limiting absorbance is observed. This is caused by a greater fraction of the B species being



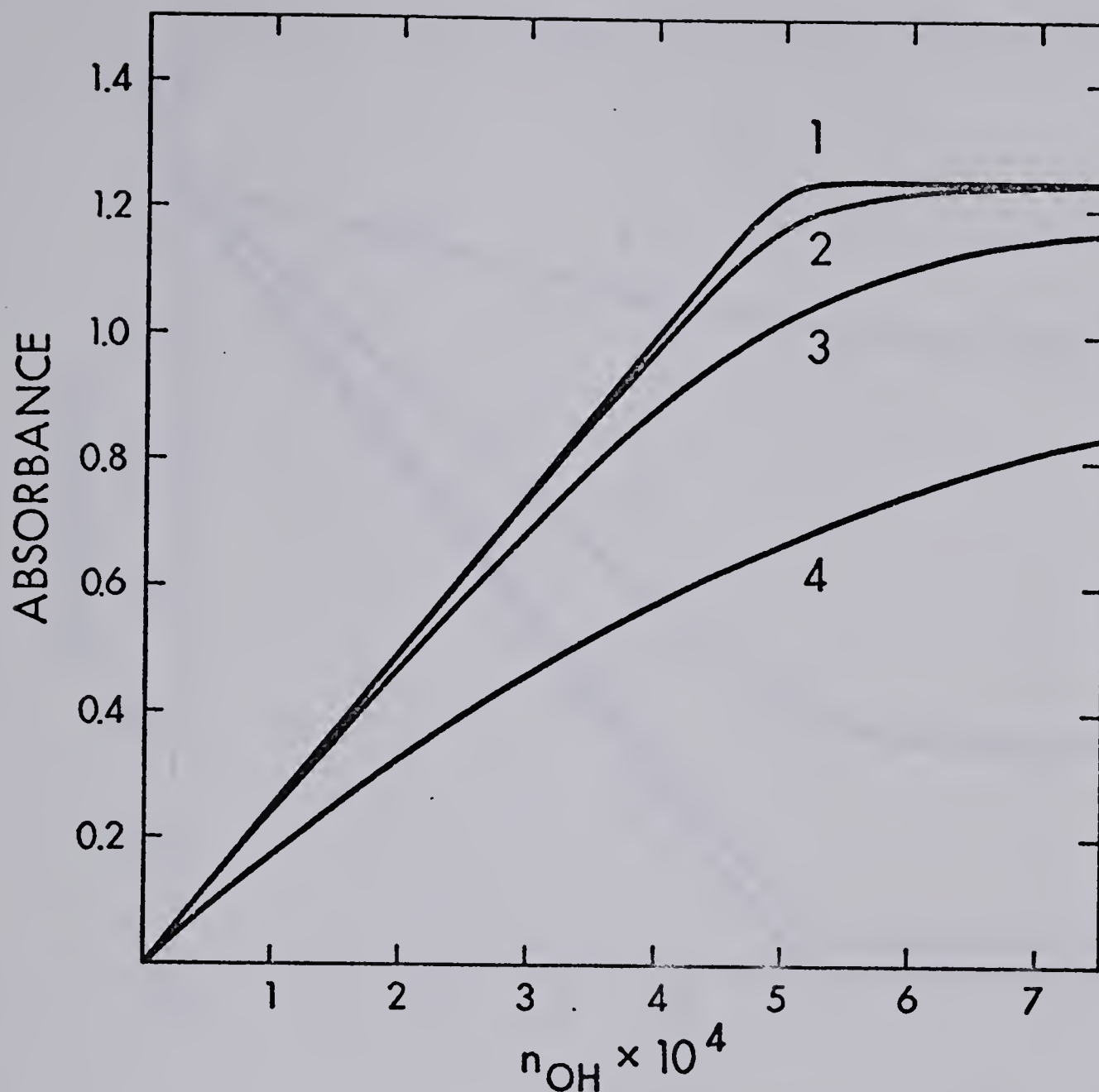


FIGURE 12. Theoretical titration curves for acid  $\text{BH}^+$  in a two phase system. Second effect of  $K_I$  on the shape of the titration curve.

(Curves calculated from Equation 16 for absorbance of aqueous phase.)

$$\gamma_H = \gamma_{OH} = 1.0; K_B = 0.0; \epsilon'_{BH} = 0.0; \epsilon'_B = 200; K_a = 1.0 \times 10^{-7}; K_w = 1.0 \times 10^{-14}; n_{BH} = 5.0 \times 10^{-4};$$

$$V_O = 0.02 \text{ L}; V = 0.08 \text{ L}$$

Curve No.	1	2	3	4
$K_I$	$10^2$	$10^3$	$10^4$	$10^5$



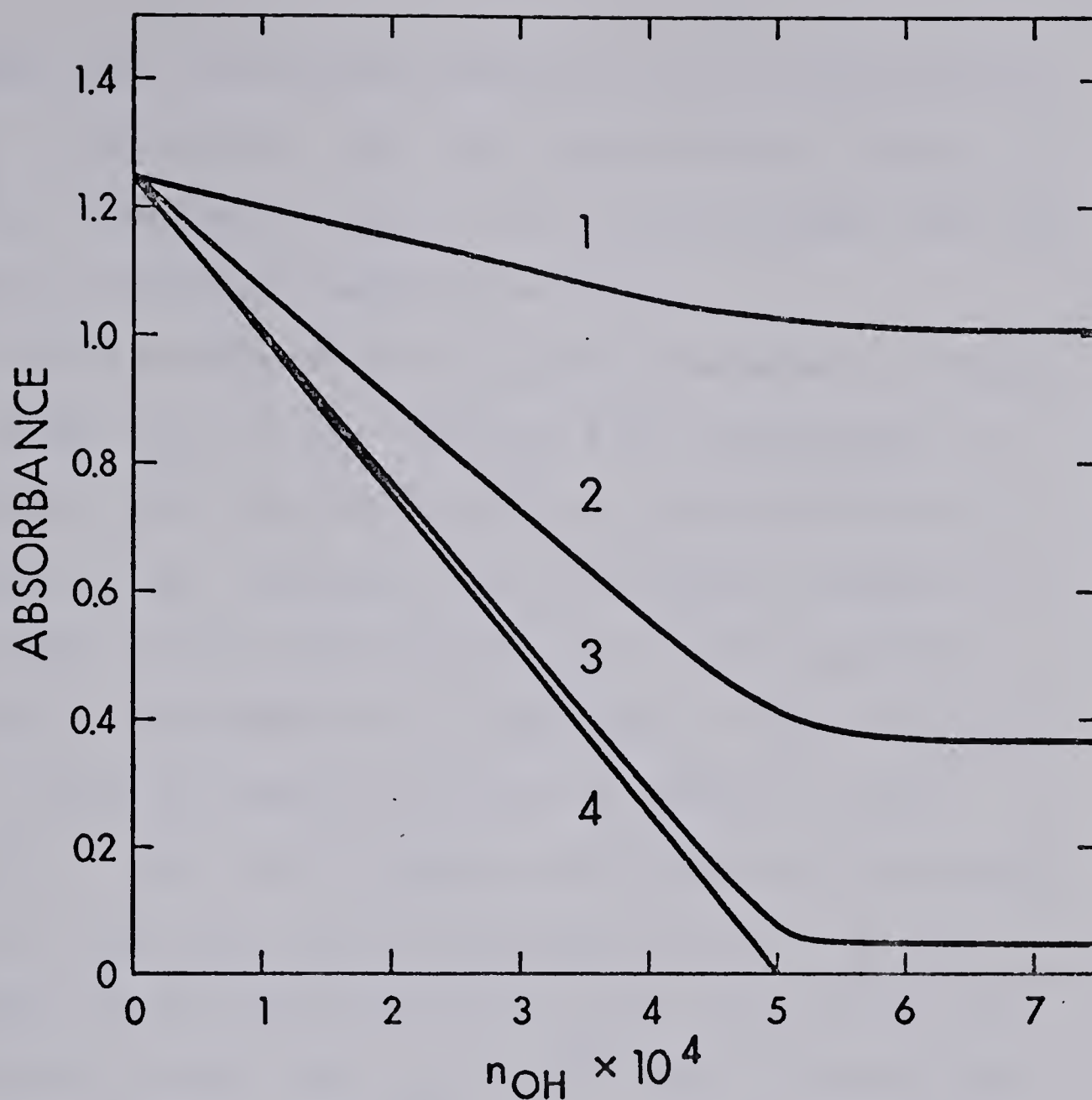


FIGURE 13. Theoretical titration curves for acid  $\text{BH}^+$  in a two phase system. First effect of  $K_B$  on the shape of the titration curve.

(Curves calculated from Equation 16 for absorbance of aqueous phase.)

$\gamma_H = \gamma_{OH} = 1.0$ ;  $\epsilon'_{BH} = \epsilon'_B = 200$ ;  $K_a = 1.0 \times 10^{-10}$ ;  
 $K_w = 1.0 \times 10^{-14}$ ;  $K_I = 0.0$ ;  $n_{BH} = 5.0 \times 10^{-4}$ ;  $V_O = 0.02 \text{ L}$ ;  $V = 0.08 \text{ L}$

Curve No.	1	2	3	4
$K_B$	1.0	10	$10^2$	$10^5$



removed from the aqueous phase into the organic phase as  $K_B$  is increased. For very large values, nearly all of the B species is found in the organic phase and the limiting absorbance approaches zero.

The second effect of  $K_B$  is illustrated in Figure 14. Since  $\epsilon'_B = 0$ , the limiting final absorbance is already at zero and is, therefore, unaffected by an increase in  $K_B$ . However, the  $K_B$  parameter appears in the second and in the third terms of the titration equation. The effect of an increase in this parameter is to cause the acid to titrate as though it were stronger. That is, it reduces the amount of curvature near the end point in the titration curve. If the strength of the acid chosen for this illustration had been much greater than  $K'_a = 10^{-10}$ , then it would also be evident that an increase in  $K_B$  increases the curvature in the early part of the curve, since this parameter occurs also in the third term of the titration equation.

The above discussion has focused on titrations in which the aqueous phase absorbance is monitored. It is evident from the symmetrical relationship of equations 17, 18, and 19 with equations 20, 21 and 22 that analogous behavior is exhibited when the organic phase absorbance is monitored. Of course, in this case the increase or decrease in absorbance would be opposite



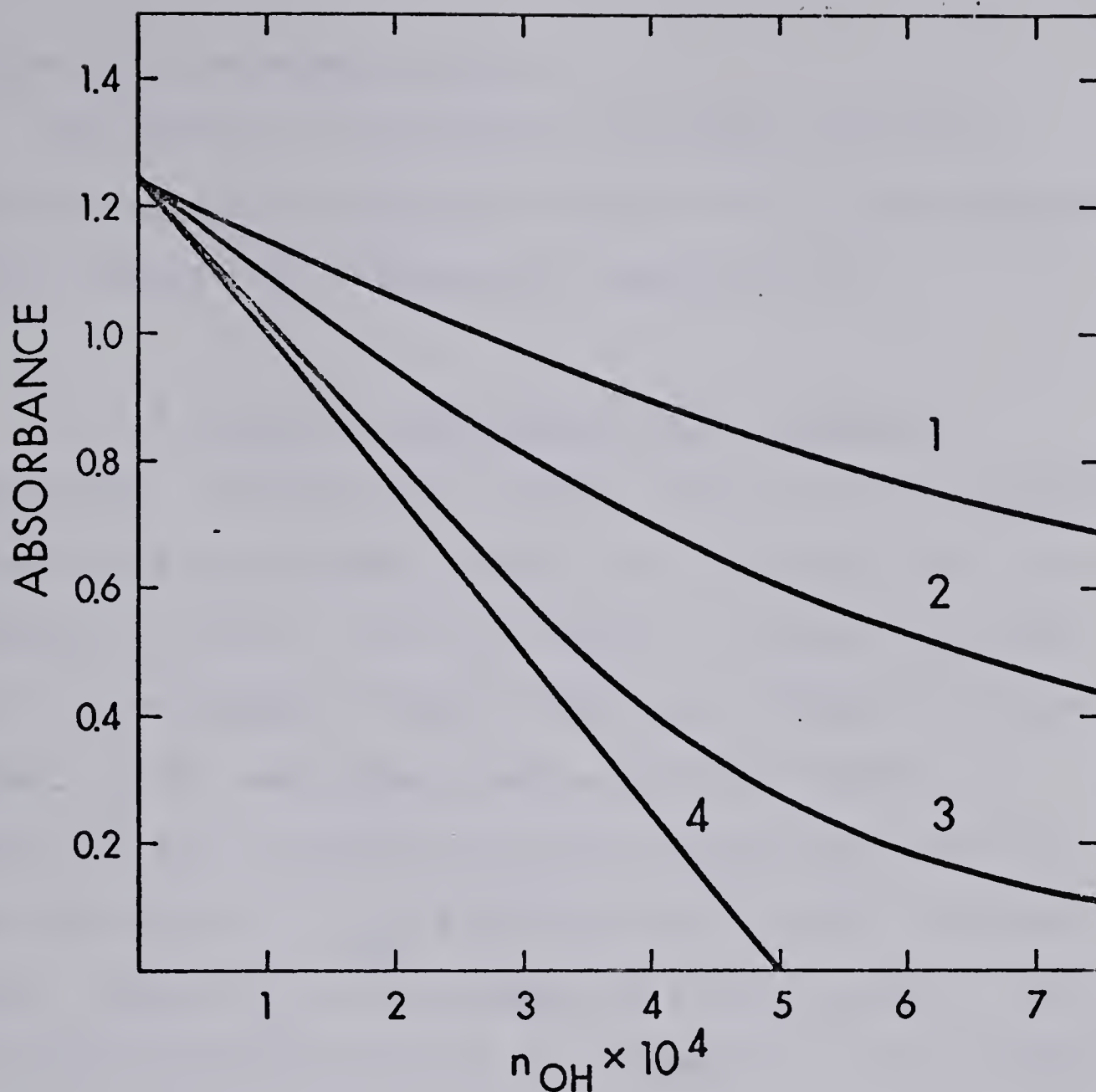


FIGURE 14. Theoretical titration curves for acid  $\text{BH}^+$  in a two phase system. Second effect of  $K_B$  on the shape of the titration curve.

(Curves calculated from Equation 16

for absorbance of aqueous phase.)

$\gamma_H = \gamma_{OH} = 1.0$ ;  $\epsilon'_B = 0.0$ ;  $\epsilon'_{BH} = 200$ ;  $K'_a = 1.0 \times 10^{-12}$ ;  
 $K_w = 1.0 \times 10^{-14}$ ;  $K_I = 0.0$ ;  $n_{BH} = 5.0 \times 10^{-4}$ ;  $V = 0.08 \text{ L}$ ;  
 $V_O = 0.02 \text{ L}$ .

Curve No.	1	2	3	4
$K_B$	1.0	10	$10^2$	$10^5$



to that in the aqueous phase.

The merits of two-phase acid-base titrations relative to other acid-base titrations will be discussed in the Results and Discussion (Section 4.1).

2.1.3 Dilution Correction for Acid-Base Titrations. Addition of titrant results in an increasing volume of aqueous phase during the titration and a consequent dilution. In a photometric titration carried out in homogeneous solution this has a simple dilution effect on the absorbing species and can readily be corrected for by multiplying each absorbance value by the quantity  $(V + V_{\text{OH}})/V$  before plotting the titration curve. Here  $V_{\text{OH}}$  is the volume of titrant added. In a two-phase titration medium the situation is more complex. Photometric titration end points are usually evaluated by extrapolation of the linear portions of the curve before and after the end point. This means that over most of the length of the segment of the titration curve before the equivalence point the "X" term in equation 16 is much larger than the other two terms on the right-hand-side of that equation. Therefore, the dilution correction before the equivalence point can be deduced for titration curves which do not show much curvature by considering only the "X" term in equation 16.



Consider first the case in which the aqueous phase absorbance is monitored (equations 16-19).

Making the very likely assumptions that  $\epsilon'_{BH}(V + K_B \cdot V_O) \gg \epsilon'_B(V + K_I \cdot V_O)$  and considering only the "X" term on the right-hand side, then equation 16 becomes:

$$n_{OH} \approx n_{BH} - \frac{A_{obs}(V + K_I \cdot V_O)}{\epsilon'_{BH}} \quad (30)$$

Now the constant  $K_I$  depends on the concentration of anion  $X^-$  according to equation 15. If the dilution is only slight then  $\gamma_{BH}$  and  $\gamma_X$  will not change and it becomes evident that  $K_I \propto [X^-]$ . Since  $[X^-]$  decreases directly with increasing dilution, provided that there is a large excess of inert salt MX present, then the initial value,  $K_{I,initial}$ , (i.e., that which prevails at the initial salt concentration at the beginning of the titration) should be multiplied by  $V/(V + V_{OH})$  to correct for dilution. At the same time, the volume  $V$  in equation 30 should be replaced by  $(V + V_{OH})$  to correct it for dilution.

Thus, to correct for both effects, before the equivalence point one should plot:

$$A_{obs} \cdot \frac{(V+V_{OH}) + K_{I,initial} \frac{(V/V+V_{OH}) \cdot V_O}{(V + K_{I,initial} \cdot V_O)}}{\quad} \text{ vs. } n_{OH} \quad (31)$$

to obtain the titration curve. The dilution correction given by equation 31 can take two limiting forms:



If the extraction of ion pairs is slight so that  $K_I \cdot V_O \ll V$ , then the correction is made by multiplying  $A_{\text{obs}}$  by  $(V + V_{\text{OH}})/V$ . At the other extreme, if ion pair extraction is extensive and  $K_I \cdot V_O \gg V$ , then the correction is made by multiplying  $A_{\text{obs}}$  by  $V/(V + V_{\text{OH}})$ .

The value of  $K_{I,\text{initial}}$  need not be measured in a separate experiment, since a good approximation can be obtained from the titration curve itself. If the straight line portion of the curve is extrapolated back to the  $A_{\text{obs}}$  axis where  $n_{\text{OH}} = 0$ , the intercept will have the value:

$$A_{\text{obs,extrap.}} = \frac{n_{\text{BH}} \cdot \epsilon'_{\text{BH}}}{(V + K_{I,\text{initial}} \cdot V_O)} \quad (32)$$

If the extent of dilution is not very great, then a fairly accurate value of  $n_{\text{BH}}$  can be had from the end-point obtained before dilution correction. Therefore, if the value of  $\epsilon'_{\text{BH}}$  is known for the compound, it is a simple matter to obtain  $K_{I,\text{initial}}$  from equation 32. This method of obtaining  $K_{I,\text{initial}}$  assumes that other absorbing compounds are absent from the sample. In the titration reported in this thesis the initial aqueous phase volume was 80.42 mL and the titrant volume required to reach the end point was only about 0.7 mL so that dilution corrections, though used, are relatively small.

The linear segment of the titration curve obtained



after the equivalence point is given by the equation:

$$A_{\text{obs}} = \frac{n_{\text{BH}} \cdot \epsilon'_B}{(V + K_B \cdot V_O)} \quad (33)$$

It is a constant, independent of added titrant, except for the dilution effect which is compensated for by plotting:

$$A_{\text{obs}} \cdot \frac{(V + V_{\text{OH}}) + K_B \cdot V_O}{V + K_B \cdot V_O} \quad \text{vs. } n_{\text{OH}} \quad (34)$$

Normally,  $K_B$  is large so that  $A_{\text{obs}}$  is very small, and the dilution correction after the equivalence point is negligible.

It may be noted that if the titrant solution is made to contain the same concentration of sodium chloride as is present in the sample solution aqueous phase, then there would be no dilution of  $\text{Na}^+$  and  $\text{Cl}^-$  and, therefore, no change in the value of  $K_I$  during the titration. In that case,  $(V/(V + V_{\text{OH}}))$  would disappear from the  $K_{I,\text{initial}}$  terms in equation 31.

Dilution corrections when the organic phase is monitored are not discussed here since no experiments were done. Such corrections for ion-pair titrations are discussed in Section 2.2.3.

## 2.2 Ion-Pair Titrations

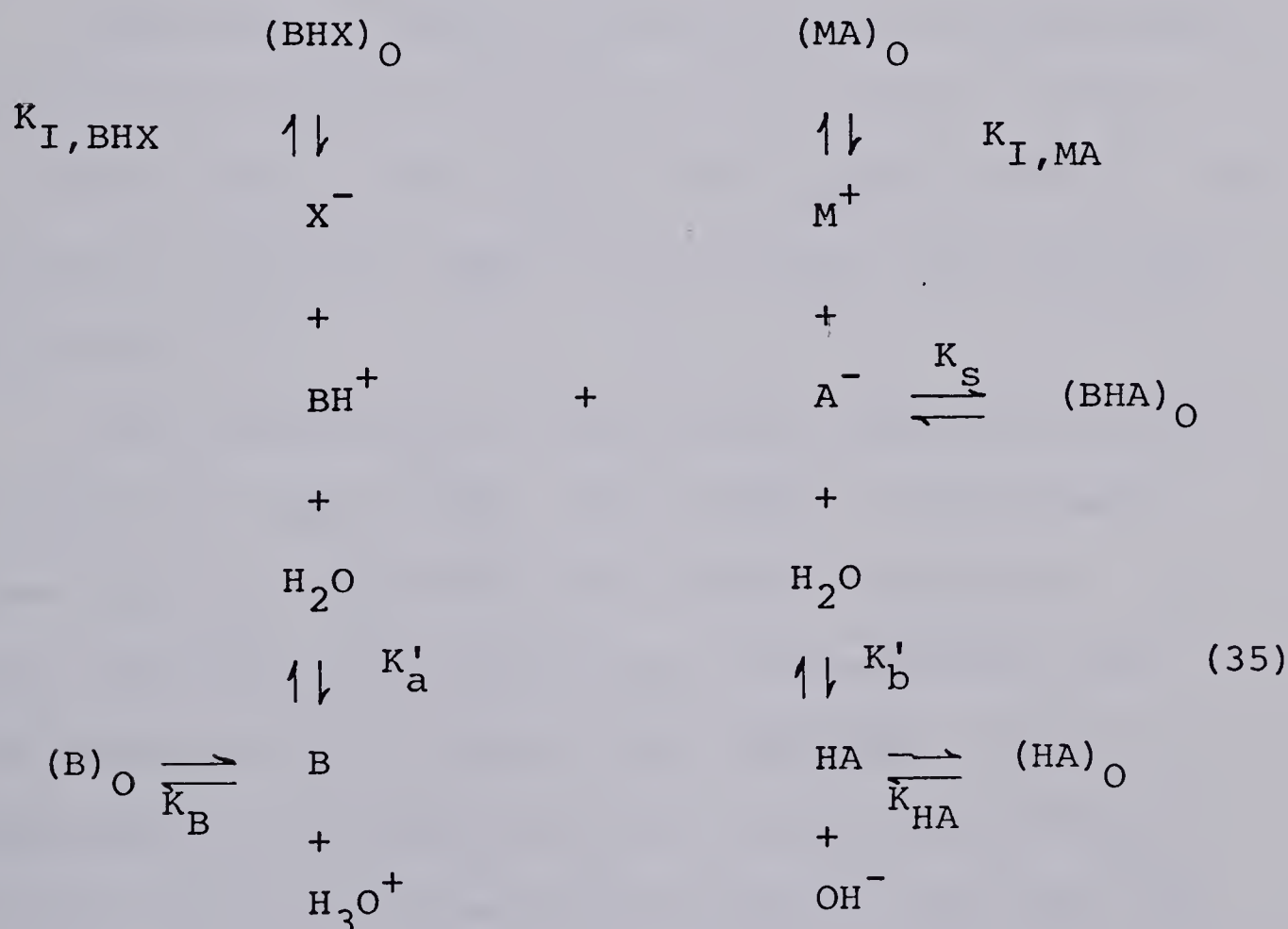
Two phase photometric ion-pair titrations of a weak



acid  $\text{BH}^+$  with titrant  $\text{A}^-$ , and of weak base  $\text{A}^-$  with titrant  $\text{BH}^+$  will be described for the cases in which the absorbance of the aqueous or of the organic phase is monitored.

2.2.1 Proposed Model. In this section, a physico-chemical model will be established. The details of the derivations are given in Appendices IV and V.

The chemical and phase distribution equilibria which prevail in the heterogeneous titration involving  $\text{BH}^+$  and  $\text{A}^-$  are summarized in equation 35.



Species without subscripts are in the aqueous phase and those with the subscript 0 are in the organic



phase. Here  $M^+$  and  $X^-$  are the cation and anion of the buffer which has been added to the aqueous phase and/or of some inert salt that may also have been added to the aqueous phase (e.g. NaCl). The titration reaction between the analyte species  $BH^+$  and the titrant  $A^-$  is quantitatively characterized by the "ion pair extraction constant"  $K_S$ . The cation  $BH^+$  is a weak acid which is in a pH-dependent equilibrium with its conjugate base B. The latter is distributed between the organic and aqueous phases. The species  $BH^+$  itself also forms an extractable ion pair with anion(s)  $X^-$ .

The anion  $A^-$  (e.g. picrate) is in a pH-dependent equilibrium with its conjugate acid, and the latter partitions between the organic and aqueous phases. The species  $A^-$  may also form an extractable ion pair with the cation  $M^+$ .

The possibility of significant concentration of the ion pair species  $BHX$ ,  $MA$  and  $BHA$  in the aqueous phase has been ignored in the present treatment. In cases where the aqueous ion pair concentration has been measured it is always small (28,110). Also neglected is the possibility of dissociation of the ion pair species in the organic phase. For some ion pairs this might be significant especially at low concentrations and when the organic solvent has a



relatively high dielectric constant (28,111). Dissociation in the organic phase becomes much less pronounced with increasing size of the organic ions involved. Gustavii and Schill (111) were unable to detect it for picrate ion pairs formed with the cation conjugate acids of atropine and codeine in methylene chloride.

Two other possible side reactions have been ignored: association of ion pairs with one another in the organic phase to form dimers or larger aggregates, and self-association of titrant anions or sample cations in the aqueous phase (e.g. micelle formation). At the low concentrations encountered in a titration these side reactions are not expected to occur to a significant extent. Gustavii and Schill (111) found no evidence of either in their studies of picrate ion pairs. At higher concentrations or with low dielectric constant organic solvents such association reactions might have to be taken into account (28). It is also assumed that all the chemical species are in one or another of the bulk liquid phases.

Thermodynamic constants describing all of the equilibria in equation 35 are presented in the left-hand column of Table V. In practice, a titration is performed with a buffered aqueous phase. The buffer, because of its relatively high concentration, provides a constant pH, constant  $M^+$ , constant  $X^-$ , and constant



TABLE V.

Equilibrium Constant Expressions.<sup>a</sup>  
For the Ion-Pair Titrations

Thermodynamic Constants

$$K_S^T = \frac{a_{\text{BHA},o}}{a_{\text{BH}} \cdot a_A}$$

$$K_a^T = \frac{a_B}{a_{\text{BH}} \cdot a_H}$$

$$K_{\text{I,BHX}}^T = \frac{a_{\text{BHX},o}}{a_{\text{BH}} \cdot a_X}$$

$$K_B^T = \frac{a_{\text{B},o}}{a_B}$$

$$K_b^T = \frac{a_{\text{HA}} \cdot a_{\text{OH}}}{a_A}$$

$$K_{\text{I,MA}}^T = \frac{a_{\text{MA},o}}{a_M \cdot a_A}$$

$$K_{\text{HA}}^T = \frac{a_{\text{HA},o}}{a_{\text{HA}}}$$

$$K_w = a_H \cdot a_{\text{OH}}$$

Constants Used

$$K_S = \frac{[\text{BHA}]_o}{[\text{BH}] [\text{A}]}$$

$$K'_a = \frac{[\text{B}]}{[\text{BH}] \cdot a_H}$$

$$K_{\text{I,BHX}} = \frac{[\text{BHX}]_o}{[\text{BH}]}$$

$$K_B = \frac{[\text{B}]_o}{[\text{B}]}$$

$$K'_b = \frac{[\text{HA}] \cdot a_{\text{OH}}}{[\text{A}]}$$

$$K_{\text{I,MA}} = \frac{[\text{MA}]_o}{[\text{A}]}$$

$$K_{\text{HA}} = \frac{[\text{HA}]_o}{[\text{HA}]}$$

$$K_w = a_H \cdot a_{\text{OH}}$$

a. The symbol  $a_i$  represents the activity of species  $i$ .

The subscript  $o$  designates the organic phase.



ion strength. As a consequence of this the thermodynamic constants can be replaced with the constants shown on the right-hand side of Table V. This can be shown by reasoning like that used in section 2.1.1 above.

By combining the equilibrium constant expressions from the right-hand side of Table V with mass balance and electroneutrality expressions and with Beer's Law expressions for all absorbing species in the aqueous phase (i.e. B,  $BH^+$ , HA,  $A^-$ ) the following two relationships can be derived for a titration of sample ion  $BH^+$  with titrant ion  $A^-$  in which the aqueous phase absorbance is monitored (Appendix III).

$$[BH]^2 \cdot K_S \cdot V_O \left[ \frac{(\epsilon'_{BH} + \epsilon'_B \cdot K'_a / a_H)}{(\epsilon'_A + \epsilon'_{HA} \cdot (K'_b \cdot a_H) / K_w)} \right] - [BH] \cdot \left[ V + \frac{K'_a \cdot V}{a_H} + \right.$$

$$\left. \frac{A_{obs} \cdot K_S \cdot V_O}{(\epsilon'_A + \epsilon'_{HA} \cdot \frac{K'_b \cdot a_H}{K_w})} + K_{I,BHX} \cdot V_O + \frac{K_B \cdot K'_a \cdot V_O}{a_H} \right] + n_{BH} = 0 \quad (36)$$

$$n_A = \frac{A_{obs} - [BH] (\epsilon'_{BH} + \epsilon'_B \cdot K'_a / a_H)}{(\epsilon'_A + \epsilon'_{HA} \cdot \frac{K'_b \cdot a_H}{K_w})} \cdot \left[ V + \frac{K'_b \cdot a_H \cdot V}{K_w} + K_S \cdot [BH] \cdot V_O \right. \\ \left. + K_{I,MA} \cdot V_O + \frac{K_{HA} \cdot K'_b \cdot a_H \cdot V_O}{K_w} \right] \quad (37)$$



When this titration is followed by monitoring the absorbance in the organic phase the following two equations apply:

$$\begin{aligned}
 & [\text{BH}]^2 \cdot K_S \cdot \left[ \epsilon'_{\text{BHA},\text{O}} \left( V + \frac{K'_a \cdot V}{a_H} + K_{\text{I,BHX}} \cdot V_O + \frac{K'_a \cdot K_B \cdot V_O}{a_H} \right) \right. \\
 & \left. - \left( \epsilon'_{\text{BHX},\text{O}} \cdot K_{\text{I,BHX}} \cdot V_O + \frac{\epsilon'_{\text{B},\text{O}} \cdot K_B \cdot K'_a \cdot V_O}{a_H} \right) \right] + [\text{BH}]^+ \cdot \\
 & \left[ \epsilon'_{\text{HA},\text{O}} \cdot \frac{K_{\text{HA}} \cdot K'_b}{K_w} \cdot (a_H \cdot V + K'_a \cdot V + K_{\text{I,BHX}} \cdot a_H \cdot V_O + K'_a \cdot K_B \cdot V_O) \right. \\
 & + \epsilon'_{\text{MA},\text{O}} \cdot K_{\text{I,MA}} \cdot \left( V + \frac{K'_a \cdot V}{a_H} + K_{\text{I,BHX}} \cdot V_O + \frac{K'_a \cdot K_B \cdot V_O}{a_H} \right) \\
 & \left. + K_S (A_{\text{obs},\text{O}} \cdot V_O - \epsilon'_{\text{BHA},\text{O}} \cdot n_{\text{BH}}) \right] - n_{\text{BH}} \cdot \left( \epsilon'_{\text{HA},\text{O}} \cdot \frac{K_{\text{HA}} \cdot K'_b \cdot a_H}{K_w} \right. \\
 & \left. + \epsilon'_{\text{MA},\text{O}} \cdot K_{\text{I,MA}} \right) = 0 \tag{38}
 \end{aligned}$$

$$\begin{aligned}
 n_A = & \frac{A_{\text{obs},\text{O}} - [\text{BH}] \cdot \left( \epsilon'_{\text{BHX},\text{O}} \cdot K_{\text{I,BHX}} + \epsilon'_{\text{B},\text{O}} \cdot \frac{K_B \cdot K'_a}{a_H} \right)}{\epsilon'_{\text{BHA},\text{O}} \cdot K_S \cdot [\text{BH}] + \epsilon'_{\text{MA},\text{O}} \cdot K_{\text{I,MA}} + \epsilon'_{\text{HA},\text{O}} \cdot \frac{K_{\text{HA}} \cdot K'_b \cdot a_H}{K_w}} \cdot \\
 & \left[ V + \frac{K'_b \cdot a_H \cdot V}{K_w} + K_S \cdot [\text{BH}] \cdot V_O + K_{\text{MA}} \cdot V_O + \frac{K_{\text{HA}} \cdot K'_b \cdot a_H \cdot V_O}{K_w} \right] \tag{39}
 \end{aligned}$$

In all of these equations  $n_A$  and  $n_{\text{BH}}$  are moles of titrant and sample added to the titration vessel;

$\epsilon'_{\text{BH}}$ ,  $\epsilon'_{\text{B}}$ ,  $\epsilon'_{\text{A}}$ ,  $\epsilon'_{\text{HA}}$ ,  $\epsilon'_{\text{BHA},\text{O}}$ ,  $\epsilon'_{\text{BHX},\text{O}}$ ,  $\epsilon'_{\text{B},\text{O}}$ ,  $\epsilon'_{\text{HA},\text{O}}$  and  $\epsilon'_{\text{MA},\text{O}}$  are the products of molar absorptivities at the



wavelength used and cell pathlength;  $A_{\text{obs}}$  and  $A_{\text{obs},0}$  are the observed absorbance of the aqueous and the organic phase, corrected for dilution if necessary;  $V$  and  $V_0$  are volumes of aqueous and organic phase in liters;  $a_{\text{H}}$  is the activity of hydrogen ion in the aqueous phase.

Equation 36 is a quadratic equation whose two roots have real, positive values corresponding to the concentrations of  $\text{BH}^+$  on the two branches of the titration curve (see Figure 30). This equation can be solved by substituting the experimentally measured values of all of the constants and an assumed value of  $A_{\text{obs}}$ . The two root-values of  $[\text{BH}]$  are each substituted into equation 37 to calculate the corresponding values of  $n_{\text{A}}$ . The process is repeated with new assumed values of  $A_{\text{obs}}$  until the entire titration (plot of  $A_{\text{obs}}$  vs.  $n_{\text{A}}$ ) curve has been calculated.

Only one root of equation 38 will have a real, positive value of  $[\text{BH}]$ . Equations 38 and 39 can be solved in the same manner as equations 36 and 37.

For the case in which a sample  $\text{A}^-$  is titrated with titrant  $\text{BH}^+$  and the organic phase absorbance is monitored, the titration equations are:

$$\begin{aligned}
 & [\text{A}]^2 \cdot K_{\text{S}} \cdot \left[ \epsilon'_{\text{BHA},\text{O}} \cdot V + \epsilon'_{\text{BHA},\text{O}} \cdot \frac{K'_{\text{b}} \cdot a_{\text{H}} \cdot V}{K_{\text{W}}} - \epsilon'_{\text{MA},\text{O}} \cdot K_{\text{I}}, \quad - \epsilon'_{\text{HA},\text{O}} \cdot K_{\text{HA}} \cdot \right. \\
 & \left. \frac{K'_{\text{b}} \cdot a_{\text{H}} \cdot V_0}{K_{\text{W}}} \right] + [\text{A}] \cdot \left[ \epsilon'_{\text{BHX},\text{O}} \cdot K_{\text{I},\text{BHX}} \left( V + \frac{K'_{\text{b}} \cdot a_{\text{H}} \cdot V}{K_{\text{W}}} \right) + \epsilon'_{\text{B},\text{O}} \cdot \frac{K_{\text{B}} \cdot K'_{\text{a}} \cdot V}{a_{\text{H}}} \cdot \right. \\
 & \left. \left( 1 + \frac{K'_{\text{b}} \cdot a_{\text{H}}}{K_{\text{W}}} \right) + \epsilon'_{\text{BHA},\text{O}} \cdot K_{\text{S}} \cdot (K_{\text{I},\text{MA}} \cdot V_0 + \frac{K_{\text{HA}} \cdot K'_{\text{b}} \cdot a_{\text{H}} \cdot V_0}{K_{\text{W}}} - n_{\text{A}}) + K_{\text{S}} \cdot A_{\text{obs},\text{O}} \cdot V_0 \right]
 \end{aligned}$$



$$+ \epsilon'_{B,O} \cdot K_B \cdot \left( \frac{K'_a \cdot K_{I,MA} \cdot V_O}{a_H} + \frac{K'_a \cdot K'_b \cdot K_{HA} \cdot a_H \cdot V_O}{a_H} \right) - \frac{K_a \cdot n_A}{a_H} = 0 \quad (40)$$

and

$$n_{BH} = \frac{A_{obs,O} - [A] \cdot \left( \epsilon'_{HA,O} \cdot \frac{K_{HA} \cdot K'_b \cdot a_H}{K_w} + \epsilon'_{MA,O} \cdot K_{I,MA} \right)}{\epsilon'_{BHA,O} \cdot K_S \cdot [A] + \epsilon'_{BHX,O} \cdot K_{I,BHX} + \epsilon'_{B,O} \cdot \frac{K_B \cdot K'_a}{a_H}} \quad (41)$$

$$\left[ V + \frac{K'_a \cdot V}{a_H} + K_S \cdot [A] \cdot V_O + K_{I,BHX} \cdot V_O + \frac{K_B \cdot K'_a \cdot V_O}{a_H} \right]$$

These equations can be solved in the same manner as equations 36 and 37.

2.2.2 Predicted Ion-Pair Titration Behavior (112, 113). In this section the effects of the various constants on the titration curves in both the aqueous and the organic phase will be considered.

2.2.2.1 Absorbance of Aqueous Phase Monitored; Titrant  $A^-$ . Because of the relatively complex equilibria involved, it is of value to examine the influence of the various equilibrium constants on the titration curves calculated from equations 36 and 37. For this purpose it will be assumed that both titrant and sample absorb radiation at the wavelength of interest. Only the parameters  $K_S$ ,  $K'_a$ ,  $K_B$ ,  $K_{I,BHX}$ ,  $K'_b$ ,  $K_{HA}$ ,  $K_{I,MA}$ , and pH (i.e.,  $a_H$ ) will be considered. In each of the



Figures 15 through 22 all of the parameters have been fixed except the one of interest. Dilution of the aqueous phase is neglected. The values of the fixed parameters in any figure have been chosen in such a way as to clearly reveal the influence of the parameter whose value is being varied.

Figure 15 demonstrates the effect of  $K_s$ , the ion pair extraction constant. When  $K_s$  is small (curve 1) there is no reaction between  $BH^+$  and  $A^-$ . The initial absorbance value, before any titrant is added, is that due to  $BH^+$  in the aqueous phase. When titrant is added the observed absorbance is simply the sum of that due to  $BH^+$  and  $A^-$ . On the other hand when  $K_s$  is large (curve 7) the reaction between  $BH^+$  and  $A^-$  is quantitative throughout the titration and the addition of  $n_A$  moles of titrant  $A^-$  prior to the equivalence point results in the same number of moles of BHA being extracted into the organic phase. The absorbance thus decreases linearly with added titrant because of the loss of  $BH^+$  from the aqueous phase. Beyond the equivalence point the absorbance increase linearly, since  $BH^+$  has already been quantitatively consumed, and adding  $A^-$  beyond the equivalence point has the same effect as adding it to a two-phase system which contains no  $BH^+$ . Note that the slope of curve 7 after the equivalence point is the same as that of curve 1.





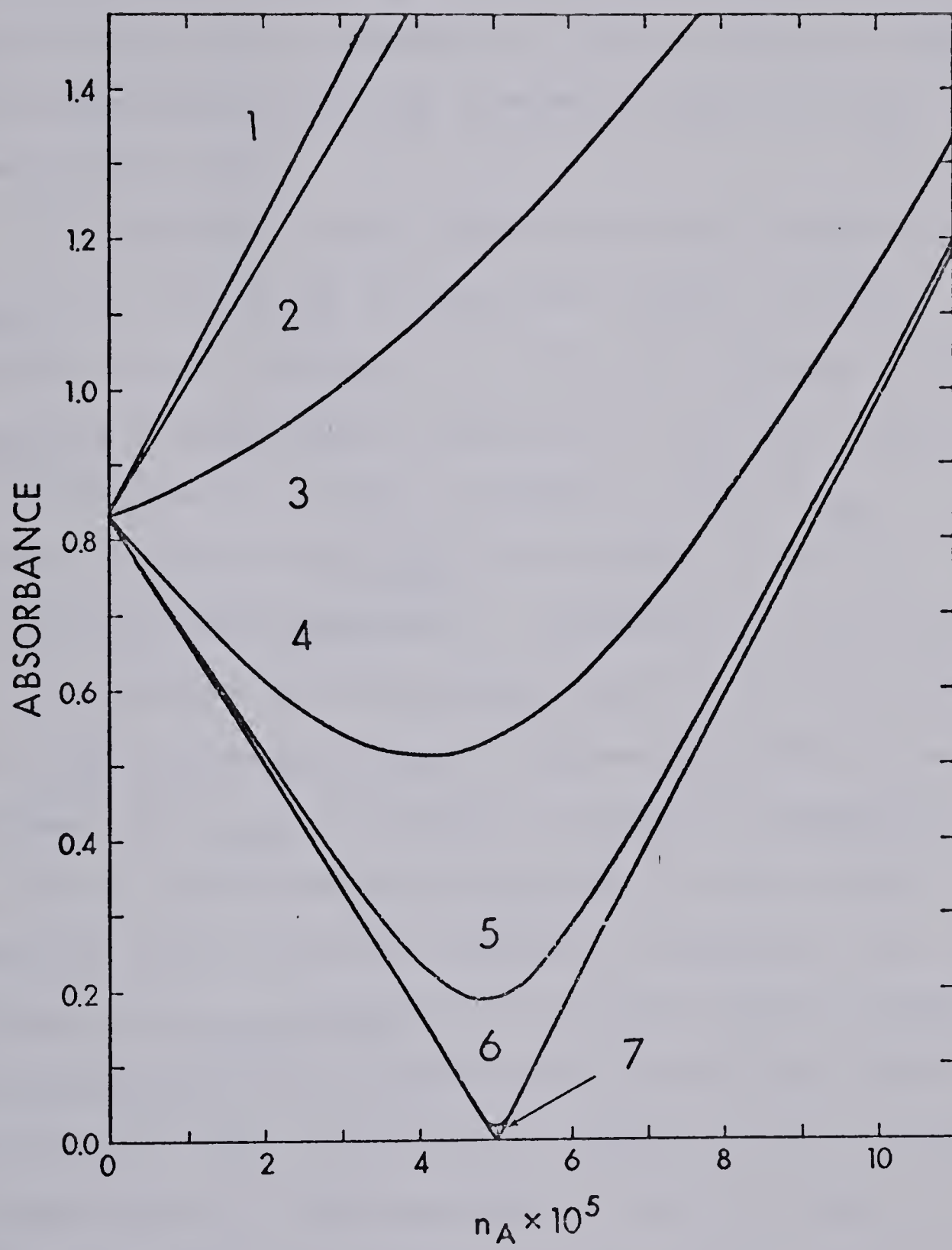
FIGURE 15. Theoretical titration curves for acid  $BH^+$  in a two phase system. Effect of  $K_S$  on the shape of the titration curve (curves calculated from Equations 36 and 37 for absorbance of aqueous phase.)

---

$n_{BH} = 5.00 \times 10^{-5}$  mole;  $V = 0.080$  L;  $V_O = 0.020$  L;  
 $K'_a = 10^{-9}$ ;  $K'_b = 10^{-14}$ ;  $K_{I,BHX} = 1.0$ ;  $K_{I,MA} = 1.0$ ;  
 $K_B = 10^6$ ;  $K_{HA} = 10^2$ ;  $\epsilon'_{BH} = \epsilon'_B = \epsilon'_A = 2 \times 10^3$ ;  $\epsilon'_{HA} = 10^4$ ;  
 $pH = 3.00$ .

Curve No.	1	2	3	4	5	6	7
$K_S$	0	$10^3$	$10^4$	$10^5$	$10^6$	$10^8$	$10^{12}$

---





Curves 2 through 6 show intermediate stages between the limiting cases of 1 and 7. From curves 7 and 6 it is obvious that, when  $K_s$  is large enough, the equivalence point may be obtained by linear extrapolation of the two branches of the titration curve to their intersection point.

An increase in any one of the three parameters  $K_{I,BHX}$ ,  $K'_a$ , or  $K_B$  has the same two effects on the titration curve, Figures 16 - 18. The influence of  $K_{I,BHX}$  is illustrated in Figure 16. The first effect is illustrated by curves 1 through 4. As  $K_{I,BHX}$  becomes larger the initial concentration of  $BH^+$  in the aqueous phase decreases. Consequently, the slope of the curve before the equivalence point decreases toward zero with increasing  $K_{I,BHX}$ . The second effect of an increase in  $K_{I,BHX}$  is evident in curves 4 through 7 and may be understood qualitatively in terms of Le Chatelier's principle by reference to equation 35. An increase in  $K_{I,BHX}$  removes  $BH^+$  from the aqueous phase and thereby shifts the equilibrium between  $BH^+$  and  $A^-$  to the left. The net effect is similar to that obtained by decreasing  $K_s$ . The branches of the titration curves approach one another in slope until, in curve 7, the situation is the same as that obtained by adding  $A^-$  to a two-phase system containing no  $BH^+$ . The difference between curve 7 in Figure 16 and curve 1 in



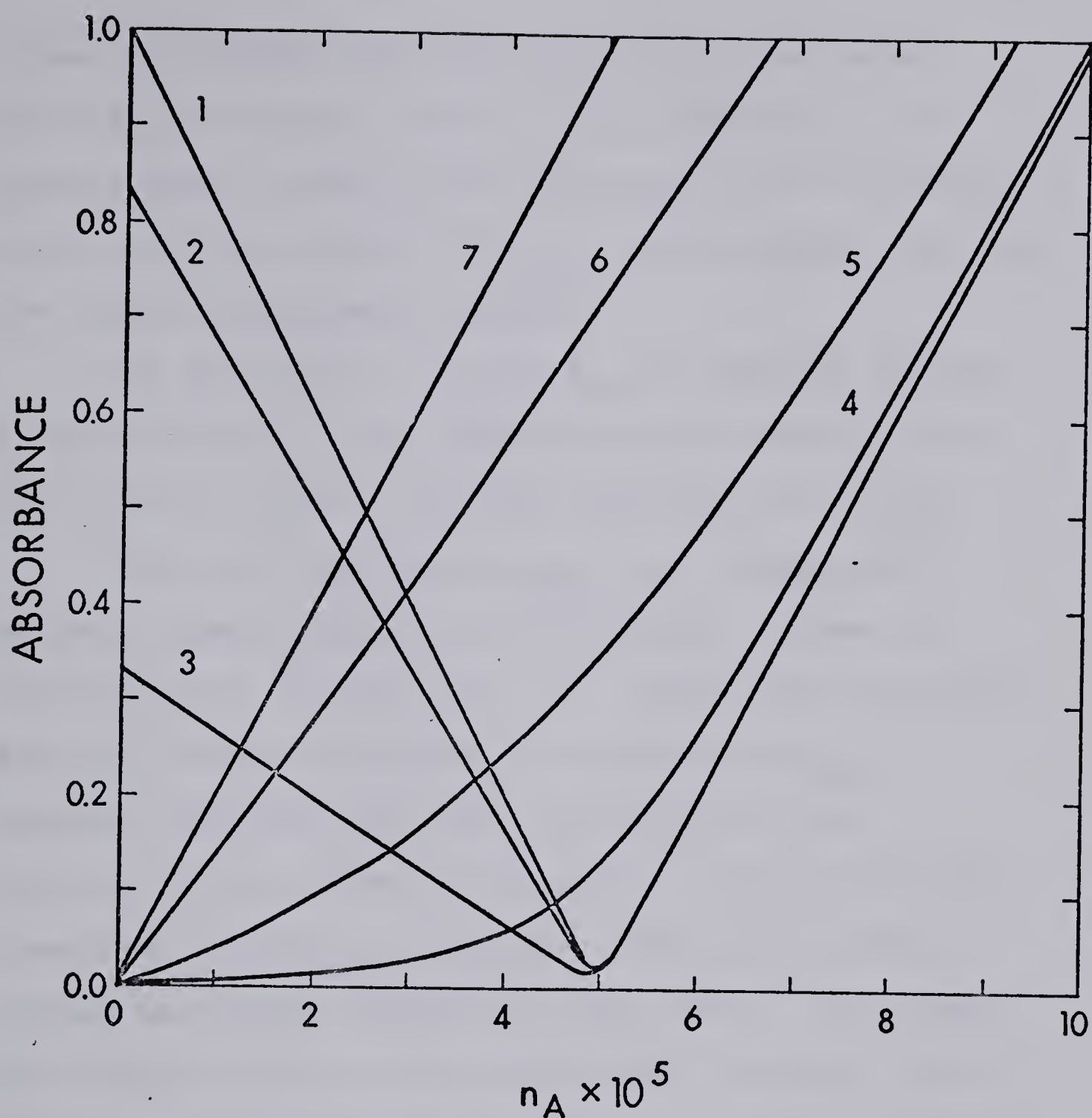


FIGURE 16. Theoretical titration curves for acid  $\text{BH}^+$  in a two phase system. Effect of  $K_{\text{I,BHX}}$  on the shape of the titration curve. (Curves calculated from Equations 36 and 37 for absorbance of aqueous phase.)

All parameters as in Figure 15 except  $K_{\text{S}} = 10^8$ .

Curve No.	1	2	3	4	5	6	7
$K_{\text{I,BHX}}$	0	1.0	10	$10^3$	$10^4$	$10^5$	$10^{10}$



Figure 15 results from the fact that in the former case essentially all of the  $BH^+$  is initially in the organic phase as BHX at the beginning of the titration (i.e. the first effect of  $K_{I,BHX}$ , noted above), so that the initial absorbance is zero.

The influence of  $K'_a$  and  $K_B$  are shown in Figures 17 and 18 where it can readily be seen that they produce effects similar to those discussed for  $K_{I,BHX}$ .

The three constants  $K_{I,MA}$ ,  $K'_b$ , and  $K_{HA}$  also produce effects similar to one another. These are illustrated in Figures 19 - 21. Figure 19 illustrates the two effects caused by an increase in  $K_{I,MA}$ . Curves 1 through 4 show that the slope of the titration curve after the equivalence point decreases toward zero as  $K_{I,MA}$  increases. This is because a larger and larger fraction of the added  $A^-$  goes into the organic phase as the species MA. A second effect of an increase in  $K_{I,MA}$  is evident in curves 4 through 7 and is analogous to the second effect of  $K_{I,BHX}$  noted above. It, too, may be understood in terms of Le Chatelier's principle, with an increase in  $K_{I,MA}$  having an effect similar to a decrease in  $K_s$ . The slopes of the two branches of the titration curve approach one another until, in curve 7, the situation is the same as if no  $A^-$  were being added to the system (i.e., the absorbance remains constant, due only to



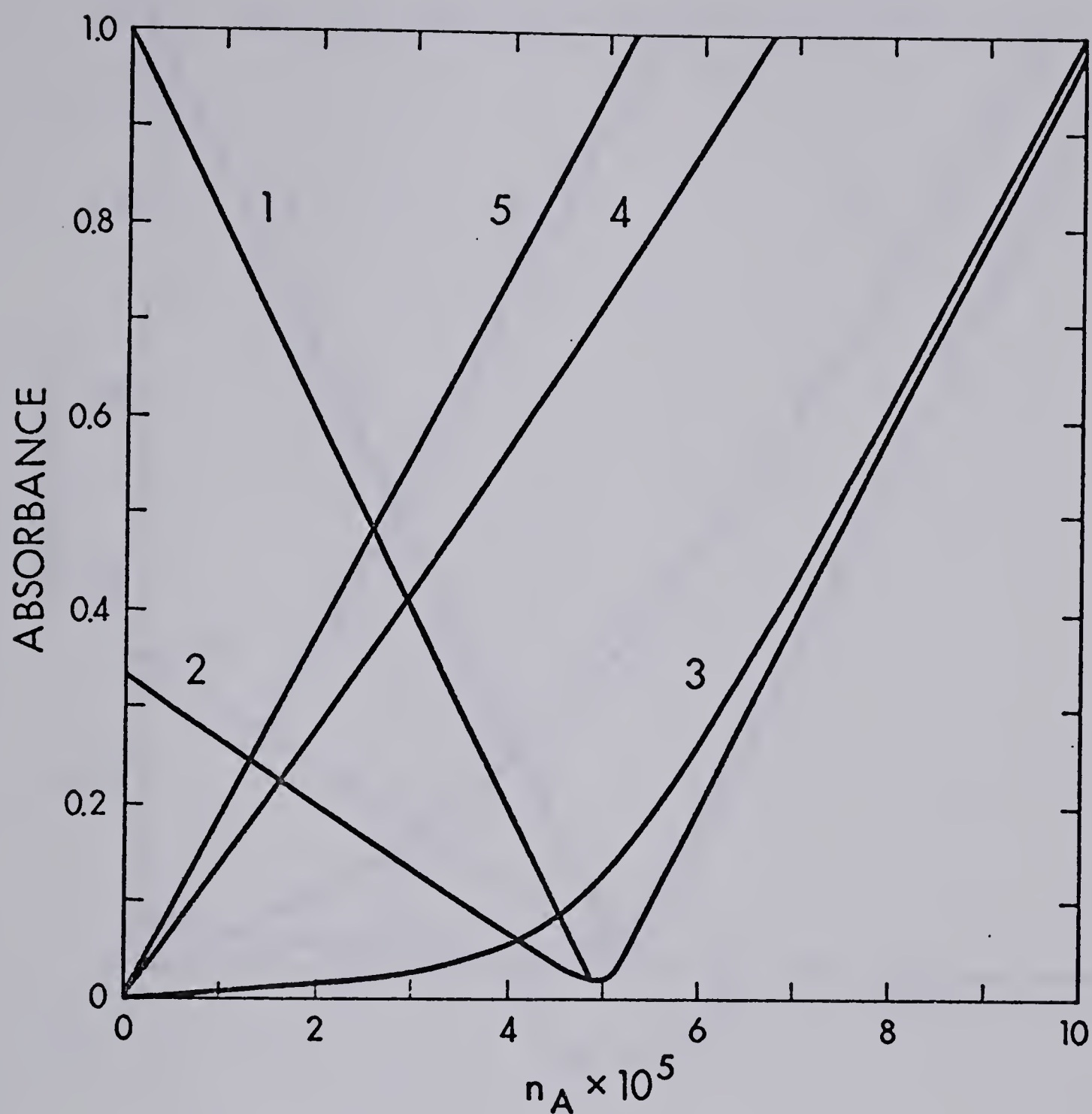


FIGURE 17. Theoretical titration curves for acid  $\text{BH}^+$  in a two phase system. Effect of  $K'_a$  on the shape of the titration curve. (Curves calculated from equations 36 and 37 for absorbance of aqueous phase.)

All parameters as in Figure 15 except  $K_S = 10^8$ .

Curve No.	1	2	3	4	5
$K_a$	$10^{-12}$	$10^{-8}$	$10^{-6}$	$10^{-4}$	$10^{-3}$



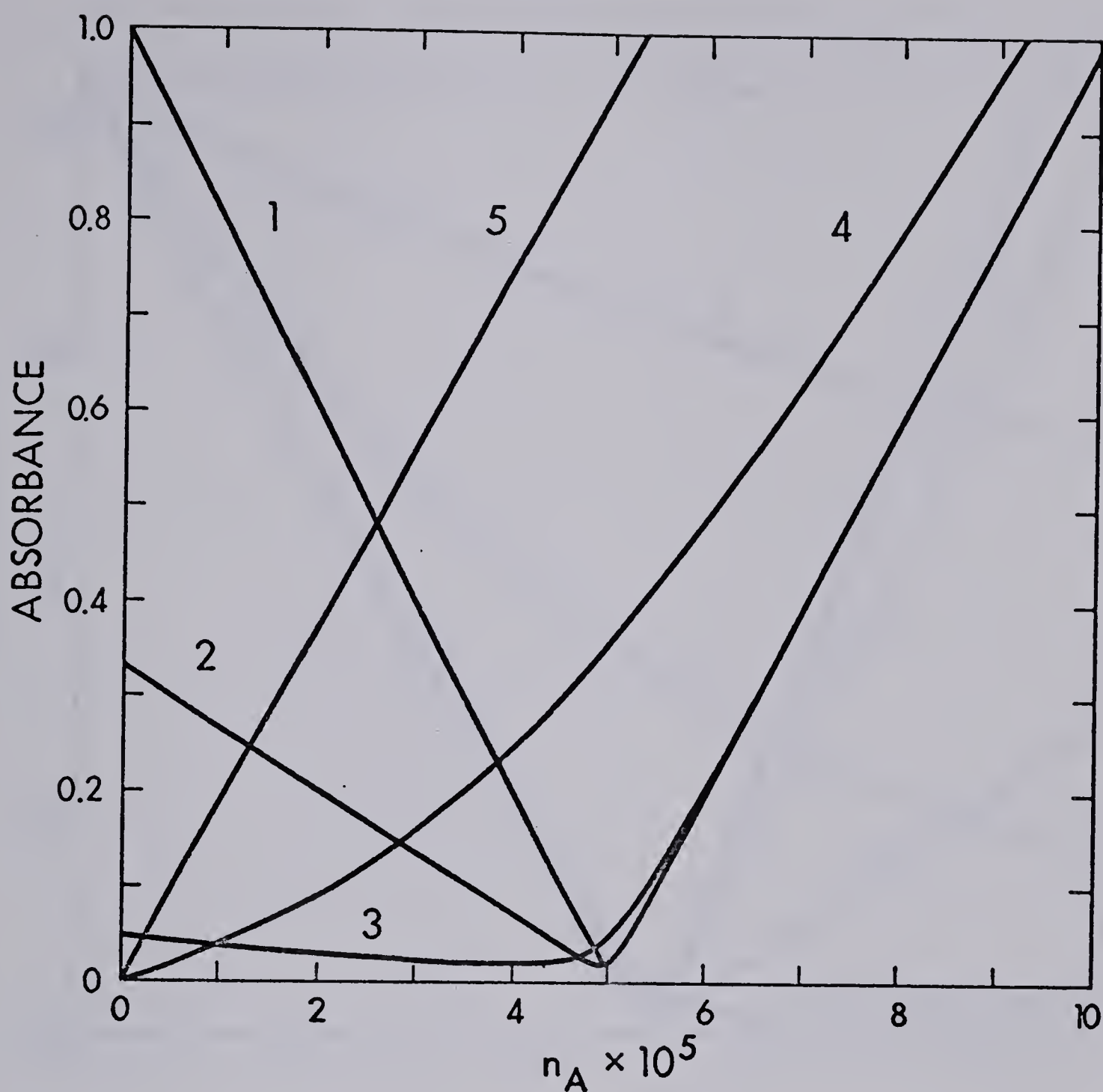


FIGURE 18. Theoretical titration curves for acid  $\text{BH}^+$  in a two phase system. Effect of  $K_B$  on the shape of the titration curve. (Curves calculated from Equations 36 and 37 for absorbance of aqueous phase.)

All parameters as Figure 15 except  $K_S = 10^8$ .

Curve No.	1	2	3	4	5
$K_B$	0.0	$10^7$	$10^8$	$10^{10}$	$10^{12}$



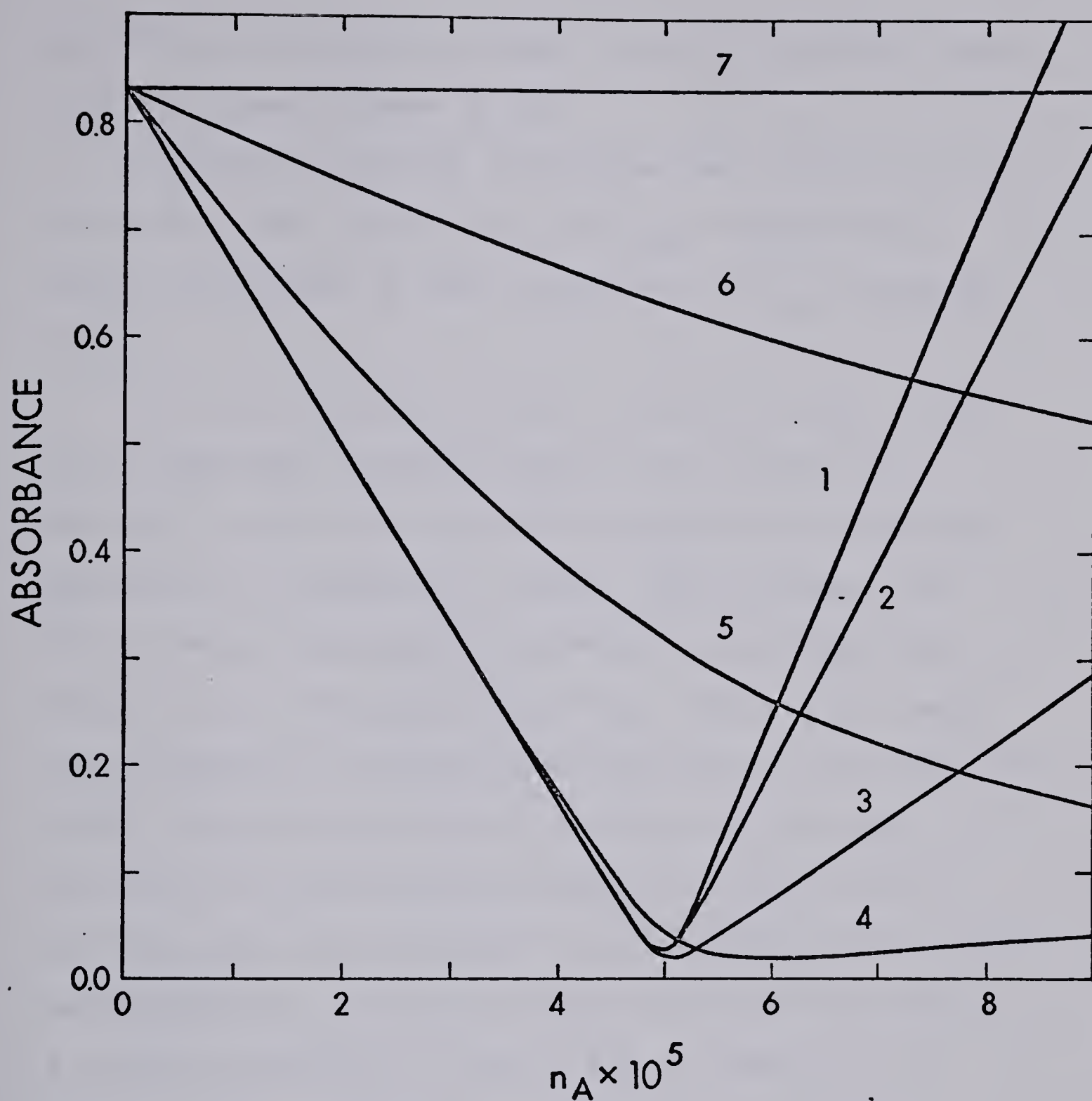


FIGURE 19. Theoretical titration curves for acid  $BH^+$  in a two phase system. Effect of  $K_{I,MA}$  on the shape of the titration curve. (Curves calculated from equations 36 and 37 for absorbance of aqueous phase.)

All parameters as in Figure 15 except  $K_S = 10^8$ .

Curve No.	1	2	3	4	5	6	7
$K_{I,MA}$	0	1.0	10	$10^2$	$10^4$	$10^5$	$10^{12}$



the  $\text{BH}^+$  in the aqueous phase), since all added  $\text{A}^-$  goes into the organic phase as MA.

Figures 20 and 21 illustrate the influence of an increase in the value of  $K'_b$  and  $K_{\text{HA}}$ , respectively. These are similar to the influence of  $K_{\text{I,MA}}$  discussed above.

A final parameter to be considered is pH. This is an important variable since it can readily be altered in order to obtain an optimum curve shape by selection of a different buffer. The influence of pH is exerted through the acid-base equilibria described by the constants  $K'_a$  and  $K'_b$ . Since a pH change simultaneously influences both equilibria, the observed effect of pH on the titration curve will be some combination of the effects shown in Figures 16-21. In Figure 22 are presented titration curves which would be obtained at various pH values between 0 and 9 for a titrant with  $\text{pK}'_b = 11$  and a sample with  $\text{pK}'_a = 9$ . At low pH the protonation reaction of the titrant  $\text{A}^-$  becomes more extensive and shifts the ion-pair equilibrium between  $\text{BH}^+$  and  $\text{A}^-$  to the left (Le Chatelier). On the other hand, at high pH the deprotonation of the sample species  $\text{BH}^+$  becomes more extensive and has a similar effect. Consequently, if both titrant anion  $\text{A}^-$  and sample cation  $\text{BH}^+$  can undergo acid-base side reactions there will be some inter-



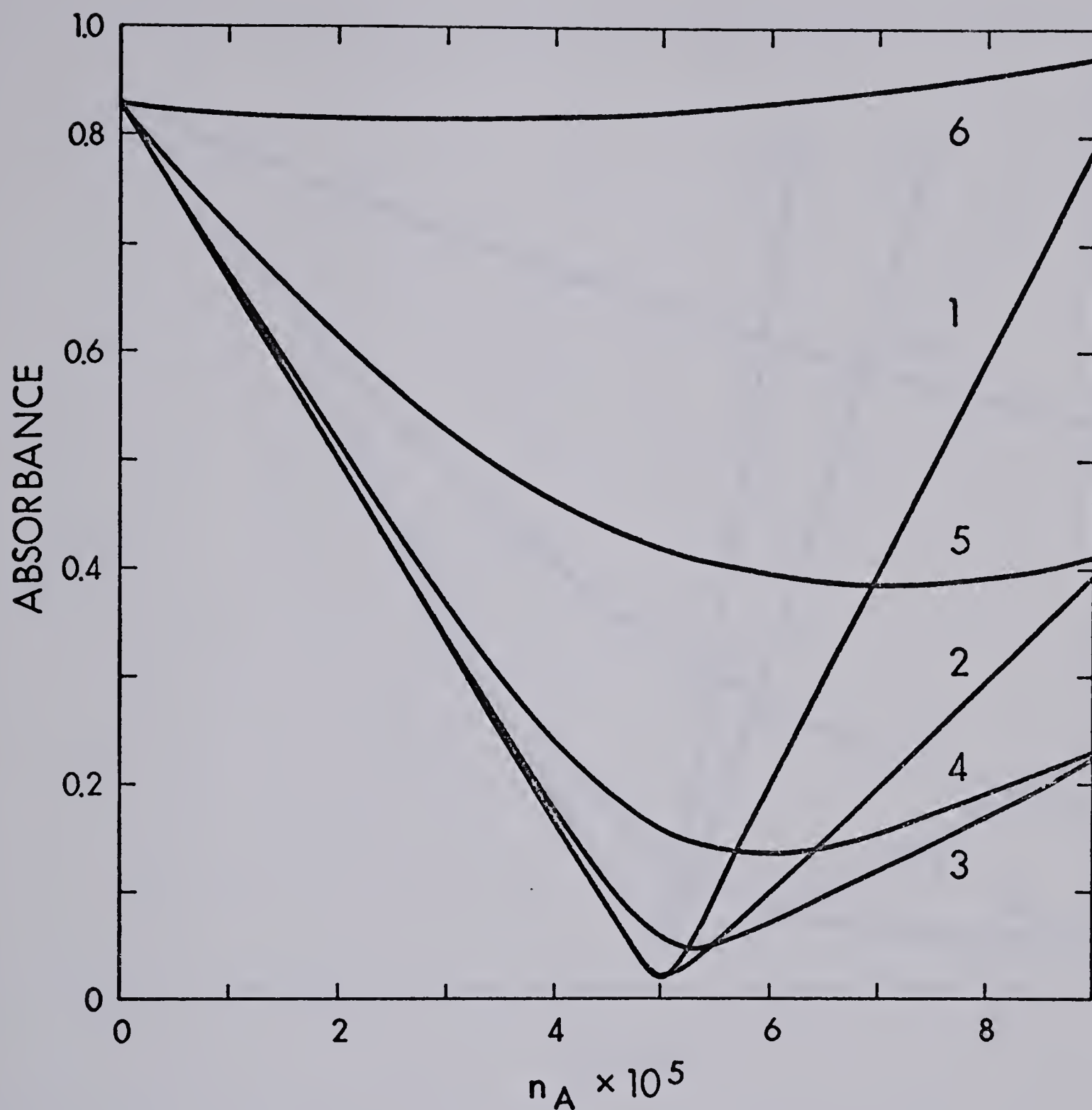


FIGURE 20. Theoretical titration curves for acid  $BH^+$  in a two phase system. Effect of  $K'_b$  on the shape of the titration curve. (Curves calculated from Equations 36 and 37 for absorbance of aqueous phase.)

All parameters as Figure 15 except  $K_S = 10^8$ .

Curve No.	1	2	3	4	5	6
$K_b$	$10^{-14}$	$10^{-12}$	$10^{-11}$	$10^{-10}$	$10^{-9}$	$10^{-8}$



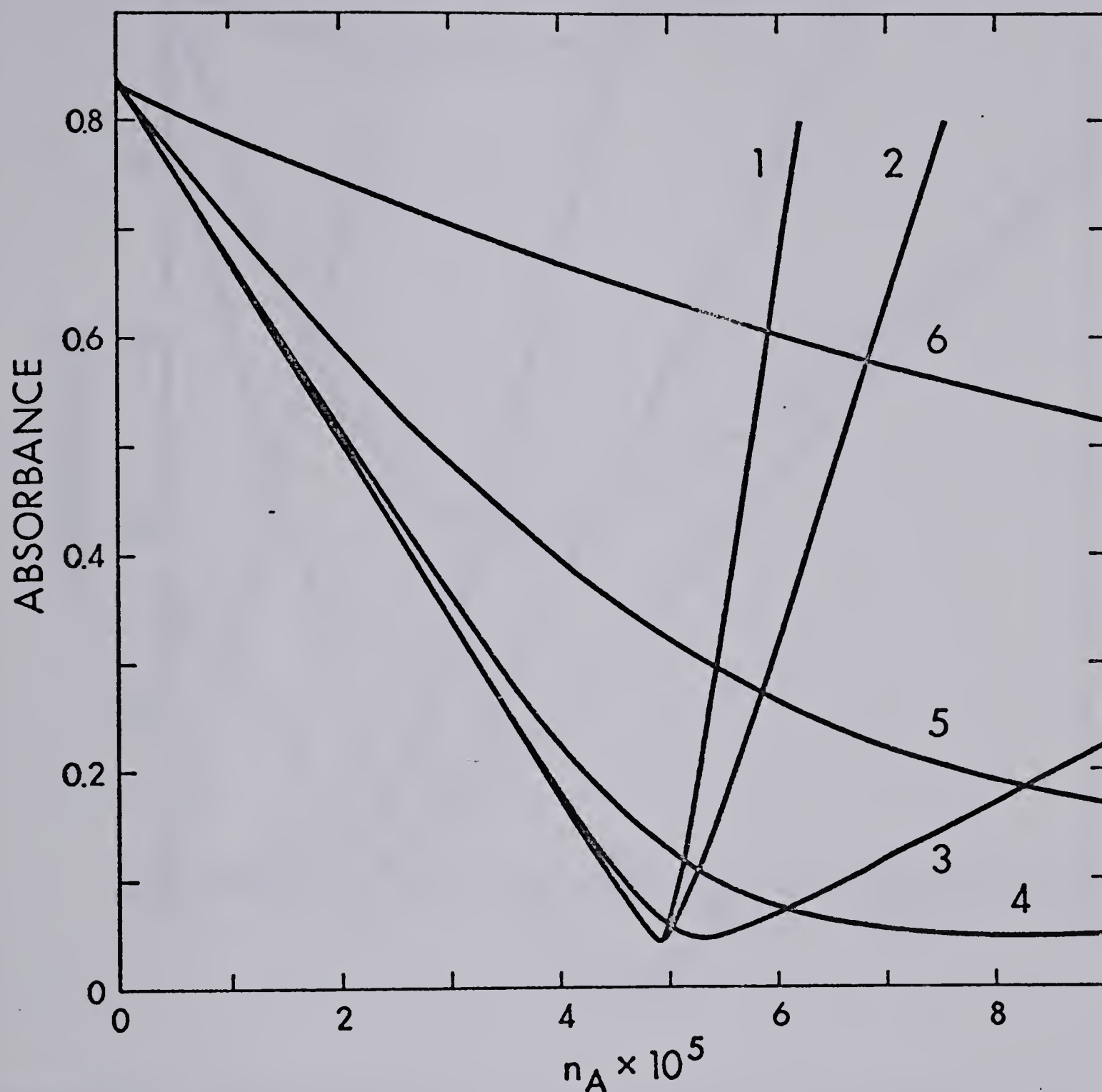


FIGURE 21. Theoretical titration curves for acid  $BH^+$  in a two phase system. Effect of  $K_{HA}$  on the shape of the titration curve. (Curves calculated from equations 36 and 37 for absorbance of aqueous phase.)

All parameters as Figure 15 except  $K_S = 10^8$ ;  $K'_b = 10^{-11}$ .

Curve No.	1	2	3	4	5	6
$K_{HA}$	0	1.0	$10^2$	$10^3$	$10^4$	$10^5$



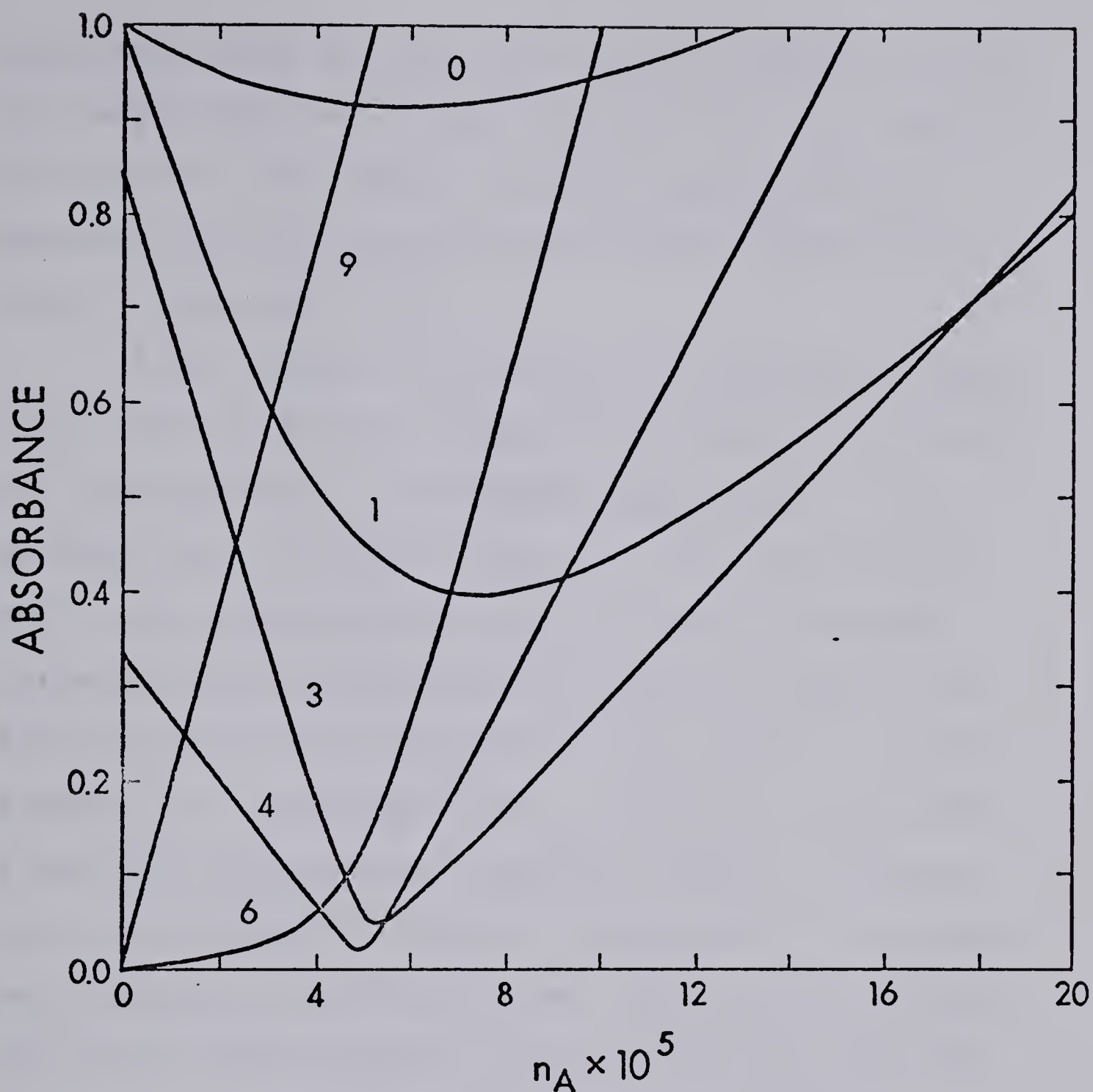


FIGURE 22. Theoretical titration curves for acid  $\text{BH}^+$  in a two phase system (monitoring the aqueous phase). Effect of pH on the shape of the titration curve. (Curves calculated from equations 36 and 37 for absorbance of aqueous phase.) All parameters as in Figure 15 except  $K_s = 10^8$ ;  $K_b = 10^{-11}$ . Numbers on the curves are pH values.



mediate pH value at which the reaction between titrant and sample will be most quantitative. For the example in Figure 22 the endpoint could be most accurately obtained by linear extrapolation of the branches of curve 4, obtained at  $\text{pH} = 4$ .

If the values of  $K'_a$  and  $K'_b$  are both fairly large (e.g.  $10^{-4}$ ) it may be impossible to find a pH at which the titration can be successfully performed. If  $K'_a$  is very small or equal to zero, as would be the case for a quaternary ammonium cation, then a successful titration can be performed at a high pH at which the titrant would not be protonated. Conversely, if the titrant is a sulfonate anion or some other anion with a very low  $K'_b$ , then the titration could be performed at a low pH where a negligible amount of the conjugate base species B would be formed. If both  $K'_a$  and  $K'_b$  are low, as in the titration of a quaternary ammonium ion with a sulfonate ion, then the choice of pH is not critical. It should be understood that the shapes of the curves shown in Figures 15 - 22 are markedly dependent on the values of the parameters which have been held constant in those figures. These values were chosen simply because they made it possible to illustrate the effects of the variable under consideration.

Another frequently encountered situation is that



in which the titration is performed at a wavelength at which only the titrant absorbs. In this case the left branch of the titration curve is horizontal. Conversely, if only the sample absorbs then the right branch is horizontal.

Although it is sometimes convenient to account for the effects of any side reactions on the main ion-pair forming reaction by the use of a "conditional" ion pair extraction constant (28), there is no particular advantage to that approach in the present case. This is because it is necessary to account explicitly (i.e. in terms of the appropriate individual equilibrium constant) for the concentration of each absorbing species in the titration equation.

2.2.2.2 Absorbance of Organic Phase Monitored; Titrant  $A^-$ . Equations 38 and 39 can be used to predict titration curves, under various experimental conditions, for cases in which any or all of the chemical species in the organic phase absorb radiation at the wavelength of interest. However, it is anticipated that the technique will be most attractive for the titration of non-colored sample ions (e.g. surfactants) with colored titrant ions, since such a titration can be performed in a colorimeter. For this reason, only titrant-containing species are assumed to absorb in



the theoretical curves shown in Figures 23 and 24. Since the effects produced by varying the parameters in equations 38 and 39 are analogous (though opposite in sign) to those in Figures 15 - 22, it is not necessary to discuss them in detail. Only the role of  $K_S$  (which will be effected by choice of titrant  $A^-$ ) and the role of pH (which is readily controlled by the choice of buffer) will be discussed.

The influence of  $K_S$  on the titration curve of a sample  $BH^+$  with titrant  $A^-$  is shown in Figure 23. Values of all of the other parameters, given in the caption, are about what would apply to the titration of an organic ammonium sample ion with a titrant like picrate. It is evident from the figure that a titrant should be chosen which gives as large a value of  $K_S$  as possible, all other things being equal. In general, it can be shown that larger values of  $K'_b$ , larger values of  $K'_a$ , and more dilute sample solutions (larger  $V$  or smaller  $n_{BH}$ ) will have an effect similar to that produced by smaller values of  $K_S$ . A larger volume of organic solvent ( $V_O$ ), however, will improve the curve shape, though the effect is not pronounced. An increase in any of the side reaction equilibrium constants  $K_B$ ,  $K_{I,BHX}$ ,  $K_{HA}$  and  $K_{I,MA}$  will yield poorer titration curves.

Figure 24 shows that the correct choice of pH



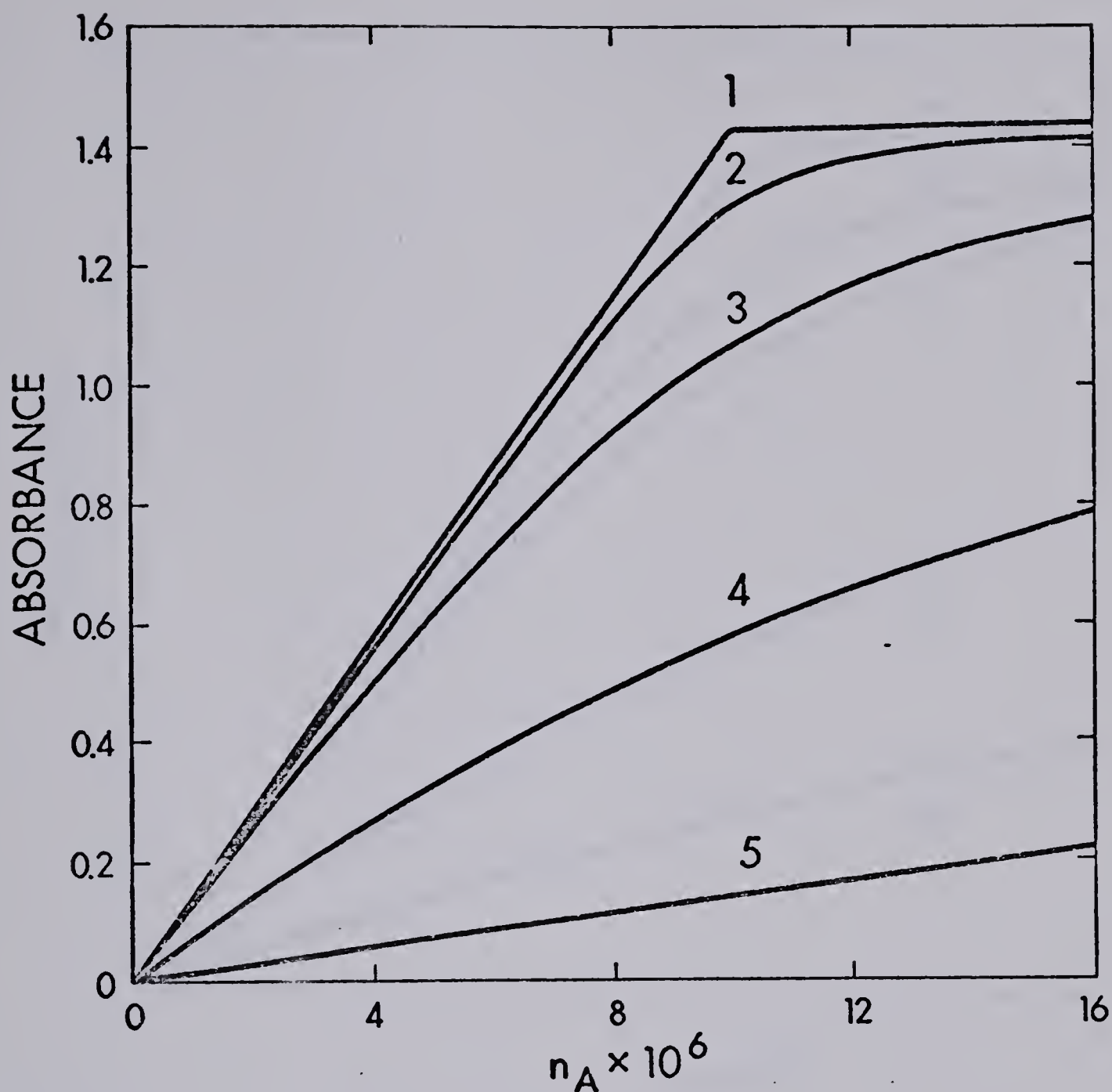


FIGURE 23. Theoretical titration curves for acid  $BH^+$  in a two phase system (monitoring the organic phase). Effect of  $K_S$  on the shape of the titration curve. (Curves calculated from Equations 38 and 39.)

---


$$\begin{aligned}
 &K'_a = 10^{-9}; K_B = 10^6; K_I = 1.0; K_{I,NaA} = 0.0; K'_b = 10^{-14}; \\
 &K_{HA} = 10^2; K_w = 10^{-14}; V = 0.03 \text{ L}; V_o = 0.07 \text{ L}; \epsilon'_{BHA} = 10^4; \\
 &\epsilon'_{NaA} = 10^4; \epsilon'_{HA} = 500; \epsilon'_{BH} = 0.0; \epsilon'_B = 0.0; n_{BH} = 10^{-5}; \\
 &a_H = 10^{-3}.
 \end{aligned}$$


---

Curve No.	1	2	3	4	5
$K_S$	$10^{10}$	$10^6$	$10^5$	$10^4$	$10^3$

---



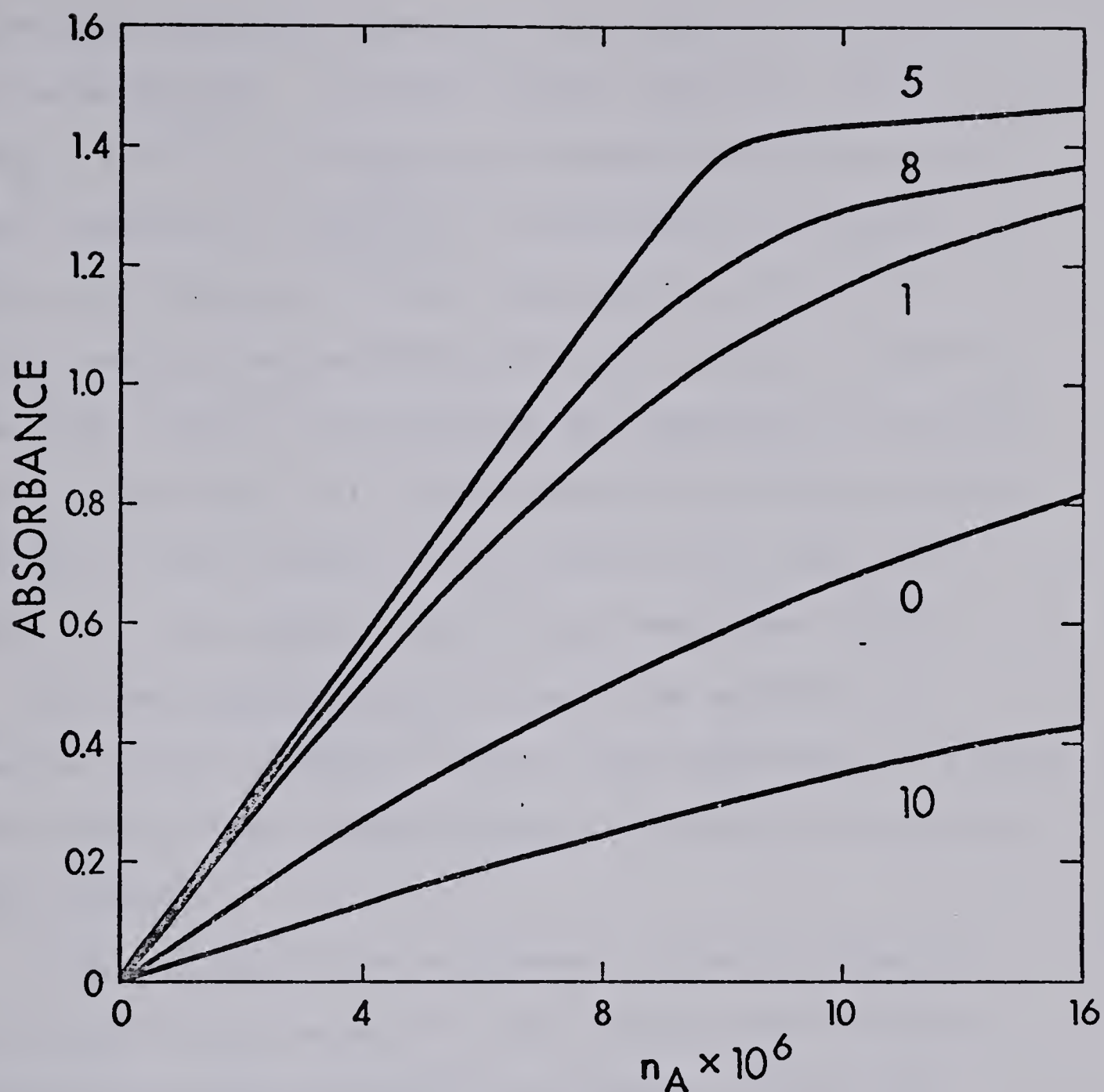


FIGURE 24. Theoretical titration curves for acid  $BH^+$  in a two phase system (monitoring the organic phase). Effect of pH on the shape of the titration curve. (Curves calculated from equations 37 and 38.) All parameters as Figure 23 except  $K_s = 10^{10}$ ,  $K'_b = 10^{-10}$ . Numbers on the curves are pH values.



can be very important when  $BH^+$  is a weak acid and/or  $A^-$  is a weak base. In this example, with  $K'_a = 10^{-9}$  and  $K'_b = 10^{-10}$ , it is only at intermediate pH values in the vicinity of  $(K'_a \cdot \frac{K'_b}{K_w})^{1/2}$  that sharp titration curves are obtained. At low pH protonation of the  $A^-$  ion competes successfully with the ion-pair reaction between  $BH^+$  and  $A^-$ , and at high pH deprotonation of  $BH^+$  is too competitive. It is therefore desirable not only that the titrant yield a large value of  $K_s$  with the sample, but also that it be a very weak base (small  $K'_b$ ). In such circumstances it will be possible to select a pH low enough to repress the hydrolysis reaction of the sample ion without incurring excessive hydrolysis of the titrant.

Considering the more general titration case in which all of the species in the organic phase absorb radiation at the wavelength of interest, it can be shown that the linear segments of the titration curve well before and well after the equivalence point will have the following properties: Before the equivalence point both the slope of the line and its ordinate intercept can have zero or positive values. After the equivalence point the slope of the line can be zero or positive and its intercept can be negative, zero or positive.

Discussions of theoretical titration behavior in



this section have emphasized the titration of sample  $BH^+$  with titrant  $A^-$ . Analogous conclusions can readily be drawn concerning the reverse titration and therefore it will not be discussed in section 2.2.2 (Predicted Titration Behavior) of this thesis.

### 2.2.3 Dilution Correction for Ion-Pair Titrations

Consider first titrations in which the aqueous phase is monitored. The adjustment which must be made on the observed absorbance value to correct for dilution of the aqueous phase which results from addition of titrant may not be the same as that which applies to a one-phase titration medium. The form of the dilution correction can be deduced, as in Section 2.1.3, by considering only the linear terms in the titration expression. It can be shown that there are two linear terms. The first one describes the straight line contribution to the left branch of the titration curve, before the equivalence point, and can be shown to be:

$$n_A = n_{BH} - \frac{A_{obs}}{(\epsilon'_{BH} + \epsilon'_B \cdot K_a / a_H)} \cdot \left[ V + \frac{K'_a \cdot V}{a_H} + K_{I,BHX} \cdot V_O + \frac{K_B \cdot K'_a \cdot V_O}{a_H} \right] \quad (42)$$

The second linear term describes the straight line contribution to the right branch of the curve, after the equivalence point, and has the form:



$$n_A = n_{BH} + \frac{A_{\text{obs}}}{(\epsilon'_A + \epsilon'_{HA} \cdot \frac{K'_b \cdot a_H}{K_w})} \cdot \left[ V + \frac{K'_b \cdot a_H \cdot V}{K_w} + K_{I,MA} \cdot V_O + \frac{K_{HA} \cdot K'_b \cdot a_H \cdot V_O}{K_w} \right] \quad (43)$$

The several different consequences of diluting the aqueous phase with titrant have been described in section 2.1.3 and it may be shown by using the same reasoning that dilution effects can be compensated for as follows: Before the equivalence point, plot:

$$A_{\text{obs}} \cdot \frac{(V + V_A) + \frac{K'_a \cdot (V + V_A)}{a_H} + K_{I,BHX,\text{initial}} \cdot \frac{V}{V + V_A} \cdot V_O + \frac{K_B \cdot K'_a \cdot V_O}{a_H}}{V + \frac{K'_a \cdot V}{a_H} + K_{I,BHX,\text{initial}} \cdot V_O + \frac{K_B \cdot K'_a \cdot V_O}{a_H}} \quad \text{vs. } n_A \quad (44)$$

and after the equivalence point, plot:

$$A_{\text{obs}} \cdot \frac{(V + V_A) + \frac{K'_b \cdot a_H \cdot (V + V_A)}{K_w} + K_{I,MA,\text{initial}} \cdot \frac{V}{V + V_A} \cdot V_O + \frac{K_{HA} \cdot K'_b \cdot a_H \cdot V_O}{K_w}}{V + \frac{K'_b \cdot a_H \cdot V}{K_w} + K_{I,MA,\text{initial}} \cdot V_O + \frac{K_{HA} \cdot K'_b \cdot a_H \cdot V_O}{K_w}} \quad \text{vs. } n_A \quad (45)$$

where  $V$  is the initial volume of aqueous phase,  $V_A$  is the volume of titrant added at any point, and  $K_{I,BHX,\text{initial}}$  and  $K_{I,MA,\text{initial}}$  are the values that prevail at the



initial concentration of the salt MX at the beginning of the titration. It may be noted that if the titrant solution is made to contain the same concentration of buffer and inert salt as is present in the sample solution aqueous phase, then there would be no dilution of  $M^+$  and  $X^-$  and, therefore, no change in the value of  $K_{I,BHX}$  and  $K_{I,MA}$  during the titration. In that case  $(V/V + V_A)$  would disappear from the  $K_I$  terms in equations 44 and 45. Also, when the dilution correction is small as in the present study, it would be possible to render it unnecessary by standardizing the picrate titrant against a primary standard amine drug in the two-phase titration medium without using a dilution correction. When a sample is titrated and the dilution correction is again omitted the small titration error will cancel out. This assumes, of course, that the phase volumes, the titrant volume, and the values of  $K_{I,BHX}$  are not greatly different for the standard and sample compound. In any event, if the volume of titrant required to complete the titration is very small compared to the initial volume of aqueous phase all dilution effects can be ignored.

Consider next titrations in which the organic phase is monitored. When the titration is performed at a wavelength at which only titrant-containing species absorb (e.g. BHA, HA, and MA) and the titrant



is added as an aqueous solution, there is no dilution correction in the linear region of the curve before the equivalence point. This is in contrast to the case in which aqueous phase absorbance is measured. Before the equivalence point in the titration of  $BH^+$  with  $A^-$ , the linear region is given by the expression:

$$A_{\text{obs}} = \frac{\epsilon'_{BHA} \cdot n_A}{V_O} \quad (46)$$

which shows that  $A_{\text{obs}}$  is independent of  $V$ , the volume of aqueous phase. After the equivalence point the linear region is given by the expression:

$$A_{\text{obs}} = \frac{\epsilon'_{BHA} \cdot n_{BH}}{V_O} + (n_A - n_{BH}) \cdot \left[ \frac{\epsilon'_{HA} \cdot \frac{K'_b \cdot K_{HA} \cdot a_H}{K_w} + \epsilon'_{MA} \cdot K_{I,MA}}{V + \frac{K'_b \cdot a_H \cdot V}{K_w} + K_{I,MA} \cdot V_O + \frac{K'_b \cdot k_{HA} \cdot a_H \cdot V_O}{K_w}} \right] \quad (47)$$

In titrations where the pH is high enough that the species HA is negligible, and where the species MA is negligible, the numerator term in the bracketed quantity of equation 47 is essentially zero and the linear portion of the titration curve beyond the equivalence point is a line with slope zero and ordinate intercept  $(\epsilon'_{BHA} \cdot n_{BH} / V_O)$  which has no dilution correction. In cases where the numerator term has a non-zero value so that the linear region beyond the equivalence point has a positive slope a dilution



correction is necessary but it applies only to the second term on the R.H.S. of equation 47. In many cases this correction is small enough to be neglected as it was in all of the titrations described in this thesis for which the organic phase absorbance was measured.



## CHAPTER 3

### EXPERIMENTAL

#### 3.1 Apparatus

The titration apparatus is shown in Figures 25 and 26. The magnetic stirrer (Model 4815, Cole-Parmer Instrument Co., Chicago, Ill.) must be one with a powerful magnet in order to avoid "spin-out" of the 1.5 inch Teflon covered stirring bar at the high speeds necessary to achieve rapid distribution equilibrium. The Teflon lid is held in place against the flat ground glass rim of the titration vessel with an aluminum clamp (not shown in figure). The lid need not be air tight but should provide a snug fit to minimize evaporation of the organic solvent and uptake of CO<sub>2</sub> from the atmosphere. Holes in the lid provide access for the glass buret tip, the filter-probe, the Teflon return tubing and the shaft of the "spoiler". The latter is a 16-mm diameter Teflon rod, to the end of which a 39-mm diameter disc of Teflon is fastened with a force-fit glass pin. The teflon disc is cut along six radii and the pie shaped sections twisted to give the disc a propeller shape. The "spoiler" does not rotate. Its purpose is to minimize vortex formation in the rapidly stirred solution and to increase the shearing effect which facilitates efficient dispersion of one solvent phase into the

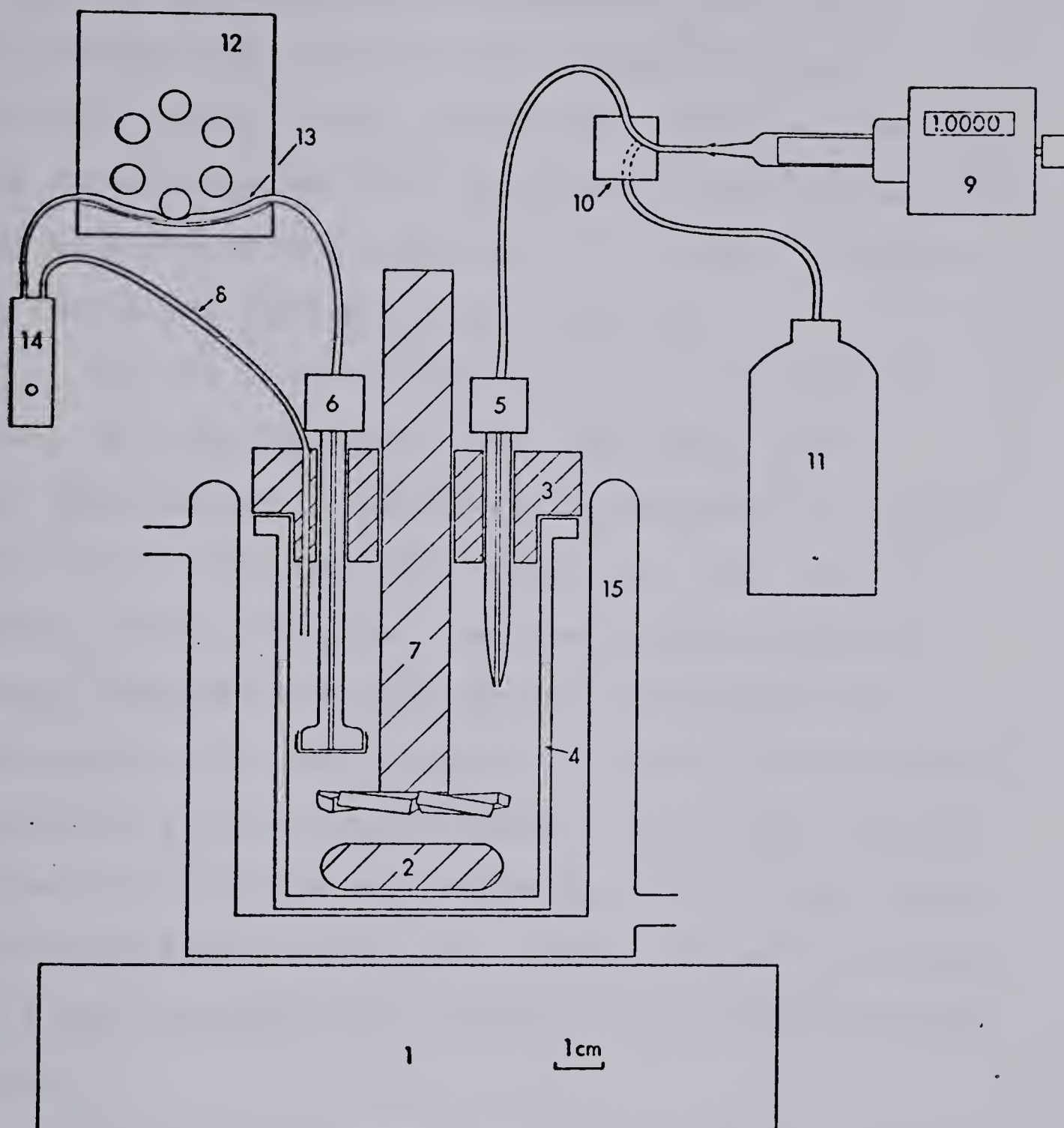




FIGURE 25. Diagram of the titration apparatus.

1. Magnetic stirrer;
2. Stirring bar;
3. Lid;
4. Titration vessel;
5. Buret tip;
6. Filter-probe;
7. Spoiler;
8. Return line;
9. Micrometer buret;
10. Three-way valve;
11. Titrant reservoir;
12. Peristaltic pump;
13. Acidflex pump tubing;
14. Flow cell;
15. Water jacketed beaker.

Only items 2 - 7 are drawn to scale.





other. A properly stirred suspension will appear milk-white with no individual droplets of either solvent visible to the unaided eye. This is necessary for rapid achievement of distribution equilibrium after the addition of each increment of titrant. Stirring is continuous throughout the titration.

Titrant is delivered from a 1-mL micrometer buret (Digipet, Monostat Corp., New York, N.Y.). The glass barrel of the buret is connected to a three-way valve (Model CAV 3031, Laboratory Data Control, Riviera Beach, Florida). Another length of Teflon tubing connects the valve to the glass buret tip. The third valve port is connected to the titrant stored in either a polyethylene reservoir bottle in the case of sodium hydroxide or a volumetric flask, and allows rapid refilling of the buret barrel between titrations by simply switching the valve and retracting the buret piston.

The micrometer buret was calibrated at 6 points over the range 0 to 1 mL by filling it with 0.4763 M NaOH and potentiometrically titrating aliquots of accurately standardized 0.01510 M HCl solution. The buret was found to be accurate and precise to within 1 part per thousand over its entire range.

The filter-probe, shown in exploded view in Figure 26, is constructed by fusing a 13 mm diameter center-



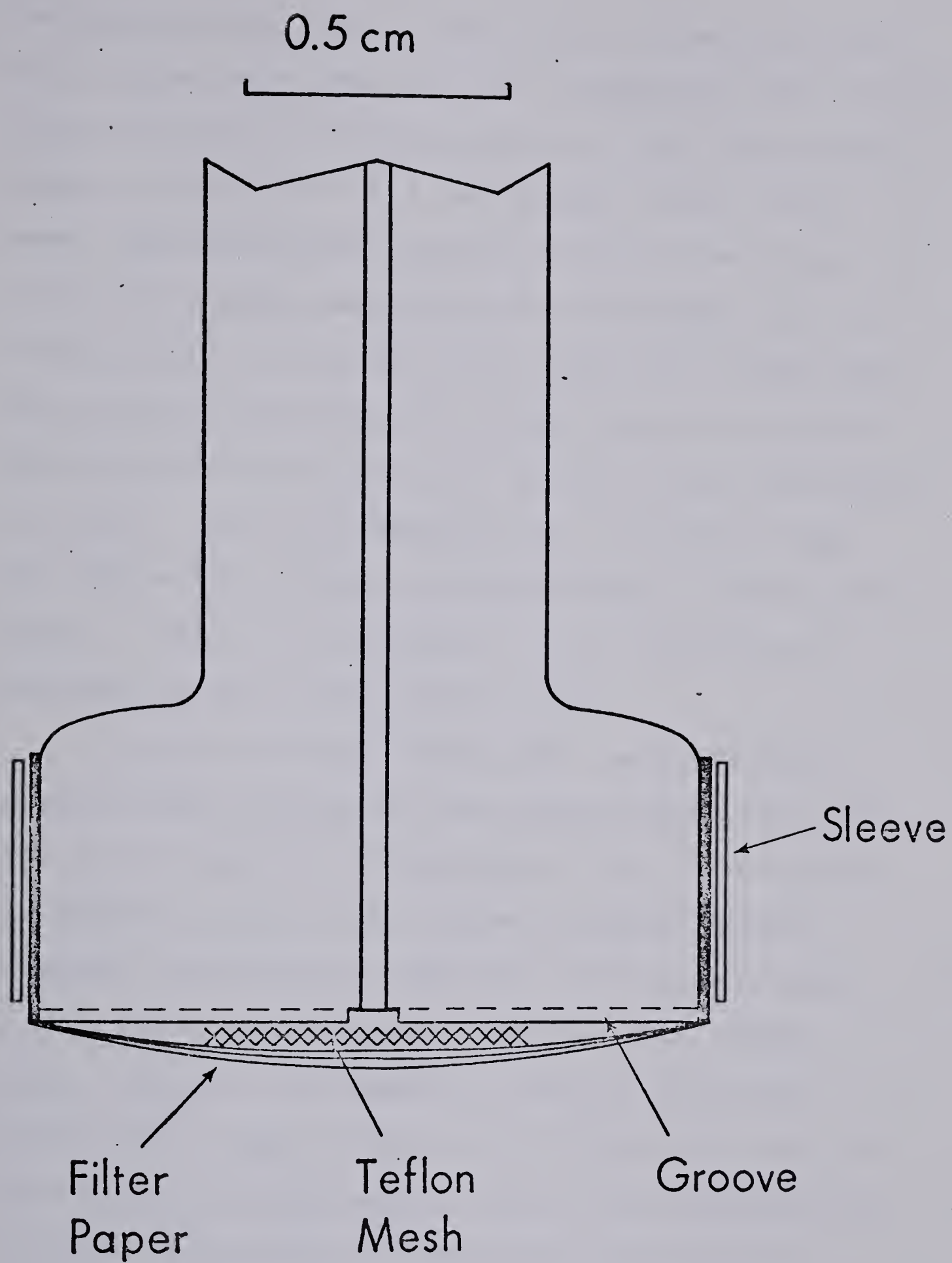


FIGURE 26. Exploded view of the end of the filter-probe.



perforated glass disc to the end of a 1 mm ID by 6.5 mm OD glass tube (part no. G2-C, Laboratory Data Control). The bottom of the probe is grooved. When the aqueous phase is monitored a 6.3 mm diameter coarse Teflon mesh (Laboratory Data Control) is placed over the center of the disc and three 18 mm diameter discs of filter paper are placed over the mesh and folded onto the probe by pressing into a short piece of 13 mm ID Teflon tubing which acts as a sleeve to hold the paper in place. The two innermost discs of filter paper are Whatman No. 5 and the outermost one is Whatman No. 1 paper. Discs of the correct size are conveniently punched out with a No. 10 cork borer.

In order to selectively pump the immiscible organic phase through the spectrophotometer flow cell the triple layer of filter paper on the filter-probe is replaced with a double layer of porous Teflon membrane (Zitex Filter Membrane, 10-20  $\mu$ m pore size, 4 mils thick, NO. E249-122, Chemplast Inc., Wayne, N.J.). Because the membrane is easily perforated by the sharp edges of the coarse Teflon mesh which is used with the filter paper, the mesh is replaced with a 0.8 mm thick wafer of Teflon which is cut to a diameter equal to the bottom of the filter probe and is extensively perforated and lapped smooth. Thus constructed, and with due caution against striking



the membrane surface of the probe against sharp objects, the filter probe has been used for over a hundred titrations without the need to change the Teflon membrane.

The upper end of the filter-probe is connected, via a short piece of Teflon tubing, to either a 1.65 mm ID by 7 cm long or a 1.14 mm ID by 18 cm long piece of Acidflex peristaltic pump tubing (Technicon Corporation, Tarrytown, N.Y.). Connections of Teflon tubing to the glass buret tip and the filter-probe are made with a standard Cheminert fitting (Laboratory Data Control).

Either a Mini-Micro 2/6 peristaltic pump (Brinkmann Instruments Corp., Toronto) or a variable speed Minipuls-2 peristaltic pump (Gibson France S.A., Villiers-leBel, France) were used. The flow rate of the solution is adjusted to about 1.5 mL/min. Solution from the pump passes via Teflon tubing into an 80  $\mu$ L flow cell with a 1.00 cm pathlength (part 178-QS, Hellma Corp., Toronto) and then back into the titration vessel via the return line.

When monitoring the organic phase a porous Teflon filter is placed between the pump and the flow cell to trap the occasional particle of rubber abraded off the inside of the pump tube. This is constructed by sandwiching a small circle of 28 mil thick, 30-50  $\mu$ m pore size Zitex Teflon filter membrane (No. K1064-



222) between two small Teflon rings which are, in turn, held between the flaired ends of the Teflon tubing in a Cheminert tube end fitting (No. TEF 107 and 107A3, Laboratory Data Control). A ten foot length of 0.3 mm ID Teflon tubing is used as a return line to connect the spectrophotometer outlet back to the titration vessel in order to suppress bubble formation in the organic phase at high pumping rates.

A Cary 118 spectrophotometer (Varian Instruments, Palo Alto, Calif.) is used for absorbance measurements. The special cell compartment cover available for this instrument (part 01-640575-00) facilitates initial positioning of the flow cell. All Teflon tubing in the flow system is either 0.3 or 0.5 mm ID. The total volume of the filter-probe, pump tube, flow cell, and associated transmission tubing is either 0.42 or 0.58 mL.

The flat bottomed titration vessel is made from 51 mm ID Pyrex glass tubing with a wide rim that has been lapped flat. During an analysis the titration vessel is placed in a glass jacketed beaker filled with water, and water at  $25 \pm 1^{\circ}\text{C}$  is pumped through the glass jacket from a constant temperature bath.

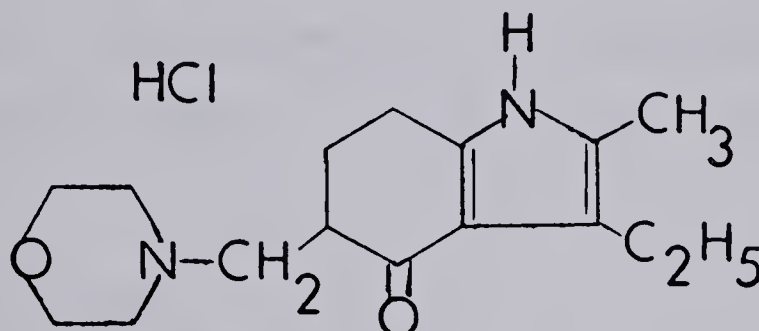
The pH meter was described in the first part of the thesis.



### 3.2 Chemicals

Dextromethorphan Hydrobromide has been described in the first part of this thesis.

Molindone Hydrochloride was supplied by Endo Laboratories. It was analyzed by Fajan's and non-aqueous titration (65) as 99.0%. Its structure is:



Diphenhydramine Hydrochloride was supplied by L. Chatten, Pharmacy Department, University of Alberta. It was analyzed by Fajan's and non-aqueous titration as 99.9% and 99.8% respectively.

Diphenylpyraline Hydrochloride was supplied by L. Chatten. It was analyzed by Fajan's and non-aqueous titration as 98.4% and 98.5% respectively.

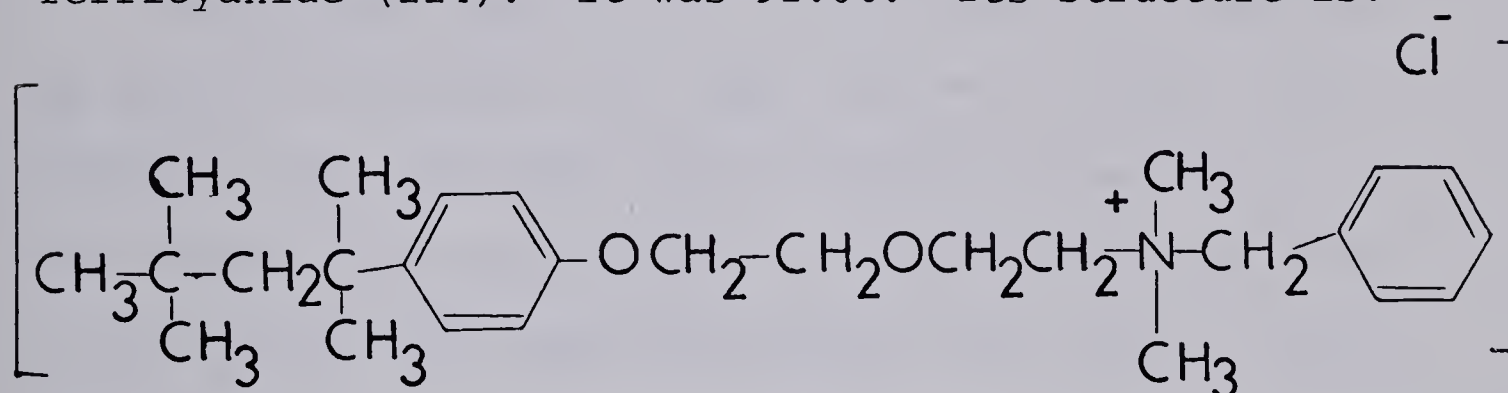
Promethazine Hydrochloride was supplied by Endo Laboratories, Garden City, New York. It was analyzed by Fajan's and non-aqueous titration as 100.0%.

Phenyltoloxamine Citrate was supplied by L. Chatten. It was analyzed by non-aqueous titration as 99.8%.



Dimethoxanate Hydrochloride was supplied by L. Chatten. It was analyzed by Fajan's and non-aqueous titration as 98.6%.

Benzethonium Chloride was supplied by K & K, Plainview, N.Y. It was analyzed by precipitation of ferricyanide salt of the quaternary ammonium ion, filtration, and iodometric determination of excess ferricyanide (114). It was 92.0%. Its structure is:



Hexadecyltrimethylammonium Bromide (Analyzed

Reagent) was supplied by J. T. Baker Chem. Co., Phillipsburg, N.J. It was analyzed as for benzethonium chloride as 96.0%.

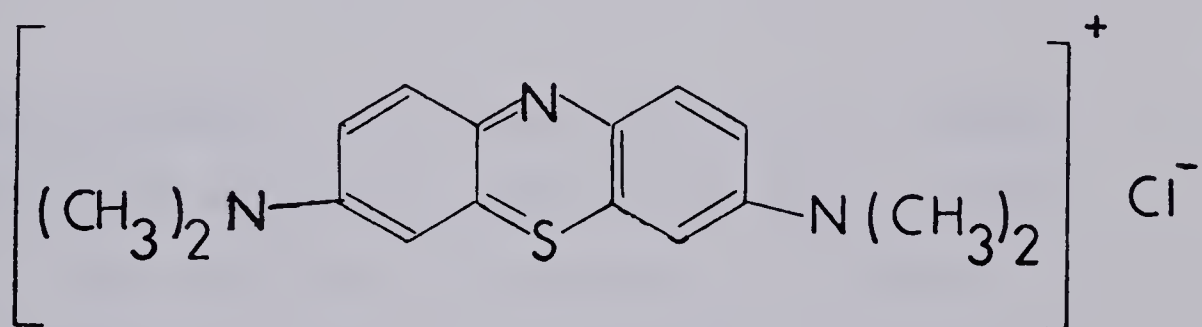
Sodium Lauryl Sulfate (U.S.P. Equivalent) was supplied by Fisher Scientific Co. It was analyzed by two phase ion-pair titration to a visual end point with benzethonium chloride titrant and methylene blue indicator, according to the method of Blank (115) as described in reference 104. It was 81.2%.



Sodium Dodecylbenzene sulfonate was supplied by K & K, Plainview, N.Y. It was analyzed as for sodium lauryl sulfate as 72.3% or 57.9% (see text).

Picric Acid (Reagent Grade) was supplied by Matheson Coleman & Bell Manufacturing Chemists (Catalog No. PX1165).

Methylene Blue (U.S.P. Equivalent) was supplied by Fisher Scientific Co., Cat. No. M-225 (Note: the ordinary grade of this compound which is used for biological staining should not be used, since it has a relatively high impurity content (Ref. 116)). Its structure is:



Other Chemicals including sodium chloride, sodium hydroxide, sodium acetate, potassium phosphate mono-basic, potassium phosphate dibasic, phosphoric acid, ammonium hydroxide, glacial acetic acid, silver nitrate, and perchloric acid, were all analytical reagent grade chemicals. Potassium acid phthalate was primary standard grade.



### 3.3 Reagents

Double distilled water and 1 Molar Sodium Hydroxide have been described in the first part of this thesis.

1 Molar Sodium Chloride was prepared by dissolving 58.5 g of sodium chloride in 1 liter of double distilled water.

Phosphate Buffer (i) pH 2.90 was prepared by combining  $\text{KH}_2\text{PO}_4$  and phosphoric acid to give a final analytical concentration of phosphate of 0.059 M.

(ii) pH 7.50 was prepared by combining  $\text{K}_2\text{HPO}_4$  and sodium hydroxide to give a final analytical concentration of phosphate of 0.075 M.

Acetate Buffer pH 5.00 was prepared by adding sodium hydroxide solution to 400 mL of acetic acid solution. This solution is transferred to 500 mL volumetric flask and diluted to volume with distilled water to give a final analytical acetate concentration of 0.1 M.

Picrate Titrant (0.03868 M) was prepared by dissolving picric acid in double distilled water and was standardized by potentiometric titration with sodium hydroxide titrant.



0.05 Molar Methylene Blue was prepared by dissolving methylene blue in 0.075 M phosphate buffer (pH 7.50), repetitively extracting this solution with chloroform until the chloroform phase was colorless, and diluting to volume with phosphate buffer. This solution was standardized by titrating aliquots of picric acid using the two-phase photometric ion-pair titration method that is the subject of this thesis.

Carbon tetrachloride was supplied by Caledon Laboratories, Georgetown, Ontario.

Chloroform was either analyzed reagent grade (J. T. Baker Chemical Co., Phillipsburg, N.J.) or A.C.S. reagent grade (Caledon Laboratories).

Chloroform/Carbon tetrachloride (1:1) was prepared by mixing the two solvents in a 1:1 ratio and the mixture was stored in gallon quantities for use in the acid-base titrations.



### 3.4 Distribution Isotherms and Molar Absorptivities

The values of all distribution coefficients were determined by batch equilibration experiments. The distribution coefficient of dextromethorphanium ion to be used for calculating the acid-base titration curves was determined between  $\text{CHCl}_3/\text{CCl}_4$  (1:1) and 0.01 M aqueous HCl (pH = 2) that was also 0.10 M in NaCl, by agitating at  $25 \pm 0.1^\circ\text{C}$  and spectrophotometrically determining the dextromethorphan content of the phases. The distribution coefficients were measured at five different equilibrium aqueous phase concentrations of dextromethorphanium ion ranging from  $1 \times 10^{-4}$  M to  $1.3 \times 10^{-3}$  M. The resulting isotherm plot of molarity in organic phase vs molarity in aqueous phase is linear with zero intercept. The slope is numerically equal to the distribution coefficient (Figure 29, below).

Distribution coefficients of dextromethorphanium ion were also measured at single points in 0.50 M NaCl and 0.01 M NaCl, both of which also contained 0.01 M HCl. Distribution coefficients that would prevail in 0.50, 0.10 and 0.01 M total chloride concentrations were calculated from these experimental values using the appropriate activity coefficients and equation 15 (vide infra). The distribution isotherm of dextromethorphan base between  $\text{CHCl}_3/\text{CCl}_4$  (1:1) and dilute NaOH (pH = 13) that was also 0.1 M in NaCl, was



measured in an identical manner to that described above, at equilibrium aqueous concentrations between  $1 \times 10^{-5}$  M and  $1.5 \times 10^{-5}$  M, and yield zero intercept and a linear slope (Figure 29, below).

The molar absorptivities of dextromethorphanium ion ( $\epsilon'_{BH}$ ) and dextromethorphan base ( $\epsilon'_B$ ) were measured in 0.1 M aqueous hydrochloric acid and 0.1 M aqueous sodium hydroxide, respectively, with the measurements made in the spectrophotometer flow cell from the titration apparatus. Beer's law plots were linear on the Cary 118 spectrophotometer up to absorbance values of at least 1.5.

The remaining measurements, described next, were used for calculating ion-pair titration results. The distribution coefficient of promethazinium ion between chloroform and aqueous 0.052 M phosphate buffer (pH = 2.90) was determined at three different equilibrium aqueous phase concentrations of promethazine hydrochloride ranging from  $2 \times 10^{-4}$  M to  $1.0 \times 10^{-3}$  M. The distribution coefficient was constant for all values. The distribution coefficient for dimethoxanatum ion was determined in the same way, except that the measurement was performed at only one sample concentration (ca.  $5 \times 10^{-4}$ ).

The value of  $K_{I,MA}$ , the ion pair distribution coefficient for sodium picrate, was determined between



chloroform and  $\text{pH} = 2.9_0$  phosphate buffer by equilibrating the two phases containing an amount of picric acid sufficient to yield an aqueous phase concentration of about  $7.7 \times 10^{-3}$  M and recording the absorption spectrum of the chloroform. The observed spectrum could be accounted for quantitatively by the small amount of extracted picric acid, indicating the absence of any extracted picrate species. The value of zero for  $K_{I,MA}$  is consistent with the value reported for the distribution coefficient of sodium picrate between methylene chloride and aqueous solution (111).

The distribution coefficient (extraction constant,  $K_S$ ) of promethazinium picrate between chloroform and 0.052 M aqueous phosphate buffer ( $\text{pH} = 2.9_0$ ) was determined by dissolving approximately equimolar amounts of promethazine hydrochloride and picric acid in the two-phase system, agitating at  $25^\circ\text{C} \pm 1^\circ\text{C}$ , and spectrophotometrically measuring the picrate concentration of the aqueous phase. The concentration of promethazinium picrate (BHA) in the organic phase was determined from the mass balance of picrate. The concentration of promethazinium cation in the aqueous phase was determined from its mass balance in the system, and was corrected for the amount extracted as BHX (vide infra). The extraction constant,  $K_S$ , was measured at six different equilibrium aqueous concentrations of promethazinium



ion ranging from  $1.0 \times 10^{-3}$  M to  $7.3 \times 10^{-3}$  M and was found to be constant over this range.

The molar absorptivities of promethazinium ion ( $\epsilon'_{BH}$ ) and promethazine free base ( $\epsilon'_B$ ) in the aqueous phase were determined by procedures analogous to those used above for dextromethorphanium ion and dextromethorphan free base. The molar absorptivity of promethazinium picrate in chloroform at 400 nm was measured by adding an excess of picrate to aqueous solutions containing several different concentrations of promethazine hydrochloride, equilibrating with an accurately known volume of chloroform allowing the phases to separate, and pumping the chloroform phase through the Teflon filter membrane into the flow cell. After correcting for the small amount of neutral picric acid extracted at  $\text{pH} = 2.9_0$  a linear "Beer's Law" plot was obtained for promethazinium picrate.

The distribution coefficient of benzethonium picrate between chloroform and 0.063 M aqueous phosphate buffer ( $\text{pH} = 7.50$ ) at  $25 \pm 1^\circ\text{C}$ , and the molar absorptivity of benzethonium picrate in chloroform were determined by procedures analogous to those used above for promethazinium picrate. The distribution coefficient of benzethonium ion between chloroform and 0.063 M phosphate buffer ( $\text{pH} = 7.50$ ) was determined in the same manner as that used for promethazinium ion.



The molar absorptivity of picric acid in chloroform was determined after a single extraction of a 0.1 M HCl solution of picric acid. The amount of picric acid extracted into chloroform was calculated from the known  $pK_a$  and the distribution coefficient of the neutral picric acid species.

The molar absorptivities of diphenylpyrilinium ion, diphenhydraminium ion, and molindonium ion ( $\epsilon'_{BH}$ ) were measured in 0.1 M HCl.

### 3.5 Titration Procedure

Distilled water to be used in the acid-base titrations is sparged with nitrogen to remove  $CO_2$ . Sparging is not done on water to be used in ion-pair titrations. The organic solvent is shaken in a separatory funnel immediately before use with an equal volume of  $CO_2$ -free water and filtered through dry Whatman No. 2 paper. This washing removes both the ethanol preservative and the small amount of HCl that is usually formed in  $CHCl_3$  upon standing.

In acid-base titrations, a volume of 60.00 mL of  $CO_2$ -free distilled water, 10.00 mL of aqueous NaCl solution, and 10.00 mL of drug solution are pipetted into the titration vessel along with 20.00 mL of  $CHCl_3/CCl_4$  (1:1).



In ion-pair titrations in which the aqueous phase absorbance is monitored, 70.00 mL of 0.059 M phosphate buffer (pH = 2.90), 20.00 mL of chloroform and 10.00 mL of aqueous drug solution are combined in the beaker.

In ion-pair titrations in which the organic phase absorbance is monitored, 25.00 mL of phosphate buffer (pH = 7.50 or 2.90), 70.00 mL of chloroform and 5.00 mL of aqueous sample solution are used.

The lid is fastened in place, with the filter probe, spoiler, return line, and the buret tip in place, and the titration vessel is placed in the water bath. Stirring and pumping are begun. The spectrophotometer is set to 100% T with the aqueous or the organic phase, but before adding sample solution. Now the sample solution is added and after about 4 min the absorbance will have risen to a constant value as distribution equilibrium is reached in the titration vessel. Titrant is now added. After the addition of each increment a period of about 1.5 minutes is required for the absorbance to reach its new plateau value. Figure 27 shows the decrease in the absorbance after each increment of titrant added for dextromethorphan hydrobromide titrated with sodium hydroxide. The photometric titration curve is a plot of plateau absorbance, corrected for dilution if necessary, vs. moles of added titrant.



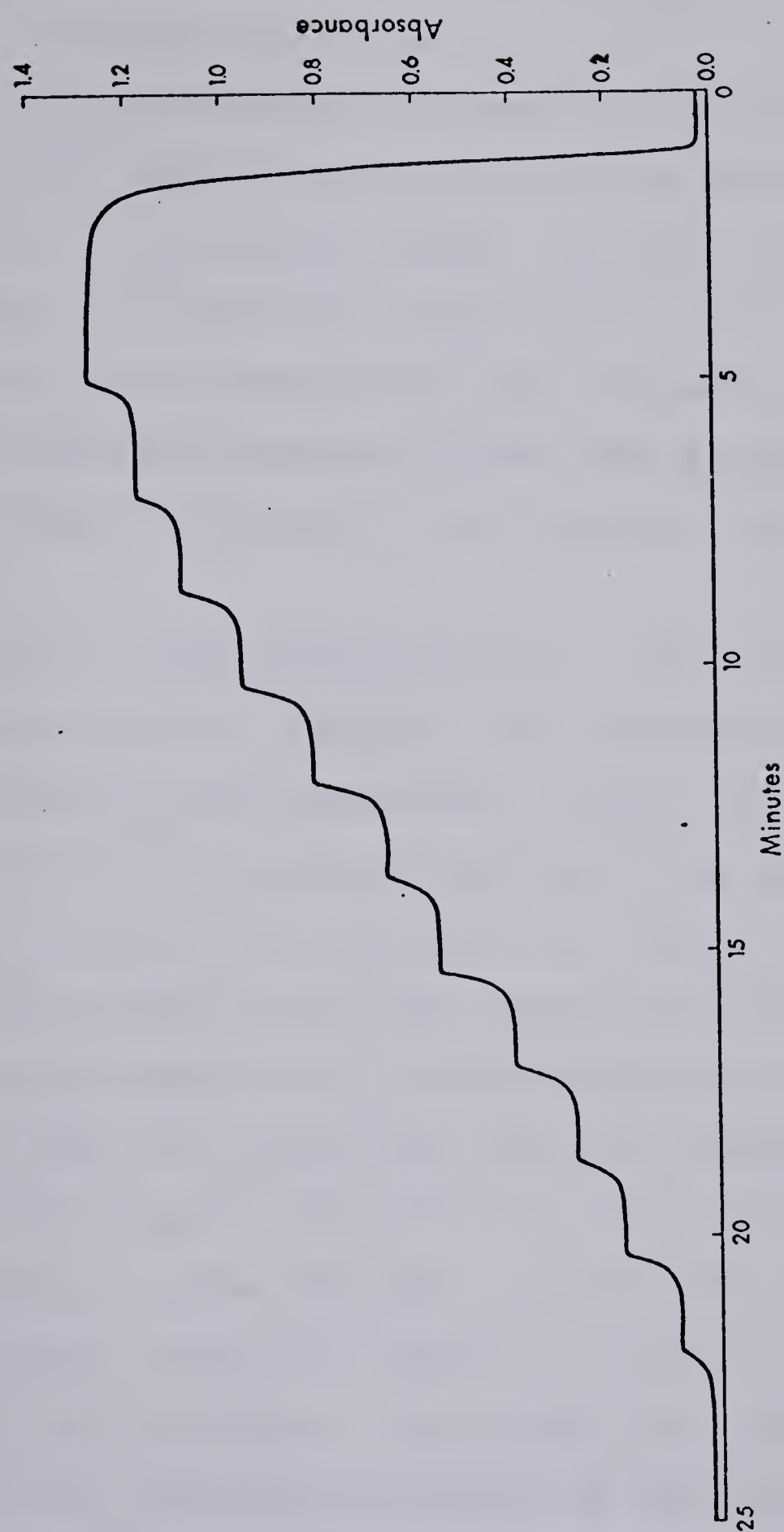


FIGURE 27. Spectrophotometric recorder tracing for the titration of dextromethorphan hydrobromide with sodium hydroxide at 275 nm.



## CHAPTER 4

### RESULTS AND DISCUSSION

#### 4.1 Acid-Base Titrations

The heterogeneous photometric titration equation was tested experimentally by titrating dextromethorphan.HBr with sodium hydroxide titrant. In order to determine the accuracy and precision of the method several pharmaceutical amine hydrohalides were titrated using this system including dextromethorphan.HBr, diphenylpyriline.HCl, diphenylhydramine.HCl and molindone.HCl.

4.1.1 Dextromethorphan.HBr. The heterogeneous titration equation (equation 16) was verified by titrating dextromethorphan.HBr, which is a  $BH^+$  type acid with sodium hydroxide titrant in the presence of a 1:1 mixture of  $CCl_4$  and  $CHCl_3$  as organic phase. Extensive studies have been reported on the ion pair extraction behavior of dextromethorphanium cation with halide ions (30,117,118) and they have demonstrated that 1:1 ion pairs are involved. The titration was performed at three different concentrations of added salt (NaCl) to show the effect of ion pair extraction of BHX on curve shape. The results are presented in Figure 28. The points in Figure 28 are the observed experimental values corrected for dilution using equations 31 and 34, while the solid lines are the





FIGURE 28. Photometric titration curves for dextromethorphan hydrobromide with sodium hydroxide titrant. Lines are calculated from equation 16 and points are experimental.

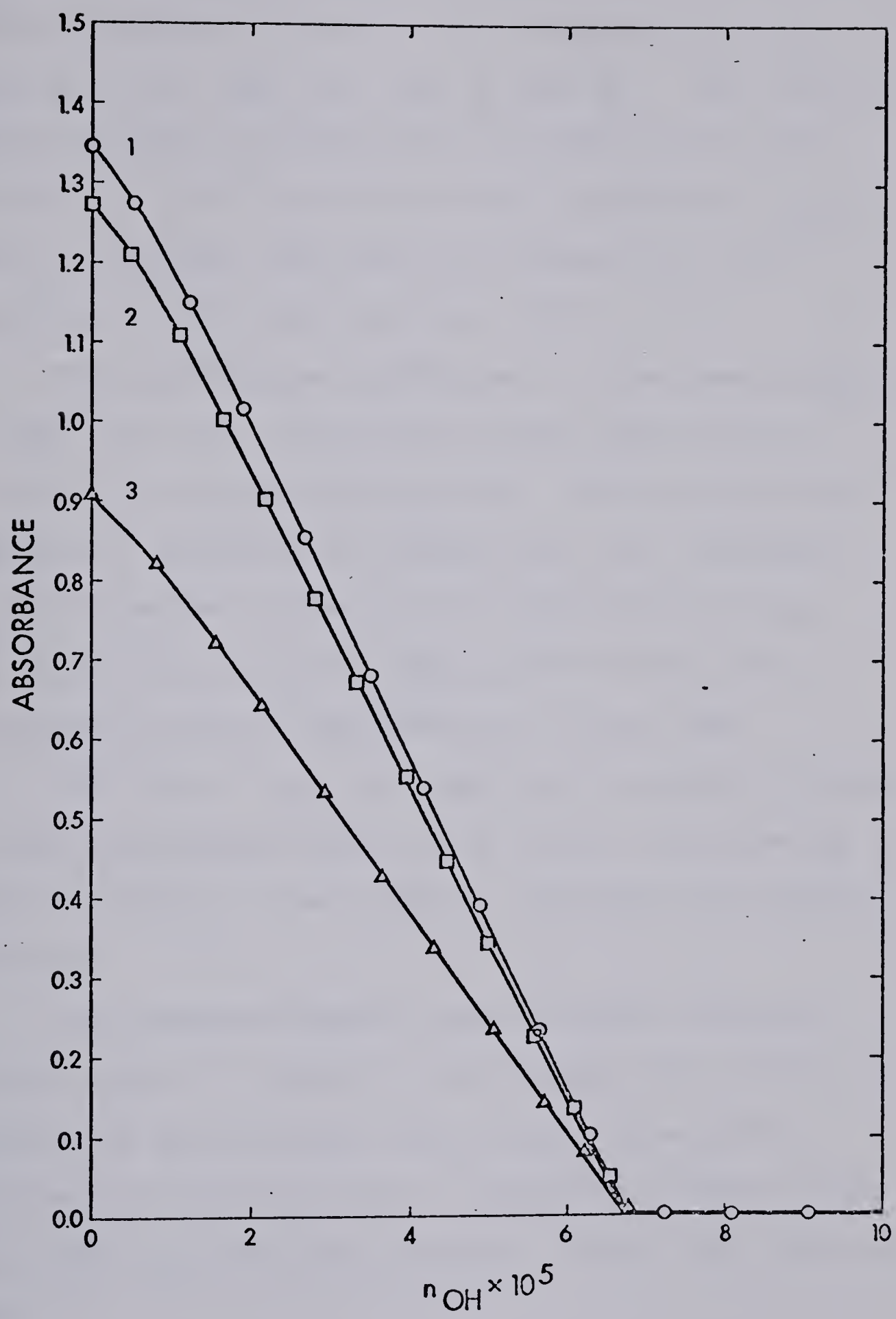
---

$n_{\text{BH}} = 6.72 \times 10^{-5}$  mole;  $\epsilon'_B = 1800$ ;  $\epsilon'_{\text{BH}} = 1840$ ;  
 $K_B = 2.70 \times 10^3$ ;  $K_w = 1.00 \times 10^{-14}$ ;  $V_O = 0.02000$  L;  
 $V = 0.08042$  L;  $\lambda = 275$  nm.

---

Curve No.	$K_I$	$K'_a$	$\gamma_H$	$\gamma_{\text{OH}}$	[NaCl]
1	0.30	$4.57 \times 10^{-9}$	0.91	0.90	0.01 M
2	0.55	$4.11 \times 10^{-9}$	0.83	0.75	0.10 M
3	2.49	$3.81 \times 10^{-9}$	0.76	0.69	0.5 M

---





theoretical curves calculated from equation 16 using known or measured values for the parameters  $K_I$ ,  $K_B$ ,  $\epsilon'_{BH}$ ,  $\epsilon'_B$ ,  $V$ ,  $V_O$ ,  $n_{BH}$ ,  $\gamma_H$ ,  $\gamma_{OH}$ ,  $K_w$  and  $K'_a$ . The value of  $K'_a$  was obtained by multiplying the literature value (30) of  $5.0 \times 10^{-9}$  by the activity coefficient,  $\gamma_{BH}$ , which is computed from tabulated values (119,120) assuming an ionic size parameter of  $8 \times 10^{-8}$ .

The distribution coefficient of dextromethorphanium ion ( $BH^+$ ) at pH = 2 in 0.10 M sodium chloride was determined by batch equilibration. The distribution isotherm, Figure 29A, is linear with zero intercept. The distribution isotherm of dextromethorphan base (B) at pH = 13 in 0.10 M sodium chloride was also determined by batch equilibration (Figure 29B).

The value of  $n_{BH}$  was equal to the number of moles of dextromethorphan hydrobromide taken multiplied by 0.954, the assay value found by nonaqueous and Fajan's titration.

The agreement between predicted and observed results shown in Figure 28 demonstrates the validity of equation 16 and clearly illustrates that accurate photometric titrations may be performed on amine salts which show no significant spectral change upon deprotonation.

In the region just before the end point, the experimental absorbance values fall slightly above the



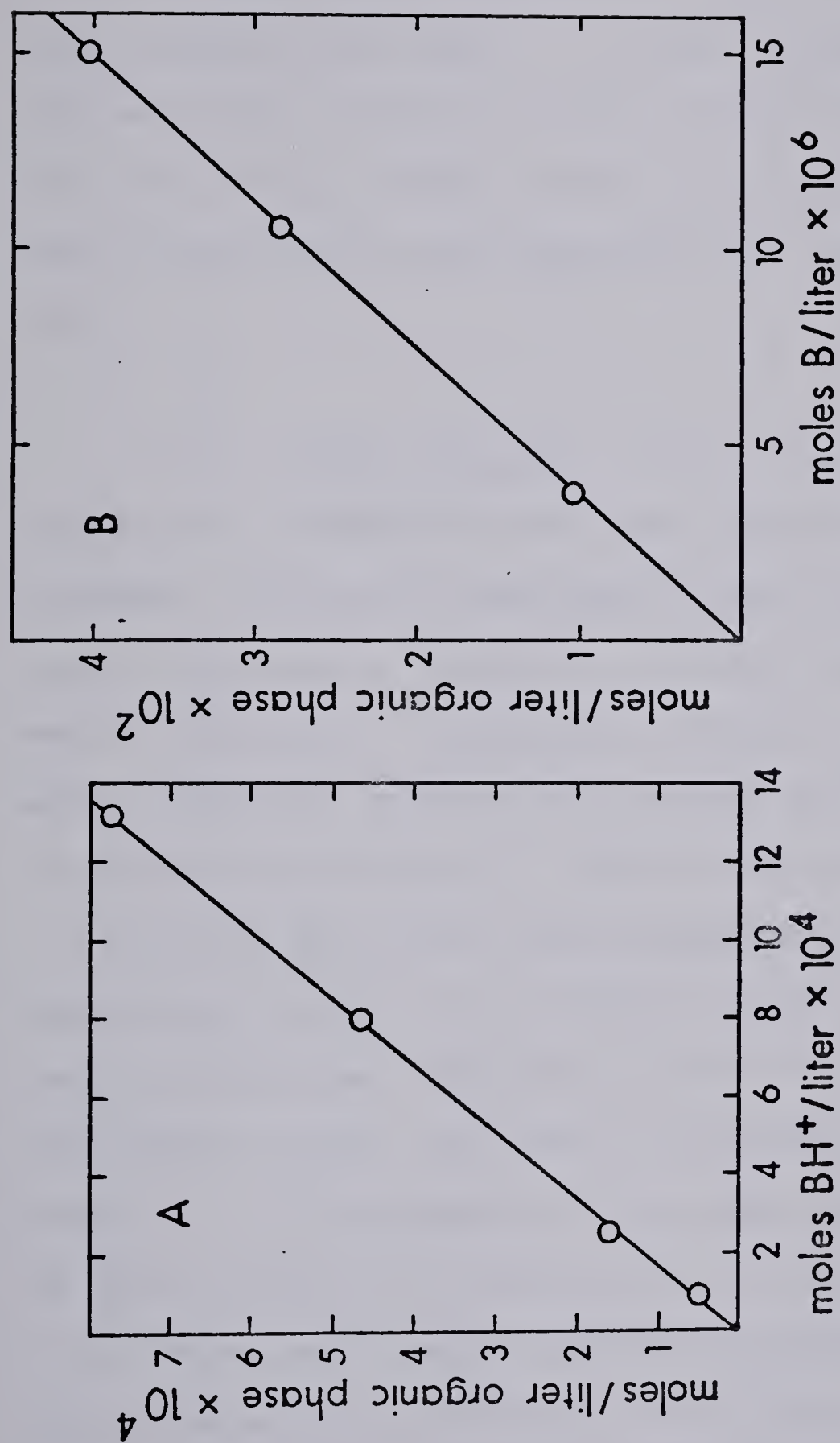


FIGURE 29. Distribution isotherm for dextromethorphanium ion ( $BH^+$ ) and dextromethorphan base (B) between  $CCl_4/CHCl_3$  (1:1) and 0.1 M NaCl aqueous electrolyte. Curve A, pH = 2 ( $BH^+$ ); Curve B, pH = 13 (B).



theoretical line. The reason for this is not known but may be the presence of small amounts of  $\text{CO}_2$  in the titrant. It is not seen when higher (e.g.,  $10^{-2}$  M) sample concentrations are used. It causes no error in locating the end point, if the steepest straight line consistent with the data is drawn through the points before the equivalence point when performing the linear extrapolation.

4.1.2 Assay of Drugs. Four common amine hydrohalide drug substances were each analyzed by three different titration techniques: Fajan's titration for halide, nonaqueous titration, and heterogeneous photometric titration. Results are summarized in Table VI which shows the averages and average deviations obtained in replicate titrations. Sample concentrations were  $> 0.01$  M for the Fajan's and nonaqueous titrations. Approximate sample concentrations during the photometric titrations, assuming all of the compound is in the aqueous phase, are given in the last column of Table VI. All photometric titrations were performed in 80.42 mL of 0.10 M NaCl and 20.00 mL of  $\text{CHCl}_3/\text{CCl}_4$  (1:1) using as titrant standardized solutions of sodium hydroxide between 0.05 M and 0.5 M, depending on drug concentration. Endpoints of the photometric titrations were obtained by linear extrapolation of plots of



TABLE VI.  
Assay Values (%) for Several Drugs by Three Titration Methods

<u>Compound</u>	<u>Nonaqueous</u>	<u>Fajan's</u>	<u>Photometric</u>	<u><math>\lambda</math> nm</u>	<u>Molarity<sup>b</sup></u>
Dextromethorphan·HBr	95.3 $\pm$ 0.07	95.4 $\pm$ 0.07	95.4 $\pm$ 0.1	275	8 $\times$ 10 <sup>-4</sup>
Diphenylpyriline·HCl	98.5 $\pm$ 0.1 <sup>a</sup>	98.4 $\pm$ 0.1	98.3 $\pm$ 0.2	258	3 $\times$ 10 <sup>-3</sup>
Diphenhydramine·HCl	99.8 $\pm$ 0.1 <sup>a</sup>	99.9 $\pm$ 0.1	99.8 $\pm$ 0.05	256	1.7 $\times$ 10 <sup>-3</sup>
Molindone·HCl	99.0 $\pm$ 0.1	99.0 $\pm$ 0.2	99.0 $\pm$ 0.1	300	4.0 $\times$ 10 <sup>-3</sup>

<sup>a</sup>Average deviations are based on at least three replicate titrations in all cases except for these two nonaqueous titrations, where they are based on duplicate titrations.

<sup>b</sup>Approximate molarity of the sample during the photometric titration, assuming that it is all in the aqueous phase.



absorbance (corrected for dilution) versus moles of added sodium hydroxide.

The value of  $K_{I,initial}$  for diphenylpyriline.HCl, diphenhydramine.HCl and molindone.HCl were calculated by using equation 32 and the measured values of  $\epsilon'_{BH}$  as discussed in the theoretical section. This value was substituted in equations 31 and 34 for making the dilution correction.

Assay values found by the photometric titration and the two indicator titrations agree within 1 - 2 ppt. Precisions for all three methods, as indicated by average and average deviations, are also in the range of 1 - 2 ppt.

4.1.3 Advantages of the Method. Considering the additional instrumentation required, it might be asked why one would choose the photometric technique over an indicator titration. The answer is that the photometric titration contains both qualitative and quantitative information about the sample, while indicator titrations contain only quantitative information. For example, if an acid  $BH^+$  with a  $pK_a$  of 9 happened to contain as an unexpected impurity another acid of the  $BH^+$  charge-type with a  $pK_a$  of 5, an indicator titration would yield only one endpoint corresponding to the sum of both compounds. A potentiometric titration with NaOH



titrant would give two endpoints in this case, but if it happened that the impurity also had a  $pK_a$  near 9 then even a potentiometric titration would not detect the presence of the impurity. On the other hand if, as is likely, the impurity had a different molar absorptivity than the acid of interest then, whether or not it had the same  $pK_a$ , the shape of the titration curve of the sample would be different than that for a pure standard of this material. In particular, the slope of the linear portion of the curve before the endpoint would be different for the sample and standard. Looking at it in another way, a photometric titration provides both a photometric and a titrimetric assay and if the two assay values do not agree the analyst is alerted to a peculiarity of the sample.

A distinct advantage of heterogeneous acid-base photometric titrations is the fact that the conjugate species of the sample compound do not need to have different molar absorptivities (86). This is true because the analytical concentration of the sample compound is changing in the phase whose absorbance is monitored during the titration. Such titrations have been called "formal titrations" (86). Major alterations are produced in photometric titration curves as a result of the heterogeneous distribution of acid-base conjugate species between the two phases.



Another advantage is that it is possible to alter the apparent strength of a weak acid ( $BH^+$ ) or base ( $A^-$ ) titrated with NaOH or HCl. This is because the titration product B or HA is distributed into the organic phase, shifting the acid-base equilibrium in the product direction and causing the acid  $BH^+$  to appear as though it was a stronger acid and the base  $A^-$  as a stronger base.

It also becomes possible to differentially titrate mixtures of acids and bases with similar ionization constants but different charge types. Titration of a mixture of acids  $BH^+$  and HA gives two breaks because the neutral acid species HA will distribute to the organic phase and leave most of the  $BH^+$  species in the aqueous phase. The first break will be due to  $BH^+$  species and the second break due to HA species. Two breaks will also arise when titrating bases B and  $A^-$  with HCl.

## 4.2 Ion-Pair Titrations

### 4.2.1 Monitoring the Absorbance of the Aqueous Phase.

Equations 36 and 37 were verified experimentally by titrating promethazine hydrochloride with picrate anion. Four common drugs were titrated with picrate including promethazine.HCl, dextromethorphan.HBr, phenyltoloxamine citrate, and dimethoxanate.HCl in order to demonstrate the precision and accuracy of the method.

4.2.1.1. Promethazine.HCl. In order to test the validity of the proposed titration model for an



acid  $\text{BH}^+$  in chloroform-aqueous buffer medium, promethazine hydrochloride was titrated with picrate titrant. The conditions of the titration are summarized in the caption of Figure 30 which shows a comparison between the predicted and observed titration behavior. The points in Figure 30 (centers of circles) are the observed experimental titration results, not corrected for dilution. The solid line is the theoretical titration curve calculated from Equations 36 and 37 as discussed in the theoretical section. Since the dilution corrections are not completely negligible, the effect of dilution was incorporated in the theoretical curve in order to allow a direct comparison of theory and results over the entire length of the curve.

The values of  $K_S$ ,  $K_{I,\text{BHX}}$ ,  $K_{I,\text{MA}}$ ,  $\epsilon'_{\text{BH}}$  and  $\epsilon'_B$  to be used in calculating the theoretical titration curve were experimentally measured as described in the experimental section and are presented in the caption of Figure 30. The distribution isotherm for promethazinium ion between chloroform and aqueous phosphate buffer, shown in Figure 31, is linear with zero intercept.

The values of  $K'_a$  for promethazinium ion, and of  $K_B$  for the partitioning of promethazine-free base between chloroform and aqueous solution were obtained from the literature and are shown in Table VII. The



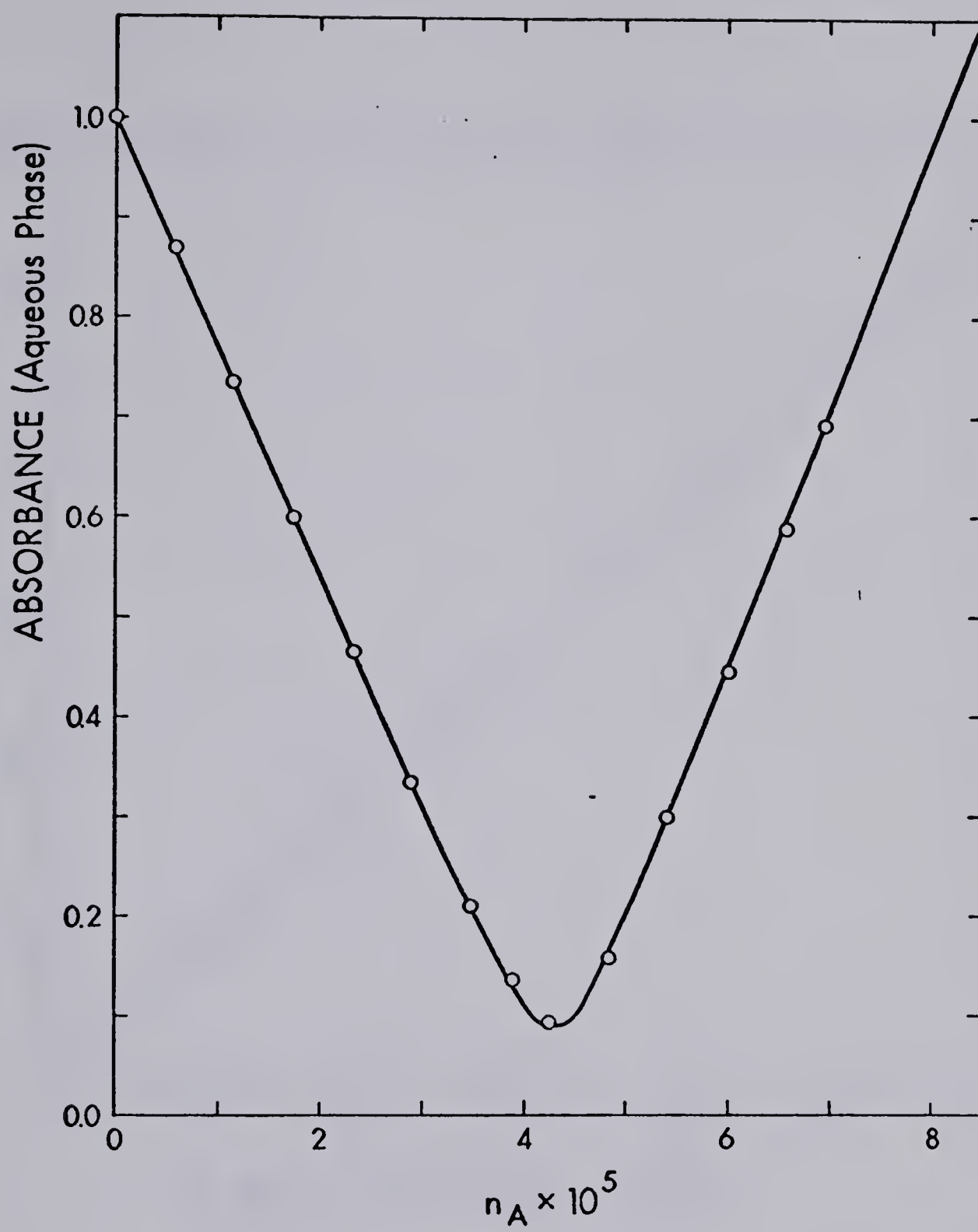


FIGURE 30. Titration curve for promethazine hydrochloride with picrate titrant. The line is calculated from equations 36 and 37 using the values below. Points are experimental.

---

$$\begin{aligned} n_{\text{BH}} &= 4.338 \times 10^{-5} \text{ mole}; V = 0.0800 \text{ L}; V_{\text{O}} = 0.0200 \text{ L}; \\ K'_{\text{a}} &= 1.0 \times 10^{-9}; K'_{\text{b}} = 2.14 \times 10^{-14}; K_{\text{I,BHX}} = 0.90; \\ K_{\text{I,MA}} &= 0.0; K_{\text{B}} = 7.9 \times 10^5; K_{\text{HA}} = 29.5; K_{\text{w}} = 1.00 \times 10^{-14}; \\ \epsilon'_{\text{BH}} &= 2.56 \times 10^3; \epsilon'_{\text{B}} = 1.8_0 \times 10^3; \epsilon'_{\text{A}} = 2.20 \times 10^3; \\ \epsilon'_{\text{HA}} &= 9.1_0 \times 10^3; K_{\text{S}} = 7.2_4 \times 10^6; \text{pH} = 2.9_0. \text{ Wavelength} = \\ &285 \text{ nm.} \end{aligned}$$

---





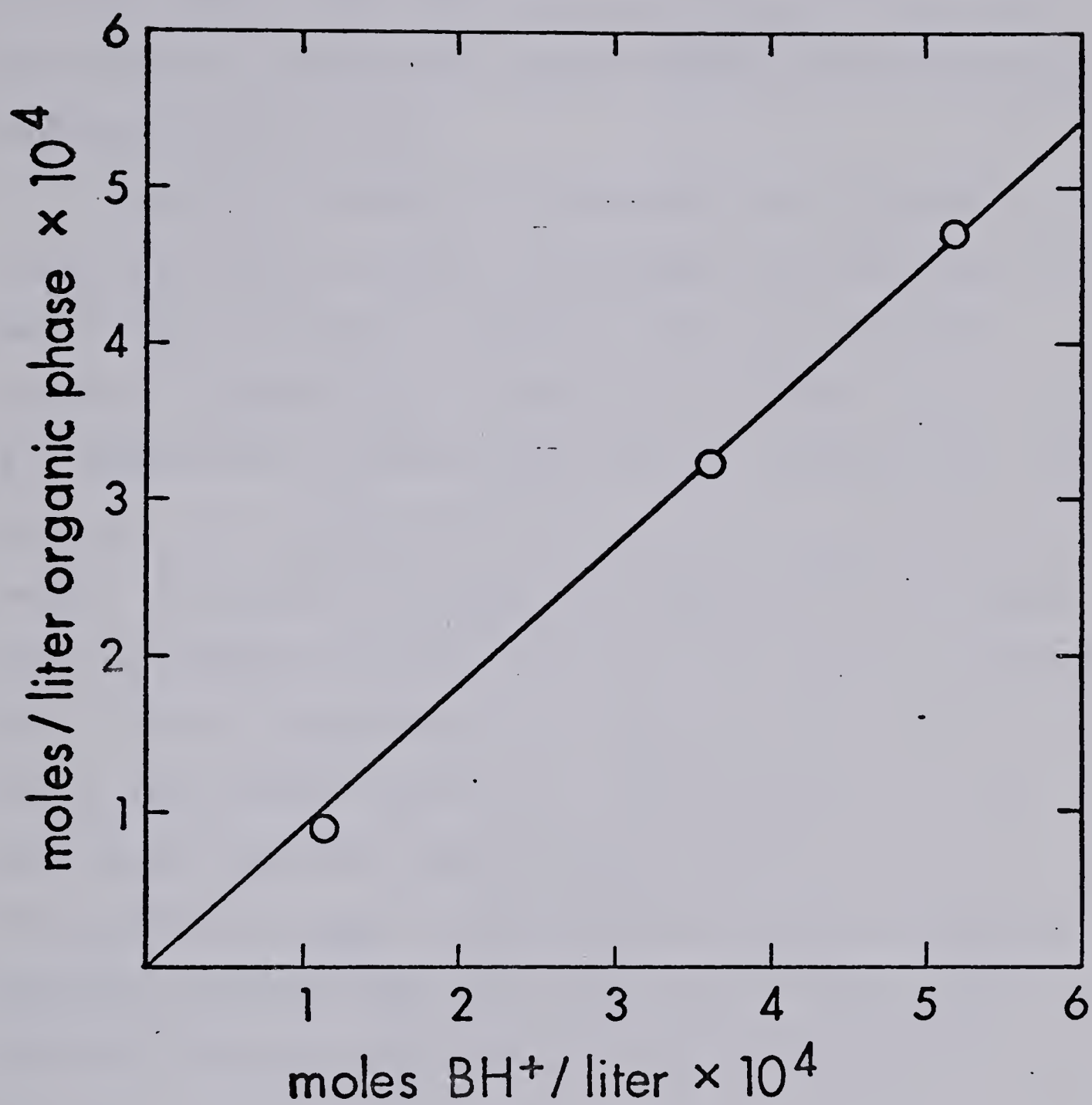


FIGURE 31. Distribution isotherm for promethazinium ion between chloroform and aqueous 0.052 M phosphate buffer pH = 2.90.



value of  $K'_b$ , the basicity constant of picrate ion, is  $2.1 \times 10^{-14}$  (111) and the value of  $K_{HA}$  for the partitioning of picric acid between chloroform and aqueous solution is 29.5 (111).

Agreement between the predicted and observed titration curve in Figure 30 verifies that equations 36 and 37 are an accurate titration function for this system. A comment is in order on the nature of the anion  $X^-$ , which forms an extractable species BH $X$  with the drug cation. It is likely that  $X^-$  is in fact more than one anion. The anions chloride and bromide from the drugs form extractable species with many drug cations (Section 4.1), and it is possible that  $H_2PO_4^-$  from the buffer could also fulfill this role. The composition of the extractable species was not investigated, but the constancy of  $K_{I,BHX}$  for promethazinium ion distributed between chloroform and the buffer was demonstrated at several different drug concentrations (Figure 31).

4.2.1.2 Assay of Drugs. The general utility of picrate as an ion-pair forming titrant for amine drugs was demonstrated by titrating three additional compounds: dextromethorphan.HBr, phenyltoloxamine citrate, and dimethoxanate.HCl. Since  $K_B$  is known for dextromethorphan and phenyltoloxamine (Table VII) the values of  $K_{I,BHX}$  for dextromethorphanium and phenyl-



TABLE VII.  
Values of Constants  
For the Ion-Pair Titrations

<u>Compound</u>	<u>K'<sub>a</sub></u>	<u>K<sub>B</sub></u>	<u>K<sub>I, BHX</sub></u>
Dextromethorphan.HBr	$5.0 \times 10^{-9} \text{ }^a$	$6.3 \times 10^3 \text{ }^a$	0.65
Promethazine.HCl	$1.0 \times 10^{-9} \text{ }^a$	$7.9 \times 10^5 \text{ }^a$	0.90
Phenyltoloxamine.Citrate	$7.9 \times 10^{-10} \text{ }^a$	$6.3 \times 10^5 \text{ }^a$	0.12
Dimethoxanate.HCl	$10^{-9} \text{ }^b$	$3.2 \times 10^5 \text{ }^c$	0.33

<sup>a</sup>Values from Reference 30.

<sup>b</sup>Estimated value for use in equation 41 when making dilution correction.

<sup>c</sup>Measured experimentally in this study.



toloxaminium ions were calculated from equation 42 as follows: Substitute into equation 42 the value of  $n_A$  before adding titrant (i.e.,  $n_A = 0$ ) and rearrange:

$$A_{\text{obs}} = \frac{n_{\text{BH}} \cdot (\epsilon'_{\text{BH}} + \epsilon'_B \frac{K'_a}{a_H})}{(V + \frac{K'_a \cdot V}{a_H} + K_{\text{I,BHX}} \cdot V_0 + \frac{K_B \cdot K'_a \cdot V_0}{a_H})} \quad (48)$$

which is true at the beginning of a titration. Now by knowing all of the other constants in equation 48 and  $A_{\text{obs}}, K_{\text{I,BHX}}$  can be calculated.

The value of  $K_{\text{I,BHX}}$  for dimethoxanatum ion was determined by batch equilibration at pH = 1 for a single point since  $K_B$  was not available in the literature. Then  $K_B$  was calculated from equation 48 from the initial point in the titration.

Dilution corrections were made with equation 44 and 45 using the values of the constants  $K'_a$ ,  $K_B$  and  $K_{\text{I,BHX}}$  shown in Table VII. End points were obtained by linear extrapolation. Neglect of the dilution correction in these titrations would have caused a negative titration error of only 5 parts per thousand.

A comparison of the results obtained for the four amine drugs by the ion-pair titration with the results obtained by nonaqueous titration and, in the case of hydrohalide salts, by Fajan's argentimetric titration is presented in Table VIII. Average values for the



TABLE VIII.

Assay Values (%) and Average Deviations for Several Drugs by Three Titration Methods

<u>Compound</u>	<u>Nonaqueous</u>	<u>Fajan's</u>	<u>Ion Pair</u>	<u><math>\lambda</math> nm</u>	<u>Molarity<sup>b</sup></u>
Dextromethorphan.HBr	95.3 $\pm$ 0.07	95.4 $\pm$ 0.07	95.4 $\pm$ 0.3	275	5.8 $\times 10^{-4}$
Promethazine.HCl	100.0 $\pm$ 0.06	100.0 $\pm$ 0.06	99.5 $\pm$ 0.03	285	5.4 $\times 10^{-4}$
Phenyltoloxamine. Citrate	98.8 $\pm$ 0.05 <sup>a</sup>	---	98.7 $\pm$ 0.2	275	5.9 $\times 10^{-4}$
Dimethoxanate.HCl	98.6 $\pm$ 0.01	98.6 $\pm$ 0.02	98.7 $\pm$ 0.03	285	4.9 $\times 10^{-4}$

<sup>a</sup>Average deviation based on duplicate titrations in this case. For all others it is based on triplicate titrations.

<sup>b</sup>Approximate molarity of the sample during the photometric ion pair titration, assuming that it is all in the aqueous phase.



three titration techniques are all within  $\pm 1$  ppt except in the case of promethazine hydrochloride, for which the ion-pair titration result is 5 ppt lower than the other two. The precision of the ion-pair titration method varies between 0.3 and 3 ppt. It should be kept in mind when comparing the results of the ion-pair titration with those of the other two techniques that the sample concentration is only about  $5 \times 10^{-4}$  M for the former, whereas it is  $> 0.01$  M for the latter two titrations.

The two-phase photometric titration curves of drugs such as diphenhydramine hydrochloride, which have a significantly smaller value of  $K_s$  with picrate ion than do the drugs in Table VIII, show greater curvature in the region of the equivalence point. In the case of quite small or highly polar drug cations, such as that of phenylephrine hydrochloride,  $K_s$  is so small that no accurate linear extrapolations can be made.

4.2.2 Monitoring the Absorbance of the Organic Phase. Cationic and anionic detergents, and cationic drugs are titrated with picrate or methylene blue titrant in a chloroform-aqueous buffer mixture by measuring the absorbance of the chloroform phase.



4.2.2.1. Titration of Cations. Two quaternary ammonium surfactants (benzethonium chloride and hexadecyltrimethylammonium bromide) and the ammonium form of a tertiary amine drug (promethazine hydrochloride) were titrated with picrate titrant in order to test the validity of equations 38 and 39.

Figure 32 shows a comparison between the theoretical titration curve (solid line) and the observed experimental points for benzethonium chloride. The values of  $K_{I,BHX}$ ,  $K_S$ ,  $\epsilon'_{MA}$ ,  $\epsilon'_{HA}$  and  $\epsilon'_{BHA}$  to be used in calculating the theoretical titration curve were experimentally measured as described in the experimental section and are presented in the caption of Figure 32. The distribution isotherm for BHX is shown in Figure 33.

The points, obtained in the actual titration (Figure 32), are seen to lie on the predicted curve suggesting the validity of equations 36 and 37. Since the pH is high (pH = 7.50) so that the amount of the neutral picric acid species (HA) is negligible and since sodium picrate (MA) does not extract (section 3.4), the linear region beyond the equivalence point has a zero slope, and no dilution correction is necessary. In the non-linear region of the titration curve, very near the equivalence point, one should in principle employ a dilution correction. However, the non-linearity is so slight that even in this region the correction is negligibly small.



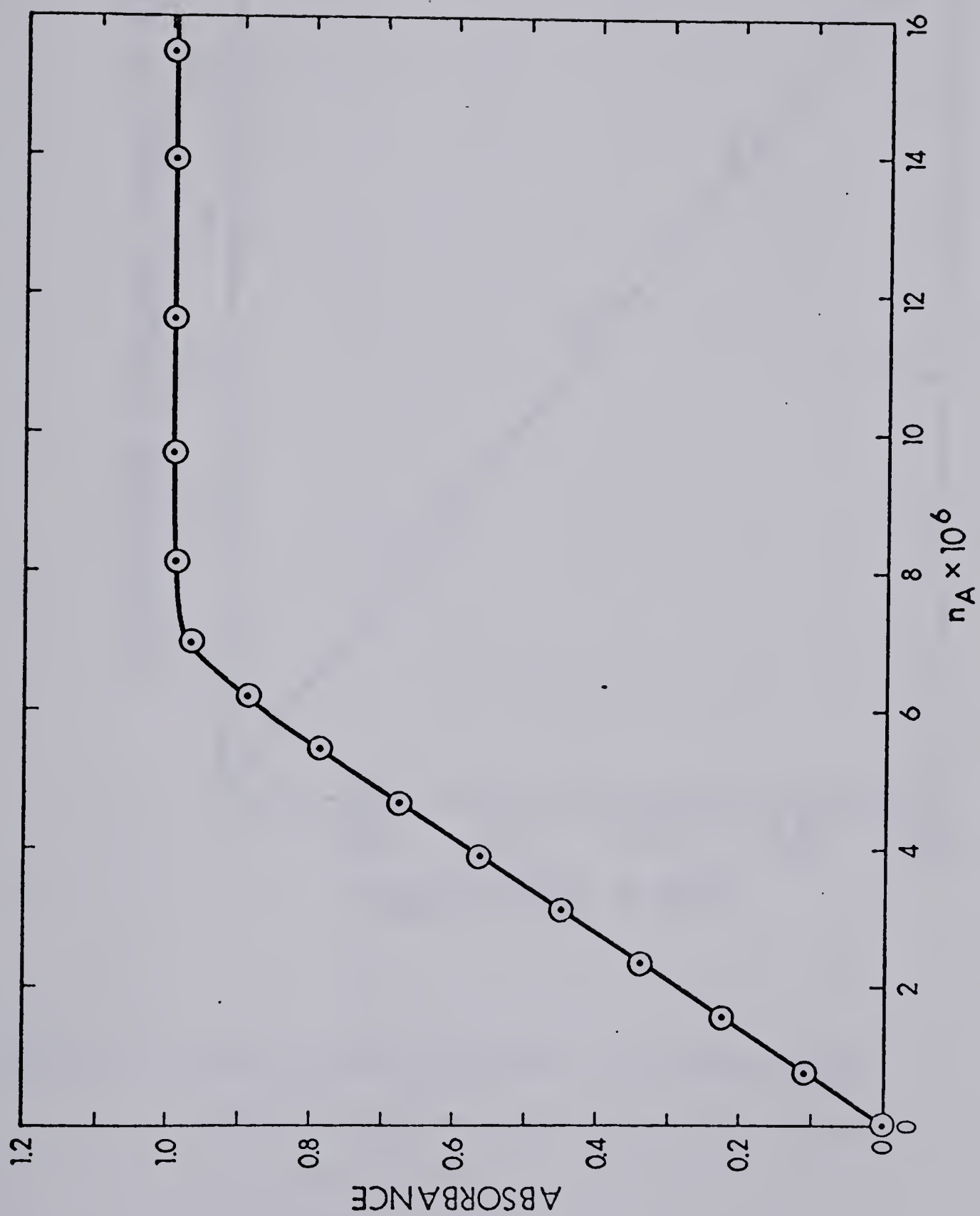


FIGURE 32. Titration of benzethonium chloride with picrate. The line is calculated from Equations 37 and 38 using the values below. The points are experimental.

---


$$\begin{aligned}
 n_{\text{BH}} &= 6.82 \times 10^{-6} \text{ mole}; V = 0.0300 \text{ L}; V_{\text{O}} = 0.0706 \text{ L}; \\
 K'_{\text{a}} &= 0, K'_{\text{b}} = 2.14 \times 10^{-14}; K_{\text{I,BHX}} = 6.5; K_{\text{I,MZ}} = 0.0; \\
 K_{\text{B}} &= 0; K_{\text{HA}} = 29.5; K_{\text{S}} = 2.34 \times 10^7; \epsilon'_{\text{BHX}} = 0; \epsilon'_{\text{B}} = 0; \\
 \epsilon'_{\text{MA}} &= 10^4; \epsilon'_{\text{HA}} = 430; \epsilon'_{\text{BHA}} = 1.02_5 \times 10^4; \text{pH} = 7.5_0; \\
 \text{Wavelength} &= 400 \text{ nm}.
 \end{aligned}$$


---





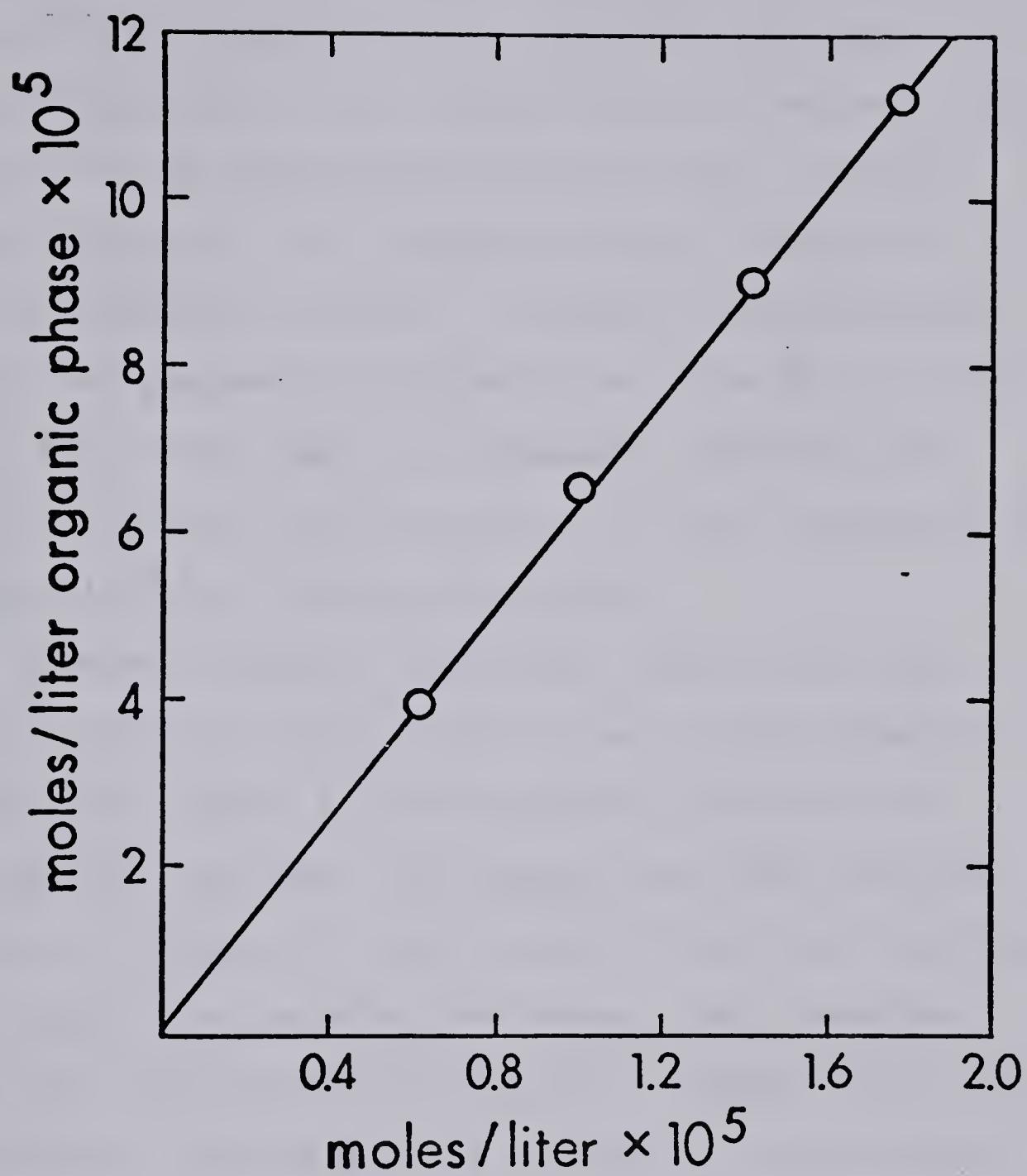


FIGURE 33. Distribution isotherm for benzethonium chloride between chloroform and aqueous buffer pH = 7.50.



The assay value and precision, based on end points obtained by linear extrapolation of the titration curves, are presented in Table IX along with the results obtained for the determination of benzethonium chloride by the ferricyanide method (114). Similar data are shown for the determination of hexadecyltrimethylammonium bromide. In general the agreement between the photometric titration and the ferricyanide method is several parts per thousand, which for an ion pair titration carried out at a sample concentration of about  $10^{-4}$  M, is quite acceptable.

Figure 34 shows a comparison between the theoretical titration curve (solid line) and the observed experimental points for promethazine hydrochloride titrated with picrate. The assay value and precision are shown in Table IX. The values of all the constants to be used in calculating the theoretical titration curve were experimentally measured as described in the experimental section and are presented in the caption of Figure 34. It will be noted in Figure 34 that the experimental points in the vicinity of the equivalence point fall below the theoretical curve. A possible explanation of this phenomenon is non-equilibrium in the ion-pair extraction process at the very low concentration of  $BH^+$  and  $A^-$  encountered near the equivalence point. A similar effect was not observed



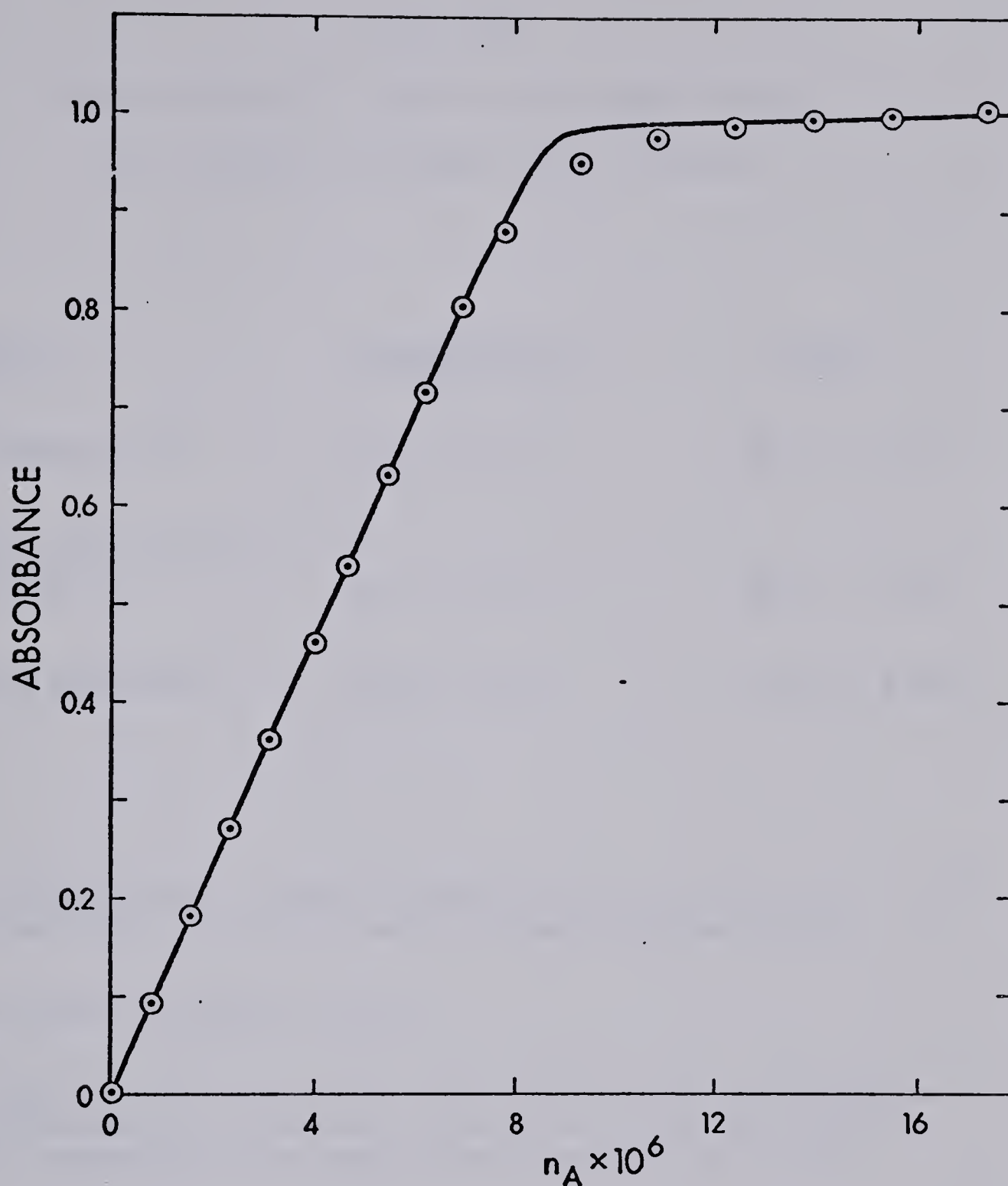


FIGURE 34. Titration of promethazine hydrochloride with picrate. The line is calculated from Equations 37 and 38 using the values below.

The points are experimental.

$n_{BH} = 8.55 \times 10^{-5}$  moles;  $K'_a = 1.0 \times 10^{-9}$ ;  $K_{I,BHX} = 0.9$ ;  
 $K_B = 7.9 \times 10^5$ ;  $K_S = 7.24 \times 10^6$ ;  $\epsilon'_{BHA} = 8.20 \times 10^3$ ;  
0. (All other parameters as in Figure 32.)



TABLE IX  
Assay Values (%) and Average Deviations  
for Cations Titrated with Picrate

<u>Compound</u>	<u>Photometric</u> <sup>a</sup>	<u>Other</u>
Benzethonium.Cl	92.1 ± 0.4	92.0 ± 0.1 <sup>b</sup>
Hexadecyltrimethyl- ammonium.Br	95.6 ± 0.1	96.0 ± 0.4 <sup>b</sup>
Promethazine.HCl	99.8 ± 0.6	99.8 ± 0.05 <sup>c</sup>

<sup>a</sup>Present method. Sample concentration about  $2.5 \times 10^{-4}$  M, assuming that it is all in the aqueous phase.

<sup>b</sup>Ferricyanide method (114).

<sup>c</sup>Average and average deviation of Fajan's, nonaqueous, and photometric ion-pair titration in which aqueous phase absorbance was monitored (Section 4.2.1.1).



when the aqueous phase absorbance was monitored (Figure 30). In other words, the departure of ions from the bulk aqueous phase may be more rapid than their appearance in the bulk organic phase, suggesting that the slow process may be related to the rate of interfacial desorption. At any rate, the phenomenon is not evident outside the immediate region of the equivalence point, and the end points obtained by linear extrapolation yield assay values in good agreement with the other methods (Table IX). Since the slope of the titration curve beyond the equivalence point is only slightly greater than zero, dilution corrections are negligible. Again, neglect of the dilution correction in the non-linear region of the titration curve near the equivalence point is justified by its small value, and it is certainly not this which is responsible for the discrepancy between theoretical and observed behavior in this vicinity.

4.2.2.2 Titration of Anions. Two anionic surfactants, sodium lauryl sulfate and sodium dodecylbenzene sulfonate, were titrated with methylene blue cation. The resulting assay values are compared in Table X with those obtained by the visual indicator titration. A typical titration curve for sodium lauryl sulfate is shown in Figure 35.



TABLE X.

Assay Values (%) and Average Deviations  
for Anions Titrated with Methylene Blue

<u>Compound</u>	<u>Photometric</u>	<u>Other<sup>d</sup></u>
Sodium lauryl sulfate	80.1 ± 0.2 <sup>a</sup>	81.2 ± 0.2
Sodium dodecylbenzene sulfonate	74.0 ± 0.4 <sup>b</sup>	72.3 ± 0.1
	58.3 ± 0.03 <sup>c</sup>	57.9 ± 0.3

<sup>a</sup>Present method. Sample concentration about  $3 \times 10^{-4}$  M in aqueous phase.

<sup>b</sup>Present method. Sample concentration about  $4 \times 10^{-5}$  M in aqueous phase.

<sup>c</sup>Present method, but aqueous phase was 0.2 M in  $\text{Na}_2\text{SO}_4$  and absorbance was measured after shutting off stirrer and allowing phases to separate (Section 4.2.2.3). Sample concentration about  $1.5 \times 10^{-4}$  M in aqueous phase.

<sup>d</sup>Method of Blank (115).



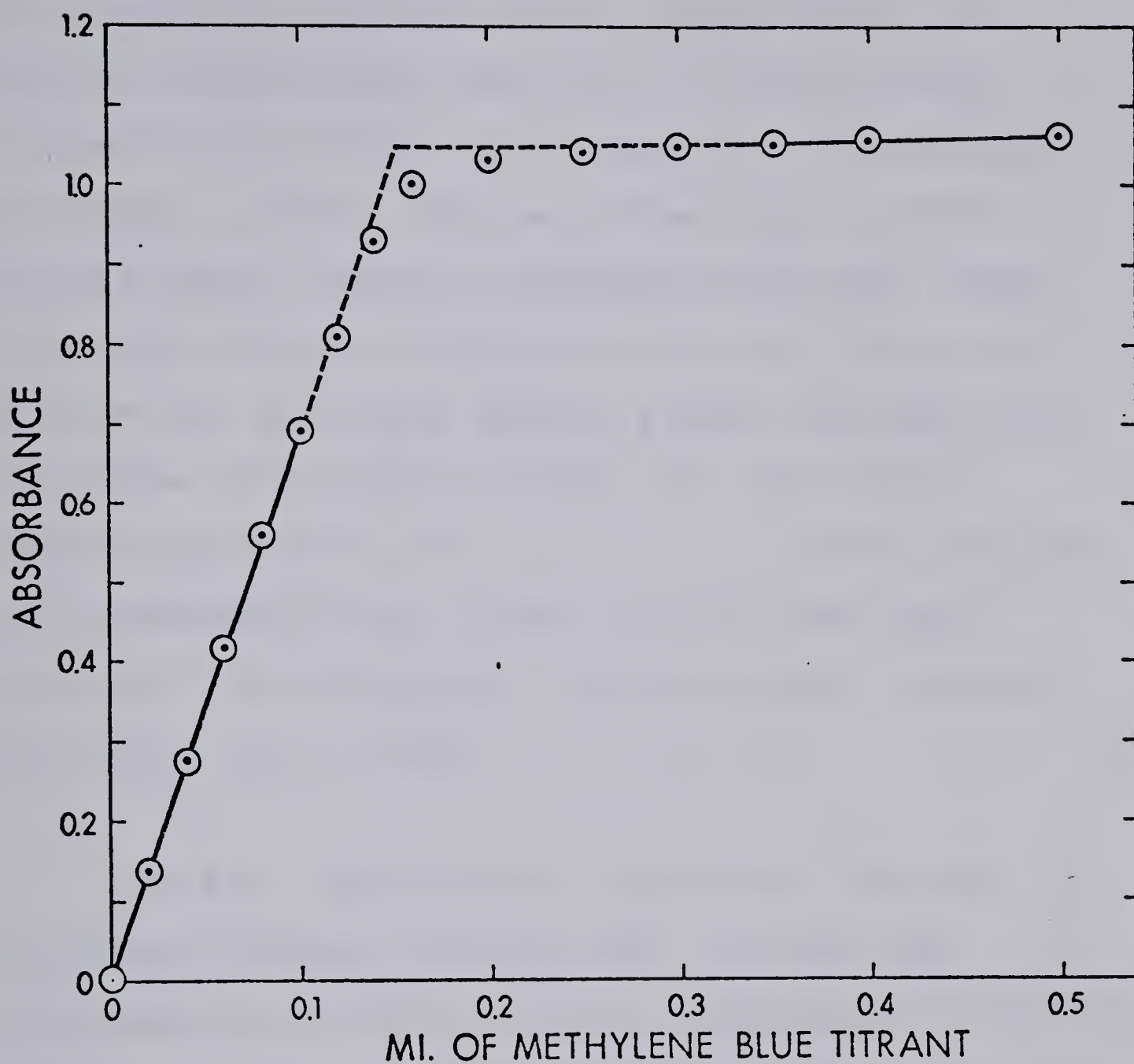


FIGURE 35. Experimental titration curve of sodium lauryl sulfate with methylene blue.  $n_{\text{BH}} = 9.52 \times 10^{-6}$  moles;  $V = 0.0300$  L;  $V_0 = 0.0700$  L; pH = 7.50; Wavelength - 658 nm. The lines are fitted to the experimental points.



The sodium dodecylbenzene sulfonate sample was an inhomogeneous syrup so that it was necessary to prepare a dilute stock solution of it and to assay aliquots of the stock solution by both the photometric and visual methods. Because of the sample inhomogeneity, stock solutions prepared at different times contained different amounts of surfactant (e.g., 58% and 73%) but both assay methods yielded the same value on a given stock solution (Table X). Even with a sample concentration of  $4 \times 10^{-5}$  M the results obtained by the proposed method agree within 2% with those obtained by the recognized indicator method (in which the sample concentration is  $6 \times 10^{-4}$  M).

4.2.2.3. Emulsions and Adsorption. When the titration of sodium dodecylbenzene sulfonate was originally performed at a sample concentration of  $10^{-4}$  M employing continuous stirring of the phases an emulsion formed and small amounts of the aqueous phase passed through the Teflon filter probe membrane. Performing the titration at  $4 \times 10^{-5}$  M sample concentration eliminated this problem. Although satisfactory precision and accuracy were obtained at this lower sample concentration (Table X) there is, as predicted, greater curvature in the vicinity of the equivalence point.

It was found that increasing the ionic strength



of the aqueous phase (e.g. 0.2 M  $\text{Na}_2\text{SO}_4$ ) eliminated emulsification at sample concentrations of  $10^{-4}$  M but, at the same time, caused low assay values (e.g. 10% relative). That is, the "plateau" after the equivalence point occurred at a lower absorbance value than predicted. However, when the same titration was repeated, but the absorbance of the organic phase was measured after shutting off the stirrer and allowing the phase to separate, an accurate end point was obtained (Table X).

The dependence of organic phase absorbance on stirring was a reversible phenomenon -- i.e., turning the stirrer off increased the absorbance and turning it on again decreased the absorbance. Also, the absorbance decrease caused by stirring was greater for higher sample concentrations. It is evident that this phenomenon is a consequence of interfacial adsorption of the ion pair formed between the sulfonate and methylene blue. During vigorous stirring the ratio of the interfacial area between the two phases to their bulk solution volume is increased by several orders of magnitude over that for the unstirred system. Thus, while a barely detectable fraction of the ion pairs might be adsorbed at the interface between 70 mL of quiescent chloroform and 30 mL of water, this fraction could become quite significant in a stirred solution.



Of the systems reported only methylene blue-dodecylbenzene sulfonate exhibited a detectable amount of interfacial adsorption.



## CHAPTER 5

### CONCLUSIONS

In this work it has been shown that photometric titrations in the presence of an immiscible organic solvent permit the accurate determination of acids of the  $BH^+$  charge type, anionic and cationic compounds, including drugs and surfactants. These titrations were carried out by monitoring the absorbance of either the aqueous or the organic phase.

Acid-base titrations were carried out in an aqueous- $CHCl_3/CCl_4$  mixture to minimize the ion pair extraction of BHX into the organic phase. It is possible to use other organic solvents for this purpose to yield a particular distribution coefficient. The method is applicable to the titration of other charge type acid (e.g. HA) with NaOH titrant, and to the titration of bases of various charge types with a strong acid titrant. Since the non-linear portion of the titration curve in the vicinity of the equivalence point is related to the strength of the acid or base being titrated, it should be possible to evaluate the  $pK_a$  of very weak acids and bases by this technique.

Photometric ion-pair titrations were performed by titrating ions of the  $BH^+$  charge type with picrate ion in a two-phase medium by monitoring the absorbance of both the aqueous and the organic phase. It would be



useful to have available anionic titrants which have higher ion-pair extraction constants,  $K_s$ , with amine drugs. This would make possible the accurate titration of smaller drug molecules. Preliminary investigations have shown the utility of some other anionic titrants such as dipicrylamine, laurylsulfate, and the azo-sulfonate dye Orange II. Photometric ion-pair titrations were also performed by titrating cations with picrate and monitoring the absorbance of the organic phase. Finally, anionic samples were titrated with methylene blue cationic titrant with the organic phase absorbance measured.

When titrant is added as an aqueous solution and the organic phase absorbance is monitored it is often possible to neglect dilution corrections. This is an advantage over using the absorbance of the aqueous phase. However, interfacial adsorption, which was seen at higher sample concentrations in the titration of dodecylbenzene sulfonate with methylene blue, and slow transfer of the ion-pair from the interface into the bulk organic phase, which was possibly seen in the titration of promethazinium ion with picrate, are potential sources of titration error when the absorbance of the organic phase is used to follow the titration. On the other hand, when the aqueous phase absorbance is used, the error in the linear regions before and



after the equivalence point, which are used to locate the endpoint by extrapolation, is likely to be negligible. This is because an ion-pair present at the interface has already left the bulk aqueous phase and produced the corresponding decrease in absorbance. This is an advantage to using aqueous phase absorbance. However, it is evident from the results in sections 4.2.1 and 4.2.2, that accurate and precise determinations can be performed by monitoring the absorbance of either phase in cases where interfacial influences are absent.

The absence of adsorption effects can readily be demonstrated in the prepared titration system by comparing absorbances observed during stirring with those observed after phase separation or alternatively by comparing assay values obtained in titrations of several different sample concentrations. It is also recommended, as with all photometric measurements, that photometric linearity of the spectrophotometer be verified using the same flow cell and over the same absorbance range encountered during a titration.

A variety of water immiscible solvents can be used as the organic phase in ion-pair titrations. Although the strong ion-pair extracting solvent methylisobutyl ketone (MIBK) is incompatible with Acidflex peristaltic pump tubing, mixtures of MIBK with chloroform up to at least a 1:1 ratio can be used. Non-



polar solvents such as carbon tetrachloride are also compatible with the tubing. Provided that values of  $K_s$  are large enough to yield sharp titration curves, it is preferable to use a less polar organic solvent, since the likelihood of aqueous phase "carryover" into the flow cell is reduced.

Photometric titrations can also be used to perform complexometric titrations of metal ions using as titrants ligands (e.g. dithizone) which form extractable complexes. Figure 36 shows the titration of silver ion with dithizone at pH = 5.00, monitoring the absorbance of the organic phase.

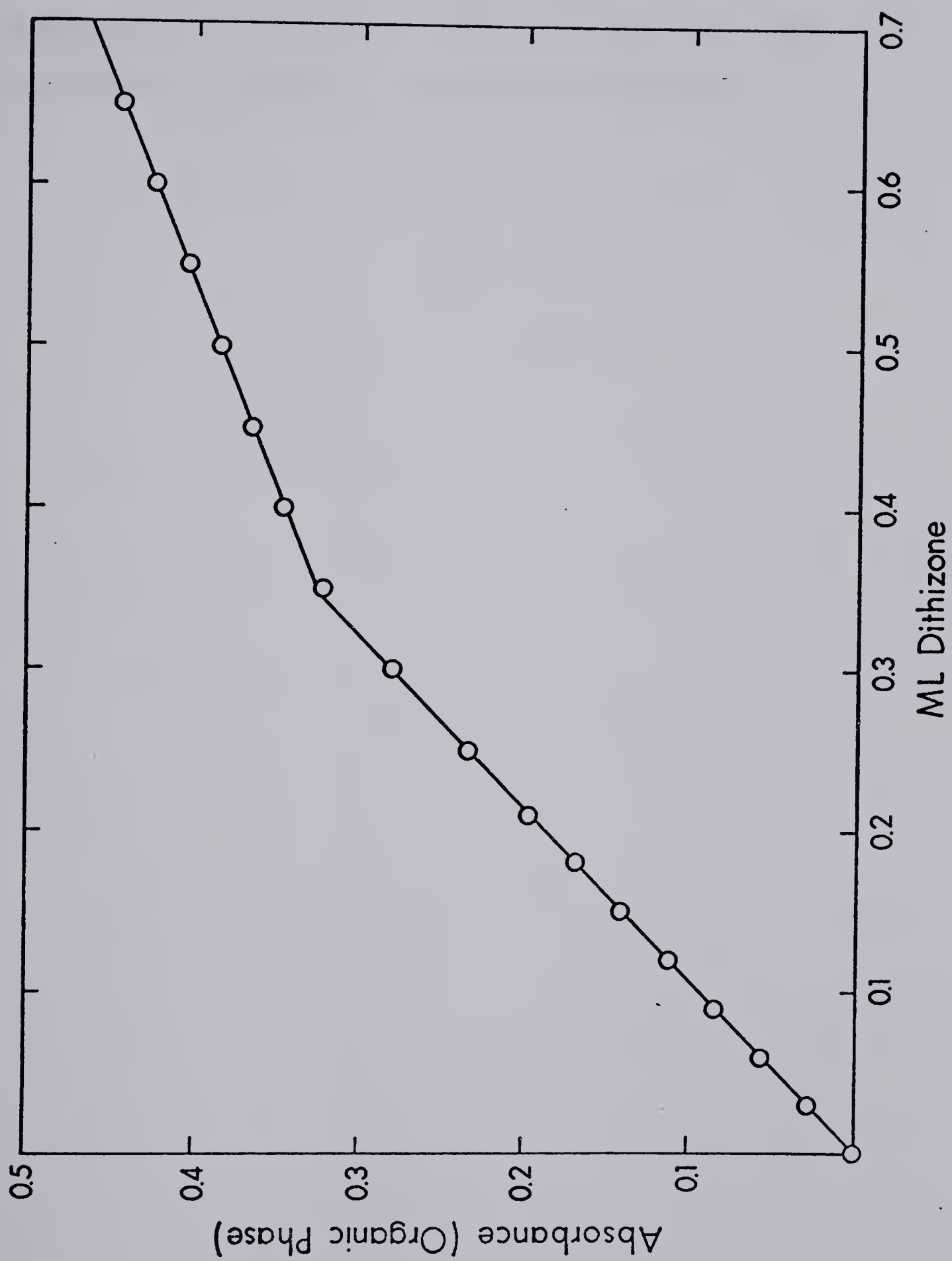
The time required to achieve a constant plateau absorbance value after each addition of titrant depends upon the efficiency of stirring, the pumping rate, the fraction of the total aqueous phase which is contained in the pumping system and flow cell, and the flow pattern through these (e.g. laminar flow in tubing, efficiency of rinsing of the flow cell) as well as on the chemical and phase-transfer rate constants. Studies are underway using faster flow rates and low dead volume flow cells such as those used in liquid chromatographic detectors.

Finally, it should be mentioned that other properties of the phases than absorbance can be used to continuously follow the course of a two-phase





FIGURE 36. Experimental titration curve of silver ion  
with dithizone.  $n_{\text{Ag}} = 7.4 \times 10^{-7}$  mole;  
 $V = 0.0300$  L;  $V_{\text{O}} = 0.0700$  L; pH = 5.0;  
Wavelength = 465 nm.





titration. In particular, the titration apparatus employed in this work should be well suited to radiometric titrations (121,122) which can only be performed in systems of more than one phase.



## CHAPTER 6

### FURTHER WORK

(a) The apparatus used in the photometric titrations is being automated. A stepping motor has been attached to the micrometer buret and the delivery of titrant can be done in three different modes, continuous addition, automatic incremental addition, and manual incremental addition.

(b) Most of the applications discussed in the second part of this thesis can be done by using the automatic titrator system.

(c) Studies are underway to determine the factors that cause the slow equilibration of sample compound between aqueous and organic solvent during the course of the titration. Also there is some thought about a new design of the whole titration system to give a better equilibration time.

(d) This photometric titration system can be used for the determination of indicators such as calmagite and orange II). These indicators can be titrated with acids of the  $BH^+$  charge type as ion-pair formers since the indicator has  $A^-$  form. The absorbance of the organic or the aqueous phase can be monitored.

(e) Freiser (123) has studied the extraction kinetics of Cu(II) with the hydroxyoximes (HL) between chloroform and dilute aqueous acid solution. Sample



was removed from the reaction vessel by purging the vessel with nitrogen to force a few mL's of solution into a test tube. After centrifuging, the aqueous phase was analyzed for copper with an atomic absorption spectrophotometer. There is a delay time for the phases to separate after sampling, which causes a systematic error in the intercept of the graph. However, the apparatus used for the photometric titration (part II of this thesis) can be used to follow such kinds of kinetics without any time required for the phases to separate.



## REFERENCES

1. C. R. Fontan, W. C. Smith and P. L. Kirk, Anal. Chem., 35, 591 (1963).
2. E. W. Cipelinski, Anal. Chem., 35, 256 (1963).
3. A. MacDonald and R. T. Pflaum, J. Pharm. Sci., 53, 887 (1964).
4. G. B. Lawless, J. J. Sciarra and A. Monte-Bovi, J. Pharm. Sci., 54, 273 (1965).
5. M. Elefant, L. Chaftz and J. M. Talmage, J. Pharm. Sci., 56, 1181 (1967).
6. J. Hudanick, J. Pharm. Sci., 59, 238 (1970).
7. W. R. Maynard, Jr., and R. B. Bruce, J. Pharm. Sci., 59, 1346 (1970).
8. L. J. Combrowski, P. M. Comi and E. L. Pratt, J. Pharm. Sci., 62, 1761 (1973).
9. S. Hanna and A. Tang, J. Pharm. Sci., 63, 1954 (1974).
10. R. A. Zwiedinger, F. M. Weinberg, and R. W. Handy, J. Pharm. Sci., 65, 427 (1976).
11. L. Neelakantan and H. B. Kostenbauder, J. Pharm. Sci., 65, 740 (1976).
12. R. E. Madsen and D. F. Magin, J. Pharm. Sci., 65, 924 (1976).
13. F. M. Plakogiannis and A. M. Saad, J. Pharm. Sci., 66, 604 (1977).



14. H. Kinsun, M. A. Moulin and E. C. Savini, J. Pharm. Sci., 67, 118 (1978).
15. H. V. Street, W. Vycudilik and G. Machata, J. Chromatogr. 168, 117 (1979).
16. F. L. Fricke, J. Assoc. Offic. Anal. Chem., 55, 1162 (1972).
17. E. Mario and L. G. Meehen, J. Pharm. Sci., 59, 539 (1970).
18. C. Hishta and R. G. Laubach, J. Pharm. Sci., 58, 745 (1968).
19. J. R. Watson and R. C. Lawrence, J. Pharm. Sci., 66, 560 (1977).
20. J. D. Nicholson, Analyst, 103, 1 (1978).
21. Ibid., 103, 193 (1978).
22. T. SpriECK, J. Pharm. Sci., 63, 591 (1974).
23. "Gas Chrom. Newsletter," Vol. 13, no. 6, Applied Science Laboratories, Inc., State College, Pa., Nov./Dec. 1972.
24. I. L. Honigberg, J. T. Stewart, and P. A. Smith, J. Pharm. Sci., 63, 766 (1974).
25. P. J. Twitchett and A. C. Moffat, J. Chromatogr., 111, 149 (1975).
26. A. Menyharth, F. P. Mahn and J. E. Heveran, J. Pharm. Sci., 63, 430 (1974).
27. "Analysis of Pharmaceutical Products," Technical Bulletin, Water Associates, Inc., Millford,



Massachusetts, 1976.

28. G. Schill, in J. A. Marinsky and Y. Marcus (Eds.), "Advances in Ion Exchange and Solvent Extraction," Vol. 6, Marcel Dekker, N.Y., 1974, Ch. 1.
29. T. D. Doyle and J. Levine, *Anal. Chem.*, 39, 1282 (1967).
30. T. D. Doyle and J. Levine, *J. Assoc. Offic. Anal. Chem.*, 51, 191 (1968).
31. S. Eksborg and B.-A. Persson, *Acta Pharm. Suecica*, 8, 205 (1971).
32. S. Eksborg and G. Schill, *Anal. Chem.*, 45, 2092 (1973).
33. S. Eksborg, P.-O. Lagerström, R. Modin and G. Schill, *J. Chromatogr.*, 83, 99 (1973).
34. J. C. Kraak and J. F. K. Huber, *J. Chromatogr.*, 102, 333 (1974).
35. B.-A. Persson and B. L. Karger, *J. Chromatogr. Sci.*, 12, 521 (1974).
36. B. L. Karger, S. C. Su, S. Marchese and B.-A. Persson, *J. Chromatogr. Sci.*, 12, 678 (1974).
37. E. Fitzgerald, *Anal. Chem.*, 48, 1734 (1976).
38. A. G. Ghanekar and V. D. Gupta, *J. Pharm. Sci.*, 67, 873 (1978).
39. E. L. Johnson, *Ind. Res./Dev.*, June, p. C2,C6 (1978).



40. "Paired-Ion Chromatography," Technical Bulletin, Waters Associates, Inc., Milford, Massachusetts, 1976.
41. D. P. Wittmer, N. O. Nuessle, and W. G. Haney, Jr., *Anal. Chem.*, 47, 1422 (1975).
42. S. P. Sood, L. E. Sartori, D. P. Wittmer, and W. G. Haney, *Anal. Chem.*, 48, 796 (1976).
43. J. Korpi, D. P. Wittmer, B. J. Sandmann, and W. G. Haney, Mr., *J. Pharm. Sci.*, 65, 1087 (1976).
44. J. H. Knox and J. Jurand, *J. Chromatogr.*, 110, 103 (1975).
45. J. H. Knox and A. Pryde, *J. Chromatogr.* 112, 171 (1975).
46. R. Gloor and E. L. Johnson, *J. Chromatogr. Sci.*, 15, 413 (1977).
47. "Amberlite XAD-2", Technical Bulletin, Rohm and Haas Co., Philadelphia, Pa., 1972.
48. G. A. Junk, C. D. Chriswell, R. C. Chang, L. D. Kissinger, J. J. Richard, J. S. Fritz, and H. J. Svec, *Fresenius Z. Anal. Chem.*, 282, 331 (1976).
49. M. W. Scoggins and J. W. Miller, *Anal. Chem.*, 40, 1155 (1968).
50. L. L. Zaika, *J. Chromatogr.*, 49, 222 (1970).
51. C. H. Chu and D. J. Pietrzyk, *Anal. Chem.*, 46, 330 (1974).



52. D. J. Pietrzyk and C. H. Chu, *Anal. Chem.*, 49, 757 (1977).
53. *Ibid.*, 49, 860 (1977).
54. D. J. Pietrzyk, E. P. Kroeff and T. D. Rotsch, *Anal. Chem.*, 50, 497 (1978).
55. E. P. Kroeff and D. J. Pietrzyk, *Anal. Chem.*, 50, 502 (1978).
56. F. F. Cantwell, *Anal. Chem.*, 48, 1854 (1976).
57. H. Y. Mohammed and F. F. Cantwell, *Anal. Chem.*, 50, 491 (1978).
58. F. F. Cantwell, H. Y. Mohammed, R. G. Baum and S. Puon, Paper No. 67, Analytical Division, 175th National Convention, American Chemical Society, Anaheim, California, March 1978.
59. Industrial Research/Development, June 1978, p. C1.
60. R. L. Gustafson, R. L. Albright, J. Heisler, J. Lirio and O. T. Reid, Jr., *Ind. Eng. Chem., Prod. Res. Dev.*, 7, 107 (1968).
61. J. Paleos, *J. Colloid Interfac. Sci.*, 31, 7 (1968).
62. M. W. Socggins, *Anal. Chem.*, 44, 1285 (1972).
63. F. F. Cantwell and S. Puon, *Anal. Chem.*, 51, 623 (1979).
64. J. S. Fritz, and R. B. Willis, *J. Chromatogr.*, 79, 107 (1973).



65. "United States Pharmacopea," 19th rev., Mack Publishing Co., Easton, Pa., 1975.
66. K. Fuzita, *Nippon Kagaku Kaishi*, 1975 (5), 846.
67. B. L. Karger, L. R. Snyder and C. Horvath, "An Introduction to Separation Science," Wiley-Interscience, Toronto, 1973.
68. R. G. Baum and F. F. Cantwell, *Anal. Chem.*, 50, 280 (1978).
69. M. D. Grieser and D. J. Pietrzyk, *Anal. Chem.*, 45, 1348 (1973).
70. A. Albert and E. P. Serjeant, "Ionization Constants of Acids and Bases," Wiley, N.Y., 1962.
71. F. A. Long and W. F. McDevit, *Chem. Rev.*, 51, 119 (1952).
72. S. Puon and F. F. Cantwell, *Anal. Chem.*, 49, 1256 (1977).
73. R. G. Baum, R. Saetre and F. F. Cantwell, submitted to *Anal. Chem.*
74. S. Puon, Ph.D. Thesis, University of Alberta, 1979.
75. R. G. Bates, "Determination of pH. Theory and Practice," Wiley, N.Y., 1964.
76. International Critical Tables, Vol. 111, McGraw-Hill, New York, N.Y., 1928, pp. 115-116.
77. S. P. Massie, *Chem. Revs.*, 54, 797 (1954).
78. R. F. Goddu and D. N. Hume, *Anal. Chem.*, 26, 1679 (1954).



79. J. F. Headrige, Photometric Titrations, Pergamon Press, London, 1961.
80. M. A. Leonard, Chapter 3 in G. Svehla, Ed., Comprehensive Analytical Chemistry, Vol. VIII, Elsevier, N.Y., 1977.
81. J. S. Fritz, Acid-Base Titrations in Nonaqueous Solvents, Allyn and Bacon, Boston, Mass. 1973.
82. J. Kucharsky and L. Safarik, Titration in Non-aqueous Solvents, Elsevier Publishing Co., New York, 1965.
83. R. G. Bates and R. M. Robinson in B. E. Conway and R. G. Barrades, Eds., Chemical Physics of Ionic Solutions, Wiley, New York, 1966.
84. F. F. Cantwell, Ph.D. Thesis, University of Iowa, December, 1972.
85. F. F. Cantwell and D. J. Pietrzyk, Anal. Chem., 46, 344 (1974).
86. Ibid., 46, 1450 (1974).
87. F. F. Cantwell and H. Y. Mohammed, Anal. Chem., 51, 218 (1979).
88. D. Dyrssen, Svensk. Kem. Tidskr., 64, 213 (1952).
89. J. A. Christiansen, Acta Chem. Scand., 16, 2363 (1963).
90. W. W. Davis and C. J. Kreutler, Abstracts, 167th National Meeting, Am. Chem. Soc., Washington, D.C., Sept. 1971, No. 9.



91. D. Ratajewicx and Z. Ratajewics, *Z. Chem. Anal.*, (Warsaw), 16, 1299 (1971).
92. M. P. Komar, *Industrial Laboratory (U.S.S.R.)* 34, 617 (1968).
93. A. Galik, *Talanta*, 13, 109 (1966).
94. A. Galik and M. Knizek, *Talanta*, 13, 589 (1966).
95. *Ibid.*, 13, 1169 (1966).
96. A. Galik, *Talanta*, 14, 731 (1967).
97. *Ibid.*, 15, 771 (1968).
98. A. Galik, in "Chelates in Analytical Chemistry," Vol. 3, p. 1, 1972.
99. K. W. Han, *Tenside*, 3, 265 (1966).
100. V. W. Reid, G. F. Longman and E. Heinerth, *Tenside*, 4, 292 (1967).
101. *Ibid.*, 5, 90 (1968).
102. S. O. Jansson, R. M. Modin and G. Schill, *Talanta*, 21, 905 (1974).
103. E. Heinerth, Chapter 6 in J. Cross, Ed., Anionic Surfactants-Chemical Analysis, Marcel Dekker, N.Y., 1977.
104. D. Hummel, Identification and Analysis of Surface Active Agents, Vol. 1, Interscience, N.Y., 1962.
105. J. T. Cross, Chapter 13 in E. Jungermann, Ed., Cationic Surfactants, Marcel Dekker, N.Y., 1970.
106. E. D. Carkhuff and W. F. Boyd, *J. Amer. Pharm. Assoc., Sci. Ed.*, 43, 240 (1954).



107. G. N. Thomis and A. Z. Kotionis, *Anal. Chim. Acta*, 14, 457 (1956).
108. K. Behrends, *Z. Anal. Chem.*, 250, 241 (1970).
109. *Ibid.*, 250, 246 (1970).
110. G. J. Divatia and J. A. Biles, *J. Pharm. Sci.*, 50, 916 (1961).
111. K. Gustavii and G. Schill, *Acta Pharm. Suecica*, 3, 241 (1966).
112. H. Y. Mohammed and F. F. Cantwell, *Anal. Chem.*, 51, 1006 (1979).
113. H. Y. Mohammed and F. F. Cantwell, submitted to *Anal. Chem.*
114. "Tests and Standards for New and Nonofficial Remedies," Lippincott, Phila., 1953; p. 28.
115. Reference 104; p. 228.
116. D. C. Abbot, *Analyst*, 87, 286 (1962).
117. T. Higuchi, A. Michaelis, T. Tan, and A. Hurwitz, *Anal. Chem.*, 39, 974 (1967).
118. T. Higuchi and A. F. Michaelis, *Anal. Chem.*, 40, 1925 (1968).
119. J. Kielland, *J. Am. Chem. Soc.*, 59, 1675 (1937).
120. R. A. Robinson and R. H. Stokes, "Electrolyte Solutions," 2nd ed., Butterworth, London, 1959.
121. T. Braun and J. Tolgyessy, "Radiometric Titrations," Pergamon, N.Y., 1967.
122. Y. A. Zolotov "Extraction of Chelate Compounds"



Ann-Arbor, Mich., 1970; Chapter 6.

123. S. P. Carter and H. Frieser, *Anal. Chem.*, 51, 1100 (1979).
124. D. D. Perrin, "Dissociation Constants of Organic Bases in Aqueous Solution," Butterworths, London, 1965.



## APPENDIX I

Tables of all of the data in Figures 2, 3 and 4.



Data for Figure 2 (A & B),  
 0.010 M  $\text{NH}_3$ , Methanol/water

Compound/ % Water	Net Retention Volume (ml)					
	5%	10%	15%	25%	35%	50%
1	1.1	1.7	2.6	6.9		
2	1.2	2.0	3.2	9.8		
3	1.6	2.8	4.7	16.3		
4	2.1	3.6	6.1			
5	2.3	4.0	6.6			
6	2.6	4.5	7.9			
7	3.6	5.2	11.6			
8	4.5	8.8	17.7			
9			0.9	1.5		9.3
10	7.4	15.3				
11			0.4	0.6		2.9
12	3.8	7.9	15.7			
13		1.4	2.7	5.8		
14	3.8	7.2	12.9			
15	1.5	2.3	3.5	9.1		
16	2.3	4.5	8.1			
17	3.2	6.3	11.7			
18	3.6	6.6	11.6			
19	5.7	11.0	22.5			
20	4.2	8.3	15.8			
21	4.0	7.3	11.9			
22			0.3	0.5		2.7
23	0.9	0.9	0.9	1.1		2.9
24			0.8	1.2		8.8



## Data for Figure 2 (C &amp; D)

0.1 M HCl, Methanol/water

Compound/ % Water	Net Retention Volume (ml)								
	30%	40%	50%	60%	65%	75%	85%	95%	100%
1						0.4	1.1	4.8	22.8
2						.5	1.9	10.1	
3					.5	1.7	5.8		
4					.8	2.8	10.0		
5						0.7	1.8	8.6	
6						.7	2.1	10.0	
7						.4	1.4	4.9	
8	1.0	2.9	8.3						
9					.6	1.3	2.9		
10			1.8	4.7	8.2				
11						.7	1.7	3.8	
12	.9	2.5	7.2						
13				.5	.7	2.3			
14	1.6	4.0	10.1						
15				1.5	2.3	6.2			
16		1.7	3.8	14.3					
17	1.2	3.8	10.9						
18	1.3	3.5	11.1						
19	1.5	4.4	12.4						
20	1.0	2.7	8.1						
21	.9	2.2	5.8						
22			2.8	6.7	11.0				
23		1.6	2.5	4.3	5.6	14.3			
24	1.4	3.7	8.0						
25				.6	.8	1.5		4.9	10.7
26		1.1	2.2	4.7	6.9				
27							.4	.8	1.8



## Data for Figure 2E

## Methanol/Water

Compound/% Water	Net Retention Volume (ml)			
	40%	60%	75%	85%
23	1.6	4.6	14.8	
24	3.5	23.6		
25		.6	1.6	3.3
26	1.1	4.9	17.3	
27	3.0	5.8		
28	4.6	13.1		
29	2.2	10.7		



Data for Figure 3 A & B)

0.01 M  $\text{NH}_3$ , Acetonitrile/Water

Compound/% Water	Net Retention Volume (ml)			
	40%	45%	50%	60%
3	1.7		3.4	7.3
4	1.9		3.8	9.2
5	1.9		3.6	8.4
6	2.4		4.6	9.8
8	4.8		10.9	28.9
12	6.6	9.6	15.4	
14	7.1		14.5	43.9
16	2.9		6.5	15.7
17	3.2		7.7	18.9
18	2.4		5.55	12.6
19	7.3		15.7	43.1
20	4.4		9.8	27.9
21	5.3		11.9	22.9



## Data for Figure 3C

Acetonitrile/Water

Compound/% Water	Net Retention Volume (ml)		
	80%	90%	95%
22	0.9	5.1	20.9
23	0.5	1.9	7.4
26	1.8	6.5	17.1



Figure 4 (A &amp; B)

0.01 M  $\text{NH}_3$ , Dioxane/Water

Compound/% Water	Net Retention Volume (ml)			
	40%	45%	50%	60%
3	0.7		1.8	5.9
4	0.8		2.0	7.2
5	0.85		2.2	6.95
6	1.0		2.7	9.0
8	1.65		5.8	25.9
12	3.3	5.9	13.5	
14	1.55		5.0	22.0
16	1.3		3.9	14.7
18	0.8		2.3	9.3
19	1.7		5.9	31.5
20	1.8		6.1	26.9
21	1.85		5.4	19.0



Figure 4C  
Dioxane/Water

Compound/% Water	Net Retention Volume (ml)		
	80%	90%	95%
22	1.2	4.3	11.8
23	0.4	1.2	3.2
26	1.9	5.4	11.4

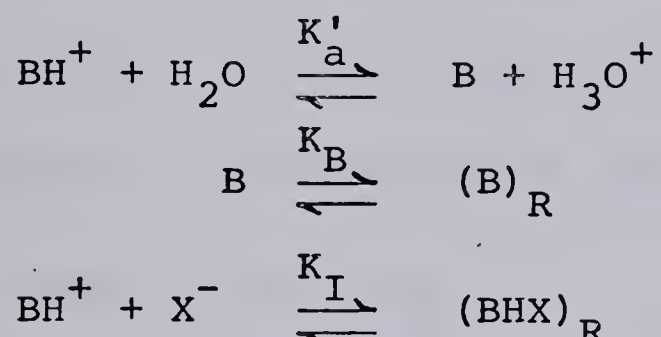


## APPENDIX II

Derivation of the distribution ratio expressions for acids  $BH^+$  and  $BH_2^{2+}$  in the presence of XAD-2 resin.

### A. Monobasic ( $BH^+$ )

Three equilibria can be written for  $BH^+$ :



Subscript R in the above equilibria indicates the resin phase and those without a subscript are in the aqueous phase. In the presence of a large excess of  $X^-$  (72,74) three equilibrium constants can be written for the three equilibria above:

$$K'_a = [B] \cdot a_H / [BH] \quad (1)$$

$$K_B = [B]_R / [B] \quad (2)$$

$$K_I = [BHX]_R / [BH] \quad (3)$$

Although the  $K_I$  equilibrium is represented as an ion pairing, this is done only for simplicity and is not intended to suggest that  $BH^+$  is adsorbed as an ion pair (72,74). However, the same conclusions would



be valid for a more complex sorption mechanism. Note that  $\text{Cl}^-$  ( $\text{X}^-$ ) is in excess and therefore is constant (63).

The distribution ratio,  $D$ , can be defined in terms of the total concentration of B-containing species in each phase.

$$D = \frac{[\text{C}]_R}{[\text{C}]} = \frac{[\text{B}]_R + [\text{BH}]_R}{[\text{B}] + [\text{BH}]} \quad (4)$$

Equations 1 - 3 can be rearranged to express all the variables as a function of  $[\text{B}]$ :

$$[\text{BH}] = [\text{B}] \cdot a_{\text{H}} / K'_a \quad (5)$$

$$[\text{B}]_R = K_B \cdot [\text{B}] \quad (6)$$

$$[\text{BHX}]_R = K_I \cdot [\text{BH}] = K_I \cdot [\text{B}] \cdot a_{\text{H}} / K'_a \quad (7)$$

Substituting the values of  $[\text{BH}]$ ,  $[\text{B}]_R$  and  $[\text{BHX}]_R$  from (5), (6) and (7) respectively into (4) and rearranging gives:

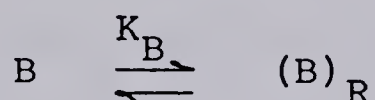
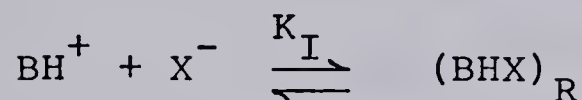
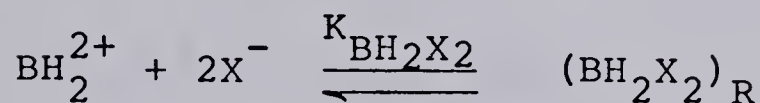
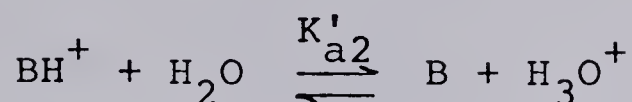
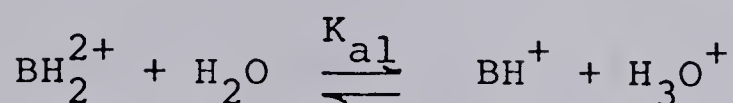
$$D = \frac{K'_a \cdot K_B + K_I \cdot a_{\text{H}}}{K'_a + a_{\text{H}}} \quad (8)$$

(equation 7 in text)



B. Dibasic ( $\text{BH}_2^{2+}$ )

Five equilibria can be written for  $\text{BH}_2^{2+}$ :



There are five equilibrium constants associated with the five equilibria above. In the presence of a large excess of  $\text{X}^-$  they have the form (72,74):

$$K'_{a1} = [\text{BH}^+] \cdot a_\text{H} / [\text{BH}_2^{2+}] \quad (9)$$

$$K'_{a2} = [\text{B}] \cdot a_\text{H} / [\text{BH}^+] \quad (10)$$

$$K_{\text{BH}_2\text{X}_2} = [\text{BH}_2\text{X}_2]_\text{R} / [\text{BH}_2^{2+}] \quad (11)$$

$$K_\text{I} = [\text{BH}]_\text{R} / [\text{BH}] \quad (12)$$

$$K_\text{B} = [\text{B}]_\text{R} / [\text{B}] \quad (13)$$

Here, as in Appendix IA, the use of an ion-pair retention equation is merely for simplicity.

The distribution ratio  $D$ , is given by:

$$D = \frac{[\text{C}]_\text{R}}{[\text{C}]} = \frac{[\text{B}]_\text{R} + [\text{BHX}]_\text{R} + [\text{BH}_2\text{X}_2]_\text{R}}{[\text{B}] + [\text{BH}] + [\text{BH}_2^{2+}]} \quad (14)$$



Equations 9 - 13 can be rearranged to express all the variables as a function of [B]:

$$[\text{BH}_2^{2+}] = [\text{BH}^+] \cdot a_{\text{H}} / K'_{\text{a1}} = [\text{B}] \cdot a_{\text{H}}^2 / K'_{\text{a1}} \cdot K'_{\text{a2}} \quad (15)$$

$$[\text{BH}] = [\text{B}] \cdot a_{\text{H}} / K'_{\text{a2}} \quad (16)$$

$$\begin{aligned} [\text{BH}_2\text{X}_2]_{\text{R}} &= K_{\text{BH}_2\text{X}_2} \cdot [\text{BH}_2^{2+}] \\ &= K_{\text{BH}_2\text{X}_2} \cdot [\text{B}] \cdot a_{\text{H}}^2 / K'_{\text{a1}} \cdot K'_{\text{a2}} \end{aligned} \quad (17)$$

$$[\text{BH}]_{\text{R}} = K_{\text{I}} \cdot [\text{BH}] = K_{\text{I}} \cdot [\text{B}] \cdot a_{\text{H}} / K'_{\text{a2}} \quad (18)$$

$$[\text{B}]_{\text{R}} = K_{\text{B}} \cdot [\text{B}] \quad (19)$$

Substituting the values of  $[\text{BH}_2^{2+}]$ ,  $[\text{BH}]$ ,  $[\text{BH}_2\text{X}_2]_{\text{R}}$ ,  $[\text{BHX}]_{\text{R}}$  and  $[\text{B}]_{\text{R}}$  from (15), (16), (17), (18), and (19) respectively into (14), and rearranging gives:

$$D = \frac{K_{\text{B}} \cdot K'_{\text{a1}} \cdot K'_{\text{a2}} + K_{\text{I}} \cdot K'_{\text{a1}} \cdot a_{\text{H}} + K_{\text{BH}_2\text{X}_2} a_{\text{H}}^2}{a_{\text{H}}^2 + K'_{\text{a1}} \cdot a_{\text{H}} + K'_{\text{a1}} \cdot K'_{\text{a2}}} \quad (20)$$

(equation 12  
in text)



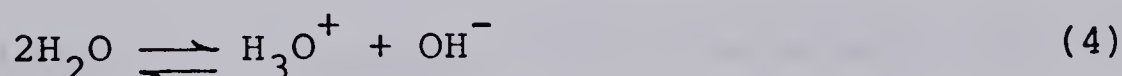
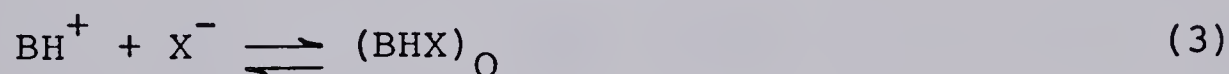
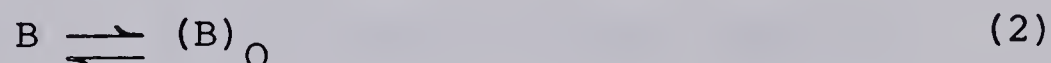
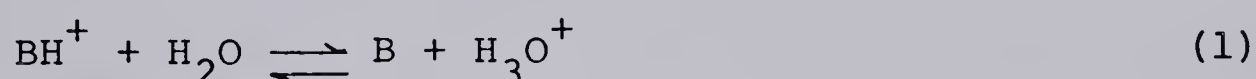
# APPENDIX III

## DERIVATION OF PHOTOMETRIC ACID-BASE TITRATION EQUATIONS FOR A WEAK ACID $BH^+$ TITRATED WITH NaOH

### A. Absorbance of Aqueous Phase Monitored

Photometric titration of  $n_{BH}$  moles of acid  $BH^+$  with strong base NaOH in dilute aqueous solution of salt MX, in the presence of an immiscible organic solvent.

The equilibria prevailing in this system are given below.



Species without a subscript are in the aqueous phase and those with the subscript O are in the organic phase. Here  $X^-$  is the conjugate base of a strong acid (e.g.,  $Cl^-$ ).

Equilibrium constants and distribution coefficients for the equilibria above are: (charges are omitted for simplicity.)

$$K'_a = [B] \cdot a_H / [BH] \quad (5)$$



$$K_B = [B]_O/[B] \quad (6)$$

$$K_I = [BHX]_O/[BH] \quad (7)$$

$$K_w = a_H \cdot a_{OH} \quad (8)$$

The following relationships can be obtained by arranging equations 5 - 8.

$$a_H = K'_a \cdot [BH]/[B] \quad (9)$$

$$[B]_O = K_B \cdot [B] \quad (10)$$

$$[BHX]_O = K_I \cdot [BH] \quad (11)$$

$$a_{OH} = K_w/a_H \quad (12)$$

Electroneutrality of the aqueous phase requires

$$[BH] + [H] + [Na] = [OH] + [X] \quad (13)$$

The mass balance relationship for B-containing species in the system may be expressed as concentration,

$n_i = [i] \cdot V$ , where  $n_i$  is moles of species  $i$  and  $V$  is the volume of the aqueous phase.

$$n_{BH} = [BH] \cdot V + [B] \cdot V + [B]_O \cdot V_O + [BHX]_O \cdot V_O \quad (14)$$

Now substituting into (14) the values of  $[B]_O$  and  $[BHX]_O$  from (10) and (11), and rearranging gives:



$$[BH] = \frac{n_{BH} - [B](V + K_B \cdot V_O)}{(V + K_I \cdot V)} \quad (15)$$

Assuming that Beer's law applies and that measurements of absorbance are made in a 1.000 cm pathlength cell, the following relationship applies.

$$A_{obs} = \epsilon'_{BH} \cdot [BH] + \epsilon'_B \cdot [B] \quad (16)$$

where  $A_{obs}$  is the absorbance of the aqueous phase, corrected for dilution if necessary. Rearranging this expression gives:

$$[BH] = \frac{A_{obs} - \epsilon'_B \cdot [B]}{\epsilon'_{BH}} \quad (17)$$

Equation (15) with (17) and rearranging gives:

$$[B] = \frac{[\epsilon'_{BH} \cdot n_{BH} - A_{obs}(V + K_I \cdot V_O)]}{\epsilon'_{BH} \cdot (V + K_B \cdot V_O) - \epsilon'_B (V + K_I \cdot V_O)} \quad (18)$$

The mass balance for [X] in the aqueous phase is:

$$[X] = [BH] + [B] + [B]_O \cdot V_O / V \quad (19)$$

Substitute into (19) the value of  $[B]_O$  from (10) give:

$$[X] = [BH] + [B] + K_B \cdot [B] \cdot V_O / V \quad (20)$$

Substituting into (13) the value of [X] from (20) and rearranging gives:



$$[\text{Na}] = [\text{OH}] + [\text{B}] \cdot (1 + K_B \cdot V_O / V) - [\text{H}] \quad (21)$$

Since  $[\text{Na}]$  is the concentration of the base added in the titration, it can be rewritten as  $[\text{Na}] = n_{\text{OH}} / V$ , so equation (21) becomes

$$n_{\text{OH}} = [\text{OH}] \cdot V + [\text{B}] \cdot (V + K_B \cdot V_O) - [\text{H}] \cdot V \quad (22)$$

combining (9) with the relationship  $a_{\text{H}} = \text{H} \cdot \gamma_{\text{H}}$  yields:

$$[\text{H}] = K'_a \cdot [\text{BH}] / [\text{B}] \cdot \gamma_{\text{H}} \quad (23)$$

where  $\gamma_{\text{H}}$  is the single ion aqueous activity coefficient for  $\text{H}^+$  ions. Combining (12) with (9) gives:

$$a_{\text{OH}} = K_w \cdot [\text{B}] / K'_a \cdot [\text{BH}] \quad (24)$$

Combining (24) with the relationship  $a_{\text{OH}} = [\text{OH}] \cdot \gamma_{\text{OH}}$  yields:

$$[\text{OH}] = K_w \cdot [\text{B}] / K'_a \cdot [\text{BH}] \cdot \gamma_{\text{OH}} \quad (25)$$

where  $\gamma_{\text{OH}}$  is the single ion aqueous activity of  $\text{OH}^-$  ion. Substituting into (22) the value of  $[\text{H}]$  and  $[\text{OH}]$  from (23) and (25) respectively:

$$n_{\text{OH}} = \frac{[\text{B}] \cdot K_w \cdot V}{[\text{BH}] \cdot K'_a \cdot \gamma_{\text{OH}}} - \frac{[\text{BH}] \cdot K'_a \cdot V}{[\text{B}] \cdot \gamma_{\text{H}}} + [\text{B}] \cdot (V + K_B \cdot V_O) \quad (26)$$

Now substituting the expression for  $[\text{B}]$  from (18) and the expression for  $[\text{BH}]$  from (15) into (26), simplifying and rearranging yields:



$$n_{OH} = X + Y \cdot \frac{K_w \cdot V}{K'_a \cdot \gamma_{OH}} - Z \cdot \frac{K'_a \cdot V}{\gamma_H} \quad (27)$$

where

$$X = \frac{[\epsilon'_{BH} \cdot n_{BH} - A_{obs} (V + K_I \cdot V_O)] \cdot (V + K_B \cdot V_O)}{\epsilon'_{BH} \cdot (V + K_B \cdot V_O) - \epsilon'_B \cdot (V + K_I \cdot V_O)}$$

$$Y = \frac{n_{BH} \cdot \epsilon'_{BH} - A_{obs} \cdot (V + K_I \cdot V_O)}{A_{obs} \cdot (V + K_B \cdot V_O) - n_{BH} \cdot \epsilon'_B}$$

$$Z = 1/Y$$

Equation 27 is the desired titration equation relating  $A_{obs}$  and  $n_{OH}$ . All of the other quantities in this equation are constants under the experimental conditions. A computer program in Fortran IV for equation (27) is presented on the next page. Use of this equation to calculate the titration curve is discussed in the Theory section, Chapter 2.

#### B. Absorbance of Organic Phase Monitored

Now considering the absorbance of the organic phase, the following relationships are derived:

$$A_{obs,O} = \epsilon'_{B,O} \cdot [B]_O + \epsilon'_{BHX,O} \cdot [BHX]_O \quad (28)$$

where  $A_{obs,O}$  is the absorbance of the organic phase,



```

1  /COMPILE NOLIST
2  C    THIS IS THE COMPUTER PROGRAM FOR THE PHOTOMETRIC ACID-BASE
3      *TITRATION EQUATION OF BH TYPE ACID TITRATED WITH NAOH
4      *(MONITORING THE AQUEOUS PHASE).
5      REAL KI,KB,KW,NBH,NOH,KA
6      READ,GH,GOH,KB,KI,E1,E2,KA,KW,NBH,VO,V
7      PRINT,GH,GOH,KB,KI,E1,E2,KA,KW,NBH,VO,V
8      PRINT 6
9      6  FORMAT('O',T10,'AOBS',T23,'FIRST TERM',T41,'SECOND TERM',
10     *T57,'THIRD TERM',T78,'NOH')
11      A1=E1*NBH
12      A2=V+KI*VO
13      A2DASH=A2/20.
14      A3=V+KB*VO
15      D2=(E1*A3-E2*A2)
16      C1=KW*V/(KA*GOH)
17      C2=KA*V/GH
18      DO 51 I=1,40
19      D1=(A1-I*A2DASH)
20      X=D1*A3/D2
21      Y=D1*A2/(NBH*D2-D1*A3)
22      Z=1./Y
23      G1=Y*C1
24      G2=Z*C2
25      NOH=X+G1-G2
26      PRINT,' '
27      51 PRINT,I/20.,X,G1,G2,NOH
28      STOP
29      END

```



corrected for dilution if necessary. Substituting into (28) the values of  $[B]_O$  and  $[BHX]_O$  from (10) and (11), and rearranging gives:

$$[BH] = \frac{A_{obs,O} - \epsilon'_{B,O} \cdot K_B \cdot [B]}{\epsilon'_{BHX,O} \cdot K_I} \quad (29)$$

Equating (15) with (29), and rearranging gives:

$$[B] = \frac{[\epsilon'_{BHX,O} \cdot n_{BH} \cdot K_I - A_{obs,O} (V + K_I \cdot V_O)]}{[\epsilon'_{BHX,O} \cdot K_I (V + K_B \cdot V_O) - \epsilon'_{B,O} \cdot K_B (V + K_I \cdot V_O)]} \quad (30)$$

Now substituting the expression for  $[B]$  from (30) and the expression for  $[BH]$  from (15) into (26), simplifying and rearranging yields:

$$n_{OH} = X + Y \frac{K_w \cdot V}{K'_a \cdot \gamma_{OH}} - Z \frac{K'_a \cdot V}{\gamma_H} \quad (31)$$

where

$$X = \frac{[\epsilon'_{BHX,O} \cdot n_{BH} \cdot K_I - A_{obs,O} (V + K_I \cdot V_O)] (V + K_B \cdot V_O)}{[K_I \cdot \epsilon'_{BHX,O} (V + K_B \cdot V_O) - \epsilon'_{B,O} \cdot K_B (V + K_I \cdot V_O)]}$$

$$Y = \frac{\epsilon'_{BHX,O} \cdot n_{BH} \cdot K_I - A_{obs,O} (V + K_I \cdot V_O)}{A_{obs,O} (V + K_B \cdot V_O) - n_{BH} \cdot \epsilon'_{B,O} \cdot K_B}$$

$$Z = 1/Y$$



## APPENDIX IV

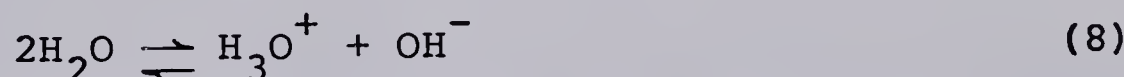
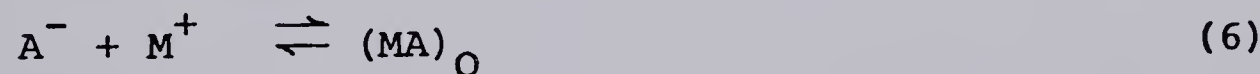
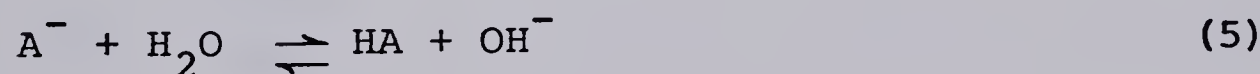
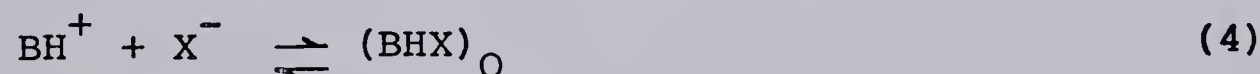
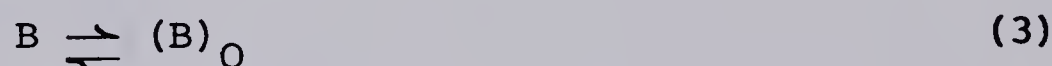
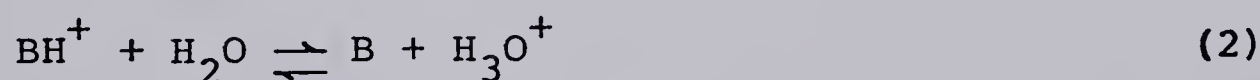
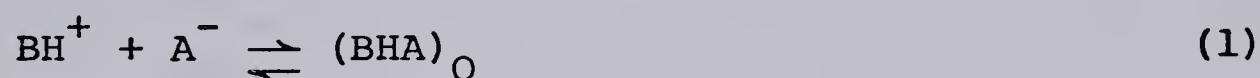
### DERIVATION OF PHOTOMETRIC ION-PAIR TITRATION

#### EQUATIONS FOR A WEAK ACID CATION WITH ANIONIC TITRANT

##### A. Absorbance of Aqueous Phase Monitored

Photometric titration of  $n_{\text{BH}}$  moles of acid  $\text{BH}^+$  with picric acid in dilute aqueous solution of salt MX, in presence of an immiscible organic solvent.

The equilibria prevailing in this system are given below.



Species without a subscript are in the aqueous phase and those with the subscript 0 are in the organic phase. Here  $\text{M}^+$  and  $\text{X}^-$  are the cation and anion of the buffer which has been added to the aqueous phase, and/or of some inert salt that may also have been added to the



aqueous phase (e.g., NaCl). The species  $A^-$  is the titrant anion (e.g., picrate).

Equilibrium constants and distribution coefficients for the equilibria above are:

$$K_S = \frac{[BHA]_O}{[BH][A]} \quad (9)$$

$$K'_a = \frac{[B]}{[BH]} \cdot a_H \quad (10)$$

$$K_B = \frac{[B]_O}{[B]} \quad (11)$$

$$K_{I,BHX} = \frac{[BHX]_O}{[BH]} \quad (12)$$

$$K'_b = \frac{[HA]}{[A]} \cdot a_{OH} \quad (13)$$

$$K_{I,MA} = \frac{[MA]_O}{[A]} \quad (14)$$

$$K_{HA} = \frac{[HA]_O}{[HA]} \quad (15)$$

$$K_w = a_H \cdot a_{OH} \quad (16)$$

The mass balance relationship for B-containing species in the system may be expressed as concentration,

$$n_i = [i] \cdot V:$$

$$n_{BH} = [BH] \cdot V + [B] \cdot V + [BHA]_O \cdot V_O + [B]_O \cdot V_O + [BHX] \cdot V_O \quad (17)$$



Substituting into (17), the values of  $[BHA]_O$ ,  $[B]_O$  and  $[BHX]_O$  from (9), (11) and (12) respectively:

$$n_{BH} = [BH] \cdot V + [B] \cdot V + K_S \cdot [BH] \cdot [A] \cdot V_O + K_B \cdot [B] \cdot V_O + K_{I,BHX} \cdot [BH] \cdot V_O \quad (18)$$

Substituting into (18) the value of  $[B]$  from (10):

$$n_{BH} = [BH] \cdot V + [BH] \cdot V \cdot K'_a / a_H + K_S \cdot [BH] \cdot [A] \cdot V_O + [BH] \cdot K_B \cdot V_O \cdot K'_a / a_H + K_{I,BHX} \cdot [BH] \cdot V_O \quad (19)$$

Rearranging this expression gives

$$n_{BH} = [BH] \cdot (V + V \cdot K'_a / a_H + K_S \cdot [A] \cdot V_O + K_B \cdot V_O \cdot K'_a / a_H + K_{I,BHX} \cdot V_O) \quad (20)$$

The mass balance expression for A-containing species is:

$$n_A = [A] \cdot V + [HA] \cdot V + [BHA]_O \cdot V_O + [MA]_O \cdot V_O + [HA]_O \cdot V_O \quad (21)$$

Substituting into (21) the values of  $[BHA]_O$ ,  $[MA]_O$  and  $[HA]_O$  from (9), (14) and (15) respectively gives:

$$n_A = [A] \cdot V + [HA] \cdot V + K_S \cdot [BH] \cdot [A] \cdot V_O + K_{I,MA} \cdot [A] \cdot V_O + K_{HA} \cdot [HA] \cdot V_O \quad (22)$$

Substituting into (22) the value of  $[HA]$  from (13):



$$n_A = [A] \cdot V + [A] \cdot V \cdot K'_b / a_{OH} + K_S \cdot [BH] \cdot [A] \cdot V_O + K_{I,MA} \cdot [A] \cdot V_O + [A] \cdot K_{HA} \cdot V_O \cdot K'_b / a_{OH} \quad (23)$$

Rearranging this expression gives

$$n_A = [A] \cdot (V + V \cdot K'_b / a_{OH} + K_S \cdot [BH] \cdot V_O + K_{I,MA} \cdot V_O + K_{HA} \cdot V_O \cdot K'_b / a_{OH}) \quad (24)$$

Assuming that Beer's law applies and that measurements of absorbance are made in 1.000 cm a pathlength cell, the following relationship applies:

$$A_{obs} = \epsilon'_{BH} \cdot [BH] + \epsilon'_B \cdot [B] + \epsilon'_A \cdot [A] + \epsilon'_{HA} \cdot [HA] \quad (25)$$

where  $A_{obs}$  is the absorbance of the aqueous phase, corrected for dilution if necessary. Substituting into (25) the values of  $[B]$  and  $[HA]$  from (10) and (13) respectively yields:

$$A_{obs} = \epsilon'_{BH} \cdot [BH] + \epsilon'_B \cdot [BH] \cdot K'_a / a_H + \epsilon'_A \cdot [A] + \epsilon'_{HA} \cdot [A] \cdot K'_b / a_{OH} \quad (26)$$

$$A_{obs} = [BH] \cdot (\epsilon'_{BH} + \epsilon'_B \cdot K'_a / a_H) + [A] \cdot (\epsilon'_A + \epsilon'_{HA} \cdot K'_b / a_{OH}) \quad (27)$$

Rearranging this expression gives:

$$[A] = \left[ \frac{A_{obs, aq} - [BH] \cdot (\epsilon'_{BH} + \epsilon'_B \cdot K'_a / a_H)}{(\epsilon'_A + \epsilon'_{HA} \cdot K'_b / a_{OH})} \right] \quad (28)$$



Substituting into (20) and (24) the value of [A] from (28) :

$$n_{BH} = [BH] \left( V + V \cdot K'_a / a_H + K_S \cdot V_O \left[ \frac{A_{obs,aq} - [BH] \cdot (\epsilon'_{BH} + \epsilon'_B \cdot K'_a / a_H)}{(\epsilon'_A + \epsilon'_{HA} \cdot K'_b / a_{OH})} \right] \right. \\ \left. + K_B \cdot V_O \cdot K'_a / a_H + K_{I,BHX} \cdot V_O \right) \quad (29)$$

$$n_A = \left[ \frac{A_{obs,aq} - [BH] \cdot (\epsilon'_{BH} + \epsilon'_B \cdot K'_a / a_H)}{\epsilon'_A + \epsilon'_{HA} \cdot K'_b / a_{OH}} \right] \cdot (V + V \cdot K'_b / a_{OH} \\ + K_S \cdot [BH] \cdot V_O + K_{I,MA} \cdot V_O + K_{HA} \cdot V_O \cdot K'_b / a_{OH}) \quad (30)$$

Substituting in (29) and (30) the value of  $a_{OH}$  from (16), and rearranging both equations gives:

$$[BH]^2 \cdot K_S \cdot V_O \cdot \left[ \frac{(\epsilon'_{BH} + \epsilon'_B \cdot K'_a / a_H)}{(\epsilon'_A + \epsilon'_{HA} \cdot (K'_b \cdot a_H) / K_w)} \right] - [BH] \cdot \left[ V + K'_a \cdot V / a_H + \right. \\ \left. \frac{A_{obs} \cdot K_S \cdot V_O}{(\epsilon'_A + \epsilon'_{HA} \cdot (K'_b \cdot a_H) / K_w)} \right] + K_{I,BHX} \cdot V_O + \frac{K_B \cdot K'_a \cdot V_O}{a_H} + n_{BH} = 0 \quad (31)$$

$$n_A = \frac{A_{obs} - [BH] \cdot (\epsilon'_{BH} + \epsilon'_B \cdot K'_a / a_H)}{(\epsilon'_A + \epsilon'_{HA} \cdot (K'_b \cdot a_H) / K_w)} \cdot \left[ V + \frac{K'_b \cdot a_H \cdot V}{K_w} + K_S \cdot [BH] \cdot V_O \right. \\ \left. + K_{I,MA} \cdot V_O + \frac{K_{HA} \cdot K'_b \cdot a_H \cdot V_O}{K_w} \right] \quad (32)$$

Equation (31) is a quadratic equation whose two roots



have real, positive values corresponding to the concentrations of  $BH^+$  on the two branches of the titration curve. Equations (31) and (32) are used to calculate a theoretical titration curve, using a Fortran IV computer program, which is given on the next page.

#### B. Absorbance of the Organic Phase Monitored

Now considering the absorbance of the organic phase the following relationships are derived:

$$A_{obs,O} = \epsilon'_{BHA} \cdot [BHA]_O + \epsilon_{MA} [MA]_O + \epsilon'_{HA} \cdot [HA]_O \\ + \epsilon'_{BHX} \cdot [BHX]_O + \epsilon'_B \cdot [B]_O \quad (33)$$

Substituting into (33) the values of  $[BHA]_O$ ,  $[MA]_O$ ,  $[HA]_O$ ,  $[BHX]_O$  and  $[B]_O$  from (9), (14), (15), (12), and (11) respectively gives:

$$A_{obs,O} = \epsilon'_{BHA} \cdot K_S \cdot [BH] \cdot [A] + \epsilon'_{MA} \cdot K_{I,MA} \cdot [A] + \\ \epsilon'_{HA} \cdot K_{HA} \cdot [HA] + \epsilon'_{BHX} \cdot K_{I,BHX} \cdot [BH] + \\ \epsilon'_B \cdot K_B \cdot [B] \quad (34)$$

Substituting the value of  $[HA]$  and  $[B]$  from (13) and (10), respectively:

$$A_{obs,O} = \epsilon'_{BHA} \cdot K_S \cdot [BH] [A] + \epsilon'_{MA} \cdot K_{I,MA} \cdot [A] \\ + \epsilon'_{HA} \cdot K_{HA} [A] \cdot K'_b / a_{OH} + \epsilon'_{BHX} \cdot K_{I,BHX} \cdot [BH] \\ + \epsilon'_B \cdot K_B \cdot [BH] \cdot K'_a / a_H \quad (35)$$



```

1  /COMPILE  NOLIST
2  C      THIS IS THE COMPUTER PROGRAM FOR THE PHOTOMETRIC ION-PAIR
3  *TITRATION EQUATION FOR A WEAK ACID CATION WITH ANIONIC
4  *TITRANT(MONITORING THE AQUEOUS PHASE.
5  IMPLICIT REAL*8 (A-H,N-Z)
6  REAL*8 KABH,KS,KB,KIBHX,KINAA,KBA,KHA,KW,U,UO,E1,E2,E3,E4,NBH,AH
7  READ,KS,KABH,KB,KIBHX,KINAA,KBA,KHA,KW,U,UO,E1,E2,E3,E4,NBH,AH
8  PRINT,KS,KABH,KB,KIBHX,KINAA,KBA,KHA,KW,U,UO,E1,E2,E3,E4,NBH,AH
9  PRINT 6
10 6      FORMAT('0',T13,'AOBS',T29,'X',T47,'Y',T64,'NAX',T82,'NAY')
11      A1=E1+E2*(KABH/AH)
12      A2=E3+E4*(KBA*AH/KW)
13      A3=KS*UO
14      A4=A3*(A1/A2)
15      A5=KABH*U/AH
16      A6=KIBHX*UO
17      A7=KB*(KABH*UO/AH)
18      A8=A3/A2
19      A9=U+A5+A6+A7
20      A10=KBA*U*AH/KW
21      A11=KINAA*UO
22      A12=KHA*KBA*UO*AH/KW
23      A15=2*A4
24      A14=2*A15*NBH
25      A16=U+A10+A11+A12
26      DO 51 I=10,20
27      AOBS=I/20.
28      X=((A9+A8*AOBS)+DSQRT((A9+A8*AOBS)**2-A14))/A15
29      Y=((A9+A8*AOBS)-DSQRT((A9+A8*AOBS)**2-A14))/A15
30      NAX=((AOBS-X*A1)*(A16+A3*X))/A2
31      NAY=((AOBS-Y*A1)*(A16+A3*Y))/A2
32      PRINT,' '
33 51      PRINT 7,AOBS,X,Y,NAX,NAY
34 7      FORMAT('0',10X,F6.4,4(3X,E15.7))
35      STOP
36      END

```



Rearranging this expression gives

$$A_{\text{obs},O} = [A] \cdot (\epsilon'_{\text{BHA}} \cdot K_S \cdot [\text{BH}] + \epsilon'_{\text{MA}} \cdot K_{\text{MA}} + \epsilon'_{\text{HA}} \cdot K_{\text{HA}} \cdot K'_b / a_{\text{OH}}) \\ + [\text{BH}] \cdot (\epsilon'_{\text{BHX}} \cdot K_{\text{I,BHX}} + \epsilon'_B \cdot K_B \cdot K'_a / a_H) \quad (36)$$

$$[A] = \left[ \frac{A_{\text{obs},O} - [\text{BH}] \cdot (\epsilon'_{\text{BHX}} \cdot K_{\text{I,BHX}} + \epsilon'_B \cdot K_B \cdot K'_a / a_H)}{(\epsilon'_{\text{BHA}} \cdot K_S \cdot [\text{BH}] + \epsilon'_{\text{MA}} \cdot K_{\text{MA}} + \epsilon'_{\text{HA}} \cdot K_{\text{HA}} \cdot K'_b / a_{\text{OH}})} \right] \quad (37)$$

Substituting the value of [A] from (37) into (20), and rearranging gives:

$$\epsilon'_{\text{BHA}} \cdot K_S \cdot [\text{BH}] \cdot n_{\text{BH}} + \epsilon'_{\text{MA}} \cdot K_{\text{I,MA}} \cdot n_{\text{BH}} + \epsilon'_{\text{HA}} \cdot K_{\text{HA}} \cdot n_{\text{BH}} \cdot K'_b / a_{\text{OH}} = \epsilon'_{\text{BHA}} \cdot K_S \cdot \\ [\text{BH}]^2 \cdot V + \epsilon'_{\text{MA}} \cdot K_{\text{I,MA}} \cdot [\text{BH}] \cdot V + \epsilon'_{\text{HA}} \cdot K_{\text{HA}} \cdot [\text{BH}] \cdot V \cdot K'_b / a_{\text{OH}} \\ + \epsilon'_{\text{BHA}} \cdot K_S \cdot [\text{BH}]^2 \cdot V \cdot K'_a / a_H + \epsilon'_{\text{MA}} \cdot K_{\text{I,MA}} \cdot [\text{BH}] \cdot V \cdot K'_a / a_H \\ + \epsilon'_{\text{HA}} \cdot K_{\text{HA}} \cdot [\text{BH}] \cdot V \cdot (K'_b \cdot K'_a) / K_w + \epsilon'_{\text{BHA}} \cdot K_S \cdot [\text{BH}]^2 \cdot K_{\text{I,BHX}} \cdot V_O \\ + \epsilon'_{\text{MA}} \cdot K_{\text{MA}} \cdot K_{\text{I,BHX}} \cdot [\text{BH}] \cdot V_O + \epsilon'_{\text{HA}} \cdot K_{\text{HA}} \cdot K'_b / a_{\text{OH}} \cdot [\text{BH}] \cdot V_O \\ + \epsilon'_{\text{BHA}} \cdot K_S \cdot [\text{BH}]^2 \cdot V_O \cdot (K_B \cdot K'_a) / a_H + \epsilon'_{\text{MA}} \cdot K_{\text{MA}} \cdot [\text{BH}] \cdot V_O \cdot (K_B \cdot K'_a) / a_H \\ + \epsilon'_{\text{HA}} \cdot K_{\text{HA}} \cdot [\text{BH}] \cdot V_O \cdot (K_B \cdot K'_b \cdot K'_a) / K_w + K_S \cdot [\text{BH}] \cdot V_O \cdot A_{\text{obs},O} \\ - K_S \cdot [\text{BH}]^2 \cdot V_O \cdot \epsilon'_{\text{BHX}} \cdot K_{\text{I,BHX}} - K_S \cdot [\text{BH}]^2 \cdot V_O \cdot \epsilon'_B \cdot K_B \cdot K'_a / a_H \quad (38)$$

Substituting the value of  $a_{\text{OH}}$  from (16) into (38), and rearranging gives:



$$\begin{aligned}
& [\text{BH}]^2 \cdot K_S \cdot \left[ \epsilon'_{\text{BHA}} \cdot (V + K'_a \cdot V/a_H + K_{\text{I,BHX}} \cdot V_O + (K'_a \cdot K_B \cdot V_O)/a_H) \right. \\
& \left. - (\epsilon'_{\text{BHX}} \cdot K_{\text{I,BHX}} \cdot V_O + (\epsilon'_B \cdot K_B \cdot K'_a \cdot V_O)/a_H) \right] + [\text{BH}^+] \cdot \\
& \left[ \epsilon'_{\text{HA}} \cdot (K_{\text{HA}} \cdot K'_b)/K_w \cdot (a_H \cdot V + K'_a \cdot V + K_{\text{I,BHX}} \cdot a_H \cdot V_O \right. \\
& \left. + K'_a \cdot K_B \cdot V_O) + \epsilon'_{\text{MA}} \cdot K_{\text{I,MA}} \cdot (V + (K'_a \cdot V)/a_H + K_{\text{I,BHX}} \cdot V_O \right. \\
& \left. + (K'_a \cdot K_B \cdot V_O)/a_H + K_S \cdot (A_{\text{OVS,O}} \cdot V_O - \epsilon'_{\text{BHA}} \cdot n_{\text{BH}}) \right] \\
& - n_{\text{BH}} \cdot (\epsilon'_{\text{HA}} \cdot (K_{\text{HA}} \cdot K'_b \cdot a_H)/K_w + \epsilon'_{\text{MA}} \cdot K_{\text{I,MA}}) = 0 \tag{39}
\end{aligned}$$

Substituting the value of [A] from (37) into (24) gives

$$\begin{aligned}
n_A = & \frac{A_{\text{obs,O}} - [\text{BH}] \cdot (\epsilon'_{\text{BHX}} \cdot K_{\text{I,BHX}} + \epsilon'_B (K_B \cdot K'_a)/a_H)}{\epsilon'_{\text{BHA}} \cdot K_S \cdot [\text{BH}] + \epsilon'_{\text{MA}} \cdot K_{\text{I,MA}} + \epsilon'_{\text{HA}} \cdot (K_{\text{HA}} \cdot K'_b \cdot a_H)/K_w} \\
& \left[ V + \frac{K'_b \cdot a_H \cdot V}{K_w} + K_S \cdot [\text{BH}] \cdot V_O + K_{\text{MA}} \cdot V_O + \frac{K_{\text{HA}} \cdot K'_b \cdot a_H \cdot V_O}{K_w} \right] \tag{40}
\end{aligned}$$

Equations (39) and (40) are used to calculate a theoretical titration curve, using a Fortran IV computer program, which is given on the next page.



```

1  /COMPILE NOLIST
2  C   THIS IS THE COMPUTER PROGRAM FOR THE PHOTOMETRIC ION-PAIR
3  *TITRATION EQUATION FOR A WEAK ACID CATION WITH ANIONIC
4  *TITRANT(MONITORING THE ORGANIC PHASE).
5  IMPLICIT REAL*8 (A-H,N-Z)
6  REAL*8 KABH,KS,KB,KIBHX,KINAA,KHA,KW,NA,NBH
7  *,KBA
8  READ,KS,KABH,KB,KIBHX,KINAA,KBA,KHA,KW,U,UO,E1,E2,E3,NBH,AH
9  *,E4,E5
10 PRINT,KS,KABH,KB,KIBHX,KINAA,KBA,KHA,KW,U,UO,E1,E2,E3,NBH
11 *,AH,E4,E5
12 PRINT 6
13 6   FORMAT('O',T13,'AOBS',T29,'X',T47,'Y',T64,'NAX',T82,'NAY')
14     A1=E1*KS
15     A2=KABH/AH
16     A3=KIBHX*UO
17     A4=KB*UO
18     A5=A1*U
19     A6=A2*A5
20     A7=A1*A3
21     A8=A1*A2*A4
22     AA=KS*UO
23     AB=E4*KIBHX
24     AC=E5*KB
25     AD=AA*AB
26     AE=AA*AC*A2
27     AF=AC*A2
28     A9=A5+A6+A7+A8-AD-AE
29     A10=E2*KINAA
30     A11=A10*U
31     A12=E3*KHA
32     A13=A12*U
33     A14=KBA/KW
34     A15=A14*AH
35     A16=A13*A15
36     A17=A11*A2
37     A18=A14*KABH
38     A19=A13*A18
39     A20=A3*A10
40     A21=A3*A12*A15
41     A22=A2*A4*A10
42     A23=A4*A12*A18
43     A24=A1*NBH
44     A25=A10*NBH
45     A26=A12*A15*NBH
46     A27=A11+A16+A17+A19+A20+A21+A22+A23-A24
47     A29=A25+A26
48     A30=4*A9*A29
49     A31=A12*A15
50     A32=A10+A31
51     A33=A15*U
52     A34=KINAA*UO
53     A35=KHA*A15*UO
54     A36=U+A33+A34+A35
55     DO 51 I=1,40
56     AOBS=I/20.
57     X=((-1)*(A27+AA*AOBS)+DSQRT((A27+AA*AOBS)**2+A30))/(2*A9)
58     Y=((-1)*(A27+AA*AOBS)-DSQRT((A27+AA*AOBS)**2+A30))/(2*A9)
59     NAX=(AOBS-X*(AB+AF))*(A36+AA*X)/(A1*X+A32)
60     NAY=(AOBS-Y*(AB+AF))*(A36+AA*Y)/(A1*Y+A32)
61 51   PRINT 7,AOBS,X,Y,NAX,NAY
62 7   FORMAT('O',10X,F6.4,4(3X,E15.7))
63 STOP
64 END

```



## APPENDIX V

DERIVATION OF PHOTOMETRIC ION-PAIR TITRATION EQUATION FOR  
A WEAK BASE ANION WITH CATIONIC TITRANT. ABSORBANCE OF  
ORGANIC PHASE MONITORED.

The case in which a sample  $A^-$  is titrated with titrant  $BH^+$  can be derived with the aid of some of the expressions used in Appendix IV.

Rearranging (35) gives:

$$A_{\text{obs},O} = [BH] \cdot (\epsilon'_{BHA} \cdot K_S \cdot [A] + \epsilon'_{BHX} \cdot K_{I,BHX} + \epsilon'_B \cdot K_B \cdot K_a / a_H) \\ + [A] \cdot (\epsilon'_{MA} \cdot K_{I,MA} + \epsilon'_{HA} \cdot K_{HA} \cdot K_b \cdot a_H / K_w) \quad (41)$$

Rearranging this expression gives:

$$[BH] = \frac{A_{\text{obs},O} - [A] \cdot (\epsilon'_{MA} \cdot K_{I,MA} + \epsilon'_{HA} \cdot K_{HA} \cdot K_b \cdot a_H / K_w)}{(\epsilon'_{BHA} \cdot K_S [A] + \epsilon'_{BHX} \cdot K_{I,BHX} + \epsilon'_B \cdot K_B \cdot K_a / a_H)} \quad (42)$$

Substituting the value of  $[BH]$  from (42) into (24) and rearranging gives:

$$[A]^2 \cdot K_S \cdot \left[ \epsilon'_{BHA} \cdot V + \epsilon'_{BHA} \cdot \frac{K'_b \cdot a_H \cdot V}{K_w} - \epsilon'_{MA} \cdot K_{MA} \cdot V_O - \epsilon'_{HA} \cdot K_{HA} \cdot \frac{K'_b \cdot a_H \cdot V_O}{K_w} \right] \\ + [A] \cdot \left[ \epsilon'_{BHX} \cdot K_{BHX} \cdot (V + \frac{K'_b \cdot a_H \cdot V}{K_w}) + \epsilon'_B \cdot \frac{K_B \cdot K'_a \cdot V}{a_H} \cdot (1 + \frac{K'_b \cdot a_H}{K_w}) \right. \\ \left. + \epsilon'_{BHA} \cdot K_S \cdot (K_{MA} \cdot V_O + \frac{K_{HA} \cdot K'_b \cdot a_H \cdot V_O}{K_w} - n_A) + K_S \cdot A_{\text{obs}} \cdot V_O \right] + \epsilon'_{BHX} \cdot K_{BHX} \cdot$$



$$\begin{aligned}
& (K_{MA} \cdot V_O + \frac{K_{HA} \cdot K'_b \cdot a_H \cdot V_O}{K_w} - n_A) + \epsilon'_B \cdot K_B \cdot \left( \frac{K'_a \cdot K_{MA} \cdot V_O}{a_H} + \frac{K'_a \cdot K'_b \cdot K_{HA} \cdot a_H \cdot V_O}{K_w} \right. \\
& \left. - \frac{K_a \cdot n_A}{a_H} \right) = 0
\end{aligned} \tag{43}$$

Substituting the value of [BH] from (42) into (20) gives

$$\begin{aligned}
n_{BH} &= \frac{A_{obs,O} - [A] \cdot \left( \epsilon'_{HA} \cdot \frac{K_{HA} \cdot K'_b \cdot a_H}{K_w} + \epsilon'_{MA} \cdot K_{MA} \right)}{\epsilon'_{BHA} \cdot K_S \cdot [A] + \epsilon'_{BHA} \cdot K_{BHX} + \epsilon'_B \cdot \frac{K_B \cdot K'_a}{a_H}} \\
&\left[ V + \frac{K'_a \cdot V}{a_H} + K_S \cdot [A] \cdot V_O + K_{BHX} \cdot V_O + \frac{K_B \cdot K'_a \cdot V_O}{a_H} \right]
\end{aligned} \tag{44}$$

Equations (43) and (44) can be used to calculate the theoretical titration curve.





**B30262**